UCLA
UCLA Electronic Theses and Dissertations

Title
Disease-specific differences in glycosylation of mouse and human skeletal muscle

Permalink
https://escholarship.org/uc/item/73v762qp

Author
McMorran, Brian James

Publication Date
2017

Peer reviewed|Thesis/dissertation

eScholarship.org Powered by the California Digital Library
University of California

UNIVERSITY OF CALIFORNIA

Los Angeles

Disease-specific differences in glycosylation of mouse and human skeletal muscle

A dissertation submitted in partial satisfaction of the

requirements for the Degree of Philosophy

in Cellular and Molecular Pathology

by

Brian James McMorran

2017

© Copyright by

Brian James McMorran

2017

ABSTRACT OF THE DISSERTATION

Disease-specific differences in glycosylation of mouse and human skeletal muscle

by

Brian James McMorran

Doctor of Philosophy in Cellular and Molecular Pathology

University of California, Los Angeles, 2017

Professor Linda G. Baum, Chair

Proper glycosylation of proteins at the muscle cell membrane, or sarcolemma, is critical for proper muscle function. The laminin receptor alpha-dystroglycan (α-DG) is heavily glycosylated and mutations in 24 genes involved in proper α-DG glycosylation have been identified as causing various forms of congenital muscular dystrophy. While work over the past decade has elucidated the structure bound by laminin and the enzymes required for its creation, very little is known about muscle glycosylation outside of α-DG glycosylation. The modification of glycan structures with terminal GalNAc residues at the rodent neuromuscular junction (NMJ) has remained the focus of work in mouse muscle glycosylation, while qualitative lectin histochemistry studies performed three decades ago represent the majority of human muscle glycosylation research.

This thesis quantifies differentiation-, species-, and disease-specific differences in mouse and human skeletal muscle glycosylation. Following differentiation of mouse myotubes, increased binding was found of lectins specific for GalNAc and *O*-glycans. Additionally,

analysis of binding preferences of four GalNAc-specific lectins, which historically have been used to identify the rodent NMJ, identified differences in the glycan types bound on distinct glycoproteins by each lectin. Following differentiation of human myotubes, specific increases in binding of high mannose *N*-glycan specific lectin NPA, asialo core 1 *O*-glycan specific lectin PNA, α2,3-linked sialic acid specific lectin MAA-II and GalNAc specific lectin WFA were observed. Disease-specific differences in binding of NPA, Jac (sialylated core 1 *O*-glycans), TJA-I (α2,3-linked sialic acid) and WFA were observed quantitatively when comparing binding to healthy and dystrophic myotubes as well as qualitatively via lectin staining of healthy and dystrophic human skeletal muscle tissue sections. This work provides the first quantitative characterization of mouse and human muscle glycosylation, identifies lectin biomarkers for differentiation-, species-, and disease-specific differences in mouse and human muscle glycosylation, and lays the groundwork for future studies which further our understanding of the relationship between proper muscle glycosylation and muscle function.

The dissertation of Brian James McMorran is approved.

M. Carrie Miceli

Stanley F. Nelson

Michael A. Teitell

Linda G. Baum, Committee Chair

University of California, Los Angeles

2017

“And now that you don’t have to be perfect, you can be good”
-John Steinbeck, East of Eden

This work is dedicated to Ryan,
without whom I would still be seeking perfect.

TABLE OF CONTENTS

LIST OF FIGURES……vii

LIST OF TABLES……..……...ix

LIST OF ABBREVIATIONS……..x

ACKNOWLEDGMENTS…….……..……..xii

VITA……...……...……....xv

CHAPTER 1: Introduction……..1

References……...…21

CHAPTER 2: The potential of sarcospan in adhesion complex replacement therapeutics for the treatment of muscular dystrophy…….…...……35

References……...…48

CHAPTER 3: Differentiation-related glycan epitopes identify discrete domains of the muscle glycocalyx…….……..…56

References……...…67

CHAPTER 4: Lectin binding characterizes the healthy human skeletal muscle glycophenotype and identifies disease specific changes in dystrophic muscle…….……...…70

References……..……..103

CHAPTER 5: Conclusions and future directions……..……...…111

References……....118

APPENDIX A: C2C12 myoblast and myotube glycotranscript expression…….……...…121

APPENDIX B: Glycan structures preferentially bound by nominally GalNAc-specific lectins: WFA, VVA-B4, SBA and DBA…….……128

APPENDIX C: Healthy and dystrophic, human myoblast and myotube glycotranscript expression…….……...…131

LIST OF FIGURES

CHAPTER 1

Figure 1-1: Mammalian glycosylation……...…15

Figure 1-2: Major sarcolemmal adhesion complexes…….……17

Figure 1-3: α-DG *O*-mannosylation……...19

CHAPTER 2

Figure 2-1: UGC- and α7β1 integrin-mediated replacement therapy for the DGC in DMD…...….40

Figure 2-2: Glycosylation of α-DG…….……41

Figure 2-3: Effects of SSPN overexpression in *mdx* mice on the cell surface protein expression and processing and possible outcomes of truncated dystrophin within the cell……..45

CHAPTER 3

Figure 3-1: The DGC, UGC and α7-integrin are not requisite for binding of GalNAc-specific lectins…….59

Figure 3-2: Distinct increases in binding of GalNAc-specific lectins following differentiation of C2C12 myotubes…….……60

Figure 3-3: GalNAc-specific lectins precipitate different glycoproteins……...61

Figure 3-4: Reduced expression of β4Galnt3, β3Galnt2, and Neu2 drive distinct changes in binding of GalNAc-specific lectins…….……..……..62

Figure 3-5: Complex *N*-glycans are required for binding of WFA……...63

CHAPTER 4

Figure 4-1: Changes in cell surface glycosylation following differentiation of primary and immortalized healthy human myotubes……..93

Figure 4-2: Disease-specific changes in lectin binding to human skeletal muscle cells……..95

Figure 4-3: Different lectins precipitate different glycoproteins from healthy and dystrophic human myotubes……97

Figure 4-4: Disease-specific differences in *O*-glycan and sialic acid-specific lectin binding to human skeletal muscle……..99

Figure 4-5: Lectin binding to frozen versus fixed skeletal muscle……..……101

LIST OF TABLES

CHAPTER 3

Table 3-1: Panel of lectins with varying specificities utilized to characterize changes in muscle glycosylation following differentiation of C2C12 myotubes……..……60

Table 3-2: Twenty-three glycosyltransferase and glycosidase transcripts upregulated following C2C12 differentiation and identified via glycotranscriptome analysis…..…61

Table 3-3: Seventeen glycans with terminal GalNAc residues on CFG glycan arrays were identified as binding at least one of the four GalNAc-specific lectins……...64

CHAPTER 4

Table 4-1: Primary and immortalized, healthy and dystrophic human myoblast cell sources …....91

Table 4-2: Panel of lectins with varying glycan structure specificities ……..….92

LIST OF ABBREVIATIONS

AAV- adeno-associated virus

AChR- acetylcholine receptor

α-BTX- alpha bungarotoxin

α-DG- alpha-dystroglycan

B3GALNT2- β1,3-*N*-Acetylgalactosaminyltransferase 2

B4GALNT2- β1,4-*N*-Acetylgalactosaminyltransferase 2

B4GAT1- β1,4-glucuronyltransferase 1

BMD- Becker muscular dystrophy

β-DG- beta-dystroglycan

β-Xyl- beta-xylose

cGMP- cyclic guanosine monophosphate

CMAH- cytidine monophosphate acid hydrolase

CMD- congenital muscular dystrophy

ConA- Concanavalin A

DBA- *Dolichos biflorus* agglutinin

DGC- dystrophin-glycoprotein complex

DMD- Duchenne muscular dystrophy

DMNJ- deoxymannojirimycin

ECM- extracellular matrix

FDA- Food and Drug Administration

FFPE- formalin-fixed, paraformaldehyde embedded

FKTN- fukutin

FKRP- fukutin-related protein

FMD- Fukuyama muscular dystrophy

GAG- glycosaminoglycan

Gal-1- galectin-1

GalNAc- *N*-acetylgalactosamine

GlcA- glucuronic acid

GlcNAc- *N*-acetylglucosamine

GPI- glycosylphosphatidylinositol

GTDC2- glycosyltransferase-like domain containing

HPA- *Helix pomatia* agglutinin

HSMC- human skeletal muscle cells

Hsp- heat shock proteins

HTS- high throughput screen

iDRMs- inducible, directly reprogrammable myotubes

ILK- integrin-linked kinase

ISPD- isoprenoid synthase domain containing

Jac- jacalin

LARGE1/2- like-acetylglucosaminyltransferase 1/2

LG- laminin globular

LGMD- limb-girdle muscular dystrophy

MAA-II- *Maackia amurensis* agglutinin-II

MGAT5b- Mannosyl (α1,6)-Glycoprotein β1,6-*N*-Acetyl-Glucosaminyltransferase

MTJ- myotendinous junction

Neu2- sialidase/neuraminidase 2

NeuAc- *N*-acetylneuraminic acid

NeuGc- *N*-glycolylneuraminic acid

NMJ- neuromuscular junction

nNOS- neuronal nitric oxide synthase

NO- nitric oxide

NP-40- Nonidet P-40

NPA- *Narcissus psuedonarcissus* agglutinin

PDE-5A- phosphodiesterase-5A

PHA-L- *Phaseolus vulgaris* leucoagglutinin

pI- isoelectric point

PNA- peanut agglutinin

PNGaseF- Peptide-*N*-glycosidase F

POMT1/2- Protein *O*-Mannosyltransferases 1 and 2

POMGNT1/2- Protein *O*-Linked Mannose *N*-Acetylglucosaminyltransferase 1/2

RboP- ribitol-phosphate

RCA 120- *Ricinus communis* agglutinin I

RXYLT1- Ribitol β-1,2 Xylosyltransferase 1

SA-HRP- streptavidin-horseradish peroxidase

SBA- soybean agglutinin

SG- sarcoglycan

SNA- *Sambucus nigra* agglutinin

SSPN- sarcospan

TJA-I- *Tricosanthes japonica* agglutinin-I

TMEM5- transmembrane protein 5

UGC- utrophin-glycoprotein complex

VVA- *Vicia villosa* agglutinin

WFA- *Wisteria floribunda* agglutinin

WGA- wheat germ agglutinin

WWS- Walker-Warburg syndrome

ACKNOWLEDGEMENTS

I would like to thank my mentor, Dr. Linda Baum, for her continued support in my pursuit of science at the bench as well as my professional development outside the lab. She has been a constant source of inspiration throughout my graduate career. In addition to Dr. Baum, my committee members, Dr. Carrie Miceli, Dr. Stanley Nelson, and Dr. Michael Teitell, have been an invaluable source of feedback and critique as my research has progressed. I would like to thank all of the Baum lab members—past and present—but especially Mabel Pang, Sandra Thiemann and Katrin Schaefer for the all the technical knowledge they provided me, as well as their friendship throughout my graduate career, and my undergraduate researcher Frannie McCarthy for all her hard work and dedication as an aspiring glycobiologist. I would also like to thank all the members of the UCLA Center for Duchenne Muscular Dystrophy for the multiple collaborations that have brought this work to fruition, the supportive and collaborative environment they have provided, as well as the funding I was provided as a UCLA CDMD Fellow this past year. Lastly, I would like to thank my friends, family, and most importantly, my husband, all of who have provided unwavering support throughout my PhD and provided the light when my lamp of knowledge has dimmed.

Chapter 2 is the published manuscript "Marshall, J. L., Kwok, Y., McMorran, B. J., Baum, L. G. & Crosbie-Watson, R. H. The potential of sarcospan in adhesion complex replacement therapeutics for the treatment of muscular dystrophy. *FEBS J* **280**, 4210-4229 (2013)." reproduced here with permission from Wiley Online. The authors thank A.W. Kwok, J. Lee, and J. Oh for critically reading the manuscript. The work was supported by the Genetic Mechanisms Pre-doctoral Training Fellowship USPHS National Research Service Award GM07104, the Edith Hyde Fellowship, the Eureka Pre-doctoral Training Fellowship, and the

Ruth L. Kirschstein National Service Award T32AR059033 (to JLM), Muscular Dystrophy Association RG 135449 (to RCW), NIH P30 AR057230 (to LGB) and NIH/NIAMS R01 AR048179 (to RCW).

Chapter 3 is the published manuscript "McMorran, B. J. *et al.* Differentiation-related glycan epitopes identify discrete domains of the muscle glycocalyx. *Glycobiology* **26**, 1120-1132 (2016)", reproduced here with permission from Oxford University Press. The authors acknowledge like to thank Sandra Thiemann and Katrin Schaefer (UCLA, Baum lab) for their intellectual input and discussion, as well as Grace Hong (UCLA, Crosbie-Watson lab) for muscle tissue sample preparation. The work was supported by funding from Muscular Dystrophy Association RG 135449 (to LGB), RG 274143 (to RCW), NIH P30 AR057230, NIH/CATS UCLA CTSI UL1TR000124 (to LGB and RCW), R01 AR048179 (to RCW), GM103490 (to KWM), NRSA GM07104, the Edith Hyde Fellowship, the Eureka Pre-doctoral Training Fellowship, and the Ruth L. Kirschstein NRSA NIAMS T32AR059033 (to JLM).

Chapter 4 a version of a manuscript submitted to *Glycobiology* for publication. Authors for this article are Brian J. McMorran, M. Carrie Miceli and Linda G. Baum. The authors thank Mabel Pang and Katrin Schaefer for helpful discussion, Negar Khanlou for assistance with muscle tissue sample acquisition, Rachelle Crosbie-Watson for assistance with fluorescence microscopy, and Alison Nairn and Kelley Moremen for analysis of glycotranscript expression. We thank the UCLA Translational Pathology Core Laboratory for their preparation of de-identified human skeletal muscle tissue and the UCLA Center for Duchenne Muscular Tissue Repository for immortalized healthy and dystrophic human cell lines. This work was supported by Muscular Dystrophy Association RG 254647 (to LGB), NIH P30 AR057230 (to MCM) and the UCLA Center for Duchenne Muscular Dystrophy Fellowship (to BJM).

Appendix A and B are versions of Supplemental Table 1 and 2, respectively, to manuscript "McMorran, B. J. *et al.* Differentiation-related glycan epitopes identify discrete domains of the muscle glycocalyx. *Glycobiology* **26**, 1120-1132 (2016)", reproduced here with permission from Oxford University Press. Appendix C contains RNA-Seq results from glycotranscript abundance analysis as a component of work related to Chapter 4.

VITA

2010	B.S., Physiological Sciences University of Arizona Tucson, AZ
2012	M.S., Biomedical Engineering University of California, Los Angeles Los Angeles, CA
2012	Admitted to UCLA ACCESS program University of California, Los Angeles Los Angeles, CA
2013	Joined Cellular and Molecular Pathology Graduate Program University of California, Los Angeles Los Angeles, CA
2014	Teaching Assistant Department of Physiological Science University of California, Los Angeles Los Angeles, CA
2016-2017	UCLA CDMD Fellowship Center for Duchenne Muscular Dystrophy University of California, Los Angeles Los Angeles, CA
2016-2017	Technology Transfer Fellow Technology Development Group University of California, Los Angeles Los Angeles, CA

PUBLICATIONS

McMorran, B. J. *et al.* Lectin binding characterizes the healthy human skeletal muscle glycophenotype and identifies disease specific changes in dystrophic muscle. *Glycobiology*, submitted for publication

McMorran, B. J. *et al.* Differentiation-related glycan epitopes identify discrete domains of the muscle glycocalyx. *Glycobiology* **26**, 1120-1132, doi:10.1093/glycob/cww061 (2016)

Marshall, J. L., Kwok, Y., McMorran, B. J., Baum, L. G. & Crosbie-Watson, R. H. The potential of sarcospan in adhesion complex replacement therapeutics for the treatment of muscular dystrophy. *FEBS J* **280**, 4210-4229, doi:10.1111/febs.12295 (2013).

PRESENTATIONS

McMorran, B.J., McCarthy, F., Crosbie-Watson, R.H., Baum, L.G. "Discrete and specific differences in mouse and human muscle glycosylation" UCLA CDMD Muscle Cell Biology Retreat, 2014, Los Angeles, CA

McMorran, B.J., Marshall, J.L., Crosbie-Watson, R.H., Baum, L.G. "Discrete and specific changes in cell surface glycosylation following differentiation of murine myoblasts" Alternative Muscle Club Meeting, 2013, San Diego, CA

CHAPTER ONE

Introduction

Glycosylation and glycan types

Virtually all proteins at the cell surface are post-translationally modified with glycans, making them glycoproteins. Appropriate protein glycosylation is necessary for life, adds an additional layer of biologic information to proteins at the cell surface, and provides functionality to many glycoproteins[1-3]. Glycosylation of each cell surface glycoprotein adds to the heterogeneity of glycan structures presented by the cell and impacts cell-cell and cell-extracellular matrix (ECM) interactions[4]. Glycan modifications exist in various forms, including *N*-glycans added to the amine of asparagine residues and *O*-glycans attached via the hydroxyl of serine/threonine residues (Figure 1-1). Additionally glycans are added to lipid ceramide moieties (known as glycolipids or glycosphingolipids), can be present as glycan bridges in glycosylphosphatidylinositol (GPI)-anchored glycoproteins, and also exist as glycosaminoglycans (GAGs) extending from proteoglycans (Figure 1-1). My research has focused on glycoprotein glycosylation present at the skeletal muscle cell membrane, or sarcolemma.

Glycoprotein glycosylation is a non-templated biologic process affected by many factors; these include expression, localization and activity of glycosyltransferases and glycosidases, the availability of the appropriate sugar-nucleotide donor substrate, and the availability of the appropriate protein acceptor substrate decorated with the relevant glycan sub-structure. Therefore, appropriate glycosylation of a glycoprotein is the result of specific sequential enzymatic steps modifying amino acid and glycan substrates in the right order at the right time.

Glycan modifications have many roles. Addition of glycans affects protein structure, molecular mass and isoelectric point (pI), all of which can impact protein function. Addition of glycans in the endoplasmic reticulum and Golgi apparatus provides a control mechanism for

protein synthesis and aids in appropriate glycoprotein targeting[5]. Interactions between glycan receptors and/or carbohydrate binding proteins known as lectins can increase glycoprotein retention at the cell surface[6]. Additionally, glycosylation is known to vary throughout development and across both tissues and between cell types[7-9]. Glycosylation, therefore, plays a significant role in both physiologic and pathologic processes.

Glycosylation and muscle function

Proper glycosylation plays a major role in muscle function. α7 and β1 integrin isoforms, along with the membrane associated glycoprotein α-dystroglycan (α-DG), are the major ECM binding proteins displayed on the skeletal muscle surface, and all of these are highly glycosylated (Figure 1-2)[10,11]. These ECM receptors stabilize myofibers during contraction via interactions with the basal lamina, without which myofibers would not be able to withstand forces generated during contraction[12]. The various congenital muscular dystrophies (CMDs) further highlight the integral role that sarcolemmal glycosylation plays in muscle function. CMDs result from loss of function mutations in any of the proteins involved in α-DG glycosylation. Patients suffering from CMDs present with a variety of symptoms and disease pathologies due to the loss of specific glycan structures resulting from these mutations. For example, Walker-Warburg syndrome, one of the most severe muscular dystrophies, results from mutations in Protein *O*-Mannosyltransferases 1 and 2 (POMT1/2) which prevent the creation of mannosyl O-glycans (Figure 1-3)[13]. Similarly, Muscle-eye-brain disease results from mutations in Protein *O*-Linked Mannose *N*-Acetylglucosaminyltransferase 1 (POMGNT1)[14] and Fukuyama muscular dystrophy (FMD) results from mutations in Fukutin (FKTN) and Fukutin related protein (FKRP) [15]. POMGNT1, FKTN and FKRP, along with 21 other proteins, are required for

creation of glycans on α-DG bound by laminin. Therefore, mutations in any of these genes causes hypoglycosylation of α-DG, disrupts laminin binding and ultimately impacts muscle function[16].

Duchenne muscular dystrophy and the Dystrophin Glycoprotein Complex

Duchenne muscular dystrophy (DMD) is an X-linked, progressive muscular dystrophy affecting 1 in 5000 boys worldwide. Resulting from mutations in the gene encoding the cytoskeletal linker protein dystrophin[17], both skeletal and cardiac function are severely impacted by loss of dystrophin boys suffering from DMD. Onset typically occurs during late infancy, with most boys losing ambulation by puberty, and rarely surviving beyond the third decade. Recent improvements in care regimens and recently approved novel therapies may slow disease progression in some boys.

Dystrophin links actin to the intracellular domain of β-dystroglycan (β-DG)[18] which extracellularly associates with α-DG[8]. α-DG completes the link to the extracellular matrix by binding to laminin and other ECM binding partners[11,19,20]. This link between the intracellular actin cytoskeleton and extracellular binding partners transmits forces during contraction, and this complex is termed the dystrophin-glycoprotein complex (DGC). The DGC is distributed ubiquitously along the sarcolemma[21,22]. A homologous complex, the utrophin glycoprotein complex (UGC) is selectively localized at the neuromuscular and myotendinous junctions (NMJ/MTJ) where utrophin, a dystrophin homolog, substitutes for dystrophin[23,24].

The DGC/UGC complex contains many additional proteins. As mentioned above, intracellular dystrophin binds β-DG to link actin and the sarcolemma (Figure 1-2). Interactions between β-DG and the sarcoglycans (SGs) further anchor the DGC at the sarcolemma with

additional support and stability provided by associations between the tetraspan-like protein SSPN and the SG subcomplex[24-27]. Additional intracellular proteins, such as the syntrophins, neuronal nitric oxide synthase (nNOS), and Grb2, associate with β-DG and the DGC via interactions mediated by α-dystrobrevin[24]. Extracellularly, α-DG binds β-DG non-covalently, and binds laminin to complete the connection between the DGC and the ECM[2,3,8,20,28,29].

Dystroglycan glycosylation represents the wealth of our muscle glycosylation knowledge

Over the past decade a large amount of work in the field of muscle glycobiology has focused on understanding the role of α-DG glycosylation in muscle function. α/β-DG is the product of one gene, *dag1*, which produces a 895 residue precursor protein. This precursor is cleaved post-translationally via a cleavage site conserved among vertebrates into α- and β-DG subunits[11,30]. Cleavage of DG into subunits is critical for appropriate glycosylation and localization of α-DG at the sarcolemma[31]. The S654A mutation at the DG cleavage site inhibits α-DG processing and results in a muscular dystrophy phenotype in mice[32]. While glycosylation of α-DG is required for localization at the sarcolemma and laminin binding, it is not required for association with β-DG. Recombinant β-DG fragments are capable of binding deglycosylated α-DG, indicating that interaction between DG subunits is mediated via protein-protein interactions with the extracellular domain of β-DG[33].

α-DG is an extensively glycosylated, dumbbell-shaped glycoprotein consisting of two globular domains separated by an extended mucin domain. Extensive glycosylation of the mucin domain is what provides length to α-DG as this domain would collapse onto itself if it were not glycosylated, as it bears no innate secondary protein structure. Furthermore, glycosylation of the mucin domain increases the molecular weight of α-DG significantly, and though the extent of

glycosylation differs developmentally, as well as from tissue to tissue, at least half of the molecular weight of α-DG is due to glycosylation. The molecular weight of α-DG is predicted to be 74 kDa based upon the amino acid sequence, however the molecular weight of α-DG expressed in brain/nerve is 120 kDa[34] and in cardiac muscle is 140 kDa[8,20,35]. In skeletal muscle α-DG glycosylation is dependent upon innervation and myofiber development[36] and its molecular weight can be greater than 200 kDa[8].

α-DG is decorated with three types of glycans: *N*-glycans, mucin *O*-glycans and mannosyl *O*-glycans (Figure 1-1, 1-2). The addition of *N*-glycans can be predicted by the canonical sequon Asn-X-Ser/Thr, where X is any amino acid except proline. The α-DG amino acid sequence contains three canonical *N*-glycosylation sites, two on the C-terminus and one on the N-terminus[37]. Mutating sites of *N*-glycosylation closest to the α/β-DG cleavage site renders the propeptide non-cleavable[31] The extended mucin domain of α-DG contains 25 different sites of *O*-glycosylation in humans[38] and 23 sites in rabbit[39]. Of the 23 *O*-glycosylation sites identified on rabbit α-DG, seven are exclusively modified with mannosyl *O*-glycans, and two sites can be modified with either mannosyl or mucin type glycans[39]. Tran et al. demonstrated that modification of specific serines and threonines with *O*-mannosyl glycans impacts modification of downstream sites with mucin type glycans[40]. Similarly, further modification of mannosyl glycans with GlcNAc by POMGNT2 regulates whether or not mannosyl *O*-glycans are elongated to become M1, M2 or M3 *O*-mannose glycans (Figure 1-3)[41]. This interdependence of glycan type specific modification reinforces the necessity for appropriate and sequential processing of *O*-glycans on α-DG.

As *O*-mannosyl glycans are required for binding of α-DG to laminin, substantial progress has been made in elucidating the specific glycan structures present on α-DG as well as the

enzymes involved in their creation. As mentioned above, three *O*-mannosyl glycan core structures, M1, M2 and M3, have been identified on α-DG (Figure 1-3)[16]. The initial mannose residue of these core structures is added by the Protein *O*-Mannosyltransferase 1/2 (POMT1/2) complex[42]. Subsequent addition of β1,2-linked GlcNAc by Protein *O*-Linked Mannose *N*-Acetylglucosaminyltransferase 1 (POMGNT1) and β1,6-linked GlcNAc by Mannosyl (α1,6)-Glycoprotein β1,6-N-Acetyl-Glucosaminyltransferase (MGAT5b) produces core M1 and core M2 structures respectively[14,43]. Core M3 is created via addition of β1,4 linked GlcNAc to mannose by Protein *O*-Linked Mannose *N*-Acetylglucosaminyltransferase 2 (POMGNT2)[44]. Importantly, POMGNT2 acts as 'gatekeeper' in this process. POMGNT1 is promiscuous for substrates, while POMGNT2 recognizes a defined amino acid sequence, R-X-R-X-X-I-X-X-T(*O*-Man)-P-T, which is conserved, yet only present in vertebrate α-DG. Therefore, POMGNT2, through its amino acid specificity, acts as the gatekeeper for core M3 glycan creation[41]

Core M3 glycans have been of particular interest as they are terminally modified with the glucuronic acid-xylose disaccharide repeat present on α-DG known as matriglycan; matriglycan is the unique glycan that is bound by laminin and laminin globular (LG)-domain containing proteins[3]. Following POMGNT2 activity, β1,3-*N*-Acetylgalactosaminyltransferase 2 (B3GALNT2) addition of β1,3-linked GalNAc to the underlying GlcNAc residue completes the core M3 glycan structrure[45]. Subsequently, Protein *O*-Mannose Kinase (POMK) phosphorylates the 6-position of the mannose creating the phosphotrisaccharide[46]. FKTN and FKRP next act sequentially to add two ribitol-phosphate (RboP) groups. FKTN first transfers RboP to the C3 position of the GalNAc residue on the phosphotrisaccharide with FKRP subsequently adding a second, sequential RboP to the initial RboP[47,48]. In order for LARGE1/2 activity to synthesize matriglycan, this RboP moiety must be 'primed' by Ribitol β-1,2 Xylosyltransferase 1(RXYLT1)

and β1,4-glucuronyltransferase 1 (B4GAT1). RXYLT1 initiates the priming via transfer of xylose to the ribitol moiety created by FKRP/FKTN[49]. Next B4GAT1 adds a β1,4-linked glucuronic acid (GlcA) to the β-Xylose (β-Xyl)[50,51]. Once primed, the xylose and glucuronic acid disaccharide repeat ([-Xyl-α3-GlcA-β3-]$_n$) known as matriglycan is elongated by the bifunctional transferases LARGE1 and/or LARGE2[52-54].

Current and emerging therapies to treat DMD

Loss of dystrophin and subsequent loss of sarcolemmal DGC manifests as multi-organ pathology in boys suffering from DMD. Loss of the DGC directly destabilizes the sarcolemma during exercise and causes contraction-induced muscle damage. Continued muscle damage leads to constant cycling of muscle degeneration and regeneration and results in a chronic immune response and profibrotic milieu within the muscle[55,56]. Loss of the DGC also causes loss of its constituent proteins and their functions from the sarcolemma[8,29]. Specifically, loss of the DGC causes mislocalization of nNOS to the cytoplasm and therefore a loss of sarcolemmal nitric oxide (NO)[57]. Ultimately this loss of sarcolemmal NO results in functional ischemia during exercise, further exacerbating muscle damage in DMD[58,59]. Conversely, in response to loss of the DGC, utrophin and UGC utilization are increased in *mdx* mice and to a lesser extent in patients with DMD[24]. Current and emerging therapies target each aspect of this multifaceted pathophysiology and have generated many promising approaches to treating DMD.

Corticosteroid treatment remains the standard of care for DMD patients. Both prednisone and deflazacort delay cardiomyopathy, delay age of wheelchair use and reduce the need for scoliosis surgery[60-63]. While corticosteroid treatments provide benefits by modulating the immune response, they are not curative as they do not treat the underlying loss of dystrophin.

Recent approval of eteplirsen by the U.S. Food and Drug Administration (FDA) provides patients the first potentially curative therapy for a subset of DMD patients with a specific mutation in exon 51 of the gene encoding dystrophin. Eteplirsen is an antisense oligonucleotide which induces skipping of exon 51 to restore the reading frame of the dystrophin transcript in patients with genetic mutations amenable to the treatment. Restoration of the transcript reading frame leads to expression of a truncated yet functional dystrophin[64,65]. In initial clinical trials, eteplirsen-treated patients have demonstrated increased 6 minute walk distance compared to historical controls following three years of treatment[66].

Research into alternative therapies continues to target other aspects of DMD pathology. Stop-codon read through and genetic editing are two other approaches to restoring dystrophin expression. Treatment with aminoglycosides permits ribosomes to insert alternative amino acids in place of a stop codon, to allow continued translation and production of full length dystrophin[67]. While treatment with the aminoglycoside ataluren increased dystrophin production 11%[68] and decreased decline in walk ability[69], human trials have generated conflicting results[70,71]. Genetic editing of the dystrophin gene via CRISPR/Cas9 technology has shown promising results in mouse models of DMD[72-76] and represents an attractive potential therapy as genetic editing would provide permanent correction of dystrophin gene mutations.

Additional emerging therapies aim to ameliorate the dystrophic phenotype by manipulating innate muscle functions including accelerating muscle repair, increasing muscle blood flow, and modulating expression of utrophin. Myostatin acts as a negative regulator of muscle mass and plays an integral role in skeletal muscle maintenance. Therefore, myostatin inhibition, either via propetides[77] or receptor blockade[78], is actively being investigated as an approach to reduce muscle loss and potentially increase muscle mass in patients with DMD.

Phosphodiesterase-5A (PDE-5A) inhibitors such as tadalafil and sildenafil regulate muscle blood flow by prolonging the half-life of cyclic guanosine monophosphate (cGMP) produced by cytosolic nNOS displaced from the sarcolemma[79]; these compounds have shown promising results in patients with DMD and Becker muscular dystrophy (BMD). As sarcolemmal nNOS, that would be a component of the DGC, is lost in D/BMD due to loss of dystrophin (Figure 1-2), the ability of PDE-5 inhibitors to boost NO-cGMP signal and improve skeletal muscle blood flow can attenuate ischemia-related damage during exercise-induced contraction[80,81]. Another emerging therapeutic target in DMD has been increased expression and utilization of utrophin in UGC at the sarcolemma, as utrophin overexpression was shown to rescue the dystrophic *mdx* phenotype[82]. Ezutromid and SMT022357 are first and second generation utrophin modulators currently in clinical trials. Ezutromid has been found to be well tolerated and to increase utrophin production in both skeletal and cardiac human muscle[83], while SMT022357 increased utrophin production in *mdx* mice[84].

Manipulating α-DG glycosylation to increase utrophin utilization at the sarcolemma is an additional potential therapy for DMD. In rodents, α-DG is known to be differentially glycosylated in a manner that correlates with sarcolemmal localization and protein complex association. Specifically, α-DG associated with the DGC and expressed ubiquitously throughout the sarcolemma preferentially binds the sialic acid and *N*-acteylglucosamine (GlcNAc)-specific plant lectin wheat germ agglutinin (WGA) [8,18,29]. Alternatively, the *N*-acetylgalactosamine (GalNAc)-specific lectin *Wisteria floribunda* agglutinin (WFA) preferentially binds α-DG in the UGC, and has been used historically to identify the UGC at the rodent NMJ/MTJ[85-89]. Interestingly, while WFA reactivity is restricted to the NMJ/MTJ in wildtype mice, reactivity spreads extra-synaptically and correlates with redistribution of the UGC in *mdx* mouse muscle[85].

Martin and colleagues have focused on overexpression of the GalNAc-transferase β1,4-*N*-Acetylgalactosaminyltransferase 2 (B4GALNT2) as a therapeutic approach to increase WFA reactivity of α-DG, utrophin utilization, and amelioration of the dystrophic phenotype[86]. While overexpression of B4GALNT2 has ameliorated the dystrophic phenotype in mouse models of various muscular dystrophies[86,88-90], the exact mechanism by which B4GALNT2 rescues the dystrophic phenotype remains poorly understood[86,91-93]. For example, overexpression of B4GALNT2 was recently reported to ameliorate the dystrophic phenotype in a mouse model for limb-girdle muscular dystrophy (LGMD) type 2i without "substantial glycosylation of α dystroglycan with the [WFA reactive] cytotoxic T cell glycan, or increased expression of dystrophin and laminin α2 surrogates…and may do so via a mechanism that differs from its ability to induce surrogate gene expression"[93].

Furthermore, while there have been descriptions of amelioration of the dystrophic phenotype in mouse models of various muscular dystrophies following B4GALNT2 overexpression, no published research has addressed essential questions regarding the potential use of B4GALNT2 overexpression in humans. Specifically, off target glycosylation of non-endogenous glycans and glycoprotein acceptor substrates is known to occur following overexpression of glycosyltransferases[94], yet, to date, no analysis of off target effects on glycans and/or glycoproteins inadvertently modified by B4GALNT2 overexpression has been published. Furthermore, no published work has evaluated whether or not the extra-synaptic redistribution of WFA reactivity and utrophin localization on *mdx* muscle sections are linked biological processes. Do utrophin and WFA reactivity redistribute extra-synaptically in *mdx* mice lacking B4GALNT2 (*mdx*/B4GALNT2$^{-/-}$)? These critical questions should be explored prior to developing B4GALNT2 overexpression for therapy in humans.

Significance of this work

Before therapies focused on manipulating muscle glycosylation can move forward, disease- and species-specific differences in muscle glycosylation must be better understood. Outside of α-DG glycosylation, muscle glycosylation research has mainly focused on the unique GalNAc-modified glycans present at the rodent NMJ, and the correlation between utrophin localization and modification of α-DG with these glycan structures. Sanes and Cheney were the first to demonstrate that the GalNAc-specific lectin *Dolichos biflorus* agglutinin (DBA) selectively stains the murine NMJ while the high mannose *N*-glycan-specific lectin Concanavalin A (ConA) does not[95]. The rodent NMJ was determined to be uniquely modified with GalNAc-terminated glycans when additional GalNAc-specific lectins such as soybean agglutinin (SBA), *Helix pomatia* agglutinin (HPA), and *Vicia villosa* agglutinin (VVA) selectively stained the NMJ compared to lectins with other specificities (ConA- high mannose *N*-glycans, PNA- *O*-glycans, PHA-L- complex *N*-glycans) [96]. Discovery of this unique GalNAc modification at the rodent NMJ led to research into potential glycosyltransferases responsible for creating the structure[97], as well as the use of WFA to identify differentially glycosylated α-DG[85,86].

While largely overlooked at the time, follow-up work by Scott et al. in 1988 provided evidence of the first species-specific differences between rodent and human muscle glycosylation. Though VVA binding was highly specific for the NMJ on muscle sections from various rodent species, it was not NMJ-specific on human muscle sections[96]. Advances in glycobiology research have continued to highlight species-specific differences in muscle glycosylation. For example, humans lack the ability to create the sugar *N*-glycolylneuraminic acid (NeuGc), a form of sialic acid, due to loss of function mutations in the enzyme cytidine

monophosphate-sialic acid hydrolase (CMAH)[98]. Therefore, humans can only create the sialic acid *N*-acteylneuraminic acid (NeuAc) while mice and all other non-great ape mammals produce both NeuAc and NeuGc. Interestingly, mouse models of DMD and alpha-sarcolgycan null (α-SG$^{-/-}$) LGMD 2d generated to also lack CMAH activity via *cmah* knockdown suffered a more severe dystrophic phenotype, demonstrating that species-specific differences in muscle glycosylation impact dystrophic pathology[99,100].

Furthermore, WFA may not be an appropriate proxy for utrophin in human muscle. Cabrera et al. also sought to utilize WFA binding as a proxy for utrophin utilization when they performed a high throughput screen (HTS) to identify small molecules which increased WFA binding to C2C12 murine myotubes[101]. Following screening of the Prestwick library of ~1200 FDA approved compounds, lobeline, an acetylcholine receptor antagonist, was identified for its ability to increase WFA binding to and abundance of UGC component proteins in C2C12 cells as well as isolated primary wild type and *mdx* cells[101]. While WFA binding increased following treatment of murine myoblasts and myotubes with lobeline, treatment of patient derived fibroblasts that were reprogrammed as inducible, directly reprogrammable myotubes (iDRMs) did not[102]. This highlighted a potential species-specific difference in glycosylation that might confound the use of WFA as a proxy for utrophin in human skeletal muscle.

The aim of this research was to characterize both human and murine muscle glycosylation and quantify differentiation-, disease-, and species-specific differences utilizing a panel of lectins with varying glycan specificities. As described previously, four GalNAc-specific lectins, WFA, VVA, SBA and DBA, have historically been used interchangeably to identify the rodent NMJ. However, while all lectins share a nominal specificity for glycan structures terminated with GalNAc moieties, differences in the glycoproteins and specific glycan types

bound by each lectin in muscle have yet to be identified. The first half of this dissertation project focused on identifying differences in the binding preferences of these four GalNAc-specific lectins to muscle cells and tissues. This work underscores the fact that these four lectins cannot be used interchangeably to identify the NMJ as they bind distinct glycans on distinct glycoproteins. The second half of this dissertation project focused on identifying disease-specific differences in human dystrophic muscle glycosylation and a potential lectin biomarker(s) for the healthy human muscle glycophenotype.

As all historical data evaluating human or mouse muscle glycosylation consisted of qualitative, lectin histochemistry[103-106], this work provided the development of necessary methodology to perform quantitative analysis of mouse and human muscle glycosylation. Novel, quantitative lectin binding assays were developed for 13 lectins and allowed for the rigorous evaluation of differences in glycosylation due to differentiation, disease and species. Initial work in evaluating mouse glycosylation provided the proof of principle for identifying disease-specific differences in human muscle glycosylation on both immortalized and primary human myotubes as well as healthy and dystrophic human muscle sections. Understanding these specific differences in human muscle glycosylation lays the ground work for the development of a HTS to identify small molecules that restore sarcolemmal integrity and healthy muscle glycosylation in dystrophic cells. In total, this project furthers our understanding of mouse and human muscle glycosylation and provides the potential for novel types of therapy for DMD.

Figure 1-1: Mammalian Glycosylation.

N-linked glycans are covalently bound to Asn residues while *O*-linked glycans are covalently linked to Ser or Thr residues on glycoproteins. Glycosphingolipids are glycan structures bound to membrane anchored ceramide moieties. Glycosylphosphatidylinositol (GPI)-linked proteins are anchored to the cell membrane by a glycan covalently linked to the membrane lipid phosphatidylinositol. Glycosaminoglycans are composed of repeating disaccharide units linked to core proteins, to create proteoglycans, or as free chains, such as hyaluronan. In addition, many nuclear/cytoplasmic proteins are modified by *O*-linked *N*-acetylglucosamine (*O*-GlcNAc). The focus of this work is glycan structures present on glycoproteins. Symbols used to represent glycans are in accordance with the guidelines outlined by the Consortium of Functional Glycomics. This is image is reprinted with permission from *The Essentials of Glycobiology*, 3rd Edition, Cold Spring Harbor Laboratory Press.

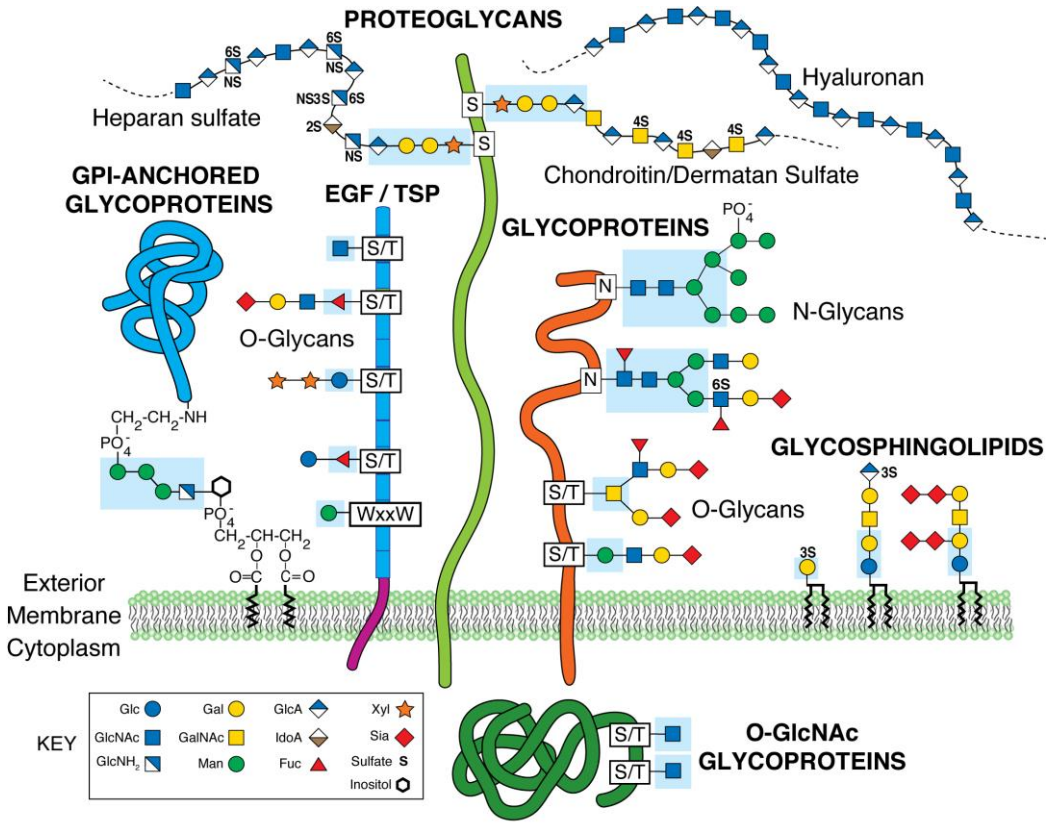

PROTEOGLYCANS
Heparan sulfate
Hyaluronan
Chondroitin/Dermatan Sulfate
GPI-ANCHORED GLYCOPROTEINS
EGF / TSP
GLYCOPROTEINS
N-Glycans
O-Glycans
GLYCOSPHINGOLIPIDS
O-Glycans
Exterior
Membrane
Cytoplasm
KEY
Glc
Gal
GlcA
Xyl
GlcNAc
GalNAc
IdoA
Sia
GlcNH2
Man
Fuc
Sulfate S
Inositol
O-GlcNAc GLYCOPROTEINS

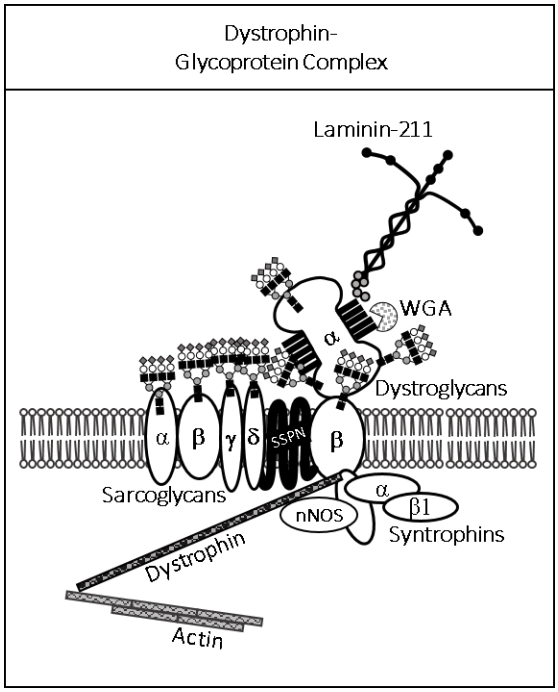
Figure 1-2: Major Sarcolemmal Adhesion Complexes- the dystrophin-glycoprotein complex (DGC), utrophin-glycoprotein complex (UGC) and the α7β1D integrin heterodimer.

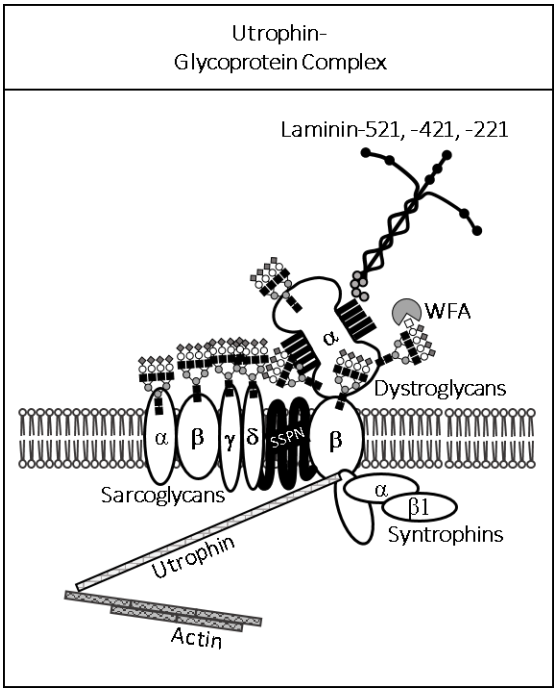
The DGC is a sarcolemmal protein complex which stabilizes muscle by connecting the intracellular actin filaments to the extracellular matrix (ECM). This connection is mediated intracellularly by the protein dystrophin which binds f-actin filaments and the transmembrane protein β-dystroglycan; β-dystroglycan is non-covalently attached to the sarcolemmal receptor α-DG which binds laminin in the ECM via highly extended glycosylaminoglycans

While the DGC is found throughout the sarcolemma, the homologous UGC is expressed at the neuromuscular junction; while most core protein components are the same, two differences exist: 1) dystrophin is replaced by its homologue utrophin and 2) glycosylation of the core protein α-DG is altered. α-DG associated with the DGC at the extra-synaptic sarcolemma preferentially binds the plant lectin wheat germ agglutinin (WGA) while α-DG associated with the UGC at the NMJ preferentially binds the lectin *Wisteria floribunda* agglutinin (WFA).

The α7β1 integrin heterodimer is a transmembrane sarcolemmal receptor for laminin binding that links the ECM to the intracellular cytoskeleton. In addition, the α7β1 integrin heterodimer also plays a significant role in both outside-in and inside-out signaling.

Symbols used to represent glycans are in accordance with the guidelines outlined by the Consortium of Functional Glycomics.


Dystrophin-
Glycoprotein Complex
Laminin-211
WGA
α
Dystroglycans
α
β
γ
δ
SSPN
β
Sarcoglycans
α
β1
nNOS
Syntrophins
Dystrophin
Actin


Utrophin-
Glycoprotein Complex
Laminin-521, -421, -221
WFA
α
Dystroglycans
α
β
γ
δ
SSPN
β
Sarcoglycans
α
β1
Syntrophins
Utrophin
Actin

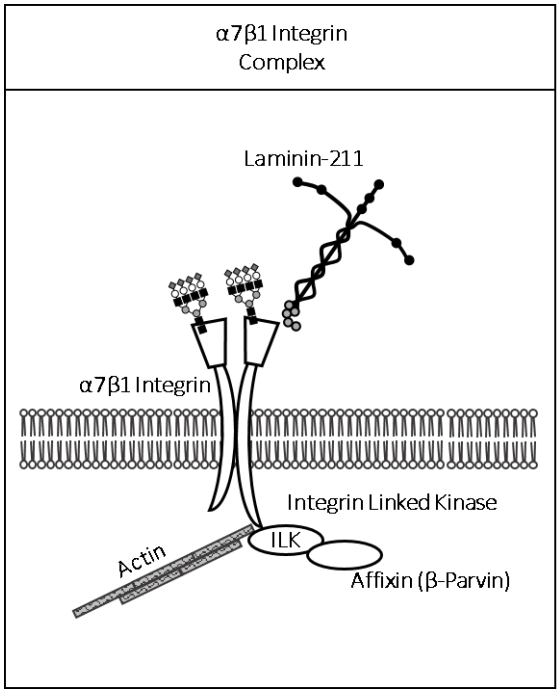
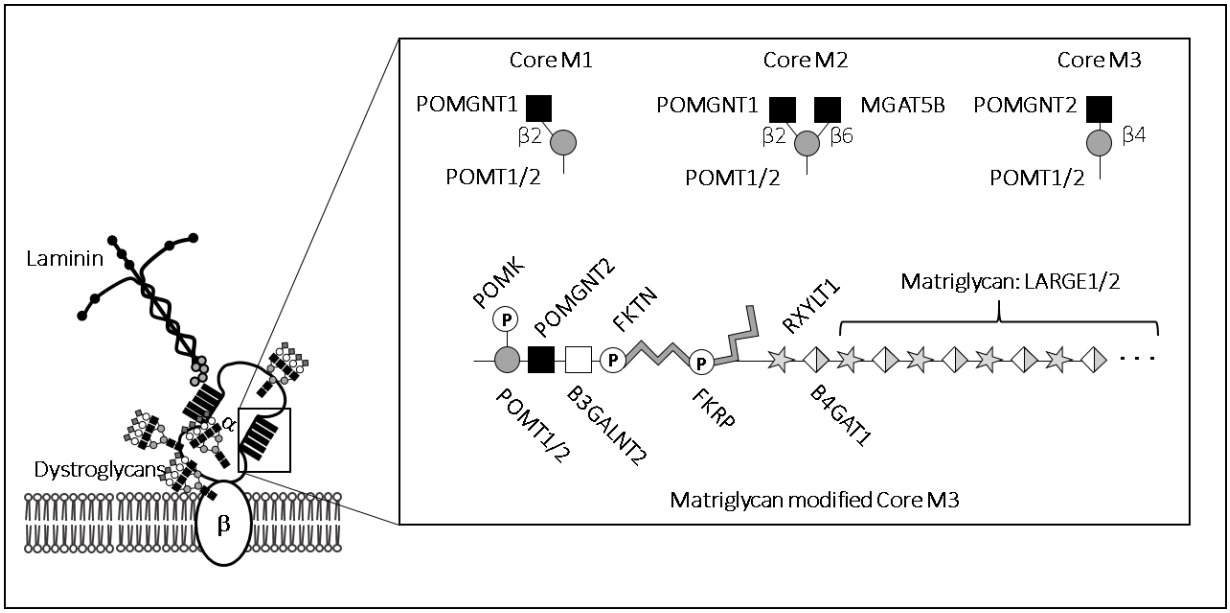

α7β1 Integrin
Complex
Laminin-211
α7β1 Integrin
Integrin Linked Kinase
ILK
Actin
Affixin (β-Parvin)

Figure 1-3: α-DG *O*-mannosylation.

The mucin domain of α-DG can be decorated with three different core mannosyl *O*-glycan structures: core M1, core M2 and core M3. All three core structures can be further elongated, including the addition of matriglycan to the core M3 glycan specifically. Enzymes responsible for synthesis of core structures and the matriglycan-bearing structure are depicted at the site of their activity. Symbols used to represent glycans are in accordance with the guidelines outlined by the Consortium of Functional Glycomics.


Core M1
Core M2
Core M3
POMGNT1
β2
POMT1/2
POMGNT1
MGAT5B
β2
β6
POMT1/2
POMGNT2
β4
POMT1/2
Laminin
α
Dystroglycans
β
POMK
POMGNT2
FKTN
RXYLT1
Matriglycan: LARGE1/2
P
P
P
POMT1/2
B3GALNT2
FKRP
B4GAT1
Matriglycan modified Core M3

References

1 Ioffe, E. & Stanley, P. Mice lacking N-acetylglucosaminyltransferase I activity die at mid-gestation, revealing an essential role for complex or hybrid N-linked carbohydrates. *Proc Natl Acad Sci U S A* **91**, 728-732 (1994).

2 Hara, Y. *et al.* Like-acetylglucosaminyltransferase (LARGE)-dependent modification of dystroglycan at Thr-317/319 is required for laminin binding and arenavirus infection. *Proc Natl Acad Sci U S A* **108**, 17426-17431, doi:10.1073/pnas.1114836108 (2011).

3 Yoshida-Moriguchi, T. & Campbell, K. P. Matriglycan: a novel polysaccharide that links dystroglycan to the basement membrane. *Glycobiology* **25**, 702-713, doi:10.1093/glycob/cwv021 (2015).

4 Rabinovich, G. A. & Vidal, M. Galectins and microenvironmental niches during hematopoiesis. *Curr Opin Hematol* **18**, 443-451, doi:10.1097/MOH.0b013e32834bab18 (2011).

5 Helenius, A. & Aebi, M. Intracellular functions of N-linked glycans. *Science* **291**, 2364-2369 (2001).

6 Grigorian, A., Torossian, S. & Demetriou, M. T-cell growth, cell surface organization, and the galectin-glycoprotein lattice. *Immunol Rev* **230**, 232-246, doi:10.1111/j.1600-065X.2009.00796.x (2009).

7 Ervasti, J. M., Burwell, A. L. & Geissler, A. L. Tissue-specific heterogeneity in alpha-dystroglycan sialoglycosylation. Skeletal muscle alpha-dystroglycan is a latent receptor for Vicia villosa agglutinin b4 masked by sialic acid modification. *J Biol Chem* **272**, 22315-22321 (1997).

8 Ervasti, J. M. & Campbell, K. P. A role for the dystrophin-glycoprotein complex as a transmembrane linker between laminin and actin. *J Cell Biol* **122**, 809-823 (1993).

9 McDearmon, E. L., Combs, A. C. & Ervasti, J. M. Differential Vicia villosa agglutinin reactivity identifies three distinct dystroglycan complexes in skeletal muscle. *J Biol Chem* **276**, 35078-35086, doi:10.1074/jbc.M103843200 (2001).

10 Gundry, R. L. *et al.* The mouse C2C12 myoblast cell surface N-linked glycoproteome: identification, glycosite occupancy, and membrane orientation. *Mol Cell Proteomics* **8**, 2555-2569, doi:10.1074/mcp.M900195-MCP200 (2009).

11 Smalheiser, N. R. & Schwartz, N. B. Cranin: a laminin-binding protein of cell membranes. *Proc Natl Acad Sci U S A* **84**, 6457-6461 (1987).

12 Claudepierre, T. *et al.* Characterization of the intermolecular associations of the dystrophin-associated glycoprotein complex in retinal Müller glial cells. *J Cell Sci* **113 Pt 19**, 3409-3417 (2000).

13 Beltrán-Valero de Bernabé, D. *et al.* Mutations in the O-mannosyltransferase gene POMT1 give rise to the severe neuronal migration disorder Walker-Warburg syndrome. *Am J Hum Genet* **71**, 1033-1043, doi:10.1086/342975 (2002).

14 Yoshida, A. *et al.* Muscular dystrophy and neuronal migration disorder caused by mutations in a glycosyltransferase, POMGnT1. *Dev Cell* **1**, 717-724 (2001).

15 Kobayashi, K. *et al.* An ancient retrotransposal insertion causes Fukuyama-type congenital muscular dystrophy. *Nature* **394**, 388-392, doi:10.1038/28653 (1998).

16 Praissman, J. L. & Wells, L. Mammalian O-mannosylation pathway: glycan structures, enzymes, and protein substrates. *Biochemistry* **53**, 3066-3078, doi:10.1021/bi500153y (2014).

17 Ervasti, J. M., Ohlendieck, K., Kahl, S. D., Gaver, M. G. & Campbell, K. P. Deficiency of a glycoprotein component of the dystrophin complex in dystrophic muscle. *Nature* **345**, 315-319, doi:10.1038/345315a0 (1990).

18 Ervasti, J. M., Kahl, S. D. & Campbell, K. P. Purification of dystrophin from skeletal muscle. *J Biol Chem* **266**, 9161-9165 (1991).

19 Bowe, M. A., Deyst, K. A., Leszyk, J. D. & Fallon, J. R. Identification and purification of an agrin receptor from Torpedo postsynaptic membranes: a heteromeric complex related to the dystroglycans. *Neuron* **12**, 1173-1180 (1994).

20 Ibraghimov-Beskrovnaya, O. *et al.* Primary structure of dystrophin-associated glycoproteins linking dystrophin to the extracellular matrix. *Nature* **355**, 696-702, doi:10.1038/355696a0 (1992).

21 Yoshida, M. & Ozawa, E. Glycoprotein complex anchoring dystrophin to sarcolemma. *J Biochem* **108**, 748-752 (1990).

22 Ohlendieck, K., Ervasti, J. M., Snook, J. B. & Campbell, K. P. Dystrophin-glycoprotein complex is highly enriched in isolated skeletal muscle sarcolemma. *J Cell Biol* **112**, 135-148 (1991).

23 Ohlendieck, K. *et al.* Dystrophin-related protein is localized to neuromuscular junctions of adult skeletal muscle. *Neuron* **7**, 499-508 (1991).

24 Marshall, J. L., Kwok, Y., McMorran, B. J., Baum, L. G. & Crosbie-Watson, R. H. The potential of sarcospan in adhesion complex replacement therapeutics for the treatment of muscular dystrophy. *FEBS J* **280**, 4210-4229, doi:10.1111/febs.12295 (2013).

25 Marshall, J. L. *et al.* Dystrophin and utrophin expression require sarcospan: loss of α7 integrin exacerbates a newly discovered muscle phenotype in sarcospan-null mice. *Hum Mol Genet* **21**, 4378-4393, doi:10.1093/hmg/dds271 (2012).

26 Marshall, J. L. *et al.* Sarcospan integration into laminin-binding adhesion complexes that ameliorate muscular dystrophy requires utrophin and α7 integrin. *Hum Mol Genet* **24**, 2011-2022, doi:10.1093/hmg/ddu615 (2015).

27 Marshall, J. L. & Crosbie-Watson, R. H. Sarcospan: a small protein with large potential for Duchenne muscular dystrophy. *Skelet Muscle* **3**, 1, doi:10.1186/2044-5040-3-1 (2013).

28 Campbell, K. P. & Kahl, S. D. Association of dystrophin and an integral membrane glycoprotein. *Nature* **338**, 259-262, doi:10.1038/338259a0 (1989).

29 Ervasti, J. M. & Campbell, K. P. Membrane organization of the dystrophin-glycoprotein complex. *Cell* **66**, 1121-1131 (1991).

30 Deyst, K. A., Bowe, M. A., Leszyk, J. D. & Fallon, J. R. The alpha-dystroglycan-beta-dystroglycan complex. Membrane organization and relationship to an agrin receptor. *J Biol Chem* **270**, 25956-25959 (1995).

31 Esapa, C. T., Bentham, G. R., Schröder, J. E., Kröger, S. & Blake, D. J. The effects of post-translational processing on dystroglycan synthesis and trafficking. *FEBS Lett* **555**, 209-216 (2003).

32 Jayasinha, V. *et al.* Inhibition of dystroglycan cleavage causes muscular dystrophy in transgenic mice. *Neuromuscul Disord* **13**, 365-375 (2003).

33 Di Stasio, E. *et al.* Structural and functional analysis of the N-terminal extracellular region of beta-dystroglycan. *Biochem Biophys Res Commun* **266**, 274-278, doi:10.1006/bbrc.1999.1803 (1999).

34 Gee, S. H. *et al.* Laminin-binding protein 120 from brain is closely related to the dystrophin-associated glycoprotein, dystroglycan, and binds with high affinity to the major heparin binding domain of laminin. *J Biol Chem* **268**, 14972-14980 (1993).

35 Klietsch, R., Ervasti, J. M., Arnold, W., Campbell, K. P. & Jorgensen, A. O. Dystrophin-glycoprotein complex and laminin colocalize to the sarcolemma and transverse tubules of cardiac muscle. *Circ Res* **72**, 349-360 (1993).

36 Leschziner, A. *et al.* Neural regulation of alpha-dystroglycan biosynthesis and glycosylation in skeletal muscle. *J Neurochem* **74**, 70-80 (2000).

37 Saito, F., Saito-Arai, Y., Nakamura, A., Shimizu, T. & Matsumura, K. Processing and secretion of the N-terminal domain of alpha-dystroglycan in cell culture media. *FEBS Lett* **582**, 439-444, doi:10.1016/j.febslet.2008.01.006 (2008).

38 Nilsson, J., Larson, G. & Grahn, A. Characterization of site-specific O-glycan structures within the mucin-like domain of alpha-dystroglycan from human skeletal muscle. *Glycobiology* **20**, 1160-1169, doi:10.1093/glycob/cwq082 (2010).

39 Stalnaker, S. H. *et al.* Site mapping and characterization of O-glycan structures on alpha-dystroglycan isolated from rabbit skeletal muscle. *J Biol Chem* **285**, 24882-24891, doi:10.1074/jbc.M110.126474 (2010).

40 Tran, D. T. *et al.* Glycosylation of α-dystroglycan: O-mannosylation influences the subsequent addition of GalNAc by UDP-GalNAc polypeptide N-

acetylgalactosaminyltransferases. *J Biol Chem* **287**, 20967-20974, doi:10.1074/jbc.M112.370387 (2012).

41 Halmo, S. M. *et al.* Protein O-Linked Mannose β-1,4-N-Acetylglucosaminyl-transferase 2 (POMGNT2) Is a Gatekeeper Enzyme for Functional Glycosylation of α-Dystroglycan. *J Biol Chem* **292**, 2101-2109, doi:10.1074/jbc.M116.764712 (2017).

42 Manya, H. *et al.* Demonstration of mammalian protein O-mannosyltransferase activity: coexpression of POMT1 and POMT2 required for enzymatic activity. *Proc Natl Acad Sci U S A* **101**, 500-505, doi:10.1073/pnas.0307228101 (2004).

43 Lee, J. K. *et al.* Developmental expression of the neuron-specific N-acetylglucosaminyltransferase Vb (GnT-Vb/IX) and identification of its in vivo glycan products in comparison with those of its paralog, GnT-V. *J Biol Chem* **287**, 28526-28536, doi:10.1074/jbc.M112.367565 (2012).

44 Ogawa, M. *et al.* GTDC2 modifies O-mannosylated α-dystroglycan in the endoplasmic reticulum to generate N-acetyl glucosamine epitopes reactive with CTD110.6 antibody. *Biochem Biophys Res Commun* **440**, 88-93, doi:10.1016/j.bbrc.2013.09.022 (2013).

45 Stevens, E. *et al.* Mutations in B3GALNT2 cause congenital muscular dystrophy and hypoglycosylation of α-dystroglycan. *Am J Hum Genet* **92**, 354-365, doi:10.1016/j.ajhg.2013.01.016 (2013).

46 Yoshida-Moriguchi, T. *et al.* SGK196 is a glycosylation-specific O-mannose kinase required for dystroglycan function. *Science* **341**, 896-899, doi:10.1126/science.1239951 (2013).

47 Kanagawa, M. *et al.* Identification of a Post-translational Modification with Ribitol-Phosphate and Its Defect in Muscular Dystrophy. *Cell Rep* **14**, 2209-2223, doi:10.1016/j.celrep.2016.02.017 (2016).

48 Gerin, I. *et al.* ISPD produces CDP-ribitol used by FKTN and FKRP to transfer ribitol phosphate onto α-dystroglycan. *Nat Commun* **7**, 11534, doi:10.1038/ncomms11534 (2016).

49 Manya, H. *et al.* The Muscular Dystrophy Gene TMEM5 Encodes a Ribitol β1,4-Xylosyltransferase Required for the Functional Glycosylation of Dystroglycan. *J Biol Chem* **291**, 24618-24627, doi:10.1074/jbc.M116.751917 (2016).

50 Praissman, J. L. *et al.* B4GAT1 is the priming enzyme for the LARGE-dependent functional glycosylation of α-dystroglycan. *Elife* **3**, doi:10.7554/eLife.03943 (2014).

51 Willer, T. *et al.* The glucuronyltransferase B4GAT1 is required for initiation of LARGE-mediated α-dystroglycan functional glycosylation. *Elife* **3**, doi:10.7554/eLife.03941 (2014).

52 Inamori, K. *et al.* Dystroglycan function requires xylosyl- and glucuronyltransferase activities of LARGE. *Science* **335**, 93-96, doi:10.1126/science.1214115 (2012).

53 Inamori, K. *et al.* Xylosyl- and glucuronyltransferase functions of LARGE in α-dystroglycan modification are conserved in LARGE2. *Glycobiology* **23**, 295-302, doi:10.1093/glycob/cws152 (2013).

54 Ashikov, A., Buettner, F. F., Tiemann, B., Gerardy-Schahn, R. & Bakker, H. LARGE2 generates the same xylose- and glucuronic acid-containing glycan structures as LARGE. *Glycobiology* **23**, 303-309, doi:10.1093/glycob/cws153 (2013).

55 Vetrone, S. A. *et al.* Osteopontin promotes fibrosis in dystrophic mouse muscle by modulating immune cell subsets and intramuscular TGF-beta. *J Clin Invest* **119**, 1583-1594, doi:10.1172/JCI37662 (2009).

56 Heydemann, A. *et al.* Latent TGF-beta-binding protein 4 modifies muscular dystrophy in mice. *J Clin Invest* **119**, 3703-3712, doi:10.1172/JCI39845 (2009).

57 Brenman, J. E., Chao, D. S., Xia, H., Aldape, K. & Bredt, D. S. Nitric oxide synthase complexed with dystrophin and absent from skeletal muscle sarcolemma in Duchenne muscular dystrophy. *Cell* **82**, 743-752 (1995).

58 Thomas, G. D. *et al.* Impaired metabolic modulation of alpha-adrenergic vasoconstriction in dystrophin-deficient skeletal muscle. *Proc Natl Acad Sci U S A* **95**, 15090-15095 (1998).

59 Thomas, G. D. & Victor, R. G. Nitric oxide mediates contraction-induced attenuation of sympathetic vasoconstriction in rat skeletal muscle. *J Physiol* **506 (Pt 3)**, 817-826 (1998).

60 Gloss, D., Moxley, R. T., Ashwal, S. & Oskoui, M. Practice guideline update summary: Corticosteroid treatment of Duchenne muscular dystrophy: Report of the Guideline Development Subcommittee of the American Academy of Neurology. *Neurology* **86**, 465-472, doi:10.1212/WNL.0000000000002337 (2016).

61 Biggar, W. D., Harris, V. A., Eliasoph, L. & Alman, B. Long-term benefits of deflazacort treatment for boys with Duchenne muscular dystrophy in their second decade. *Neuromuscul Disord* **16**, 249-255, doi:10.1016/j.nmd.2006.01.010 (2006).

62 Lebel, D. E., Corston, J. A., McAdam, L. C., Biggar, W. D. & Alman, B. A. Glucocorticoid treatment for the prevention of scoliosis in children with Duchenne

muscular dystrophy: long-term follow-up. *J Bone Joint Surg Am* **95**, 1057-1061, doi:10.2106/JBJS.L.01577 (2013).

63 Schram, G. *et al.* All-cause mortality and cardiovascular outcomes with prophylactic steroid therapy in Duchenne muscular dystrophy. *J Am Coll Cardiol* **61**, 948-954, doi:10.1016/j.jacc.2012.12.008 (2013).

64 Mann, C. J. *et al.* Antisense-induced exon skipping and synthesis of dystrophin in the mdx mouse. *Proc Natl Acad Sci U S A* **98**, 42-47, doi:10.1073/pnas.011408598 (2001).

65 Lu, Q. L. *et al.* Functional amounts of dystrophin produced by skipping the mutated exon in the mdx dystrophic mouse. *Nat Med* **9**, 1009-1014, doi:10.1038/nm897 (2003).

66 Mendell, J. R. *et al.* Longitudinal effect of eteplirsen versus historical control on ambulation in Duchenne muscular dystrophy. *Ann Neurol* **79**, 257-271, doi:10.1002/ana.24555 (2016).

67 Barton-Davis, E. R., Cordier, L., Shoturma, D. I., Leland, S. E. & Sweeney, H. L. Aminoglycoside antibiotics restore dystrophin function to skeletal muscles of mdx mice. *J Clin Invest* **104**, 375-381, doi:10.1172/JCI7866 (1999).

68 Finkel, R. S. *et al.* Phase 2a study of ataluren-mediated dystrophin production in patients with nonsense mutation Duchenne muscular dystrophy. *PLoS One* **8**, e81302, doi:10.1371/journal.pone.0081302 (2013).

69 Bushby, K. *et al.* Ataluren treatment of patients with nonsense mutation dystrophinopathy. *Muscle Nerve* **50**, 477-487, doi:10.1002/mus.24332 (2014).

70 Wagner, K. R. *et al.* Gentamicin treatment of Duchenne and Becker muscular dystrophy due to nonsense mutations. *Ann Neurol* **49**, 706-711 (2001).

71 Malik, V. *et al.* Gentamicin-induced readthrough of stop codons in Duchenne muscular dystrophy. *Ann Neurol* **67**, 771-780, doi:10.1002/ana.22024 (2010).

72 Long, C. *et al.* Postnatal genome editing partially restores dystrophin expression in a mouse model of muscular dystrophy. *Science* **351**, 400-403, doi:10.1126/science.aad5725 (2016).

73 Nelson, C. E. *et al.* In vivo genome editing improves muscle function in a mouse model of Duchenne muscular dystrophy. *Science* **351**, 403-407, doi:10.1126/science.aad5143 (2016).

74 Tabebordbar, M. *et al.* In vivo gene editing in dystrophic mouse muscle and muscle stem cells. *Science* **351**, 407-411, doi:10.1126/science.aad5177 (2016).

75 Young, C. S. *et al.* A Single CRISPR-Cas9 Deletion Strategy that Targets the Majority of DMD Patients Restores Dystrophin Function in hiPSC-Derived Muscle Cells. *Cell Stem Cell* **18**, 533-540, doi:10.1016/j.stem.2016.01.021 (2016).

76 Bengtsson, N. E. *et al.* Muscle-specific CRISPR/Cas9 dystrophin gene editing ameliorates pathophysiology in a mouse model for Duchenne muscular dystrophy. *Nat Commun* **8**, 14454, doi:10.1038/ncomms14454 (2017).

77 Bogdanovich, S., Perkins, K. J., Krag, T. O., Whittemore, L. A. & Khurana, T. S. Myostatin propeptide-mediated amelioration of dystrophic pathophysiology. *FASEB J* **19**, 543-549, doi:10.1096/fj.04-2796com (2005).

78 Béchir, N. *et al.* ActRIIB blockade increases force-generating capacity and preserves energy supply in exercising mdx mouse muscle in vivo. *FASEB J* **30**, 3551-3562, doi:10.1096/fj.201600271RR (2016).

79 Thomas, G. D. Functional muscle ischemia in Duchenne and Becker muscular dystrophy. *Front Physiol* **4**, 381, doi:10.3389/fphys.2013.00381 (2013).

80 Nelson, M. D. *et al.* PDE5 inhibition alleviates functional muscle ischemia in boys with Duchenne muscular dystrophy. *Neurology* **82**, 2085-2091, doi:10.1212/WNL.0000000000000498 (2014).

81 Martin, E. A. *et al.* Tadalafil alleviates muscle ischemia in patients with Becker muscular dystrophy. *Sci Transl Med* **4**, 162ra155, doi:10.1126/scitranslmed.3004327 (2012).

82 Tinsley, J. *et al.* Expression of full-length utrophin prevents muscular dystrophy in mdx mice. *Nat Med* **4**, 1441-1444, doi:10.1038/4033 (1998).

83 Ricotti, V. *et al.* Safety, Tolerability, and Pharmacokinetics of SMT C1100, a 2-Arylbenzoxazole Utrophin Modulator, following Single- and Multiple-Dose Administration to Pediatric Patients with Duchenne Muscular Dystrophy. *PLoS One* **11**, e0152840, doi:10.1371/journal.pone.0152840 (2016).

84 Guiraud, S. *et al.* Second-generation compound for the modulation of utrophin in the therapy of DMD. *Hum Mol Genet* **24**, 4212-4224, doi:10.1093/hmg/ddv154 (2015).

85 Marshall, J. L. *et al.* Sarcospan-dependent Akt activation is required for utrophin expression and muscle regeneration. *J Cell Biol* **197**, 1009-1027, doi:10.1083/jcb.201110032 (2012).

86 Nguyen, H. H., Jayasinha, V., Xia, B., Hoyte, K. & Martin, P. T. Overexpression of the cytotoxic T cell GalNAc transferase in skeletal muscle inhibits muscular dystrophy in mdx mice. *Proc Natl Acad Sci U S A* **99**, 5616-5621, doi:10.1073/pnas.082613599 (2002).

87 Xia, B. *et al.* Overexpression of the CT GalNAc transferase in skeletal muscle alters myofiber growth, neuromuscular structure, and laminin expression. *Dev Biol* **242**, 58-73, doi:10.1006/dbio.2001.0530 (2002).

88 Xu, R., Chandrasekharan, K., Yoon, J. H., Camboni, M. & Martin, P. T. Overexpression of the cytotoxic T cell (CT) carbohydrate inhibits muscular dystrophy in the dyW mouse model of congenital muscular dystrophy 1A. *Am J Pathol* **171**, 181-199, doi:10.2353/ajpath.2007.060927 (2007).

89 Xu, R., DeVries, S., Camboni, M. & Martin, P. T. Overexpression of Galgt2 reduces dystrophic pathology in the skeletal muscles of alpha sarcoglycan-deficient mice. *Am J Pathol* **175**, 235-247, doi:10.2353/ajpath.2009.080967 (2009).

90 Jayasinha, V., Hoyte, K., Xia, B. & Martin, P. T. Overexpression of the CT GalNAc transferase inhibits muscular dystrophy in a cleavage-resistant dystroglycan mutant mouse. *Biochem Biophys Res Commun* **302**, 831-836 (2003).

91 Xu, R., Camboni, M. & Martin, P. T. Postnatal overexpression of the CT GalNAc transferase inhibits muscular dystrophy in mdx mice without altering muscle growth or neuromuscular development: evidence for a utrophin-independent mechanism. *Neuromuscul Disord* **17**, 209-220, doi:10.1016/j.nmd.2006.12.004 (2007).

92 Yoon, J. H. *et al.* The synaptic CT carbohydrate modulates binding and expression of extracellular matrix proteins in skeletal muscle: Partial dependence on utrophin. *Mol Cell Neurosci* **41**, 448-463, doi:10.1016/j.mcn.2009.04.013 (2009).

93 Thomas, P. J., Xu, R. & Martin, P. T. B4GALNT2 (GALGT2) Gene Therapy Reduces Skeletal Muscle Pathology in the FKRP P448L Mouse Model of Limb Girdle Muscular Dystrophy 2I. *Am J Pathol* **186**, 2429-2448, doi:10.1016/j.ajpath.2016.05.021 (2016).

94 Patnaik, S. K. & Stanley, P. Mouse large can modify complex N- and mucin O-glycans on alpha-dystroglycan to induce laminin binding. *J Biol Chem* **280**, 20851-20859, doi:10.1074/jbc.M500069200 (2005).

95 Sanes, J. R. & Cheney, J. M. Lectin binding reveals a synapse-specific carbohydrate in skeletal muscle. *Nature* **300**, 646-647 (1982).

96 Scott, L. J., Bacou, F. & Sanes, J. R. A synapse-specific carbohydrate at the neuromuscular junction: association with both acetylcholinesterase and a glycolipid. *J Neurosci* **8**, 932-944 (1988).

97 Martin, P. T., Scott, L. J., Porter, B. E. & Sanes, J. R. Distinct structures and functions of related pre- and postsynaptic carbohydrates at the mammalian neuromuscular junction. *Mol Cell Neurosci* **13**, 105-118, doi:10.1006/mcne.1999.0737 (1999).

98 Chou, H. H. *et al.* A mutation in human CMP-sialic acid hydroxylase occurred after the Homo-Pan divergence. *Proc Natl Acad Sci U S A* **95**, 11751-11756 (1998).

99 Chandrasekharan, K. *et al.* A human-specific deletion in mouse Cmah increases disease severity in the mdx model of Duchenne muscular dystrophy. *Sci Transl Med* **2**, 42ra54, doi:10.1126/scitranslmed.3000692 (2010).

100 Martin, P. T. *et al.* N-Glycolylneuraminic acid deficiency worsens cardiac and skeletal muscle pathophysiology in α-sarcoglycan-deficient mice. *Glycobiology* **23**, 833-843, doi:10.1093/glycob/cwt020 (2013).

101 Cabrera, P. V. *et al.* High throughput screening for compounds that alter muscle cell glycosylation identifies new role for N-glycans in regulating sarcolemmal protein abundance and laminin binding. *J Biol Chem* **287**, 22759-22770, doi:10.1074/jbc.M111.334581 (2012).

102 Cabrera, P. V. *et al.* Haploinsufficiency of C2GnT-I glycosyltransferase renders T lymphoma cells resistant to cell death. *Blood* **108**, 2399-2406, doi:10.1182/blood-2006-04-018556 (2006).

103 Dunn, M. J., Sewry, C. A. & Dubowitz, V. Cytochemical studies of lectin binding by diseased human muscle. *J Neurol Sci* **55**, 147-159 (1982).

104 Capaldi, M. J., Dunn, M. J., Sewry, C. A. & Dubowitz, V. Altered binding of Ricinus communis I lectin by muscle membranes in Duchenne muscular dystrophy. *J Neurol Sci* **63**, 129-141 (1984).

105 Capaldi, M. J., Dunn, M. J., Sewry, C. A. & Dubowitz, V. Binding of Ricinus communis I lectin to the muscle cell plasma membrane in diseased muscle. *J Neurol Sci* **64**, 315-324 (1984).

106 Capaldi, M. J., Dunn, M. J., Sewry, C. A. & Dubowitz, V. Lectin binding in human skeletal muscle: a comparison of 15 different lectins. *Histochem J* **17**, 81-92 (1985).

CHAPTER TWO

The potential of sarcospan in adhesion complex replacement therapeutics for the treatment of muscular dystrophy

This chapter is reprinted from *FEBS Journal* 280 (2013) 4210-4229, with copyright permission from Wiley Online.

the FEBS Journal
REVIEW ARTICLE

The potential of sarcospan in adhesion complex replacement therapeutics for the treatment of muscular dystrophy

Jamie L. Marshall[1,2], Yukwah Kwok[1,2], Brian J. McMorran[2,3], Linda G. Baum[2,3,4] and Rachelle H. Crosbie-Watson[1,2,4,5]

1 Department of Integrative Biology and Physiology, University of California, Los Angeles, CA, USA
2 Center for Duchenne Muscular Dystrophy, University of California, Los Angeles, CA, USA
3 Department of Pathology and Laboratory Medicine, University of California, Los Angeles, CA, USA
4 Molecular Biology Institute, University of California, Los Angeles, CA, USA
5 Department of Neurology, University of California, Los Angeles, CA, USA

Keywords
Duchenne; dystrophin; integrin; laminin-binding; *mdx*; muscle; muscular dystrophy; sarcolemma; sarcospan; utrophin

Correspondence
R. H. Crosbie-Watson, Department of Integrative Biology and Physiology, University of California Los Angeles, 610 Charles E. Young Drive East, Terasaki Life Sciences Building Room 1121, Los Angeles, CA 90095, USA
Fax: +1 310 206 3987
Tel: +1 310 794 2103
E-mail: rcrosbie@physci.ucla.edu

(Received 13 March 2013, accepted 12 April 2013)

doi:10.1111/febs.12295

Three adhesion complexes span the sarcolemma and facilitate critical connections between the extracellular matrix and the actin cytoskeleton: the dystrophin– and utrophin–glycoprotein complexes and α7β1 integrin. Loss of individual protein components results in a loss of the entire protein complex and muscular dystrophy. Muscular dystrophy is a progressive, lethal wasting disease characterized by repetitive cycles of myofiber degeneration and regeneration. Protein-replacement therapy offers a promising approach for the treatment of muscular dystrophy. Recently, we demonstrated that sarcospan facilitates protein–protein interactions amongst the adhesion complexes and is an important potential therapeutic target. Here, we review current protein-replacement strategies, discuss the potential benefits of sarcospan expression, and identify important experiments that must be addressed for sarcospan to move to the clinic.

Introduction

Duchenne muscular dystrophy (DMD) is a progressive muscle-wasting disease caused by mutations in the dystrophin gene leading to a loss of the dystrophin–glycoprotein complex (DGC) at the sarcolemma [1]. DMD occurs in ~ 1 in 3500 male children, leading to respiratory or cardiac failure in the second decade of life. In 1986, the gene encoding dystrophin was identified, and mutations in the *dystrophin* gene were determined to

Abbreviations
MDC1A, merosin-deficient congenital muscular dystrophy 1A; AAV, adeno-associated virus; CMD, congenital muscular dystrophy; DG, dystroglycan; DGC, dystrophin-glycoprotein complex; DMD, Duchenne muscular dystrophy; ECM, extracellular matrix; ER, endoplasmic reticulum; FKRP, fukutin-related protein; GTDC2, glycosyltransferase-like domain containing; Hsp, heat shock protein; ILK, integrin-linked kinase; ISPD, isoprenoid synthase domain containing; LARGE, like-acetylglucosaminyltransferase; MTJ, myotendinous junction; NMJ, neuromuscular junction; nNOS, neuronal nitric oxide synthase; POMGnT1, protein O-linked mannose β-1,2-acetylglucosaminyltransferase; POMT, protein O-mannosyl transferase; SG, sarcoglycan; SSPN, sarcospan; TMEM5, transmembrane protein 5; UGC, utrophin-glycoprotein complex; WFA, *Wisteria floribunda* agglutinin.

be responsible for DMD [2,3]. Although dystrophin was identified over 25 years ago, there is still no cure for the disease [2]. The N-terminus of dystrophin binds directly to F-actin in the cytoplasm of the myofiber and the C-terminus of dystrophin is associated with a group of proteins including neuronal nitric oxide synthase (nNOS), α-syntrophin, α-dystrobrevin and β-dystroglycan (DG) [4,5]. Dystrobrevin binds to the intermediate filament protein syncoilin, which provides a connection between desmin and the DGC that is thought to be important for maintaining mechanical strength and structural organization necessary for muscle contractions [6]. nNOS requires binding to both dystrophin and syntrophin for sarcolemmal localization and produces nitric oxide, which stimulates the blood flow necessary to meet the metabolic demands of healthy muscle [7–11]. The DGC functions to stabilize the sarcolemma during muscle contractions by providing a critical connection between the extracellular matrix (ECM) and the intracellular actin cytoskeleton [12]. α-DG, a peripheral membrane protein, provides the connection between the transmembrane β-DG and laminin-211 in the ECM [13,14]. The central mucin domain of α-DG is heavily glycosylated and the extent of the glycosylation determines the affinity of DGC attachment to the ECM [5,13–18]. The sarcoglycan–sarcospan (SG–SSPN) subcomplex stabilizes α-DG's association with β-DG at the cell surface [19–21]. Loss of the DGC in DMD renders the sarcolemma susceptible to membrane ruptures, which initiates the cycles of myofiber degeneration and regeneration characteristic of DMD [1,12,15,22].

Many forms of muscular dystrophy result from a loss of muscle cell attachment to its surrounding ECM. In addition to the DGC, two adhesion complexes span the sarcolemma and facilitate this connection: the utrophin–glycoprotein complex (UGC) and α7β1 integrin. The UGC is homologous to the DGC, where utrophin replaces dystrophin [23,24]. α7β1 integrin is the main heterodimeric integrin expressed in adult skeletal muscle [25–27]. Mutations in genes encoding the protein components of the DGC/UGC, α7β1 integrin and ECM cause various forms of muscular dystrophy, which are classified based on the severity of disease and the muscle groups predominantly affected. Autosomal recessive limb-girdle muscular dystrophies encompass a wide array of genetic disorders and disease onset typically occurs between 10 and 30 years of age. Mutations in α-, β-, γ- and δ-SG and mutations in glycosyltransferases, resulting in the hypoglycosylation of α-DG cause autosomal recessive limb-girdle muscular dystrophies subtypes 2C-2F, 2K and 2N–2O respectively [28–37]. Congenital muscular dystrophies (CMDs) are an autosomal recessive disease characterized by severe muscular dystrophy with onset occurring within the first year of life. Various forms of CMD are also caused by hypoglycosylation of α-DG due to mutations in glycosyltransferases as well as mutations in laminin α2, collagen 6 and α7 integrin [38–42]. Notably, patient mutations in SSPN and β1D integrin have not been identified [43–45].

There are many strategies currently being investigated for the treatment of muscular dystrophy. Several therapeutic approaches focus on adenoviral delivery of gene replacement therapy or exon skipping to produce a shortened, but functional dystrophin protein. This review focuses on therapeutic strategies to replace the DGC with compensatory adhesion complexes, UGC and α7β1 integrin. In particular, this review discusses the potential of SSPN as a therapeutic target to upregulate both the UGC and α7β1 integrin. SSPN is a tetraspanin-like protein that was discovered as a core component of the DGC [46]. Although SSPN has been shown to ameliorate the pathology of the *mdx* mouse model of DMD [47,48], many questions remain to be answered before SSPN-related therapies are suitable for patients.

Restoring myofiber function with compensatory adhesion complexes

The adhesion complexes responsible for stabilizing the myofiber membrane have distinct biochemical and functional properties, including sarcolemmal localization and ECM/actin connections in normal muscle. In muscle, the DGC is the most widely expressed adhesion complex, and is found at all regions of the sarcolemma including the neuromuscular and myotendinous junctions (NMJs and MTJs) [3,49–52]. The UGC, a homologous complex to the DGC, is restricted to NMJ and MTJ regions of the sarcolemma, where utrophin replaces dystrophin [53,54]. Although utrophin and dystrophin are structurally homologous, they bind to F-actin through distinct sites [55,56] and only dystrophin contains nNOS-binding sites [57]. It is thought that muscle ischemia occurs in DMD because nNOS is not anchored to the sarcolemmal membrane [57]. The UGC also differs from the DGC in the glycosylation of α-DG, which is a critical determinant of the binding specificity for ECM ligands [47,58–60]. α7β1 integrins, which are also highly enriched within NMJ and MTJ structures and expressed at low levels at nonjunctional regions of the sarcolemma, are the predominant integrin heterodimers expressed in adult muscle [25–27]. Integrins bind F-actin through a complex of proteins including integrin-linked kinase (ILK), PINCH and

α/β-parvin [61–63]. The ILK, PINCH and parvin protein complex has been implicated in facilitating cell signaling through Akt/PKB, GSK3β/β-catenin, JNK and α-Pix/Rac1 pathways [61,62,64]. ILK interacts specifically with β1 integrin and deletion of ILK causes muscular dystrophy that resembles the α7-integrin-deficient mouse model [65]. Laminin-211 binds α7β1 integrin through laminin-type G domains (LG) 1–3, whereas binding to α-DG is mediated through LG1–3 and LG4–5 [66–70]. Given that many differences exist between the three adhesion complexes, the extent to which UGC- and integrin-based therapeutics for DMD fully replace DGC function remains an unanswered question.

The concept of the UGC and integrins acting as compensatory adhesion complexes and their potential as therapeutic targets to replace the DGC arose from studies in the *mdx* mouse model of DMD. Muscle pathology in *mdx* muscle is less severe than that observed in boys with DMD and the *mdx* mouse maintains a fairly normal lifespan [71]. It was hypothesized that increased abundance of the UGC and α7β1 integrin at extra-junctional regions of the sarcolemma in *mdx* muscle may partially compensate for the loss of the DGC, resulting in moderate dystrophic pathology without affecting lifespan, which is in stark contrast to the severe dystrophic pathology and premature lethality observed in the DMD population. To experimentally address this hypothesis, *mdx*:utrophin-null and *mdx*:α7 integrin-null double knockout mice were created. The additional loss of utrophin or α7 integrin in *mdx* mice exacerbated dystrophic symptoms to more closely resemble DMD. Furthermore, lifespan was shortened to 20 and 4 weeks, respectively for utrophin-deficient and α7 integrin-deficient *mdx* mice [72–75]. Significantly, overexpression of either utrophin or β1D integrin in *mdx* muscle prevented muscular dystrophy, demonstrating that the UGC and integrins are capable of replacing the DGC in the mouse model of DMD [76,77]. Mental retardation and brain abnormalities have been detected in ~ 30% of patients with DMD [78]. Utrophin and its smaller isoforms are expressed in the blood vessels in all brain regions, walls of the lateral ventricle, cortex, subiculum, thalamus, brainstem nuclei, superior colliculus and deep cerebellar nuclei [79]. Although utrophin stabilizes the sarcolemma in *mdx* mice, utrophin was not upregulated in a compensatory fashion in the brain of *mdx* mice [79]. Arginine butyrate alleviated *mdx* muscle disease through utrophin upregulation and increased all utrophin isoforms in the brain of *mdx* mice, but did not rescue cognitive deficits observed in behavioral assays including exploration, emotional reactivity, and spatial and fear memories [79]. These results suggest that utrophin cannot fully compensate for the loss of dystrophin in all tissues. The ability of α7β1 integrin to ameliorate cognitive deficits in *mdx* mice has not been tested.

Although the UGC and α7β1 integrin do not fully replace the DGC, they remain excellent candidates for protein-replacement therapies. The packaging limit of adeno-associated virus (AAV) capsids prevents the delivery of the most ideal protein for the treatment of DMD, the entire *dystrophin* gene [80]. Additionally, recent evidence that the expression of AAV-delivered mini-dystrophin is circumvented by an immune response to dystrophin in patient clinical trials [81], strengthens the importance of UGC and α7β1 integrin protein-replacement therapies. A thorough investigation of the biochemical, structural and functional differences between the UGC, α7β1 integrin and the DGC may lead to the future development of combinatorial therapies designed to replace the DGC. The first goal is to determine whether UGC- and α7β1-integrin-based therapies are safe and beneficial to patients with DMD. To date, only three therapies designed to replace the DGC with the UGC or integrins are near clinical trials. Two therapies designed to upregulate utrophin are currently in or near Phase 1 clinical trials: BMN195 (SMT-C1100, Summit plc, Abingdon, Oxfordshire, UK) and biglycan (Trivorsan Pharmaceuticals, Providence, RI, USA). BMN195, a 5-(ethylsulfonyl)-2-(naphthalene-2-yl) benzodoxazole, was identified in a screen for small molecules, which upregulated utrophin mRNA 25% in human myoblasts, increased utrophin protein levels twofold in DMD patient cells, and demonstrated efficacy in treatment of *mdx* mice [82]. Specifically, BMN195 reduced regeneration, inflammation, serum CK levels and fibrosis, and prevented membrane damage due to eccentric contractions in treated *mdx* mice [82]. Although BMN195 was shown to be safe at all doses in a Phase 1 clinical trial by BioMarin Pharmaceuticals (Novato, CA, USA), it did not achieve plasma concentrations, even at the highest doses, required to increase utrophin expression (http://investors.bmrn.com/releasedetail.cfm?ReleaseID =703221). Summit plc has since reformulated BMN195 to allow for better absorption and has initiated Phase 1 clinical trials. The second utrophin upregulation therapy, biglycan, is an extracellular protein that is highly expressed, similar to utrophin, in regenerating and developing muscle [83,84]. Injection of recombinant human biglycan protein improves muscle pathology in the *mdx* mouse by increasing cell-surface expression of utrophin and γ-SG [85]. Furthermore, the inability of biglycan to ameliorate dystrophic pathology of the utrophin-deficient *mdx*

mouse demonstrates the requirement of utrophin for biglycan therapies [85]. Biglycan is currently being developed for Phase 1 clinical trials by Trivorsan Pharmaceuticals. The only therapeutic designed to upregulate α7 integrin near Phase 1 clinical trials is laminin-111 protein. Laminin-111 is an ECM protein present in cardiac and skeletal muscles during embryonic development that is replaced by laminin-211 in adult muscle [69,70]. Injection of Engelbreth–Holt–Swarm-derived purified natural mouse laminin-111 protein improves dystrophic pathology in the *mdx* and laminin α2-deficient dy^W mouse models [86–89] through the upregulation of both utrophin and integrins at the sarcolemma. Prothelia (Milford, MA, USA) is currently developing laminin-111 for clinical trials and a Phase 1 trial will occur upon the completion of preclinical trials. Laminin-111 has the potential for therapeutic use in merosin-deficient congenital muscular dystrophy, DMD and LGMD2I [mutations in fukutin-related protein (FKRP)]. The outcome of these clinical trials may illuminate whether utrophin and integrin therapeutics will alleviate the symptoms of DMD (Fig. 1).

Although introduction of recombinant laminin-111 protein was initially discovered to increase α7β1 integrin protein levels, it has also been shown to increase the levels of utrophin in *mdx* muscle [89]. Given that the overexpression of neither utrophin nor α7β1 integrin fully rescues dystrophic symptoms, it would be interesting to determine whether the upregulation of both adhesion complexes would be more beneficial than targeting a single complex alone. Experiments to directly test the UGC and integrin association have not been performed and numerous murine genetic experiments are often complicated by the compensatory actions of other proteins. Migration of the three adhesion complexes in the same sucrose gradient fractions after biochemical isolation of DG-bound proteins using succinylated wheatgerm agglutinin lectin raises the interesting question of whether integrins and the UGC/DGC physically interact at the sarcolemma [90,91]. If laminin-111 is successful in Phase 1 trials, the potential benefit of targeting both the UGC and α7β1 integrin may be addressed in DMD patients. Similar to laminin-111, Adam12 and SSPN also secondarily upregulate both the UGC and integrins at extrajunctional regions of the sarcolemma when overexpressed in *mdx* mice [47,48,92] (Fig. 1). Adam12 is an active metalloproteinase that is expressed during muscle development and regeneration. The mechanism by which it promotes cell adhesion through the stabilization of the UGC and α7β1 integrin is currently unknown [93–95].

Recent studies have implicated a role for SSPN in facilitating interactions between the UGC and α7β1 integrin. SSPN, a tetraspanin-like protein, functions with the SGs to stabilize the association of α-DG with β-DG in the DGC [19,20,46]. Overexpression of threefold levels of SSPN ameliorates *mdx* muscle by increasing the levels of the UGC, α7β1 integrin and laminin-binding to α-DG [47,48]. Interestingly, the increase in laminin-binding to α-DG was not observed with 1.5-fold levels of SSPN overexpression in *mdx* mice, demonstrating that there is a minimum threshold of SSPN expression required for restoring normal ECM binding to DG [47]. To determine whether laminin-binding to α-DG is required for SSPN-mediated amelioration of dystrophic symptoms, threefold SSPN transgenic mice were crossed with $LARGE^{myd}$ mice. LARGE, like-acetylglucosaminyltransferase, is a glycosyltransferase responsible for elongating O-mannose glycans in the mucin domain of α-DG and mutations in *LARGE* abolish laminin-binding to α-DG [96]. Overexpression of SSPN does not ameliorate muscular dystrophy in the $LARGE^{myd}$ mouse model of hypoglycosylated α-DG (merosin-deficient congenital muscular dystrophy 1A) despite increasing levels of the UGC at the sarcolemma, demonstrating that functionally glycosylated α-DG capable of binding to laminin is a requisite for SSPN-mediated amelioration of dystrophic pathology [47]. Recent genetic studies demonstrated that the combined loss of SSPN and α7 integrin results in extensive muscle pathology and decreased specific force production possibly due to decreased protein levels of the DGC and UGC in 4.5-month-old diaphragm muscle [90]. These studies suggest that SSPN and integrins genetically interact and affect protein abundance of the DGC/UGC, but do not establish a direct interaction between these adhesion complexes. Investigation of the dependence of SSPN-mediated amelioration of *mdx* mice on α7 integrin and utrophin would clarify whether both adhesion complexes are essential for SSPN-based therapeutics. Interestingly, α7 integrin overexpression in *mdx*:utrophin-null mice causes a 10% reduction in regeneration, a threefold increase in mean survival age and reduced severity of joint contractures [97]. These results suggest that α7 integrin reduces the severity of muscular dystrophy in *mdx* mice partially independent of utrophin, although the muscle pathology was not significantly reduced. It is possible that utrophin is required for the full rescue effect of α7 integrin in *mdx* muscle or that higher than threefold levels of α7 integrin are needed to rescue *mdx* muscle independently of utrophin. The ability of utrophin alone to rescue *mdx*:α7 integrin-null muscle has not been tested. Thus, additional evidence is needed to

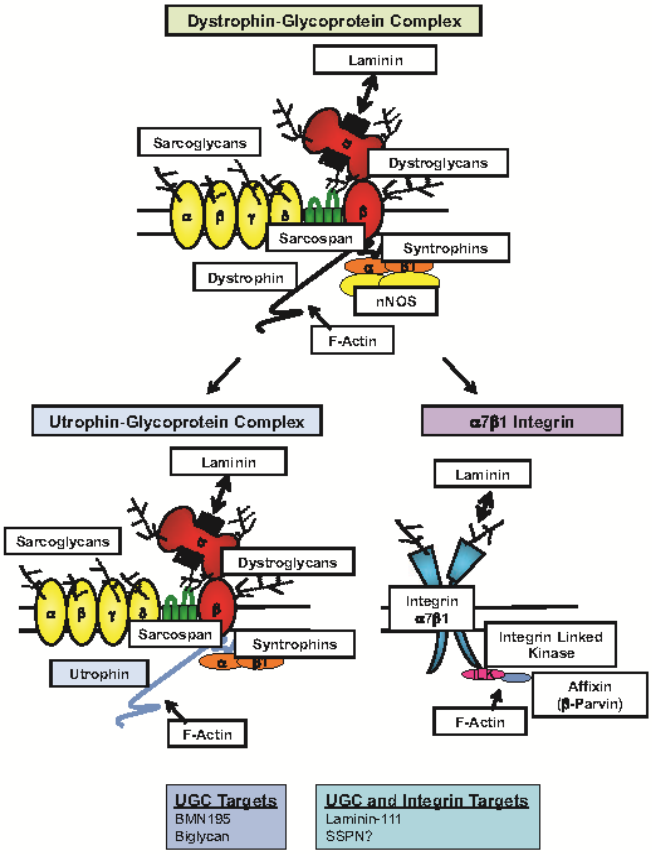


Fig. 1. UGC- and α7β1 integrin-mediated replacement therapy for the DGC in DMD. The DGC, UGC and α7β1 integrins function to prevent contraction-induced damage of the sarcolemma by maintaining connections between the actin cytoskeleton and ECM. The DGC is composed of dystrophin, the dystroglycans (α- and β-DG), the sarcoglycans (α-, β-, γ- and δ-SG), sarcospan (SSPN) and the syntrophins (α- and β-subunits). Neuronal nitric oxide synthase (nNOS) requires dystrophin and syntrophin to be anchored to the sarcolemmal membrane, where it is thought to function in preventing functional muscle ischemia. The UGC is homologous to the DGC, where utrophin replaces dystrophin. However, many differences exist between the UGC and DGC, including the glycosylation of α-DG, the domains in which actin binding occurs, and the lack of nNOS-binding sites on utrophin. α7β1 integrin differs from the UGC/DGC in the globular domains by which laminin binds and the presence of adaptor proteins that facilitate actin binding, including ILK and β-parvin. BMN195 and biglycan are two utrophin upregulation therapeutics that are near/in clinical trials and laminin-111 is the only dual (utrophin and integrin) target therapy that is near clinical trials. This review proposes that AAV delivery of SSPN should be considered as an additional dual target therapy.

establish a direct SSPN-mediated interaction between the UGC and α7β1 integrin at the sarcolemma while the benefit of upregulating both adhesion complexes for the treatment of DMD remains undetermined.

Glycosylation of α-DG and amelioration of muscular dystrophy

Appropriate glycosylation of sarcolemmal proteins is integral for proper muscle function. Over 50% of all known CMDs result from hypoglycosylation of α-DG and therefore are known as dystroglycanopathies [98]. Mutations in 13 genes are known to cause aberrant glycosylation of α-DG. These gene products include: protein *O*-mannosyl transferase-1 and -2 (POMT1 and POMT2), protein O-linked mannose β-1,2-*N*-acetylglucosaminyltransferase (POMGnT1), LARGE, fukutin, FKRP, β-1,3-*N*-acetylgalactosaminyltransferase 2, isoprenoid synthase domain containing (ISPD), dolichyl-phosphate-mannosyltransferase subunits 2 and 3, dolichol kinase, glycosyltransferase-like domain containing (GTDC2) and transmembrane protein 5 (TMEM5) [36,37,39,99 113]. POMT1/2 act collaboratively to add the initiating mannose to serine or threonine residues of the mucin domain of α-DG [114,115]. Classical mannose glycans are then elongated by the addition of a β-1,2-*N*-acetylglucosamine (β1,2GlcNAc) residue, whereas laminin-binding mannose glycans are elongated by the addition of a β-1,4-*N*-acetylglucosamine (β1,4GlcNAC) residue (Fig. 2) [37,99,116]. It was recently proposed that β-1,3-*N*-acetylgalactosaminyltransferase 2 may be the glycosyltransferase responsible for the addition of the GalNAc residue following β1,4GlcNAc addition to laminin-binding mannose glycans, however, this precise activity remains to be proven [108]. On laminin-binding glycan structures,

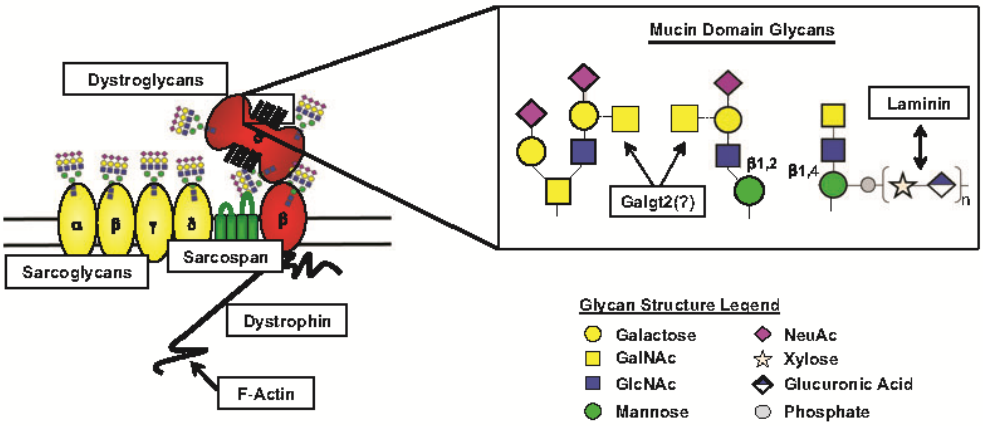


Fig. 2. Glycosylation of the DGC. Known and putative sites of glycosylation of DGC component proteins are depicted. Inset of laminin-binding glycan is provided along with potential site of Galgt2 modification. Colored symbols used to represent glycan structures are in accordance with the guidelines outlined by the Consortium of Functional Glycomics.

LARGE creates the unique moiety required for binding of α-DG to laminin as well as other ECM components (Fig. 2) [39,117,118]. Binding of α-DG to laminin has been shown to be dependent upon the xylosyl and glucuronyl transferase activities of LARGE [119]. Furthermore, knockout of LARGE activity causes a decrease in the molecular weight of α-DG [116]. Precise enzymatic functions of fukutin, FKRP, ISPD, GTDC2 and TMEM5 remain elusive; however, mutations in these genes lead to hypoglycosylation of α-DG and subsequent CMD phenotypes [100,102–104,107,120]. Dolichol kinase and dolichyl-phosphate-mannosyltransferase subunits-2 and -3 are required for synthesis of the glycosylation precursors dolichol-phosphate and dolichol-phosphate-mannose respectively [121–123]; mutations in all three give rise to dystroglycanopathies as both glycosylation precursors are required for synthesis of N-glycans and O-mannosyl glycans [124,125].

The dystroglycanopathies represent a diverse group of muscular dystrophies with broad phenotypic severities and wide ranging causative gene mutations. Walker–Warburg syndrome (WWS) cases result from the largest group of genetic mutations and can be attributed to mutations in POMT1, POMT2, LARGE, fukutin, FKRP, ISPD, β-1,3-*N*-acetylglucosaminyltransferase, β-1,3-*N*-acetylgalactosaminyltransferase 2, GTDC2 and TMEM5 [103,107,126,127]. Patients presenting with muscle–eye–brain disease represent a similarly heterogeneous population of phenotypic severities and genetic mutations. Muscle–eye–brain disease has been reported to result from mutations in POMGnT1, fukutin and FKRP [37,127,128]. LGMD types 2K, N, M, I and O result from mutations in POMT1, POMT2, fukutin, FKRP and POMGnT1, respectively [28,127–129]. CMD types 1C and 1D result from mutations in FKRP and LARGE, respectively [39,130]. Furthermore, an insertion of a retrotransposon in the *fukutin* gene is known to cause Fukuyama congenital muscular dystrophy [102]. The genetic basis for the various dystroglycanopathies is varied and the resulting phenotypes are overlapping, which reinforces the need for a thorough understanding of the connection between specific genetic mutations and resulting biochemical dysfunctions that underlie or cause muscular dystrophy.

Although DMD results from mutations in dystrophin, it is noteworthy that significant changes in glycosylation have been reported in the mouse model for DMD. The lectin *Wisteria floribunda* agglutinin (WFA) recognizes terminal β1,4-GalNAc residues of α-DG in skeletal muscle [60,131] and binding is normally restricted to the NMJ and MTJ in wild-type myofibers [59]. However, WFA binds to the extrasynaptic sarcolemma in addition to the NMJ on *mdx* muscle cryosections [47,58]. This redistribution of WFA staining to the extrasynaptic sarcolemma is concomitant with the redistribution of utrophin and the associated UGC in *mdx* mouse muscle.

Overexpression of both full-length and truncated utrophin rescues the dystrophic phenotype in *mdx* mice [77,132–135]. Because WFA preferentially binds

to α-DG in the UGC, increasing GalNAc modification of α-DG has been one approach to increase extrasynaptic utilization of utrophin as a potential therapy for DMD. The overexpression of terminal β-GalNAc glycosyltransferase *galgt2* in wild-type mice has been shown to increase levels of UGC proteins, laminin-binding and reactivity of α-DG to WFA [59,60]. Similar results were obtained from *galgt2* overexpression in *mdx* mice, where rescue of laminin-binding and the dystrophic phenotype were additionally noted [59,60]. Interestingly, transgenic overexpression of SSPN also increases the WFA reactivity of α-DG in *mdx* and $LARGE^{myd}$ muscle, whereas loss of SSPN reduces UGC levels and the reactivity of α-DG with WFA [47]. Importantly, no mitigation of dystrophic pathology or rescue of laminin-binding is observed in $LARGE^{myd}$ mice overexpressing SSPN [47]. These studies are significant because they demonstrate that laminin-binding is required for SSPN-mediated amelioration of dystrophic pathology and that the glycans detected by increasing WFA reactivity are distinct from the structure created by LARGE activity. It has been proposed that SSPN overexpression mediates changes in glycosylation via increased galgt2 activity [47]; however, this mechanism requires further validation through the creation of galgt2-deficient *mdx* SSPN transgenic mice. Interestingly, overexpression of *galgt2* has also been demonstrated to be effective in ameliorating the dystrophic phenotype in mouse models of CMD 1A (dy^W) and α-SG-deficient LGMD 2D [136,137]. It is noteworthy, however, that the overexpression of a neuronal homolog *galgt1*, which adds terminal β-GalNAc residues distinctly to ganglioside glycolipids, caused muscle pathology including decreased myofiber diameter and increased central nucleation in wild-type mice [138]. These stark differences resulting from the overexpression of either *galgt2* or *galgt1* demonstrate the tissue and acceptor substrate specificity of glycosylation and reinforce the importance of thoroughly evaluating the effects of manipulating glycosylation.

Although genetic overexpression of a glycosyltransferase provides one potential therapeutic approach for manipulating glycosylation of sarcolemmal glycoproteins, pharmacologic approaches also provide potential therapeutics. Using high-throughput screening, the small molecule lobeline was identified as a pharmacological treatment that altered C2C12 glycosylation *in vitro* [139]. Compounds from the Prestwick library of ~ 1200 FDA-approved small molecules were added to myoblasts in differentiation media and changes in glycosylation were measured after two days of treatment [139]. Specifically, binding of terminal β-GalNAc modifications as detected by WFA binding increased in C2C12 cells as well as isolated wild-type and *mdx* myoblasts following treatment with lobeline during differentiation [139]. Lobeline treatment increased the abundance of UGC proteins and laminin-binding in wild-type and *mdx* primary cell cultures [139]; these results are similar to changes resulting from *galgt2* overexpression. It is noteworthy that the increase in WFA binding following lobeline treatment was dependent upon complex N-glycans and not O-mannose glycans such as those required for laminin binding [139]. Furthermore, deoxymannojirimycin inhibition of complex N-glycans necessary for WFA binding caused a decrease in laminin binding as detected by laminin overlay [139]. Although lobeline was first FDA approved for smoking cessation, *in vitro* studies have shown that it may potentially act as a protein folding chaperone or nicotinic antagonist through the dopamine or vesicular monoamine transporter [140–143]. In the C2C12 studies, the molecular mechanism by which lobeline increased WFA binding *in vitro* was not determined. Although the ability of lobeline to alter muscle glycosylation *in vivo* remains to be demonstrated, these studies represent strong proof of the principle of pharmacologic manipulation of sarcolemmal protein glycosylation as a potential therapeutic.

Protein aggregation and amelioration in muscular dystrophies

The *mdx* mouse contains a point mutation in exon 23 [144], resulting in a premature termination codon that is predicted to result in a 115-kDa protein [145]. It has previously been shown that dystrophin mRNA levels are decreased in the skeletal muscle, cardiac muscle and brains of three *mdx* mouse strains [146]. However, dystrophin mRNA levels vary widely, depending on the causative mutation in human DMD and Becker muscular dystrophy patients [147]. It was previously thought that the 115 kDa dystrophin protein is rapidly degraded after synthesis in *mdx* muscle, but studies suggest that truncated dystrophin may be expressed at the sarcolemma [148–150] or retained in the ER/Golgi [47].

A 70–80-kDa dystrophin reactive to a C-terminal antibody was found in a group of Japanese Spitz dogs displaying progressive Duchenne-like muscular dystrophy [149]. These dogs displayed exercise intolerance, an abnormal gait and pain upon handling of muscles beginning at 10–12 weeks of age. The symptoms worsened over time, suggesting that the 70–80-kDa dystrophin was unable to restore sarcolemmal stability. In a separate study, immunohistochemical assays revealed expression of truncated dystrophin in myotubes iso-

lated from three 12-week-old aborted fetuses at risk for DMD, suggesting that mutant dystrophin is synthesized in human DMD patients [148]. Recently, the truncated form of dystrophin was detected within the ER/Golgi compartments of *mdx* mice [47], suggesting that the 115-kDa dystrophin may be retained in the ER/Golgi compartments.

The mutation in *mdx* mice leads to the loss of the β-DG-binding domain, leaving only the actin-binding domains in the dystrophin fragment [145]. The N-terminus of dystrophin binds directly to F-actin in the cytoplasm of the myofiber, whereas the C-terminus of dystrophin contains cysteine-rich domains that bind the C-terminus of β-DG [4,151]. Recent studies utilizing truncated dystrophin have provided more insight into which segments of the protein are required for sarcolemmal stability. One study utilized rAAV6 micrdystrophin to evaluate the role of the actin-binding domains in sarcolemmal stabilization [152]. Four months after injection into the tibialis anterior, muscles treated with micro-dystrophins lacking actin-binding domains displayed decreased specific force and a decreased ability to protect against contraction-induced injury [152], indicating the importance of an intact actin-binding domain in maintaining sarcolemmal stability.

Other studies have analyzed different isoforms of dystrophin. The dystrophin isoform Dp116 is expressed in Schwann cells within the peripheral nervous system [153]. This isoform lacks the actin-binding domains although it retains the complete dystroglycan-binding domain [153]. Although expression of Dp116 in *mdx*:utrophin-null mice increased muscle mass, life span and maximal force, the specific force and histopathology did not improve [153]. It is hypothesized that Dp116, or the dystroglycan-binding domain, attempts to stabilize the DGC at the sarcolemma through other interactions with the cytoskeleton, although specifics have yet to be elucidated [153]. The expression of a non-muscle isoform of dystrophin, Dp71, which lacks N-terminal actin-binding domains and spectrin-like repeats, restores the DGC in muscle, suggesting that the β-DG-binding domain is required for assembly of the DGC [154]. Thus, it would be interesting to examine other mice with C-terminal mutations in dystrophin. Such experiments would assess the ability of truncated dystrophin to be incorporated and expressed with the DGC at the sarcolemma and restore functionality of dystrophic muscle. This provides an exciting opportunity to examine ways to express fragmented dystrophin at the sarcolemma to improve dystrophic pathology. Other studies involving protein retention within cellular compartments in different muscular dystrophies may provide insights into the therapeutic translation of these findings.

Studies in Fukuyama congenital muscular dystrophy, which is caused by mutations in *fukutin* [102], have provided insight into the importance of protein processing within the ER/Golgi. The exact role of fukutin remains unclear, but mutations in *fukutin* lead to abnormal glycosylation of α-DG [155], a reduction in laminin-binding activity [155], and the mislocalization and retention of fukutin in the ER [156]. A recent study analyzed 13 missense *fukutin* constructs in C2C12 cells and discovered that four were mislocalized to the ER. To understand whether mutant fukutin still leads to the production of functionally glycosylated α-DG, site-directed mutagenesis was used to generate mutants for transfection into fukutin-null mouse embryonic stem cells [156]. Expression of the four missense fukutin mutants restored α-DG reactivity against the IIH6C4 antibody and laminin-binding to α-DG, suggesting that α-DG is functionally glycosylated with the expression of mutant fukutin [156]. Using treatments to improve protein folding, including curcumin, a molecule isolated from the spice turmeric and low temperature culturing conditions, ER retention of fukutin was corrected in the four mutants shown to be mislocalized in the ER. In order to elucidate the reasons for aberrant fukutin trafficking, brefeldin A was used to examine anterograde transport and nocodazole was used to examine retrograde transport [156]. After incubation with brefeldin A, the fukutin mutants remain accumulated in the ER [156]. The results suggest that although mutant fukutin proteins are processed in the ER, they are unable to be transported to the Golgi through the anterograde pathway, providing valuable insight into how the protein-trafficking process is affected upon the mislocalization of a mutant protein. Thus, it is possible that truncated dystrophin may be retained within the ER/Golgi compartments and is not transported to the cell surface in *mdx* muscle. It will be important for future studies to utilize a similar strategy to elucidate the effects of 115-kDa dystrophin on retrograde and anterograde transport in *mdx* cells. Additionally, treatment with pharmacological agents, such as curcumin or exposure to low temperature, may potentially alleviate accumulation of truncated dystrophin in the ER/Golgi compartments and improve the transport of DGC and UGC components to the sarcolemmal membrane.

Curcumin was found to target the NF-κB pathway [157] and has been used to treat dystrophic muscle. The activation of NF-κB, which is involved in the modulation of immune responses and regulation of myogenesis, is increased in DMD patient muscle [158].

Intraperitoneal administration of curcumin inhibits NF-κB activation and reduces dystrophic pathology in *mdx* mice [159]. However, a different study reports that curcumin treatment is unable to inhibit the NF-κB pathway and does not improve specific force in the diaphragm muscle of *mdx* mice [160]. Future studies examining the effect of curcumin on the accumulation of truncated dystrophin in the ER/Golgi will be important in determining what role, if any, it plays in pathogenesis.

Protein mislocalization has also been implicated in LGMDs 2C–F pathologies caused by mutations in the SG genes [161]. The severity of pathology in LGMDs 2C–F and cellular fate of the affected SG varies according to the mutation [161]. According to data compiled from the Leiden University mutation database, the most common mutations are α-SG (p.R77C), β-SG (p.S114F) and γ-SG (p.C283Y), which cause a mild to severe phenotype [161]. These data led to an examination of the noted point mutations and their effect on intracellular fate and expression of the SGs at the cell surface. Following treatment with kifunensine, an α-mannosidase I inhibitor that prevents ER-associated degradation [162], the expression of sarcoglycans with mild mutations thought to cause the least amount of structural modification was restored at the cell surface. Future studies manipulating ER quality control in wild-type and *mdx* cells might provide more information on how changes in the ER can affect DGC and UGC expression at the cell surface.

Heat shock proteins and proteasome inhibition in the treatment of muscular dystrophy

Heat shock proteins (Hsp) are induced to combat cellular stress when organisms are under environmental strains such as heat, or during disease and infection [163]. Analysis of skeletal muscle from young DMD patients revealed an induction of Hsp72 and Hsp65 in hypercontracted fibers and Hsp90 in regenerating muscle [164]. Hsp72 is also increased at the mRNA level following electrical stimulation for tetanic contractions in isolated single skeletal muscle fibers from *Xenopus laevis* [165] and after high-intensity exercise in normal Wistar rats [166], suggesting a role for Hsp72 in protection against muscle stress. Treatment of *mdx* and utrophin-deficient *mdx* mice with BGP-15, a pharmacologic inducer of Hsp72, showed that an increase in Hsp72 expression improved SERCA function and dystrophic pathology, decreased kyphosis and ultimately extended lifespan [167]. Targeting Hsp72 to improve protein folding and quality control during cellular stress and disease progression provides a possible avenue to improve muscle function while prolonging the lifespan of patients with muscular dystrophy.

Ubiquitin is an important component in proteasome regulation and can direct proteins towards degradation [168]. Ubiquitin was also found to be elevated in hypercontracted, regenerating and necrotic myofibers in the skeletal muscle of young DMD patients [164]. The increase in ubiquitin protein may suggest misregulation of the ubiquitin–proteasome pathway as well as an increase in protein degradation in DMD patients, which may contribute to the pathogenesis of DMD. Recent studies attempting to ameliorate dystrophic pathology using proteasome inhibitors have produced mixed results. Velcade and MLN273, two FDA-approved proteasome inhibitors, were injected into the gastrocnemius muscle of *mdx* mice [169]. A truncated 97 kDa dystrophin product, as well as an increase in α-DG, β-DG and α-SG, were detected using immunoblotting and immunohistochemistry 24 h post treatment [169]. Similarly, another proteasome inhibitor, MG-132, rescued the membrane localization of dystrophin, α-DG, β-DG and α-SG [170]. However, physiological functionality was not examined and experiments such as grip strength and force production were not performed. This information is critical for the pursuit of such pharmacological agents as treatments for DMD (Fig. 3A).

Although some drugs such as Velcade and MLN273 have shown promise for the attenuation of dystrophic pathology in *mdx* mice, other studies have described conflicting results. In a separate study, long-term administration of a MG-132 failed to restore dystrophin expression in *mdx* muscle and ultimately increased susceptibility to contraction-induced damage [171]. The effects of proteasome inhibitors on grip strength, force production and DGC protein expression need to be analyzed more rigorously to better determine their efficacy in improving muscle function and dystrophic pathology.

A possible function for sarcospan as a chaperone protein

New data suggest a role for SSPN in protein trafficking to the sarcolemma. A recent study isolated ER/Golgi membranes from *mdx* muscle and immunoblots revealed an increase in α-DG and utrophin compared with wild-type muscle [47]. This suggests a possible compensatory mechanism is at play, whereby the system attempts to utilize utrophin upon the loss of dystrophin (Fig. 3B). Interestingly, SSPN transgenic *mdx* mice revealed decreased levels of WFA-reactive α-DG

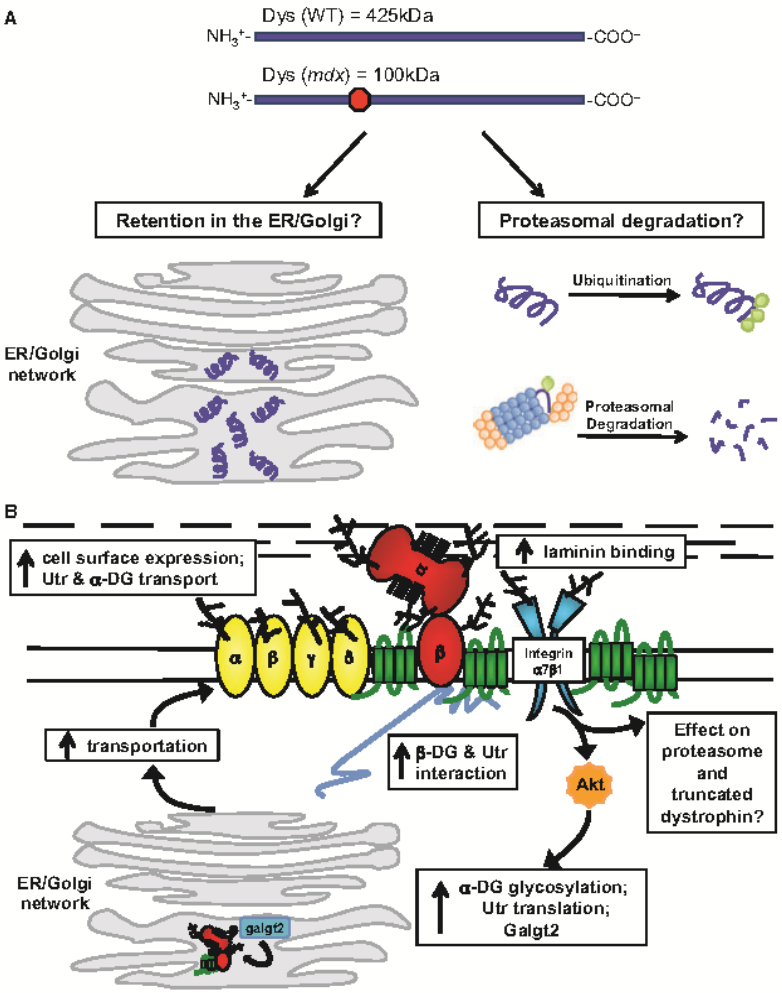


Fig. 3. Effects of SSPN overexpression in *mdx* mice on the cell surface protein expression and protein processing and possible outcomes of truncated dystrophin within the cell. (A) Wild-type mice express full-length dystrophin, which is 425 kDa. The *mdx* mutation leads to a premature stop codon that results in a truncated dystrophin of 100 kDa. Dystrophin is depicted in purple, the proteasome is blue and orange, and ubiquitin is green. Truncated dystrophin can be retained in the ER/Golgi. Alternatively, truncated dystrophin is ubiquitinated and sent to the proteasomal degradation pathway. (B) The overexpression of SSPN in *mdx* muscle leads to molecular events resulting in the restoration of laminin binding and rescue of *mdx* pathology. SSPN activates Akt, which leads to an increase in utrophin and integrins. Galgt2, one enzyme responsible for GalNAc modification of α-DG, is also increased in isolated ER/Golgi membranes. SSPN also improves utrophin-DG transportation to the sarcolemma while simultaneously restoring laminin-binding and membrane stability. SSPN's effect on the trafficking of truncated dystrophin and proteasomal degradation is still unknown. DGs (red), SGs (yellow), SSPN (green), integrins (blue) and Akt (orange) are shown. Utrophin (Utr) is depicted in gray.

and utrophin in ER/Golgi preparations, whereas immunofluorescence assays showed an increased abundance of these proteins at the sarcolemma [47]. SSPN overexpression increased WFA binding 1.8-fold per α-DG molecule as detected by WFA overlay [47]. Increased extrasynaptic binding of WFA may be the

result of general chaperone trafficking of glycoprotein complexes by SSPN. However, the increase in WFA-reactive glycosylation per α-DG protein demonstrates a role for SSPN in specific changes in glycosylation of α-DG. This modification in α-DG glycosylation may result from downstream transcriptional effects of increased Akt signaling [47] or could additionally be a more direct result of chaperone activities of SSPN in trafficking. SSPN might act directly as a chaperone to stabilize α-DG during ER/Golgi trafficking and addition of glycans resulting in increased glycan modification per α-DG molecule. Importantly, overexpression of SSPN drives changes in glycosylation of α-DG, which aid in the amelioration of *mdx* pathology [47]. These studies highlight a promising role for SSPN as a therapeutic and it would be interesting to examine SSPN overexpression in dystroglycanopathy mouse models where direct manipulation of glycosylation ameliorates dystrophic pathology [136,137]. SSPN may possess chaperone-like functions, and the overexpression of SSPN may improve overall protein folding and quality control as well as transport to the cell surface.

How to achieve forced overexpression of SSPN

Membrane proteins are synthesized by ribosomes on the ER and disulfide bonds are synthesized and rearranged in the ER lumen [172]. Because SSPN is an integral membrane protein with disulfide bonds requiring processing through the ER, it most likely cannot be administered systemically. The small size of SSPN makes it an excellent gene to be delivered through AAV. AAV delivery of α-SG in α-SG-deficient patients and γ-SG in γ-SG-deficient patients resulted in no adverse events, demonstrating that intramuscular AAV delivery is likely to be safe in adult patients [173,174]. The only patients that did not express SG following AAV delivery had pre-existing immunity to the AAV serotype used, demonstrating the need for prescreening of AAV serotypes [173,174]. However, there are many challenges to be overcome before systemic delivery of AAV is feasible. Systemic delivery of therapeutics will be required for amelioration of fatal dystrophic symptoms in the diaphragm and heart muscles. Surprisingly, a T-cell-mediated immune reaction against dystrophin prevented the expression of mini-dystrophin following AAV delivery in DMD patients [81]. The precise reason for the varied T-cell immune responses (against mini-dystrophin and against self revertant dystrophin) in the six trial patients is unknown. These results warrant caution in future AAV mini-/microdystrophin and exon skipping trials. Importantly, immune responses should not be a problem in secondary approaches to upregulate utrophin or α7β1 integrin for protein-replacement therapeutics. A drug screen for compounds that upregulate SSPN offers an additional approach to AAV-mediated SSPN therapy. A similar approach led to the discovery of BMN195 for utrophin upregulation and is currently in Phase 1 clinical trials.

Unanswered questions for SSPN-based therapeutics

Overexpression of SSPN under the human skeletal actin promoter results in a 60% reduction in regeneration in the *mdx* mouse model of DMD by replacing the DGC with the UGC and α7β1 integrin [47,48]. As with most therapeutic targets, many questions remain to be answered for SSPN-based therapeutics. For SSPN to become a viable therapeutic for the treatment of DMD, the questions below need to be addressed.

Does SSPN delivery with AAV prevent dystrophic pathology in the mdx mouse model?

This is an important question that needs to be answered, because it will determine the delivery system used for SSPN-based therapeutics. It would also be useful to further determine the feasibility of AAV delivery of SSPN in the golden retriever model of DMD, because the dog model provides a more realistic clinical model for systemic delivery.

Does SSPN eliminate/reduce dystrophic pathology in the heart and diaphragm?

The human skeletal actin promoter is not highly expressed in the diaphragm or heart muscles. Because death occurs from respiratory and/or cardiac failure in DMD patients, an ideal therapeutic target should prevent dystrophic pathology in the heart and diaphragm. This question can be addressed with systemic delivery of AAV6-SSPN in the *mdx* mouse model. AAV6 has been shown to infect the heart and the diaphragm [175,176].

Can SSPN reverse or prevent dystrophic pathology after the onset of dystrophy?

The human skeletal actin promoter is turned on early in muscle development. SSPN is likely preventing the onset of dystrophic pathology rather than reversing pathology. Boys with DMD are often diagnosed with the disease well after the onset of dystrophic pathol-

ogy, so effective treatments should reverse or halt pathology already in progress. To determine whether SSPN is effective after the onset of disease, a murine inducible transgenic system could be engineered to turn SSPN expression on later in life. Intramuscular or systemic injection of AAV-SSPN after the onset of pathology in *mdx* mice will also address this question.

Is widespread expression of SSPN safe?

The promoter used in murine studies of SSPN overexpression in the *mdx* mouse model restricted SSPN expression to striated skeletal muscle [177]. An effective treatment in patients with DMD would require systemic delivery of SSPN in order to target the heart and diaphragm. It is important to determine whether long-term systemic delivery of SSPN is safe. This question can also be addressed with systemic delivery of AAV-SSPN in *mdx* mice. Because AAV infection of particular tissues depends on the AAV serotype, it would be important to test SSPN delivery with the serotypes approved for use in patients.

Does SSPN upregulate the UGC and integrins in human myoblasts?

Many recent treatment strategies have been tested in DMD myoblasts, including BMN195 and dantrolene [82,178]. The ability to demonstrate that a therapy acts through similar targets in human cells offers a nice proof-of-principle for the approach being tested.

Which patient populations will benefit from SSPN-based therapeutics?

It is important when developing therapies for muscular dystrophy to determine how many different muscle diseases will benefit from the treatment. This will allow for the design and recruitment of appropriate patient populations for clinical trials. SSPN is effective in ameliorating pathology in the *mdx* model of DMD [47,48]. SSPN did not reduce dystrophic pathology in the $LARGE^{myd}$ model of hypoglycosylation of α-DG (merosin-deficient congenital muscular dystrophy 1A) [47]. It would be interesting to determine if SSPN can ameliorate various limb-girdle and congenital muscular dystrophies.

Conclusions

In the *mdx* model of DMD, the SSPN transgene ameliorates dystrophic pathology by increasing the UGC and α7β1 integrin extrasynaptic sarcolemma, the synapse-specific GalNAc glycosylation of α-DG, and the transport of utrophin and α-DG from the ER/Golgi to the cell surface [47,48,179]. These studies raise important questions about the mechanisms by which SSPN overexpression accomplishes these observed effects. Biochemical evidence that SSPN is a component of both the DGC and UGC complexes and genetic analysis of mice lacking both SSPN and α7 integrin have led to the proposal that SSPN stabilizes the UGC and integrins through direct interactions at the sarcolemma [46,47,90,179]. More experiments are needed to address the requirement of utrophin and α7 integrin for SSPN-mediated amelioration of *mdx* muscle, as well as the possibility that the UGC and α7β1 integrin function synergistically at the sarcolemma. In addition, SSPN may act either directly or indirectly as a chaperone protein to facilitate the efficient assembly and export of the UGC to the cell surface [47]; however, more studies are needed to elucidate the role of SSPN in the ER/Golgi. Overexpression of constitutively active Akt signaling has been shown to be beneficial in *mdx* muscle by increasing the UGC and integrins at the sarcolemma, reducing membrane damage and improving the force-generating capacity of muscle [180,181]. SSPN-mediated amelioration of *mdx* muscle results in a similar increase in active Akt signaling and downstream muscle growth pathways [47]. Many therapeutic approaches for DMD concentrate on a single target. Although experimental strategies for the treatment of DMD have been developed for over 25 years, steroids remain the only approved drugs to slow the progression of the disease. Thus, the best treatment strategy remains an open question. SSPN is unique because it incorporates several beneficial therapeutic targets into a single protein that is small and easily packaged in AAV delivery systems. SSPN is also ubiquitously expressed in other tissues throughout the body so systemic delivery and immune response should not be an issue [46]. We are currently experimentally addressing the unanswered questions for SSPN therapeutics.

Acknowledgements

We thank A. W. Kwok, J. Lee and J. Oh for critically reading this manuscript. This work was supported by grants from the Genetic Mechanisms Pre-doctoral Training Fellowship USPHS National Research Service Award GM07104, the Edith Hyde Fellowship, the Eureka Pre-doctoral Training Fellowship, and the Ruth L. Kirschstein National Service Award T32AR059033 from the National Institute of Arthritis and Musculoskeletal and Skin Diseases to JLM; Mus-

cular Dystrophy Association RG 135449 and NIH P30 AR057230 to LGB and NIH/NIAMS (R01 AR048179) to RC-W.

References

1 Ervasti JM, Ohlendieck K, Kahl SD, Gaver MG & Campbell KP (1990) Deficiency of a glycoprotein component of the dystrophin complex in dystrophic muscle. *Nature* **345**, 315–319.

2 Koenig M, Hoffman EP, Bertelson CJ, Monaco AP, Feener C & Kunkel LM (1987) Complete cloning of the Duchenne muscular dystrophy (DMD) cDNA and preliminary genomic organization of the DMD gene in normal and affected individuals. *Cell* **50**, 509–517.

3 Hoffman EP, Brown RH Jr & Kunkel LM (1987) Dystrophin: the protein product of the Duchenne muscular dystrophy locus. *Cell* **51**, 919–928.

4 Levine BA, Moir AJ, Patchell VB & Perry SV (1990) The interaction of actin with dystrophin. *FEBS Lett* **263**, 159–162.

5 Campbell KP & Kahl SD (1989) Association of dystrophin and an integral membrane glycoprotein. *Nature* **338**, 259–262.

6 Moorwood C (2008) Syncoilin, an intermediate filament-like protein linked to the dystrophin associated protein complex in skeletal muscle. *Cell Mol Life Sci* **65**, 2957–2963.

7 Sander M, Chavoshan B, Harris SA, Iannaccone ST, Stull JT, Thomas GD & Victor RG (2000) Functional muscle ischemia in neuronal nitric oxide synthase-deficient skeletal muscle of children with Duchenne muscular dystrophy. *Proc Natl Acad Sci USA* **97**, 13818–13823.

8 Lai Y, Thomas GD, Yue Y, Yang HT, Li D, Long C, Judge L, Bostick B, Chamberlain JS, Terjung RL *et al.* (2009) Dystrophins carrying spectrin-like repeats 16 and 17 anchor nNOS to the sarcolemma and enhance exercise performance in a mouse model of muscular dystrophy. *J Clin Invest* **119**, 624–635.

9 Thomas GD, Shaul PW, Yuhanna IS, Froehner SC & Adams ME (2003) Vasomodulation by skeletal muscle-derived nitric oxide requires alpha-syntrophin-mediated sarcolemmal localization of neuronal nitric oxide synthase. *Circ Res* **92**, 554–560.

10 Thomas GD & Victor RG (1998) Nitric oxide mediates contraction-induced attenuation of sympathetic vasoconstriction in rat skeletal muscle. *J Physiol* **506**, 817–826.

11 Martin EA, Barresi R, Byrne BJ, Tsimerinov EI, Scott BL, Walker AE, Gurudevan SV, Anene F, Elashoff RM, Thomas GD *et al.* (2012) Tadalafil alleviates muscle ischemia in patients with becker muscular dystrophy. *Sci Transl Med* **4**, 162ra155.

12 Petrof BJ, Shrager JB, Stedman HH, Kelly AM & Sweeney HL (1993) Dystrophin protects the sarcolemma from stresses developed during muscle contraction. *Proc Natl Acad Sci USA* **90**, 3710–3714.

13 Ervasti JM & Campbell KP (1991) Membrane organization of the dystrophin–glycoprotein complex. *Cell* **66**, 1121–1131.

14 Ibraghimov-Beskrovnaya O, Ervasti JM, Leveille CJ, Slaughter CA, Sernett SW & Campbell KP (1992) Primary structure of dystrophin-associated glycoproteins linking dystrophin to the extracellular matrix. *Nature* **355**, 696–702.

15 Ervasti JM & Campbell KP (1993) A role for the dystrophin–glycoprotein complex as a transmembrane linker between laminin and actin. *J Cell Biol* **122**, 809–823.

16 Ervasti JM, Kahl SD & Campbell KP (1991) Purification of dystrophin from skeletal muscle. *J Biol Chem* **266**, 9161–9165.

17 Ervasti JM & Campbell KP (1993) Dystrophin and the membrane skeleton. *Curr Opin Cell Biol* **5**, 82–87.

18 Yoshida M & Ozawa E (1990) Glycoprotein complex anchoring dystrophin to sarcolemma. *J Biochem* **108**, 748–752.

19 Crosbie RH, Lebakken CS, Holt KH, Venzke DP, Straub V, Lee JC, Grady RM, Chamberlain JS, Sanes JR & Campbell KP (1999) Membrane targeting and stabilization of sarcospan is mediated by the sarcoglycan subcomplex. *J Cell Biol* **145**, 153–165.

20 Crosbie RH, Lim LE, Moore SA, Hirano M, Hays AP, Maybaum SW, Collin H, Dovico SA, Stolle CA, Fardeau M *et al.* (2000) Molecular and genetic characterization of sarcospan: insights into sarcoglycan–sarcospan interactions. *Hum Mol Genet* **9**, 2019–2027.

21 Holt KH & Campbell KP (1998) Assembly of the sarcoglycan complex. Insights for muscular dystrophy. *J Biol Chem* **273**, 34667–34670.

22 Weller B, Karpati G & Carpenter S (1990) Dystrophin-deficient mdx muscle fibers are preferentially vulnerable to necrosis induced by experimental lengthening contractions. *J Neurol Sci* **100**, 9–13.

23 Pearce M, Blake DJ, Tinsley JM, Byth BC, Campbell L, Monaco AP & Davies KE (1993) The utrophin and dystrophin genes share similarities in genomic structure. *Hum Mol Genet* **2**, 1765–1772.

24 Tinsley JM, Blake DJ, Roche A, Fairbrother U, Riss J, Byth BC, Knight AE, Kendrick-Jones J, Suthers GK, Love DR *et al.* (1992) Primary structure of dystrophin-related protein. *Nature* **360**, 591–593.

25 Hynes RO (1992) Integrins: versatility, modulation, and signaling in cell adhesion. *Cell* **69**, 11–25.

26 Song WK, Wang W, Foster RF, Bielser DA & Kaufman SJ (1992) H36-alpha 7 is a novel integrin alpha chain that is developmentally regulated during skeletal myogenesis. *J Cell Biol* **117**, 643–657.

27 von der Mark H, Durr J, Sonnenberg A, von der Mark K, Deutzmann R & Goodman SL (1991) Skeletal myoblasts utilize a novel beta 1-series integrin and not alpha 6 beta 1 for binding to the E8 and T8 fragments of laminin. *J Biol Chem* **266**, 23593–23601.

28 Balci B, Uyanik G, Dincer P, Gross C, Willer T, Talim B, Haliloglu G, Kale G, Hehr U, Winkler J *et al.* (2005) An autosomal recessive limb girdle muscular dystrophy (LGMD2) with mild mental retardation is allelic to Walker-Warburg syndrome (WWS) caused by a mutation in the POMT1 gene. *Neuromuscul Disord* **15**, 271–275.

29 Bonnemann CG, Modi R, Noguchi S, Mizuno Y, Yoshida M, Gussoni E, McNally EM, Duggan DJ, Angelini C & Hoffman EP (1995) Beta-sarcoglycan (A3b) mutations cause autosomal recessive muscular dystrophy with loss of the sarcoglycan complex. *Nat Genet* **11**, 266–273.

30 Matsumura K, Tome FM, Collin H, Azibi K, Chaouch M, Kaplan JC, Fardeau M & Campbell KP (1992) Deficiency of the 50K dystrophin-associated glycoprotein in severe childhood autosomal recessive muscular dystrophy. *Nature* **359**, 320–322.

31 McNally EM, Bonnemann CG, Kunkel LM & Bhattacharya SK (1996) Deficiency of adhalin in a patient with muscular dystrophy and cardiomyopathy. *N Engl J Med* **334**, 1610–1611.

32 McNally EM, Passos-Bueno MR, Bonnemann CG, Vainzof M, de Sa Moreira E, Lidov HG, Othmane KB, Denton PH, Vance JM, Zatz M *et al.* (1996) Mild and severe muscular dystrophy caused by a single gamma-sarcoglycan mutation. *Am J Hum Genet* **59**, 1040–1047.

33 McNally EM, Duggan D, Gorospe JR, Bonnemann CG, Fanin M, Pegoraro E, Lidov HG, Noguchi S, Ozawa E, Finkel RS *et al.* (1996) Mutations that disrupt the carboxyl-terminus of gamma-sarcoglycan cause muscular dystrophy. *Hum Mol Genet* **5**, 1841–1847.

34 Nigro V, de Sa Moreira E, Piluso G, Vainzof M, Belsito A, Politano L, Puca AA, Passos-Bueno MR & Zatz M (1996) Autosomal recessive limb-girdle muscular dystrophy, LGMD2F, is caused by a mutation in the delta-sarcoglycan gene. *Nat Genet* **14**, 195–198.

35 Noguchi S, McNally EM, Ben Othmane K, Hagiwara Y, Mizuno Y, Yoshida M, Yamamoto H, Bonnemann CG, Gussoni E, Denton PH *et al.* (1995) Mutations in the dystrophin-associated protein gamma-sarcoglycan in chromosome 13 muscular dystrophy. *Science* **270**, 819–822.

36 van Reeuwijk J, Janssen M, van den Elzen C, Beltran-Valero de Bernabe D, Sabatelli P, Merlini L, Boon M, Scheffer H, Brockington M, Muntoni F *et al.* (2005) POMT2 mutations cause alpha-dystroglycan hypoglycosylation and Walker–Warburg syndrome. *J Med Genet* **42**, 907–912.

37 Yoshida A, Kobayashi K, Manya H, Taniguchi K, Kano H, Mizuno M, Inazu T, Mitsuhashi H, Takahashi S, Takeuchi M *et al.* (2001) Muscular dystrophy and neuronal migration disorder caused by mutations in a glycosyltransferase, POMGnT1. *Dev Cell* **1**, 717–724.

38 Hayashi YK, Chou FL, Engvall E, Ogawa M, Matsuda C, Hirabayashi S, Yokochi K, Ziober BL, Kramer RH, Kaufman SJ *et al.* (1998) Mutations in the integrin alpha7 gene cause congenital myopathy. *Nat Genet* **19**, 94–97.

39 Longman C, Brockington M, Torelli S, Jimenez-Mallebrera C, Kennedy C, Khalil N, Feng L, Saran RK, Voit T, Merlini L *et al.* (2003) Mutations in the human *LARGE* gene cause MDC1D, a novel form of congenital muscular dystrophy with severe mental retardation and abnormal glycosylation of alpha-dystroglycan. *Hum Mol Genet* **12**, 2853–2861.

40 Jones KJ, Morgan G, Johnston H, Tobias V, Ouvrier RA, Wilkinson I & North KN (2001) The expanding phenotype of laminin alpha2 chain (merosin) abnormalities: case series and review. *J Med Genet* **38**, 649–657.

41 Mercuri E, Yuva Y, Brown SC, Brockington M, Kinali M, Jungbluth H, Feng L, Sewry CA & Muntoni F (2002) Collagen VI involvement in Ullrich syndrome: a clinical, genetic, and immunohistochemical study. *Neurology* **58**, 1354–1359.

42 Tome FM, Evangelista T, Leclerc A, Sunada Y, Manole E, Estournet B, Barois A, Campbell KP & Fardeau M (1994) Congenital muscular dystrophy with merosin deficiency. *CR Acad Sci III* **317**, 351–357.

43 Durbeej M & Campbell KP (2002) Muscular dystrophies involving the dystrophin–glycoprotein complex: an overview of current mouse models. *Curr Opin Genet Dev* **12**, 349–361.

44 Fassler R & Meyer M (1995) Consequences of lack of beta 1 integrin gene expression in mice. *Genes Dev* **9**, 1896–1908.

45 Williamson RA, Henry MD, Daniels KJ, Hrstka RF, Lee JC, Sunada Y, Ibraghimov-Beskrovnaya O & Campbell KP (1997) Dystroglycan is essential for early embryonic development: disruption of Reichert's membrane in Dag1-null mice. *Hum Mol Genet* **6**, 831–841.

46 Crosbie RH, Heighway J, Venzke DP, Lee JC & Campbell KP (1997) Sarcospan, the 25-kDa transmembrane component of the dystrophin–glycoprotein complex. *J Biol Chem* **272**, 31221–31224.

47 Marshall JL, Holmberg J, Chou E, Ocampo AC, Oh J, Lee J, Peter AK, Martin PT & Crosbie-Watson RH (2012) Sarcospan-dependent Akt activation is required for utrophin expression and muscle regeneration. *J Cell Biol* **197**, 1009–1027.
48 Peter AK, Marshall JL & Crosbie RH (2008) Sarcospan reduces dystrophic pathology: stabilization of the utrophin–glycoprotein complex. *J Cell Biol* **183**, 419–427.
49 Hoffman EP, Knudson CM, Campbell KP & Kunkel LM (1987) Subcellular fractionation of dystrophin to the triads of skeletal muscle. *Nature* **330**, 754–758.
50 Zubrzycka-Gaarn EE, Bulman DE, Karpati G, Burghes AH, Belfall B, Klamut HJ, Talbot J, Hodges RS, Ray PN & Worton RG (1988) The Duchenne muscular dystrophy gene product is localized in sarcolemma of human skeletal muscle. *Nature* **333**, 466–469.
51 Miike T, Miyatake M, Zhao J, Yoshioka K & Uchino M (1989) Immunohistochemical dystrophin reaction in synaptic regions. *Brain Dev* **11**, 344–346.
52 Samitt CE & Bonilla E (1990) Immunocytochemical study of dystrophin at the myotendinous junction. *Muscle Nerve* **13**, 493–500.
53 Zhao J, Yoshioka K, Miyatake M & Miike T (1992) Dystrophin and a dystrophin-related protein in intrafusal muscle fibers, and neuromuscular and myotendinous junctions. *Acta Neuropathol* **84**, 141–146.
54 Matsumura K, Ervasti JM, Ohlendieck K, Kahl SD & Campbell KP (1992) Association of dystrophin-related protein with dystrophin-associated proteins in mdx mouse muscle. *Nature* **360**, 588–591.
55 Prochniewicz E, Henderson D, Ervasti JM & Thomas DD (2009) Dystrophin and utrophin have distinct effects on the structural dynamics of actin. *Proc Natl Acad Sci USA* **106**, 7822–7827.
56 Rybakova IN, Humston JL, Sonnemann KJ & Ervasti JM (2006) Dystrophin and utrophin bind actin through distinct modes of contact. *J Biol Chem* **281**, 9996–10001.
57 Li D, Bareja A, Judge L, Yue Y, Lai Y, Fairclough R, Davies KE, Chamberlain JS & Duan D (2010) Sarcolemmal nNOS anchoring reveals a qualitative difference between dystrophin and utrophin. *J Cell Sci* **123**, 2008–2013.
58 Durko M, Allen C, Nalbantoglu J & Karpati G (2010) CT-GalNAc transferase overexpression in adult mice is associated with extrasynaptic utrophin in skeletal muscle fibres. *J Muscle Res Cell Motil* **31**, 181–193.
59 Nguyen HH, Jayasinha V, Xia B, Hoyte K & Martin PT (2002) Overexpression of the cytotoxic T cell GalNAc transferase in skeletal muscle inhibits muscular dystrophy in mdx mice. *Proc Natl Acad Sci USA* **99**, 5616–5621.
60 Xia B, Hoyte K, Kammesheidt A, Deerinck T, Ellisman M & Martin PT (2002) Overexpression of the CT GalNAc transferase in skeletal muscle alters myofiber growth, neuromuscular structure, and laminin expression. *Dev Biol* **242**, 58–73.
61 Legate KR, Montanez E, Kudlacek O & Fassler R (2006) ILK, PINCH and parvin: the tIPP of integrin signalling. *Nat Rev Mol Cell Biol* **7**, 20–31.
62 Hannigan G, Troussard AA & Dedhar S (2005) Integrin-linked kinase: a cancer therapeutic target unique among its ILK. *Nat Rev Cancer* **5**, 51–63.
63 Wu C (2005) PINCH, N(i)ck and the ILK: network wiring at cell-matrix adhesions. *Trends Cell Biol* **15**, 460–466.
64 McDonald PC, Fielding AB & Dedhar S (2008) Integrin-linked kinase – essential roles in physiology and cancer biology. *J Cell Sci* **121**, 3121–3132.
65 Gheyara AL, Vallejo-Illarramendi A, Zang K, Mei L, St-Arnaud R, Dedhar S & Reichardt LF (2007) Deletion of integrin-linked kinase from skeletal muscles of mice resembles muscular dystrophy due to alpha 7 beta 1-integrin deficiency. *Am J Pathol* **171**, 1966–1977.
66 Smirnov SP, McDearmon EL, Li S, Ervasti JM, Tryggvason K & Yurchenco PD (2002) Contributions of the LG modules and furin processing to laminin-2 functions. *J Biol Chem* **277**, 18928–18937.
67 Talts JF, Mann K, Yamada Y & Timpl R (1998) Structural analysis and proteolytic processing of recombinant G domain of mouse laminin alpha2 chain. *FEBS Lett* **426**, 71–76.
68 Talts JF, Andac Z, Gohring W, Brancaccio A & Timpl R (1999) Binding of the G domains of laminin alpha1 and alpha2 chains and perlecan to heparin, sulfatides, alpha-dystroglycan and several extracellular matrix proteins. *EMBO J* **18**, 863–870.
69 Holmberg J & Durbeej M (2013) Laminin-211 in skeletal muscle function. *Cell Adh Migr* **7**, 111–121.
70 Gawlik KI & Durbeej M (2011) Skeletal muscle laminin and MDC1A: pathogenesis and treatment strategies. *Skelet Muscle* **1**, 9.
71 Tanabe Y, Esaki K & Nomura T (1986) Skeletal muscle pathology in X chromosome-linked muscular dystrophy (mdx) mouse. *Acta Neuropathol* **69**, 91–95.
72 Grady RM, Teng H, Nichol MC, Cunningham JC, Wilkinson RS & Sanes JR (1997) Skeletal and cardiac myopathies in mice lacking utrophin and dystrophin: a model for Duchenne muscular dystrophy. *Cell* **90**, 729–738.
73 Deconinck AE, Rafael JA, Skinner JA, Brown SC, Potter AC, Metzinger L, Watt DJ, Dickson JG, Tinsley JM & Davies KE (1997) Utrophin–dystrophin-deficient mice as a model for Duchenne muscular dystrophy. *Cell* **90**, 717–727.
74 Rooney JE, Welser JV, Dechert MA, Flintoff-Dye NL, Kaufman SJ & Burkin DJ (2006) Severe muscular

dystrophy in mice that lack dystrophin and alpha7 integrin. *J Cell Sci* **119**, 2185–2195.
75 Guo C, Willem M, Werner A, Raivich G, Emerson M, Neyses L & Mayer U (2006) Absence of alpha 7 integrin in dystrophin-deficient mice causes a myopathy similar to Duchenne muscular dystrophy. *Hum Mol Genet* **15**, 989–998.
76 Liu J, Milner DJ, Boppart MD, Ross RS & Kaufman SJ (2012) beta1D chain increases alpha7beta1 integrin and laminin and protects against sarcolemmal damage in mdx mice. *Hum Mol Genet* **21**, 1592–1603.
77 Tinsley J, Deconinck N, Fisher R, Kahn D, Phelps S, Gillis JM & Davies K (1998) Expression of full-length utrophin prevents muscular dystrophy in mdx mice. *Nat Med* **4**, 1441–1444.
78 Poysky J (2007) Behavior patterns in Duchenne muscular dystrophy: report on the Parent Project Muscular Dystrophy behavior workshop 8–9 December 2006, Philadelphia, USA. *Neuromuscul Disord* **17**, 986–994.
79 Perronnet C, Chagneau C, Le Blanc P, Samson-Desvignes N, Mornet D, Laroche S, De La Porte S & Vaillend C (2012) Upregulation of brain utrophin does not rescue behavioral alterations in dystrophin-deficient mice. *Hum Mol Genet* **21**, 2263–2276.
80 Goyenvalle A, Seto JT, Davies KE & Chamberlain J (2011) Therapeutic approaches to muscular dystrophy. *Hum Mol Genet* **20**, R69–R78.
81 Mendell JR, Campbell K, Rodino-Klapac L, Sahenk Z, Shilling C, Lewis S, Bowles D, Gray S, Li C, Galloway G *et al.* (2010) Dystrophin immunity in Duchenne's muscular dystrophy. *N Engl J Med* **363**, 1429–1437.
82 Tinsley JM, Fairclough RJ, Storer R, Wilkes FJ, Potter AC, Squire SE, Powell DS, Cozzoli A, Capogrosso RF, Lambert A *et al.* (2011) Daily treatment with SMTC1100, a novel small molecule utrophin upregulator, dramatically reduces the dystrophic symptoms in the mdx mouse. *PLoS ONE* **6**, e19189.
83 Casar JC, McKechnie BA, Fallon JR, Young MF & Brandan E (2004) Transient up-regulation of biglycan during skeletal muscle regeneration: delayed fiber growth along with decorin increase in biglycan-deficient mice. *Dev Biol* **268**, 358–371.
84 Lechner BE, Lim JH, Mercado ML & Fallon JR (2006) Developmental regulation of biglycan expression in muscle and tendon. *Muscle Nerve* **34**, 347–355.
85 Amenta AR, Yilmaz A, Bogdanovich S, McKechnie BA, Abedi M, Khurana TS & Fallon JR (2011) Biglycan recruits utrophin to the sarcolemma and counters dystrophic pathology in mdx mice. *Proc Natl Acad Sci USA* **108**, 762–767.
86 Goudenege S, Lamarre Y, Dumont N, Rousseau J, Frenette J, Skuk D & Tremblay JP (2010) Laminin-111: a potential therapeutic agent for Duchenne muscular dystrophy. *Mol Ther* **18**, 2155–2163.
87 Rooney JE, Gurpur PB, Yablonka-Reuveni Z & Burkin DJ (2009) Laminin-111 restores regenerative capacity in a mouse model for alpha7 integrin congenital myopathy. *Am J Pathol* **174**, 256–264.
88 Rooney JE, Knapp JR, Hodges BL, Wuebbles RD & Burkin DJ (2012) Laminin-111 protein therapy reduces muscle pathology and improves viability of a mouse model of merosin-deficient congenital muscular dystrophy. *Am J Pathol* **180**, 1593–1602.
89 Rooney JE, Gurpur PB & Burkin DJ (2009) Laminin-111 protein therapy prevents muscle disease in the mdx mouse model for Duchenne muscular dystrophy. *Proc Natl Acad Sci USA* **106**, 7991–7996.
90 Marshall JL, Chou E, Oh J, Kwok A, Burkin DJ & Crosbie-Watson RH (2012) Dystrophin and utrophin expression require sarcospan: loss of alpha7 integrin exacerbates a newly discovered muscle phenotype in sarcospan-null mice. *Hum Mol Genet* **21**, 4378–4393.
91 Han R, Kanagawa M, Yoshida-Moriguchi T, Rader EP, Ng RA, Michele DE, Muirhead DE, Kunz S, Moore SA, Iannaccone ST *et al.* (2009) Basal lamina strengthens cell membrane integrity via the laminin G domain-binding motif of alpha-dystroglycan. *Proc Natl Acad Sci USA* **106**, 12573–12579.
92 Moghadaszadeh B, Albrechtsen R, Guo LT, Zaik M, Kawaguchi N, Borup RH, Kronqvist P, Schroder HD, Davies KE, Voit T *et al.* (2003) Compensation for dystrophin-deficiency: ADAM12 overexpression in skeletal muscle results in increased alpha 7 integrin, utrophin and associated glycoproteins. *Hum Mol Genet* **12**, 2467–2479.
93 Galliano MF, Huet C, Frygelius J, Polgren A, Wewer UM & Engvall E (2000) Binding of ADAM12, a marker of skeletal muscle regeneration, to the muscle-specific actin-binding protein, alpha-actinin-2, is required for myoblast fusion. *J Biol Chem* **275**, 13933–13939.
94 Kronqvist P, Kawaguchi N, Albrechtsen R, Xu X, Schroder HD, Moghadaszadeh B, Nielsen FC, Frohlich C, Engvall E & Wewer UM (2002) ADAM12 alleviates the skeletal muscle pathology in mdx dystrophic mice. *Am J Pathol* **161**, 1535–1540.
95 Yagami-Hiromasa T, Sato T, Kurisaki T, Kamijo K, Nabeshima Y & Fujisawa-Sehara A (1995) A metalloprotease-disintegrin participating in myoblast fusion. *Nature* **377**, 652–656.
96 Grewal PK & Hewitt JE (2002) Mutation of *Large*, which encodes a putative glycosyltransferase, in an animal model of muscular dystrophy. *Biochim Biophys Acta* **1573**, 216–224.
97 Burkin DJ, Wallace GQ, Nicol KJ, Kaufman DJ & Kaufman SJ (2001) Enhanced expression of the alpha 7 beta 1 integrin reduces muscular dystrophy

and restores viability in dystrophic mice. *J Cell Biol* **152**, 1207–1218.
98 Mercuri E & Muntoni F (2012) The ever-expanding spectrum of congenital muscular dystrophies. *Ann Neurol* **72**, 9–17.
99 Beltran-Valero de Bernabe D, Currier S, Steinbrecher A, Celli J, van Beusekom E, van der Zwaag B, Kayserili H, Merlini L, Chitayat D, Dobyns WB *et al.* (2002) Mutations in the *O*-mannosyltransferase gene *POMT1* give rise to the severe neuronal migration disorder Walker–Warburg syndrome. *Am J Hum Genet* **71**, 1033–1043.
100 Beltran-Valero de Bernabe D, Voit T, Longman C, Steinbrecher A, Straub V, Yuva Y, Herrmann R, Sperner J, Korenke C, Diesen C *et al.* (2004) Mutations in the *FKRP* gene can cause muscle-eye–brain disease and Walker–Warburg syndrome. *J Med Genet* **41**, e61.
101 Brockington M, Blake DJ, Prandini P, Brown SC, Torelli S, Benson MA, Ponting CP, Estournet B, Romero NB, Mercuri E *et al.* (2001) Mutations in the fukutin-related protein gene (*FKRP*) cause a form of congenital muscular dystrophy with secondary laminin alpha2 deficiency and abnormal glycosylation of alpha-dystroglycan. *Am J Hum Genet* **69**, 1198–1209.
102 Kobayashi K, Nakahori Y, Miyake M, Matsumura K, Kondo-Iida E, Nomura Y, Segawa M, Yoshioka M, Saito K, Osawa M *et al.* (1998) An ancient retrotransposal insertion causes Fukuyama-type congenital muscular dystrophy. *Nature* **394**, 388–392.
103 Roscioli T, Kamsteeg EJ, Buysse K, Maystadt I, van Reeuwijk J, van den Elzen C, van Beusekom E, Riemersma M, Pfundt R, Vissers LE *et al.* (2012) Mutations in *ISPD* cause Walker–Warburg syndrome and defective glycosylation of alpha-dystroglycan. *Nat Genet* **44**, 581–585.
104 Silan F, Yoshioka M, Kobayashi K, Simsek E, Tunc M, Alper M, Cam M, Guven A, Fukuda Y, Kinoshita M *et al.* (2003) A new mutation of the *fukutin* gene in a non-Japanese patient. *Ann Neurol* **53**, 392–396.
105 van Reeuwijk J, Brunner HG & van Bokhoven H (2005) Glyc-O-genetics of Walker–Warburg syndrome. *Clin Genet* **67**, 281–289.
106 van Reeuwijk J, Grewal PK, Salih MA, Beltran-Valero de Bernabe D, McLaughlan JM, Michielse CB, Herrmann R, Hewitt JE, Steinbrecher A, Seidahmed MZ *et al.* (2007) Intragenic deletion in the *LARGE* gene causes Walker–Warburg syndrome. *Hum Genet* **121**, 685–690.
107 Willer T, Lee H, Lommel M, Yoshida-Moriguchi T, de Bernabe DB, Venzke D, Cirak S, Schachter H, Vajsar J, Voit T *et al.* (2012) ISPD loss-of-function mutations disrupt dystroglycan *O*-mannosylation and cause Walker–Warburg syndrome. *Nat Genet* **44**, 575–580.
108 Stevens E, Carss KJ, Cirak S, Foley AR, Torelli S, Willer T, Tambunan DE, Yau S, Brodd L, Sewry CA *et al.* (2013) Mutations in *B3GALNT2* cause congenital muscular dystrophy and hypoglycosylation of alpha-dystroglycan. *Am J Hum Genet* **92**, 354–365.
109 Barone R, Aiello C, Race V, Morava E, Foulquier F, Riemersma M, Passarelli C, Concolino D, Carella M, Santorelli F *et al.* (2012) DPM2-CDG: a muscular dystrophy–dystroglycanopathy syndrome with severe epilepsy. *Ann Neurol* **72**, 550–558.
110 Lefeber DJ, Schonberger J, Morava E, Guillard M, Huyben KM, Verrijp K, Grafakou O, Evangeliou A, Preijers FW, Manta P *et al.* (2009) Deficiency of Dol-P-Man synthase subunit DPM3 bridges the congenital disorders of glycosylation with the dystroglycanopathies. *Am J Hum Genet* **85**, 76–86.
111 Lefeber DJ, de Brouwer AP, Morava E, Riemersma M, Schuurs-Hoeijmakers JH, Absmanner B, Verrijp K, van den Akker WM, Huijben K, Steenbergen G *et al.* (2011) Autosomal recessive dilated cardiomyopathy due to DOLK mutations results from abnormal dystroglycan O-mannosylation. *PLoS Genet* **7**, e1002427.
112 Manzini MC, Tambunan DE, Hill RS, Yu TW, Maynard TM, Heinzen EL, Shianna KV, Stevens CR, Partlow JN, Barry BJ *et al.* (2012) Exome sequencing and functional validation in zebrafish identify *GTDC2* mutations as a cause of Walker–Warburg syndrome. *Am J Hum Genet* **91**, 541–547.
113 Vuillaumier-Barrot S, Bouchet-Seraphin C, Chelbi M, Devisme L, Quentin S, Gazal S, Laquerriere A, Fallet-Bianco C, Loget P, Odent S *et al.* (2012) Identification of mutations in *TMEM5* and *ISPD* as a cause of severe cobblestone lissencephaly. *Am J Hum Genet* **91**, 1135–1143.
114 Jurado LA, Coloma A & Cruces J (1999) Identification of a human homolog of the *Drosophila* rotated abdomen gene (*POMT1*) encoding a putative protein *O*-mannosyl-transferase, and assignment to human chromosome 9q34.1. *Genomics* **58**, 171–180.
115 Willer T, Amselgruber W, Deutzmann R & Strahl S (2002) Characterization of POMT2, a novel member of the PMT protein *O*-mannosyltransferase family specifically localized to the acrosome of mammalian spermatids. *Glycobiology* **12**, 771–783.
116 Yoshida-Moriguchi T, Yu L, Stalnaker SH, Davis S, Kunz S, Madson M, Oldstone MB, Schachter H, Wells L & Campbell KP (2010) *O*-Mannosyl phosphorylation of alpha-dystroglycan is required for laminin binding. *Science* **327**, 88–92.
117 Brockington M, Torelli S, Prandini P, Boito C, Dolatshad NF, Longman C, Brown SC & Muntoni F (2005) Localization and functional analysis of the LARGE family of glycosyltransferases: significance for muscular dystrophy. *Hum Mol Genet* **14**, 657–665.

118 Kanagawa M, Saito F, Kunz S, Yoshida-Moriguchi T, Barresi R, Kobayashi YM, Muschler J, Dumanski JP, Michele DE, Oldstone MB *et al.* (2004) Molecular recognition by LARGE is essential for expression of functional dystroglycan. *Cell* **117**, 953–964.

119 Inamori K, Yoshida-Moriguchi T, Hara Y, Anderson ME, Yu L & Campbell KP (2012) Dystroglycan function requires xylosyl- and glucuronyltransferase activities of LARGE. *Science* **335**, 93–96.

120 Brockington M, Yuva Y, Prandini P, Brown SC, Torelli S, Benson MA, Herrmann R, Anderson LV, Bashir R, Burgunder JM *et al.* (2001) Mutations in the fukutin-related protein gene (*FKRP*) identify limb girdle muscular dystrophy 2I as a milder allelic variant of congenital muscular dystrophy MDC1C. *Hum Mol Genet* **10**, 2851–2859.

121 Shridas P & Waechter CJ (2006) Human dolichol kinase, a polytopic endoplasmic reticulum membrane protein with a cytoplasmically oriented CTP-binding site. *J Biol Chem* **281**, 31696–31704.

122 Maeda Y, Tanaka S, Hino J, Kangawa K & Kinoshita T (2000) Human dolichol-phosphate-mannose synthase consists of three subunits, DPM1, DPM2 and DPM3. *EMBO J* **19**, 2475–2482.

123 Maeda Y, Tomita S, Watanabe R, Ohishi K & Kinoshita T (1998) DPM2 regulates biosynthesis of dolichol phosphate-mannose in mammalian cells: correct subcellular localization and stabilization of DPM1, and binding of dolichol phosphate. *EMBO J* **17**, 4920–4929.

124 Burda P & Aebi M (1999) The dolichol pathway of N-linked glycosylation. *Biochim Biophys Acta* **1426**, 239–257.

125 Manya H, Chiba A, Yoshida A, Wang X, Chiba Y, Jigami Y, Margolis RU & Endo T (2004) Demonstration of mammalian protein *O*-mannosyltransferase activity: coexpression of POMT1 and POMT2 required for enzymatic activity. *Proc Natl Acad Sci USA* **101**, 500–505.

126 Buysse K, Riemersma M, Powell G, van Reeuwijk J, Chitayat D, Roscioli T, Kamsteeg EJ, van den Elzen C, van Beusekom E, Blaser S *et al.* (2013) Missense mutations in beta-1,3-*N*-acetylglucosaminyltransferase 1 (B3GNT1) cause Walker–Warburg syndrome. *Hum Mol Genet* **22**, 1746–1754.

127 Dobson CM, Hempel SJ, Stalnaker SH, Stuart R & Wells L (2012) *O*-Mannosylation and human disease. *Cell Mol Life Sci* doi:10.1007/s00018-012-1193-0.

128 Yis U, Uyanik G, Heck PB, Smitka M, Nobel H, Ebinger F, Dirik E, Feng L, Kurul SH, Brocke K *et al.* (2011) Fukutin mutations in non-Japanese patients with congenital muscular dystrophy: less severe mutations predominate in patients with a non-Walker–Warburg phenotype. *Neuromuscul Disord* **21**, 20–30.

129 Hehr U, Uyanik G, Gross C, Walter MC, Bohring A, Cohen M, Oehl-Jaschkowitz B, Bird LM, Shamdeen GM, Bogdahn U *et al.* (2007) Novel *POMGnT1* mutations define broader phenotypic spectrum of muscle–eye–brain disease. *Neurogenetics* **8**, 279–288.

130 Brockington S & Clarke A (2001) The relative influence of temperature and food on the metabolism of a marine invertebrate. *J Exp Mar Bio Ecol* **258**, 87–99.

131 Smith PL & Lowe JB (1994) Molecular cloning of a murine N-acetylgalactosamine transferase cDNA that determines expression of the T lymphocyte-specific CT oligosaccharide differentiation antigen. *J Biol Chem* **269**, 15162–15171.

132 Deconinck N, Tinsley J, De Backer F, Fisher R, Kahn D, Phelps S, Davies K & Gillis JM (1997) Expression of truncated utrophin leads to major functional improvements in dystrophin-deficient muscles of mice. *Nat Med* **3**, 1216–1221.

133 Gilbert R, Nalbantoglu J, Petrof BJ, Ebihara S, Guibinga GH, Tinsley JM, Kamen A, Massie B, Davies KE & Karpati G (1999) Adenovirus-mediated utrophin gene transfer mitigates the dystrophic phenotype of mdx mouse muscles. *Hum Gene Ther* **10**, 1299–1310.

134 Rafael JA, Tinsley JM, Potter AC, Deconinck AE & Davies KE (1998) Skeletal muscle-specific expression of a utrophin transgene rescues utrophin-dystrophin deficient mice. *Nat Genet* **19**, 79–82.

135 Tinsley JM, Potter AC, Phelps SR, Fisher R, Trickett JI & Davies KE (1996) Amelioration of the dystrophic phenotype of mdx mice using a truncated utrophin transgene. *Nature* **384**, 349–353.

136 Xu R, Chandrasekharan K, Yoon JH, Camboni M & Martin PT (2007) Overexpression of the cytotoxic T cell (CT) carbohydrate inhibits muscular dystrophy in the dyW mouse model of congenital muscular dystrophy 1A. *Am J Pathol* **171**, 181–199.

137 Xu R, DeVries S, Camboni M & Martin PT (2009) Overexpression of Galgt2 reduces dystrophic pathology in the skeletal muscles of alpha sarcoglycan-deficient mice. *Am J Pathol* **175**, 235–247.

138 Singhal N, Xu R & Martin PT (2012) Distinct contributions of Galgt1 and Galgt2 to carbohydrate expression and function at the mouse neuromuscular junction. *Mol Cell Neurosci* **51**, 112–126.

139 Cabrera PV, Pang M, Marshall JL, Kung R, Nelson SF, Stalnaker SH, Wells L, Crosbie-Watson RH & Baum LG (2012) High throughput screening for compounds that alter muscle cell glycosylation identifies new role for N-glycans in regulating sarcolemmal protein abundance and laminin binding. *J Biol Chem* **287**, 22759–22770.

140 Santha E, Sperlagh B, Zelles T, Zsilla G, Toth PT, Lendvai B, Baranyi M & Vizi ES (2000) Multiple

cellular mechanisms mediate the effect of lobeline on the release of norepinephrine. *J Pharmacol Exp Ther* **294**, 302–307.
141 Dwoskin LP & Crooks PA (2002) A novel mechanism of action and potential use for lobeline as a treatment for psychostimulant abuse. *Biochem Pharmacol* **63**, 89–98.
142 Wilhelm CJ, Johnson RA, Eshleman AJ & Janowsky A (2008) Lobeline effects on tonic and methamphetamine-induced dopamine release. *Biochem Pharmacol* **75**, 1411–1415.
143 Lee WC, Kang D, Causevic E, Herdt AR, Eckman EA & Eckman CB (2010) Molecular characterization of mutations that cause globoid cell leukodystrophy and pharmacological rescue using small molecule chemical chaperones. *J Neurosci* **30**, 5489–5497.
144 Bulfield G, Siller WG, Wight PA & Moore KJ (1984) X chromosome-linked muscular dystrophy (mdx) in the mouse. *Proc Natl Acad Sci USA* **81**, 1189–1192.
145 Sicinski P, Geng Y, Ryder-Cook AS, Barnard EA, Darlison MG & Barnard PJ (1989) The molecular basis of muscular dystrophy in the mdx mouse: a point mutation. *Science* **244**, 1578–1580.
146 Chamberlain JS, Pearlman JA, Muzny DM, Gibbs RA, Ranier JE, Caskey CT & Reeves AA (1988) Expression of the murine Duchenne muscular dystrophy gene in muscle and brain. *Science* **239**, 1416–1418.
147 Chelly J, Gilgenkrantz H, Lambert M, Hamard G, Chafey P, Recan D, Katz P, de la Chapelle A, Koenig M, Ginjaar IB *et al.* (1990) Effect of dystrophin gene deletions on mRNA levels and processing in Duchenne and Becker muscular dystrophies. *Cell* **63**, 1239–1248.
148 Ginjaar IB, Bakker E, van Paassen MM, den Dunnen JT, Wessels A, Zubrzycka-Gaarn EE, Moorman AF & van Ommen GJ (1991) Immunohistochemical studies show truncated dystrophins in the myotubes of three fetuses at risk for Duchenne muscular dystrophy. *J Med Genet* **28**, 505–510.
149 Jones BR, Brennan S, Mooney CT, Callanan JJ, McAllister H, Guo LT, Martin PT, Engvall E & Shelton GD (2004) Muscular dystrophy with truncated dystrophin in a family of Japanese Spitz dogs. *J Neurol Sci* **217**, 143–149.
150 Helliwell TR, Ellis JM, Mountford RC, Appleton RE & Morris GE (1992) A truncated dystrophin lacking the C-terminal domains is localized at the muscle membrane. *Am J Hum Genet* **50**, 508–514.
151 Jung D, Yang B, Meyer J, Chamberlain JS & Campbell KP (1995) Identification and characterization of the dystrophin anchoring site on beta-dystroglycan. *J Biol Chem* **270**, 27305–27310.
152 Banks GB, Gregorevic P, Allen JM, Finn EE & Chamberlain JS (2007) Functional capacity of dystrophins carrying deletions in the N-terminal actin-binding domain. *Hum Mol Genet* **16**, 2105–2113.
153 Imamura M, Araishi K, Noguchi S & Ozawa E (2000) A sarcoglycan-dystroglycan complex anchors Dp116 and utrophin in the peripheral nervous system. *Hum Mol Genet* **9**, 3091–3100.
154 Cox GA, Sunada Y, Campbell KP & Chamberlain JS (1994) Dp71 can restore the dystrophin-associated glycoprotein complex in muscle but fails to prevent dystrophy. *Nat Genet* **8**, 333–339.
155 Michele DE, Barresi R, Kanagawa M, Saito F, Cohn RD, Satz JS, Dollar J, Nishino I, Kelley RI, Somer H *et al.* (2002) Post-translational disruption of dystroglycan–ligand interactions in congenital muscular dystrophies. *Nature* **418**, 417–422.
156 Tachikawa M, Kanagawa M, Yu CC, Kobayashi K & Toda T (2012) Mislocalization of fukutin protein by disease-causing missense mutations can be rescued with treatments directed at folding amelioration. *J Biol Chem* **287**, 8398–8406.
157 Singh S & Aggarwal BB (1995) Activation of transcription factor NF-kappa B is suppressed by curcumin (diferuloylmethane) [corrected]. *J Biol Chem* **270**, 24995–25000.
158 Monici MC, Aguennouz M, Mazzeo A, Messina C & Vita G (2003) Activation of nuclear factor-kappaB in inflammatory myopathies and Duchenne muscular dystrophy. *Neurology* **60**, 993–997.
159 Pan Y, Chen C, Shen Y, Zhu CH, Wang G, Wang XC, Chen HQ & Zhu MS (2008) Curcumin alleviates dystrophic muscle pathology in mdx mice. *Mol Cells* **25**, 531–537.
160 Durham WJ, Arbogast S, Gerken E, Li YP & Reid MB (2006) Progressive nuclear factor-kappaB activation resistant to inhibition by contraction and curcumin in mdx mice. *Muscle Nerve* **34**, 298–303.
161 Soheili T, Gicquel E, Poupiot J, N'Guyen L, Le Roy F, Bartoli M & Richard I (2012) Rescue of sarcoglycan mutations by inhibition of endoplasmic reticulum quality control is associated with minimal structural modifications. *Hum Mutat* **33**, 429–439.
162 Wang F, Song W, Brancati G & Segatori L (2011) Inhibition of endoplasmic reticulum-associated degradation rescues native folding in loss of function protein misfolding diseases. *J Biol Chem* **286**, 43454–43464.
163 Schlesinger MJ (1990) Heat shock proteins. *J Biol Chem* **265**, 12111–12114.
164 Bornman L, Polla BS, Lotz BP & Gericke GS (1995) Expression of heat-shock/stress proteins in Duchenne muscular dystrophy. *Muscle Nerve* **18**, 23–31.
165 Stary CM, Walsh BJ, Knapp AE, Brafman D & Hogan MC (2008) Elevation in heat shock protein 72 mRNA following contractions in isolated single

skeletal muscle fibers. *Am J Physiol Regul Integr Comp Physiol* **295**, R642–R648.
166 Carmeli E, Beiker R, Maor M & Kodesh E (2010) Increased iNOS, MMP-2, and HSP-72 in skeletal muscle following high-intensity exercise training. *J Basic Clin Physiol Pharmacol* **21**, 127–146.
167 Gehrig SM, van der Poel C, Sayer TA, Schertzer JD, Henstridge DC, Church JE, Lamon S, Russell AP, Davies KE, Febbraio MA *et al.* (2012) Hsp72 preserves muscle function and slows progression of severe muscular dystrophy. *Nature* **484**, 394–398.
168 Glickman MH & Ciechanover A (2002) The ubiquitin–proteasome proteolytic pathway: destruction for the sake of construction. *Physiol Rev* **82**, 373–428.
169 Bonuccelli G, Sotgia F, Capozza F, Gazzerro E, Minetti C & Lisanti MP (2007) Localized treatment with a novel FDA-approved proteasome inhibitor blocks the degradation of dystrophin and dystrophin-associated proteins in mdx mice. *Cell Cycle* **6**, 1242–1248.
170 Bonuccelli G, Sotgia F, Schubert W, Park DS, Frank PG, Woodman SE, Insabato L, Cammer M, Minetti C & Lisanti MP (2003) Proteasome inhibitor (MG-132) treatment of mdx mice rescues the expression and membrane localization of dystrophin and dystrophin-associated proteins. *Am J Pathol* **163**, 1663–1675.
171 Selsby J, Morris C, Morris L & Sweeney L (2012) A proteasome inhibitor fails to attenuate dystrophic pathology in mdx mice. *PLoS Curr* **4**, e4f84a944d8930.
172 Braakman I & Bulleid NJ (2011) Protein folding and modification in the mammalian endoplasmic reticulum. *Annu Rev Biochem* **80**, 71–99.
173 Mendell JR, Rodino-Klapac LR, Rosales XQ, Coley BD, Galloway G, Lewis S, Malik V, Shilling C, Byrne BJ, Conlon T *et al.* (2010) Sustained alpha-sarcoglycan gene expression after gene transfer in limb-girdle muscular dystrophy, type 2D. *Ann Neurol* **68**, 629–638.
174 Mendell JR, Rodino-Klapac L, Sahenk Z, Malik V, Kaspar BK, Walker CM & Clark KR (2012) Gene therapy for muscular dystrophy: lessons learned and path forward. *Neurosci Lett* **527**, 90–99.
175 Blankinship MJ, Gregorevic P, Allen JM, Harper SQ, Harper H, Halbert CL, Miller AD & Chamberlain JS (2004) Efficient transduction of skeletal muscle using vectors based on adeno-associated virus serotype 6. *Mol Ther* **10**, 671–678.
176 Zincarelli C, Soltys S, Rengo G, Koch WJ & Rabinowitz JE (2010) Comparative cardiac gene delivery of adeno-associated virus serotypes 1–9 reveals that AAV6 mediates the most efficient transduction in mouse heart. *Clin Transl Sci* **3**, 81–89.
177 Brennan KJ & Hardeman EC (1993) Quantitative analysis of the human alpha-skeletal actin gene in transgenic mice. *J Biol Chem* **268**, 719–725.
178 Kendall GC, Mokhonova EI, Moran M, Sejbuk NE, Wang DW, Silva O, Wang RT, Martinez L, Lu QL, Damoiseaux R *et al.* (2012) Dantrolene enhances antisense-mediated exon skipping in human and mouse models of Duchenne muscular dystrophy. *Sci Transl Med* **4**, 164ra160.
179 Marshall JL & Watson RH (2013) Sarcospan: a small protein with large potential for Duchenne muscular dystrophy. *Skelet Muscle* **3**, 1.
180 Kim MH, Kay DI, Rudra RT, Chen BM, Hsu N, Izumiya Y, Martinez L, Spencer MJ, Walsh K, Grinnell AD *et al.* (2011) Myogenic Akt signaling attenuates muscular degeneration, promotes myofiber regeneration and improves muscle function in dystrophin-deficient mdx mice. *Hum Mol Genet* **20**, 1324–1338.
181 Peter AK, Ko CY, Kim MH, Hsu N, Ouchi N, Rhie S, Izumiya Y, Zeng L, Walsh K & Crosbie RH (2009) Myogenic Akt signaling upregulates the utrophin–glycoprotein complex and promotes sarcolemma stability in muscular dystrophy. *Hum Mol Genet* **18**, 318–327.

CHAPTER THREE

Differentiation-related glycan epitopes identify discrete domains of the muscle glycocalyx

This chapter is reprinted from *Glycobiology*, 2016, vol. 26, no. 10, 1120-1132, with copyright permission from Oxford University Press.

Glycobiology, 2016, vol. 26, no. 10, 1120–1132
doi: 10.1093/glycob/cww061
Advance Access Publication Date: 28 May 2016
Original Article

OXFORD

Translational Glycobiology

Differentiation-related glycan epitopes identify discrete domains of the muscle glycocalyx

Brian J McMorran[2], Francis E McCarthy[2], Elizabeth M Gibbs[3], Mabel Pang[2], Jamie L Marshall[4], Alison V Nairn[5], Kelley W Moremen[5], Rachelle H Crosbie-Watson[3], and Linda G Baum[2,1]

[2]Department of Pathology and Laboratory Medicine, David Geffen School of Medicine, University of California Los Angeles, Los Angeles, CA 90095, USA, [3]Department of Integrative Biology and Physiology, University of California Los Angeles, Los Angeles, CA 90095, USA, [4]Program in Medical and Population Genetics, The Broad Institute of MIT and Harvard, Cambridge, MA 02142, USA, and [5]Department of Biochemistry and Molecular Biology, University of Georgia, Athens, GA 30602, USA

[1]To whom correspondence should be addressed: Tel: +1-310-206-5985; Fax: +1-310-206-0657; e-mail: lbaum@mednet.ucla.edu

Received 3 March 2016; Revised 10 May 2016; Accepted 23 May 2016

Abstract

The neuromuscular junction (NMJ) is enriched with glycoproteins modified with *N*-acetylgalactosamine (GalNAc) residues, and four nominally GalNAc-specific plant lectins have historically been used to identify the NMJ and the utrophin–glycoprotein complex. However, little is known about the specific glycan epitopes on skeletal muscle that are bound by these lectins, the glycoproteins that bear these epitopes or how creation of these glycan epitopes is regulated. Here, we profile changes in cell surface glycosylation during muscle cell differentiation and identify distinct differences in the binding preferences of GalNAc-specific lectins, *Wisteria floribunda* agglutinin (WFA), *Vicia villosa* agglutinin (VVA), soybean agglutinin (SBA) and *Dolichos biflorus* agglutinin (DBA). While we find that all four GalNAc binding lectins specifically label the NMJ, each of the four lectins binds distinct sets of muscle glycoproteins; furthermore, none of the major adhesion complexes are required for binding of any of the four GalNAc-specific lectins. Analysis of glycosylation-related transcripts identified target glycosyltransferases and glycosidases that could potentially create GalNAc-containing epitopes; reducing expression of these transcripts by siRNA highlighted differences in lectin binding specificities. In addition, we found that complex *N*-glycans are required for binding of WFA and SBA to murine C2C12 myotubes and for WFA binding to wild-type skeletal muscle, but not for binding of VVA or DBA. These results demonstrate that muscle cell surface glycosylation is finely regulated during muscle differentiation in a domain- and acceptor-substrate-specific manner, suggesting that temporal- and site-specific glycosylation are important for skeletal muscle cell function.

Key words: GalNAc, muscle glycosylation, neuromuscular junction, utrophin–glycoprotein complex, *Wisteria floribunda* agglutinin

Introduction

Skeletal muscle fibers are surrounded by an extracellular matrix (ECM) that provides mechanical support and also transmits signals into the cell via interactions with glycoproteins on the muscle cell membrane, or sarcolemma. The sarcolemma has distinct domains that vary by function, anatomic location and the array of membrane proteins concentrated in these specific domains. The neuromuscular junction (NMJ) is the domain that transmits signals from nerve

© The Author 2016. Published by Oxford University Press. All rights reserved. For permissions, please e-mail: journals.permissions@oup.com

terminals to the muscle fiber (Tintignac et al. 2015). The myotendinous junction (MTJ) is the domain that transmits forces from muscle to tendon (Tidball 1991). The extrasynaptic, or extrajunctional, domain connects the sarcolemma to the ECM to transmit force during muscle contraction. These distinct domains contain discrete sets of membrane molecules required for their different functions.

On the extrasynaptic sarcolemma, a major adhesion complex is the dystrophin–glycoprotein complex (DGC). The DGC connects the intracellular actin cytoskeleton to the ECM via the laminin receptor dystroglycan and the intracellular adaptor protein dystrophin (Ervasti and Campbell 1993). A homologous complex, the utrophin–glycoprotein complex (UGC), which localizes to the NMJ and MTJ domains, also includes dystroglycan but uses utrophin rather than dystrophin to link the ECM to the cytoskeleton (Clerk et al. 1993; James et al. 1995). Dystroglycan is a heterodimer of soluble alpha-dystroglycan (α-DG) and membrane-bound beta-dystroglycan (β-DG). α-DG has N- and C-terminal globular domains linked by an extended mucin domain. The C-terminal globular domain connects α-DG to β-DG, while the highly glycosylated mucin domain bears unique *O*-mannose-linked glycosaminoglycans that bind to proteins in the ECM (Kanagawa et al. 2005; Yoshida-Moriguchi et al. 2010). While dystroglycan is present in both the DGC and the UGC, different ECM components are bound by dystroglycan at different sites; α-DG in the DGC at extrasynaptic sarcolemma binds laminin-211 (Ervasti and Campbell 1993), while α-DG at the NMJ binds laminin-221, laminin-421 and laminin-521 (Meier and Ruegg 2000). The α7β1 integrin heterodimer is the other major adhesion complex present in skeletal muscle (Song et al. 1992; Burkin and Kaufman 1999). Splice variants of α7-integrin are also specific for either the synaptic or extrasynaptic sarcolemmal domains (Martin et al. 1996) and selectively bind different laminin isoforms (von der Mark et al. 2002).

Proper glycosylation is critical for sarcolemma–ECM interactions and muscle function. The role of integrin glycosylation in cell adhesion and migration has been characterized in many cell types, although the function of skeletal muscle integrin glycans remain poorly understood (Gundry et al. 2009). In contrast, glycosylation of α-DG has been studied extensively. Laminin binds to α-DG via O-mannose glycans modified with glycosylaminoglycans synthesized by the enzyme like-glycosyltransferase (LARGE); the ability of α-DG to bind laminin is dependent upon proper glycosylation (Yoshida-Moriguchi et al. 2010), as hypoglycosylated α-DG shows reduced binding to laminin and perlecan (Kanagawa et al. 2005; Yoshida-Moriguchi et al. 2010). Mutations in *DAG1*, the gene encoding dystroglycan, or in any of 17 genes involved in α-DG glycosylation that result in hypoglycosylation of α-DG, cause decreased cell binding to ECM and a spectrum of neuromuscular disorders (Live et al. 2013; Endo 2015).

In addition to distinct types of glycosylation on muscle cell glycoproteins, there is differential glycosylation of glycoproteins in specific sarcolemmal domains. In 1982, Sanes and Cheney used *Dolichos biflorus* agglutinin (DBA), a plant lectin that recognizes terminal *N*-acetylgalactosamine (GalNAc) residues, to selectively identify the NMJ (Sanes and Cheney 1982). Utilizing a panel of plant lectins, the Sanes group later demonstrated that the NMJ in rodent muscle is enriched with terminal GalNAc residues compared to the extrasynaptic sarcolemma (Scott et al. 1988). Historically, several lectins specific for GalNAc, including *Vicia villosa* agglutinin (VVA) and *Wisteria floribunda* agglutinin (WFA) have been used to differentiate the NMJ from extrasynaptic sarcolemma (McDearmon et al. 2001; Nguyen et al. 2002; Marshall et al. 2012). WFA specifically has been used to differentiate between complexes associated with NMJ vs. the extrasynaptic sarcolemma. WFA preferentially binds to α-DG in the UGC, while the sialic acid and *N*-acetylglucosamine (GlcNAc)-specific lectin wheat germ agglutinin (WGA) binds to α-DG associated with both the DGC and the UGC (McDearmon et al. 2001; Nguyen et al. 2002; Xia et al. 2002; Cabrera et al. 2012; Marshall et al. 2012).

Manipulating muscle glycosylation to improve muscle cell adhesion to ECM is a potential therapeutic option for some muscular dystrophies. A number of therapeutic approaches have been described in cell and animal models, including overexpression of a specific glycosyltransferase enzyme to modify sarcolemmal glycans (Nguyen et al. 2002; Xia et al. 2002), administration of a recombinant scaffolding glycoprotein that binds to the sarcolemma (Amenta et al. 2011; Van Ry et al. 2015) and pharmacologic treatment to enrich for specific saccharide residues on sarcolemmal glycoproteins (Cabrera et al. 2012). However, as there has been no comprehensive quantitative approach to characterizing glycans expressed on skeletal muscle, it is not clear what glycans are being modified by these approaches, or if there are more specific glycan targets that could be modified to improve muscle function.

While plant lectins with nominal specificity for GalNAc have been interchangeably used to distinguish the NMJ-associated UGC from the sarcolemmal DGC, we have found that these different lectins recognize unique types of glycans and discrete sets of glycoproteins that bear these glycans. These results indicate that muscle cell glycosylation is very finely regulated, implying that specific differences in glycoprotein glycosylation are important for distinct functions and that definition of these differences will enable a more precise approach to enhancing muscle cell function through manipulation of glycosylation.

Results

Four lectins that preferentially recognize GalNAc, WFA, VVA, SBA and DBA have historically been used to identify the NMJ (Sanes and Cheney 1982; Scott et al. 1988). WFA and VVA specifically have been used to detect various α-DG glycoforms, including those that associate with the UGC (McDearmon et al. 2001; Nguyen et al. 2002; Xia et al. 2002; Cabrera et al. 2012; Marshall et al. 2012). However, the assumption that these four lectins recognize the same GalNAc-containing glycans on the same glycoproteins has not been confirmed. Therefore we asked if 1) there were differences among the four lectins in specificity for the NMJ, 2) whether reactivity with VVA, SBA and DBA, like WFA, correlated with utrophin distribution and 3) if any of the major adhesion complexes (DGC, UGC or α7β1 integrin) were required for binding of the four lectins.

As previously described, in wild-type mice, DBA, VVA and SBA reactivity were highly specific for the NMJ, staining discretely and minimally in comparison to the extensive sarcolemma. (Figure 1). In contrast, while enriched at the synapse, WFA binding spread slightly beyond the NMJ. Moreover, significant differences were observed in reactivity of the four GalNAc-specific lectins with muscle from *mdx* mice. As previously described, we observed spreading of WFA reactivity throughout the sarcolemma in muscle from *mdx* mice, which correlated with utrophin staining. However, VVA, SBA and DBA staining remained highly specific for the NMJ in muscle from *mdx* mice. Interestingly, we noted similar differences between the four GalNAc-specific lectins when muscle from α7-integrin-null ($\alpha7^{-/-}$) mice was stained. While VVA, SBA and DBA staining remained highly NMJ specific, WFA staining spread extrasynaptically and correlated with utrophin staining. As WFA staining redistributed concomitantly with utrophin staining, we next asked if

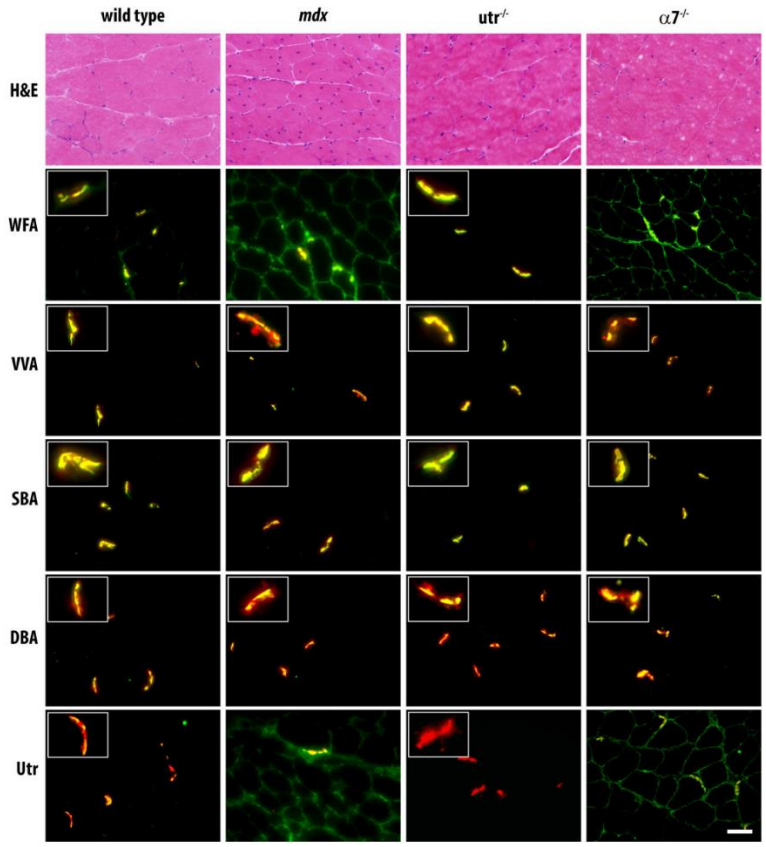


Fig. 1. The DGC, UGC and α7-integrin are not requisite for binding of GalNAc-specific lectins. Transverse 8-μm serial cryosections of murine quadriceps muscles from 12-week-old wild-type, *mdx*, utrophin-null (Utr $^{-/-}$) and alpha-7-integrin-null (α7 $^{-/-}$) mice were stained with hematoxylin and eosin (H&E, top row), anti-utrophin antibody (bottom row), and the following biotinylated reagents: WFA, VVA, SBA and DBA. Bound lectins and antibodies were detected with FITC-avidin D (green) and counterstained with Texas Red conjugated alpha-bungarotoxin (red). Merged images are depicted. Insets depict neuromuscular junctions. Scale bar is 50 μm. This figure is available in black and white in print and in color at *Glycobiology* online.

expression of utrophin was necessary for staining of WFA or the other GalNAc-specific lectins. Surprisingly, we observed no loss of reactivity for any of the four lectins with muscle from utrophin-null (Utr$^{-/-}$) mice compared to wild type, indicating that utrophin expression is not required for binding of WFA, VVA, SBA or DBA (Figure 1).

As we observed some qualitative differences in patterns of reactivity of WFA, VVA, SBA and DBA with muscle from wild-type and *mdx* mice, we developed an in vitro lectin binding assay to quantify differences in binding among the lectins. We used a panel of **11** lectins (Table I) to analyze glycosylation of C2C12 murine myoblasts and differentiated myotubes. Fixed cells were incubated with biotinylated lectins and bound lectins were detected colorimetrically. In addition to the GalNAc-specific lectins WFA, VVA, SBA and DBA, the panel included lectins specific for major classes of glycan structures found on glycoproteins. WGA, *Sambucus nigra* agglutinin (SNA) and *Maackia amurensis* agglutinin-II (MAA-II) were included for specificity for terminal sialic acid residues (Greenaway and LeVine 1973; Shibuya et al. 1987; Konami et al. 1994). Peanut agglutinin (PNA) and jacalin (Jac) recognize asialo and sialylated core **1** type *O*-glycans, respectively (Lotan et al. 1975; Wu et al. 2003), while *Phaseolus vulgaris* leucoagglutinin (PHA-L) and Concanavalin A (Con A) recognize complex and high mannose-type *N*-glycans, respectively (Cummings and Kornfeld 1982; Mega et al. 1992). Therefore, this panel of **11** lectins allowed us to detect changes in glycosylation across a wide breadth of glycan structures.

As shown in Figure 2A, reactivity of C2C12 myoblasts at day 0 with the different lectins varied considerably. Following 7 days of differentiation, we observed little change in reactivity with the sialic acid-specific lectins WGA, SNA and MAA-II. However, we observed a significant increase in PNA reactivity at day 7 compared with day 0, with a concomitant decrease in Jac binding, indicating an increase in asialo core **1** *O*-glycans following differentiation. We also observed increased PHA-L binding to cells at day 7 compared to day 0, indicating an increase in complex *N*-glycans following differentiation.

Importantly, we observed increased binding of all four GalNAc-specific lectins, WFA, VVA, SBA and DBA, with C2C12 differentiation. WFA, VVA, SBA and DBA binding increased approximately 70%, 120%, 300% and 130%, respectively. In addition to the quantitative differences in the amplitude of binding of the four GalNAc-specific lectins, we also observed temporal differences in binding during C2C12 differentiation. As shown in Figure 2B, binding of WFA, VVA, SBA and DBA increased at different rates throughout the 7 days. Binding of WFA did not increase until day 4, while increased VVA binding was detected at day 2. In contrast, increased SBA and DBA binding were not observed until day 7 (Figure 2B). The differential rates of change in reactivity of the four GalNAc-specific lectins suggested that these lectins recognize different glycoproteins or different glycoforms of the same protein.

Table I. Panel of lectins with varying specificities utilized to characterize changes in muscle glycosylation following differentiation of C2C12 myotubes

Lectin	Abbreviation	Nominal sugar specificity
Wisteria floribunda agglutinin	WFA	GalNAc
Vicia villosa agglutinin	VVA	GalNAc
Soybean agglutinin	SBA	GalNAc
Dolichos biflorus agglutinin	DBA	GalNAc
Wheat germ agglutinin	WGA	Sialic Acid, GlcNAc
Sambucus nigra agglutinin	SNA	α2,6 linked Sialic acid
Maackia amurensis agglutinin-II	MAA-II	α2,3 linked Sialic acid
Peanut agglutinin	PNA	Asialo core 1 *O*-glycans
Jacalin agglutinin	Jac	Core 1 *O*-glycans
Phaseolus vulgaris leucoagglutinin	PHA-L	Complex *N*-glycans
Concanavalin A	Con A	High mannose *N*-glycans

To determine if the GalNAc-specific lectins WFA, VVA, SBA and DBA bind different glycoproteins on muscle cells, we performed lectin precipitations. C2C12 myotubes differentiated for 7 days were biotinylated to label cell surface glycoproteins, and lectin precipitations of cell lysates were performed with the four lectins. Sarcolemmal glycoproteins precipitated by each lectin were detected with SA-HRP (Figure 3A). Multiple cell surface glycoproteins were precipitated by WFA, VVA and SBA, while DBA precipitated a smaller array of glycoproteins, with a predominant component of approximately 250 kDA. While WFA, VVA and SBA all precipitated an array of glycoproteins, we observed significant differences among the lectins in the patterns of glycoprotein reactivity, indicating that these lectins selectively recognize different repertoires of glycoproteins in C2C12 cells. In addition, the four lectins selectively recognize distinct repertoires of glycoproteins in wild-type mouse muscle. We performed lectin precipitation with extracts of skeletal muscle and detected precipitated glycoproteins with SYPRO® Ruby stain (Figure 3B). Distinct glycoprotein receptors were precipitated by each lectin from wild-type skeletal muscle lysates. Thus, WFA, VVA, SBA and DBA react with distinct sets of glycoproteins and/or protein glycoforms. As modification of α-DG with terminal GalNAc residues has been used to identify the UGC (Nguyen et al. 2002; Xia et al. 2002; Marshall et al. 2012), we asked if each of the four GalNAc-specific lectins were capable of precipitating either α-DG or β-DG. WFA, VVA and SBA precipitated both α-DG and β-DG from C2C12 myotubes and total skeletal muscle lysates, while DBA did not precipitate either α-DG or β-DG (Figure 3, A and B lower

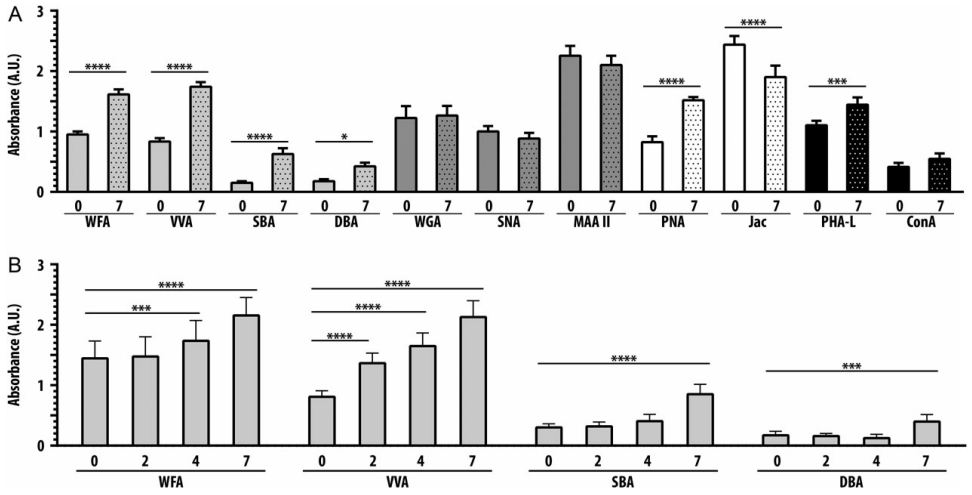


Fig. 2. Distinct increases in binding of GalNAc-specific lectins following differentiation of C2C12 myotubes. (**A**) Glycosylation of C2C12 myotubes differentiated for 7 days was detected utilizing a panel of 11 lectins with varying specificities. Increases were seen in the four GalNAc-specific lectins WFA, VVA, SBA and DBA. (**B**) Changes in binding of the four GalNAc-specific lectins were determined over a time course of 7 days. Lectin binding was performed at the time of differentiation (day 0), and following 2, 4 and 7 days of differentiation. Binding of VVA increased rapidly, WFA increased following 2 days of differentiation, whereas binding of SBA and DBA did not increase until 7 days of differentiation. Data are mean ± SEM (error bars) of triplicates from three pooled independent experiments. * $P < 0.05$; *** $P < 0.001$; **** $P < 0.0001$.

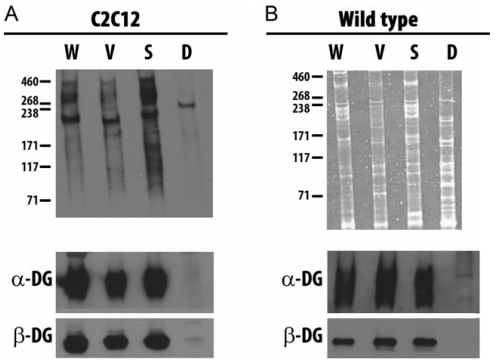


Fig. 3. GalNAc-specific lectins precipitate different glycoproteins. Equal amounts of lysates from murine C2C12 myotubes differentiated for 7 days (**A**) or wild-type murine skeletal muscle (**B**) were precipitated by WFA (W), VVA (V), SBA (S) and DBA (D) following surface biotinylation and cell lysis. Total proteins precipitated were separated by SDS-PAGE from surface biotinylated murine C2C12 myotubes and detected by SA-HRP (**A**, upper panel), while proteins from wild-type skeletal muscle were detected with SYPRO® Ruby Protein Gel stain (**B**, upper panel). Parallel blots were probed with mAb against α-DG and β-DG (**A** and **B**, lower panels).

panels). Thus, while WFA, VVA and SBA precipitated DG, it was not the only sarcolemmal glycoprotein receptor for these GalNAc-specific lectins on C2C12 myotubes or wild-type skeletal muscle, and DBA, the fourth GalNAc-specific lectin, did not recognize DG.

These results indicated that different types of glycans were being recognized by the GalNAc-specific lectins. A number of factors control cell-specific glycoprotein glycosylation, including transcription of glycan modifying genes, availability of preferred glycoprotein acceptors, availability of nucleotide-sugar donors, localization of glycosyltransferases in the secretory pathway and rate of transport through the glycosylation machinery. To determine if differential expression of specific glycosyltransferase or glycosidase gene transcripts could be responsible for the differentiation-dependent changes in lectin reactivity that we observed, we performed a glycotranscriptome analysis (Abbott et al. 2008; Gasimli et al. 2014; Magalhães et al. 2015) of C2C12 cells at day 0 and day 2 of differentiation. As we had observed changes in cell surface glycosylation by lectin binding between 2 and 7 days after addition of differentiation media, we assessed transcript expression at day 2 of differentiation. In our analysis of over 580 glycosylation-related transcripts (Supplementary data, Table S1), we found 22 different glycosyltransferases and glycosidases for which relative expression differed at least 2-fold between day 0 and day 2 (Table II).

Focusing on glycosyltransferases that could add terminal GalNAc residues or glycosidases that could unmask subterminal GalNAc residues, we identified beta-1,4-*N*-acetylgalactosaminyltransferase 3 (*β4Galnt3*) and sialidase 2 (*Neu2*), increased 4- and 18.6-fold, respectively, as candidates for further interrogation. We also included beta-1,3-*N*-acetylgalactosaminyltransferase 2 (*β3Galnt2*), expression of which increased 1.5-fold by day 2, due to the role of this enzyme in α-DG glycosylation and identification of mutations in this gene in some cases of Walker–Warburg syndrome (Stevens et al. 2013; Hedberg et al. 2014). We hypothesized that increased abundance of either β4Galnt3 or β3Galnt2 GalNAc transferases could directly contribute to increased reactivity of GalNAc-specific lectins following

Table II. Twenty-three glycosyltransferase and glycosidase transcripts upregulated following C2C12 differentiation and identified via glycotranscriptome analysis

	Gene Name	Fold Change	Function
Glycosyltransferases	Fut1	24.92	Blood group Antigen synthesis
	Extl1	22.12	Heparan polymerization
	β3Galt5	7.51	Hybrid *N*-glycan, neo-lac
	β3Galt2	6.15	Hybrid *N*-glycan, neo-lac
	Fut7	5.81	Lewis X Antigen
	St8sia4	4.86	Poly Sialic acid
	St8sia2	4.44	Poly Sialic Acid
	Fut2	4.04	Blood group Antigen synthesis
	β4Galnt3[a]	4.02	Hormone glycosylation
	Sec1	2.99	Blood group Antigen synthesis
	Fut9	2.87	Lewis X Antigen
	β3Galnt2[a,b]	1.46	α-DG glycosylation
Glycosylhydrolases	Neu2[a]	18.6	Sialidase (muscle, brain, cytosol)
	Lctl	9.13	Lactase-like protein
	Slc3a2	4.87	Solute carrier: dibasic/ neutral amino acids
	Chi3l1	4.51	Chitinase-like, cartilage protein
	Al464131	3.58	Glucosidase family
	Amy2	3.03	Amylase
	Amy1	2.82	Amylase
	Neu1	2.66	Sialic acid catabolism (lysosome)
	Gaa	2.26	Glucosidase
	Edem3	2.15	ER degradation enhancer
	Hyal1	2.05	Hyaluronic Acid catabolism

[a]Genes of interest for further investigation in this study.
[b]Although fold change for *β3Galnt2* was less than 2, this gene was included due to its known role in α-DG glycosylation (Stevens et al. 2013; Hedberg et al. 2014; Praissman et al. 2016).

differentiation. Neu2 is a cytosolic sialidase expressed in muscle that removes terminal sialic acid residues and has been reported to be essential for myoblast differentiation (Monti et al. 1999). How cytosolic Neu2 would access glycans in the secretory pathway or on the cell surface is not well understood; however, we reasoned that increased *Neu2* transcript expression and activity might remove sialic acid to reveal subterminal GalNAc residues, resulting in increased binding of GalNAc-specific lectins.

Changes in transcript abundance for *β4Galnt3*, *β3Galnt2* and *Neu2* at day 0 and day 2 of C2C12 differentiation were validated by qRT-PCR, and the fold changes in abundance were 1.85, 1.49 and 14.2, respectively (Figure 4A). To determine if reduced expression of *β4Galnt3*, *β3Galnt2* or *Neu2* abrogated the increase in binding of GalNAc-specific lectins following differentiation, we reduced expression of these three enzymes using siRNA. To determine if decreased expression of any of these enzymes reduced binding of GalNAc-specific lectins, C2C12 cells were transfected with the indicated siRNA, plated for qRT-PCR and lectin binding analysis in parallel and differentiated the same day. Following 2 days of differentiation, we achieved 60% or greater reduction in transcript abundance for each specific enzyme by this method (Figure 4B). After an

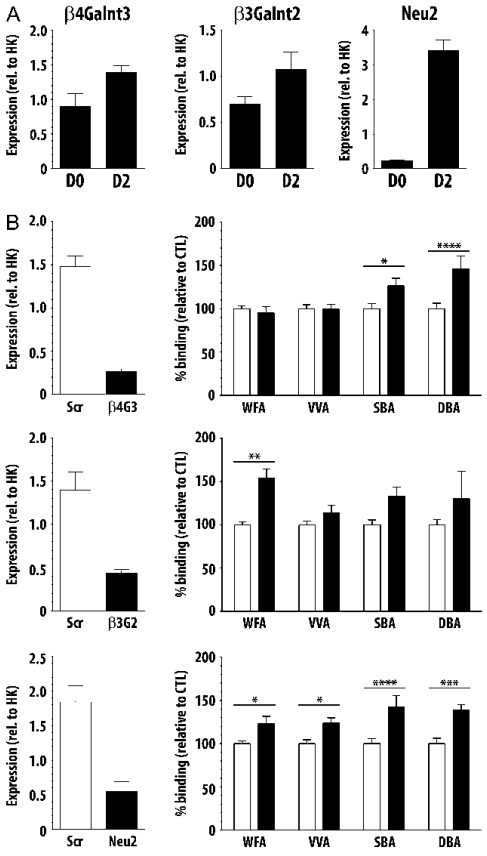


Fig. 4. Reduced expression of β4GalNt3, β3GalNt2 and Neu2 drive distinct changes in binding of GalNAc-specific lectins. (**A**) Transcript expression of β4GalNt3, β3GalNt2 and Neu2 increased between day 0 and day 2 as detected by qRT-PCR. (**B**) Cells transfected with siRNA for β4GalNt3, β3GalNt2 and Neu2 showed 60% or greater reduction in expression of each enzyme compared to cells transfected with scramble siRNA. Following siRNA knockdown, lectin binding was performed on parallel cells. No decrease was seen in binding of the GalNAc-specific lectins following siRNA knockdown; however, distinct increases were seen in specific lectins. Data are mean ± SEM (error bars) of triplicates from three pooled independent experiments. * $P < 0.05$; ** $P < 0.01$; *** $P < 0.001$; **** $P < 0.0001$

additional 2 days of differentiation (4 total days of differentiation), binding of the four GalNAc-specific lectins to myotubes plated in parallel was quantified as in Figure 2. To our surprise, knockdown of none of the enzymes reduced binding of any of the GalNAc-specific lectins. In fact, following reduction in *β4Galnt3* expression, we observed no change in WFA or VVA binding, while binding of both SBA and DBA increased (Figure 4B, upper panel). Similarly, following reduction in *β3Galnt2* expression, we observed increased WFA and SBA binding, while no change was seen in VVA or DBA binding (Figure 4B, middle panel). Finally, reducing *Neu2* expression resulted in increased binding of all four GalNAc-specific lectins (Figure 4B, lower panel). While not identifying a specific enzyme that regulates exposure or addition of terminal GalNAc residues, these results further highlight the differences among the specificities of these four lectins; WFA, VVA, SBA and DBA, while nominally GalNAc-specific, clearly recognize unique and distinct glycan structures on C2C12 cells.

Previously, we identified complex *N*-glycans modified with terminal GalNAc residues on C2C12 cells (Cabrera et al. 2012). We also found that complex *N*-glycans were required for WFA binding to C2C12 myotubes (Cabrera et al. 2012). Thus, since the glycotranscriptome analysis did not pinpoint enzymes responsible for creating GalNAc-containing ligands, we wanted to determine the type of glycan structures required for binding of the four GalNAc-specific lectins. To interrogate the requirement for complex *N*-glycans in lectin binding, C2C12 myotubes differentiated for 4 days were treated for a further 72 h with deoxymannojirimycin (DMNJ), which blocks ER alpha-mannosidase I activity and thus the elaboration of complex *N*-glycans from high mannose precursors on glycoproteins (Figure 5A, Fuhrmann et al. 1984). To confirm the efficacy of DMNJ treatment, we determined that binding of PHA-L, specific for complex *N*-glycans, was nearly completely abrogated in treated cells (Figure 5B).

As we had previously found, WFA binding to DMNJ-treated differentiated C2C12 myotubes was substantially reduced, approximately 50%. SBA binding following DMNJ treatment was also reduced, but to a lesser extent. In contrast, we observed no change in VVA or DBA binding to DMNJ-treated cells compared to control. As DMNJ treatment reduced binding of WFA and SBA, but not of VVA or DBA, we reasoned that precipitation of sarcolemmal glycoproteins by WFA and SBA might be sensitive to DMNJ treatment, and we performed lectin precipitations from lysates of control or DMNJ-treated cells with the four GalNAc-specific lectins, as in Figure 3. We observed that fewer glycoproteins were precipitated by WFA and SBA from cell lysates when the cells were treated with DMNJ, compared to control-treated cells (Figure 5C), while no differences in the pattern or abundance of glycoproteins precipitated by VVA or DBA from control- or DMNJ-treated lysates were observed. This further indicated that WFA and SBA bind, at least in part, to complex *N*-glycans on C2C12 myotubes, while complex *N*-glycans are not required for VVA and DBA binding.

To determine if *N*-glycans were required for binding of the lectins to murine muscle, tissue sections were treated with the bacterial enzyme Peptide-N-glycosidase F (PNGaseF) which cleaves *N*-glycans between the innermost GlcNAc and the underlying asparagine residue (Figure 5A, Chu 1986). As expected, PNGaseF treatment abrogated PHA-L staining of wild-type muscle compared to control-treated tissue (Figure 5D). PNGaseF treatment of tissue sections substantially reduced WFA binding, compared to control-treated sections. However, we observed no qualitative change in binding of VVA, SBA or DBA following PNGaseF treatment (Figure 5D).

Discussion

To date, qualitative lectin staining of muscle sections has provided most of our knowledge regarding muscle glycosylation; for example, the rodent NMJ was shown to preferentially bind GalNAc-specific lectins (Sanes and Cheney 1982; Scott et al. 1988). While WFA, VVA, SBA and DBA have been used to identify the NMJ, presumably due to recognition of terminal GalNAc residues, specific glycoreceptors bound by each lectin remain undetermined. Our work demonstrates significant differences in the binding characteristics of these four GalNAc-specific lectins. Thus, studies using these four

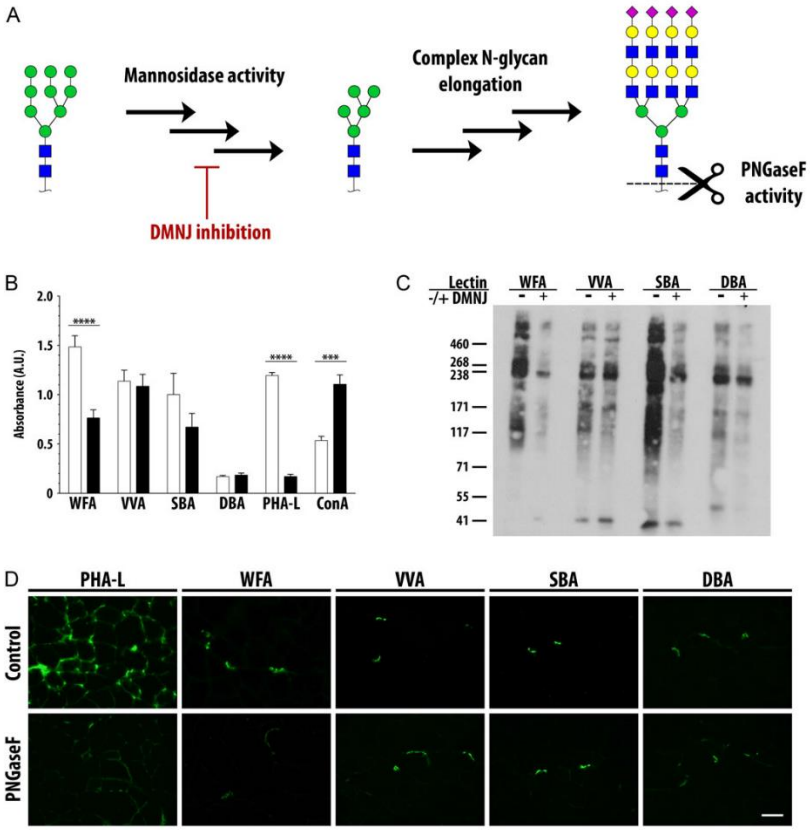


Fig. 5. Complex N-glycans are required for binding of WFA. (**A**) High mannose *N*-glycans present on glycoproteins are trimmed to truncated mannose structures by mannosidase enzyme activity, a process inhibited by the small molecule DMNJ. Glycosyltransferase activity elongates truncated mannose structures into complex *N*-glycans. The bacterial enzyme PNGaseF cleaves *N*-glycans between the asparagine and GlcNAc residues. (**B**) C2C12 myotubes were treated with DMNJ or vehicle control for 72 h. DMNJ treatment abrogated WFA binding and modestly reduced binding of SBA. (**C**) Equal amounts of lysates from murine C2C12 myotubes treated with DMNJ or vehicle control for 72 h were precipitated by WFA, VVA, SBA and DBA following surface biotinylation and cell lysis. Precipitated proteins were separated by SDS-PAGE, and blots probed with SA-HRP. (**D**) Eight-micrometer serial quadriceps cryosections from wild-type mice were incubated with PNGaseF or vehicle control for 4 h to enzymatically remove *N*-glycans. PNGaseF treatment abrogated binding of PHA-L and reduced binding of WFA. NMJs were co-stained with Texas Red conjugated alpha-bungarotoxin. Scale bar is 50 μm. Data are mean ± SEM (error bars) of triplicates from three pooled independent experiments. Monosaccharide symbols follow the SNFG (Symbol Nomenclature for Glycans) system (PMID 26543186, *Glycobiology* 25: 1323–1324, 2015) details at NCBI. *** $P < 0.001$; **** $P < 0.0001$. This figure is available in black and white in print and in color at *Glycobiology* online.

lectins interchangeably to identify the NMJ most likely identified different glycoproteins or glycoforms of proteins.

While VVA, SBA and DBA staining of muscle sections from wild-type mice and various null mutants were highly NMJ specific, WFA staining differed; WFA staining of wild-type muscle spread extrasynaptically compared to the other lectins, and redistributed throughout the sarcolemma on *mdx* and $\alpha7^{-/-}$ muscle sections (Figure 1). While WFA staining has been correlated with localization of utrophin, no loss of muscle staining was observed for any of the lectins of tissues from mice lacking utrophin. Similarly, no loss of binding was observed for tissue from mice lacking α7-integrin. Thus, while WFA reactivity may redistribute extrasynaptically in *mdx* and $\alpha7^{-/-}$ mice in a pattern similar to utrophin localization (Figure 1), utrophin expression is not requisite for WFA binding. Moreover, neither α-DG containing adhesion complex (DGC, UGC) nor α7-integrin are required for binding of these four GalNAc-specific lectins; integrins and α-DG represent only two of the many surface glycoproteins that might be decorated with glycans detected by GalNAc-specific lectins

In addition to different qualitative patterns of binding among the four GalNAc-specific lectins, a quantitative assay showed that binding of the four lectins increased at different rates during differentiation of C2C12 cell in vitro (Figure 2). These two observations led us to postulate that the four GalNAc-specific lectins bind different glycoproteins or different glycoforms of various proteins. In fact, all four GalNAc-specific lectins directly enrich for distinct subsets of cell surface glycoproteins from C2C12 cells or glycoproteins from muscle lysate. We detected no α-DG in DBA precipitates from either

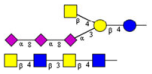
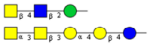
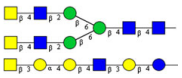
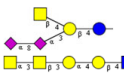
C2C12 myotubes or wild-type skeletal muscle lysates, consistent with the previously reported lack of DBA binding to α-DG from rabbit skeletal muscle (Ervasti et al. 1997). Interestingly, DBA has been shown to react with α-DG isolated from rabbit brain, demonstrating the tissue-specific heterogeneity of α-DG glycosylation (Ervasti et al. 1997). A broad band of α-DG was detected in WFA, VVA and SBA precipitates indicating all three lectins recognize multiple glycoforms of α-DG (Figure 3). While our studies demonstrate that VVA binds to α-DG in total skeletal muscle lysate, this differs from a previous result in which VVA did not bind α-DG when the DGC complex was pre-precipitated with WGA; it is possible that the VVA-reactive α-DG we detected was not included in material precipitated by WGA. This would indicate that at least two glycoforms of α-DG, one sialylated and one modified with terminal GalNAc residues, are expressed in muscle (Ervasti et al. 1997).

Several new mechanisms regulating muscle glycosylation are rapidly emerging. For example, an enzyme initially described to transfer a GlcNAc residue to mannosyl *O*-glycans on α-DG was recently determined to instead act as a primer for LARGE activity and not as a GlcNAc-transferase (Praissman et al. 2014, 2016; Willer et al. 2014). However, the product of the *β3Galnt2* gene, that modifies *O*-mannose glycans on dystrophin, was not required for binding of GalNAc-specific lectins (Figure 4). Also, while we identified increased expression of *β4Galnt3* and *Neu2* genes during C2C12 differentiation, reduction of enzyme expression differentially affected binding of the lectins; following knockdown of *β4Galnt3*, no change was observed in binding of WFA or VVA, while binding of SBA and DBA both increased. In contrast, binding of all four lectins increased following a reduction in expression of *Neu2*. What might cause these unexpected changes in binding following enzyme knockdown? Knockdown of one specific enzyme may shift the balance of glycosyltransferase activity in the Golgi, and therefore alter the glycans ultimately displayed on sarcolemmal glycoproteins. Genetic manipulation of glycosyltransferase expression is known to alter activity of unrelated glycosylation pathways and ultimately drive glycosylation of non-traditional substrates (Lee et al. 1989; Patnaik and Stanley 2005; Cabrera et al. 2006; Zhang and Hu 2012).

We also found that complex *N*-glycans contribute significantly to binding of WFA, as DMNJ treatment of C2C12 cells and PNGaseF digestion of wild-type muscle substantially reduced WFA binding. In contrast, *N*-glycans appear to contribute a fraction of binding sites for SBA as DMNJ treatment modestly reduced binding to intact C2C12 as well as C2C12 lysates. PNGaseF digestion did not reduce SBA binding to wild-type muscle tissue sections indicating glycan structures bound by SBA on C2C12 cells may differ from those bound on innervated muscle. *N*-glycans do not appear to be required for VVA and DBA binding to C2C12 cells or murine muscle (Figure 5).

To further examine which glycan structures were preferentially bound by the four GalNAc-specific lectins, we analyzed glycan array data from the Consortium for Functional Glycomics (CFG) (Supplementary data, Table S2, http://www.functionalglycomics.org/). This identified 23 glycans bound by WFA, 5 glycans bound by VVA, 12 bound by SBA and 3 bound by DBA, which were compared (Supplementary data, Table S2). Of the glycan structures recognized by any of the four GalNAc-specific lectins, 17 contained terminal GalNAc residues (Table III); linkage of terminal GalNAc residues in either the α- or β-confirmation did not affect lectin recognition. Of those 17 structures, 6 structures were bound by more than one lectin and 2 of these were recognized by three lectins (WFA, VVA and SBA). Interestingly, while the top glycan structures

Table III. Seventeen glycans with terminal GalNAc residues on CFG glycan arrays were identified as binding at least one of the four GalNAc-specific lectins

Structure	Nomenclature	WFA	VVA	SBA	DBA
	GalNAcβ1-3Galα1-4Galβ1-4GlcNAc	x		x	
	GalNAcα1-3GalNAc	x			
	GalNAcβ1-4GlcNAc	x	x	x	
	GalNAcα	x	x	x	
	GalNAcβ	x		x	
	GalNAcα1-3Gal	x			
	NeuAcα2-8NeuAcα2-8NeuAcα2-8NeuAcα2-8(GalNAcβ1-4)Galβ1-4Glc	x			
	NeuAcα2-8NeuAcα2-8NeuAcα2-8(GalNAcβ1-4)Galβ1-4Glc	x			
	GalNAcβ1-4GlcNAcβ1-3GalNAcβ1-4GlcNAc		x		
	GalNAcβ1-4GlcNAc[6S]		x		
	GalNAcβ1-4GlcNAcβ1-2Man		x	x	
	GalNAcα1-3GalNAcβ1-3Galα1-4Galβ1-4Glc			x	x
	GalNAcβ1-4GlcNAcβ1-2Man β1-6 (GalNAcβ1-4GlcNAcβ1-2Man)Manβ1-4GlcNAcβ1-4GlcNAc			x	
	GalNAcβ1-3Galα1-4Galβ1-4GlcNAcβ1-3Galβ1-4Glc			x	
	NeuAcα2-8NeuAcα2-3(GalNAcβ1-4)Galβ1-4Glcβ			x	
	GalNAcα1-3GalNAcβ1-3Galα1-4Galβ1-4GlcNAc				x
	NeuAcα2-3(GalNAcβ1-4)Galβ1-4GlcNAcβ				x

bound by WFA all had terminal GalNAc residues, several glycans also recognized by WFA did not have terminal GalNAc residues. Similarly, the glycan demonstrating the highest affinity binding by SBA was not modified with a terminal GalNAc, though the other 11 structures recognized by SBA were. Thus, these four lectins therefore have overlapping, yet distinct, preferences for glycan structures terminated with GalNAc residues, while WFA and SBA also bound glycan structures lacking terminal GalNAc residues; future work will have to precisely identify glycan structures on cells and tissues to fully understand patterns of lectin binding. While glycan structures on glycan arrays may not completely recapitulate all structures present on a muscle cell, these data clearly demonstrate differences in the binding preferences of these four lectins.

Changes in glycosylation seen in muscle disease could result from multiple aspects of pathophysiology and disease progression. Each protein in an adhesion complex may bear unique glycan structures, so that loss of one protein, or of an entire complex, from the sarcolemma would result in altered sarcolemmal glycosylation. Sarcolemmal adhesion complexes are known to regulate intracellular signaling and subsequent glycosylation of sarcolemmal proteins (Marshall et al. 2012), so that initial loss of sarcolemmal adhesion complexes could further alter glycosylation of sarcolemmal proteins. Loss of adhesion complexes results in destabilization of the sarcolemma and release of intracellular enzymes into the extracellular space. It is conceivable that release of glycosyltransferase enzymes and sugar substrates into the extracellular milieu may also result in modification of glycans on sarcolemmal glycoproteins (Iwata et al. 2013).

While precise changes in muscle glycosylation in human disease are not well described, therapies to alter muscle cell glycosylation to improve muscle cell function have been proposed. These include administration of recombinant galectin-1 (gal-1) and biglycan (Amenta et al. 2011; Van Ry et al. 2015), genetic overexpression of a glycosyltransferase (Nguyen et al. 2002), and treatment with a small molecule (Cabrera et al. 2012). Both gal-1 and biglycan may act to stabilize the sarcolemma by mediating interactions between sarcolemmal glycoproteins and between glycoproteins and the ECM.

Overexpression of the GalNAc transferase β4Galnt2 has been shown to increase abundance of the UGC, increase reactivity of α-DG with WFA and rescue the dystrophic phenotype in *mdx* mice (Nguyen et al. 2002). However, specific glycan structures modified on α-DG following β4Galnt2 enzyme overexpression remain to be determined. Moreover, overexpression of glycosyltransferases is known to result in modification of atypical substrates in some cases (Patnaik and Stanley 2005; Zhang and Hu 2012), so that the possibility that additional glycoproteins may be modified in cells expressing high levels of β4Galnt2 should be considered. Interestingly, while we saw a significant increase in binding of all four GalNAc-specific lectins following C2C12 differentiation, we did not detect expression of *β4Galnt2* (Supplementary data, Table S1).

Any potential therapy for restoring muscle viability and/or function by manipulating muscle glycosylation must address species-specific differences in glycosylation. For example, humans do not produce the sialic acid Neu5Gc due to an inactivating exon deletion in the cytidine monophosphate-*N*-acetylneuraminic acid hydroxylase (*CMAH*) gene (Chou et al. 1998). In mouse models of Duchenne muscular dystrophy (DMD) bearing this mutation (CMAH/*mdx* mice), muscle pathophysiology and disease progression are more severe than in *mdx* mice, and more accurately reflect the disease progression seen in boys with DMD (Chandrasekharan et al. 2010). Similarly alpha-sarcoglycan (α-SG) deficient mice that also bear the CMAH mutation (CMAH/Sgca$^{-/-}$) have worse cardiac and skeletal muscle pathophysiology than control mice lacking α-SG (Sgca$^{-/-}$) (Martin et al. 2013). While this difference in sialic acid usage between humans and rodents is significant, this is most likely not the only difference in muscle glycosylation between mice and humans. In 1988, it was noted that VVA staining of rodent muscle was highly specific for the NMJ, but binding to human muscle spread extrasynaptically (Scott et al. 1988). Furthermore, we found that lobeline treatment did not increase WFA binding to human inducible directly reprogrammable myotubes (Cabrera et al. 2012).

To date, characterization of muscle glycosylation has focused on murine models. While dramatic progress has been made in identification of glycosyltransferases required for creation of *O*-mannose glycans on α-DG in human muscle, future areas of investigation should focus on 1) characterization of all sarcolemmal glycoproteins and functions of the glycans, 2) identification of glycosylation changes that occur during myogenesis and 3) elucidation of glycosylation differences that occur during progression of muscle disease.

Materials and methods

Animals and cells

Wild-type and *mdx* breeders were purchased from Jackson Laboratories (Bar Harbor, ME), α7-integrin-deficient (Itga-nulls, α7$^{-/-}$) mice were a generous gift from D. Burkin (University of Nevada, Reno), and *mdx*:utrophin$^{-/-}$ mice (*mdx*:Utr$^{-/-}$) were a generous gift of J. Sanes (Harvard University, Cambridge) and sent from the mouse colony of J. Chamberlain (University of Washington, Seattle). Tissue sections from 12-week-old wild-type, *mdx*, Utr$^{-/-}$ and α7$^{-/-}$ mice were analyzed. All procedures involving mice were carried out in accordance with guidelines set by the UCLA Institutional Animal Care and Use Committee. Murine C2C12 cells were purchased from the American Type Culture Collection (Manassas, VA) and cultured and differentiated as previously described (Cabrera et al. 2012), except without antibiotics.

Antibodies and reagents

Antibodies and reagents were purchased: mouse anti-Dystrophin MANDYS1 (3B7), mouse anti-utrophin MANCHO3(8A4) (Developmental Studies Hybridoma Bank, University of Iowa, Iowa City, IA), mouse anti-α-DG IIH6-C4 (EMD Millipore, Billerica, MA), goat polyclonal IgG anti-α7-integrin (Santa Cruz Biotechnology, Dallas, TX), goat anti-mouse IgG (H+L)-HRP (Bio-Rad, Hercules, CA), goat anti-mouse IgG+M (H+L)-HRP (Jackson ImmunoResearch, West Grove, PA), streptavidin-conjugated horseradish peroxidase (SA-HRP, Jackson ImmunoResearch) and fluorescein-conjugated avidin D (A-2001, Vector Laboratories, Burlingame, CA).

Biotinylated lectins were bought from Vector Laboratories: WFA (B-1355), VVA (B-1235), SBA (B-1015), DBA (B-1035), PNA (B-1075), Jac (B-1155), SNA (B-1305), MAA-II (B-1265), WGA (B-1025), PHA-L (B-1115) and Con A (B-1005). Biotinylated bovine serum albumin (BSA, B-2007) was purchased for use as a control in lectin binding assays. The following agarose bound lectins were purchased from Vector Labs: WFA (AL-1353), VVA (AL-1233), SBA (AL-1013) and DBA (AL-1033).

Reagents were purchased as indicated: protease inhibitor cocktail (P8340, Sigma-Aldrich), SYPRO® Ruby protein gel stain (S12000), 1-Step Ultra TMB-ELISA Substrate solution (34028), EZ-Link® Sulfo-NHS-LC-Biotin (21335) (Thermo Fisher Scientific, Waltham, MA), DMNJ (EMD Millipore), Avidin/Biotin blocking kit (SP-2001), Mouse on Mouse (M.O.M.) Biotinylated Anti-Mouse

Ig Reagent (MKB-2225), VECTASHIELD™ Antifade Mounting Medium (Vector) and Texas Red conjugated α-bungarotoxin (α-BTX; 00015, Biotium, Hayward, CA).

Immunofluorescence and lectin fluorescence assays on tissue sections

Quadricep sections were mounted in 10.2% polyvinyl alcohol, 4.3% polyethylene glycol, flash frozen in liquid nitrogen-cooled isopentane and stored at −80°C. Transverse sections of 8 µm were mounted on positively charged glass slides (Thermo Fisher Scientific). For immunofluorescence assays, sections were brought to room temperature for 15 min, blocked in 3% BSA in 1× phosphate-buffered saline (1× PBS) for 1 h at room temperature, and blocked with Avidin/Biotin blocking kit according to manufacturer's instructions. Non-specific binding of mouse antibodies was blocked with M.O.M. kit. Sections were incubated in primary antibodies against utrophin (MANCHO3 1:5) in M.O.M. diluent solution overnight at 4°C. Following overnight incubation, sections were rinsed with 1× PBS, bound primary antibodies were detected with secondary antibody biotinylated anti-mouse diluted in M.O.M. diluent (Vector Labs) and tertiary fluorescein-conjugated avidin D (10 µg/mL) in 1× PBS for 1 h at room temperature. NMJs were stained with α-BTX conjugated to Texas Red (0.3 µg/mL) during incubation with fluorescein-avidin D. Control sections were incubated in tertiary fluorescein-avidin alone. To prevent photo bleaching, sections were then mounted with VECTASHIELD™. Bound antibodies were visualized on an Olympus BX51 fluorescence microscope and Olympus DP2-BSW software (Olympus America Inc., Center Valley, PA).

For lectin fluorescence assays, sections were brought to room temperature for 15 min, blocked in 3% BSA in 1X PBS for 1 h at room temperature and blocked with Avidin/Biotin blocking kit according to manufacturer's instructions. Biotinylated WFA (4 µg/mL), VVA (4 µg/mL), SBA (10 µg/mL) and DBA (20 µg/mL) were diluted in 1× PBS and added to sections overnight at 4°C. Sections were washed three times with PBS, and bound lectin detected with fluorescein-avidin (10 µg/mL) for 1 h at room temperature; NMJs were stained with α-BTX conjugated to Texas Red (0.3 µg/mL) during incubation with fluorescein-avidin D. Control slides were incubated in fluorescein-avidin alone. Slides were mounted in VECTASHIELD™ to prevent photo bleaching. Bound lectin was visualized as stated above.

N-glycans present on tissue sections were enzymatically removed by treatment with bacterial PNGaseF (New England BioLabs, Ipswich, MA) after sections were brought to room temperature for 15 min. Sections were incubated with 0.5 µL PNGaseF in 20 µL total reaction buffer for 4 h in a 37°C water bath, refreshing reaction buffer when necessary to guarantee sections did not dry out. Control-treated sections were incubated with reaction buffer alone. Following treatment with PNGaseF, sections were blocked and stained with lectins per above, as well as with the lectin PHA-L (2 µg/mL).

Lectin binding assays

Of a 96-well plate, 1.5×10^3 cells were plated per well. Cells were grown for 4 days, refreshing growth media every 2 days until cells were 90–100% confluent. Once confluent, cells were differentiated to form myotubes, refreshing differentiation media every 2 days until harvested. Cells were collected at the time of differentiation (day 0), and 2, 4 and 7 days following differentiation. At the appropriate time point, cells were rinsed with ice-cold 1× PBS and fixed overnight in 2% paraformaldehyde in PBS at 4°C. Non-specific binding to cells was blocked by incubating with 1% BSA in PBS for 1 h at room temperature. Triplicate wells were incubated with the following biotinylated lectins overnight at 4°C: WFA (0.5 µg/mL), VVA (7.5 µg/mL), SBA (0.5 µg/mL), DBA (7.5 µg/mL), PNA (2 µg/mL), Jac (2.5 µg/mL), WGA (0.2 µg/mL), SNA (0.5 µg/mL), MAA-II (1.25 µg/mL), PHA-L (0.1 µg/mL) and Con A (5 ng/mL). Control wells were incubated with biotinylated BSA (7.5 µg/mL). Following overnight incubation, unbound lectins were removed by washing with 1% BSA/0.1% Tween-20/1× PBS solution. Wells were incubated with SA-HRP (50 ng/mL) with bound lectins detected using 1-Step Ultra TMB-ELISA Substrate solution per manufacturer's instructions with a colorimetric spectrophotometer (Bio-Rad Benchmark Plus) at 450 nm.

C2C12 cell surface biotinylation

Per 10 cm dish, 2.5×10^5 cells were plated and grown until 90–100% confluent for approximately 4 days, refreshing growth media every 2 days. Once confluent, cells were differentiated to form myotubes, refreshing differentiation media every 2 days. Seven days following differentiation, cells were rinsed twice with ice-cold 1× PBS (pH 8.0) and incubated in 5 mL of 1 mg/mL EZ-Link® Sulfo-NHS-LC-Biotin in 1× PBS (pH 8.0) for 1 h at room temperature. The biotinylation reaction was quenched by rinsing twice with 5 mL of ice-cold 100 mM glycine in 1× PBS (pH 8.0). Cells were then immediately used for lectin precipitations.

Lectin precipitation

Biotinylated cells were scraped into 200 µL ice-cold Nonidet P-40 lysis buffer (NP-40 lysis buffer) consisting of 50 mM Tris-HCl, pH 7.4, 1% Nonidet P-40, 150 mM NaCl and 5 mM EDTA, homogenized with a dounce homogenizer, rotated for 30 min at 4°C and clarified via centrifugation at 13,000 rpm for 20 min at 4°C. Quadriceps from wild-type murine muscle were snap frozen in liquid nitrogen, ground to a powder using a mortar and pestle and added to NP-40 lysis buffer. Wild-type murine lysates were homogenized, rotated and clarified per above. Protein concentration was quantified by Pierce™ BCA Protein Assay kit (Life Technologies). Lectin-agarose beads were prepared by washing with ice-cold NP-40 lysis buffer. Prepared beads were loaded with 100 µg of whole-cell lysate plus 5 µL protease inhibitor cocktail adjusting the total volume to 350 µL with NP-40 lysis buffer. Beads were rotated top over bottom overnight at 4°C. Following precipitation, beads were washed three times with ice-cold NP-40 lysis buffer and protease inhibitor cocktail (Sigma-Aldrich). Precipitated proteins were denatured in NuPAGE sample buffer and reducing agent (Life Technologies), and half of the precipitated proteins were separated on a NuPAGE 3–8% Tris Acetate polyacrylamide gel (Life Technologies) before transferring to nitrocellulose membrane for immunoblotting or staining with SYPRO Ruby protein gel stain.

UGA glycotranscriptome analysis

2.5×10^5 cells were plated, grown until 90–100% confluent and differentiated as above. Cells were collected at the time of differentiation (day 0) or 48 h post differentiation (day 2) by lifting with Trypsin/EDTA (Life Technologies). Cells were pelleted for 5 min at 1200 rpm, rinsed twice with 1× PBS and snap frozen in liquid nitrogen. RNA isolation, cDNA synthesis and transcript abundance determination for 580 glycan-related genes were performed as previously described (Nairn et al. 2008).

siRNA-mediated knockdown

Cells were used for transfection when they reached approximately 65% confluency at which point 1×10^6 cells were resuspended in 100 µL of Nucleofector™ solution V (Lonza, Basel, Switzerland). Individual batches of cells were transfected via Amaxa™ Nucleofector II™ (Lonza) with optimized concentrations of siRNA to β4Galnt3 (1 µM), β3Galnt2 (0.3 µM) and Neu2 (0.3 µM) (Santa Cruz Biotechnology). Control cells were transfected with 1 µM scramble siRNA (Santa Cruz Biotechnology). Transfected cells were resuspended to a concentration of 1×10^5 cells/mL growth media and plated at 5×10^4 per well for lectin binding assays or at 7.5×10^5 cells/well of a 12-well plate. Cells were switched to differentiation media 4 h after plating. Samples were collected for analysis of transcript expression level via quantitative real-time RT-PCR (qRT-PCR) following 2 days of differentiation while samples for lectin binding assays were collected 4 days after differentiation.

Quantitative real-time RT-PCR

RNA from cells was isolated via RNeasy Mini kit per manufacturer's instructions including digestion of genomic DNA. cDNA was synthesized via qScript™ XLT cDNA SuperMix (Quantabio, Beverly, MA). cDNA was amplified with specific primers via LightCycler® 480 SYBR Green I Master reagent (Roche, Indianapolis, IN) with the LightCycler® 480 (Roche) and its detection software. The following primer sets were ordered from Integrated DNA Technologies (IDT, Coralville, IA): *β4Galnt3* (Forward: CCA AGA AAT TGC CCG AAG TAG G; Reverse: GGA GGC CAT AGT TGG TCC A), *β3Galnt2* (Forward: GTC TTG GAG TGT TCT ACG ATG C; Reverse: ACT GAA TCG GGC GAT GAA AAG), *Neu2* (Forward: CAC AGG CGT CCA TGC TTA CA; Reverse: CTG CGT GCT CAT CCG TCT T), *Gapdh* (Forward: AGG TCG GTG TGA ACG GAT TTG; Reverse: TGT AGA CCA TGT AGT TGA GGT CA). Expression of the gene of interest was normalized to expression of the housekeeping gene *Gapdh*.

Glycosylation Inhibitor treatment (DMNJ)

Deoxymannojirimycin (2 mM, DMNJ) or vehicle control was added to differentiation media of cells on day 4 of differentiation. Cells were treated for 72 h and analyzed by lectin binding assay or lectin precipitation as described above.

CFG glycan array analysis

For each lectin, the relative fluorescent units (RFU) for the most highly bound glycan was identified and all glycans with an average RFU of 10% or more of the highest bound glycan were compared. For example, the highest RFU for WFA was 54,879.56, therefore all glycans with an RFU in excess of 5488 were compared. While multiple entries for each lectin may exist in the CFG database, only those manufactured by Vector Laboratories and assayed at 10 µg/mL were included in our analysis. At this lectin concentration, RFU for all four lectins was within 3- to 4-fold of the maximum.

Supplementary data

Supplementary data for this article is available online at http://glycob.oxfordjournals.org/.

Funding

The Muscular Dystrophy Association (RG 135449 to L.G.B., RG 274143 to R.C.W.); the National Institutes of Health (NIH P30 AR057230 and NIH/CATS UCLA CTSI UL1TR000124 subprojects to L.G.B., and R.C.W. NIH R01 AR048179 to R.C.W., GM103490 to K.M.); the National Research Service Award GM07104, Edith Hyde Fellowship and Eureka Pre-doctoral Training Fellowship (to J.L.M.); Ruth L. Kirschstein National Research Service Award from National Institute of Arthritis and Musculoskeletal and Skin Diseases (NIAMS) (T32AR059033 to J.L.M. and E.M.G.) and the Broad Stem Cell Institute and the Center for Duchenne Muscular Dystrophy at UCLA.

Acknowledgements

The authors would like to thank Sandra Thiemann and Katrin Schaefer (UCLA, Baum lab) for their intellectual input and discussion, as well as Grace Hong (UCLA, Crosbie-Watson lab) for muscle tissue sample preparation.

Conflict of interest statement

None declared.

Abbreviations

$\alpha 7^{-/-}$, alpha-7-integrin-null; α-BTX, alpha-bungarotoxin; α-DG, alpha-dystroglycan; α-SG, alpha-sarcoglycan; β3Galnt2, beta-1,3-*N*-acetylgalactosaminyltransferase 2; β4Galnt3, beta-1,4-*N*-acetylgalactosaminyltransferase 3; β-DG, beta-dystroglycan; BSA, bovine serum albumin; CFG, Consortium for Functional Glycomics; CMAH, cytidine monophosphate-*N*-acetylneuraminic acid hydroxylase; Con A, concanavalin A; DBA, *Dolichos biflorus* agglutinin; DGC, dystrophin–glycoprotein complex; DMD, Duchenne muscular dystrophy; DMNJ, deoxymannojirimycin; ECM, extracellular matrix; gal-1, galectin-1; GalNAc, *N*-acetylgalactosamine; GAPDH, glyceraldehyde-3-phosphate dehydrogenase; GlcNAc, *N*-acetylglucosamine; Jac, Jacalin; LARGE, like-glycosyltransferase; MAA-II, *Maackia amurensis* agglutinin-II; MTJ, myotendinous junction; Neu2, sialidase 2; NMJ, neuromuscular junction; PBS, phosphate-buffered saline; PHA-L, *Phaseolus vulgaris* Leucoagglutinin; PNA, peanut agglutinin; PNGaseF, Peptide-N-glycosidase F; RFU, relative fluorescent unit; SBA, soybean agglutinin; SNA, *Sambucus nigra* agglutinin; UGC, utrophin–glycoprotein complex; $Utr^{-/-}$, utrophin-null; VVA, *Vicia villosa* agglutinin; WFA, *Wisteria floribunda* agglutinin; WGA, wheat germ agglutinin.

References

Abbott KL, Nairn AV, Hall EM, Horton MB, McDonald JF, Moremen KW, Dinulescu DM, Pierce M. 2008. Focused glycomic analysis of the N-linked glycan biosynthetic pathway in ovarian cancer. *Proteomics*. 8:3210–3220.

Amenta AR, Yilmaz A, Bogdanovich S, McKechnie BA, Abedi M, Khurana TS, Fallon JR. 2011. Biglycan recruits utrophin to the sarcolemma and counters dystrophic pathology in mdx mice. *Proc Natl Acad Sci USA*. 108:762–767.

Burkin DJ, Kaufman SJ. 1999. The alpha7beta1 integrin in muscle development and disease. *Cell Tissue Res*. 296:183–190.

Cabrera PV, Amano M, Mitoma J, Chan J, Said J, Fukuda M, Baum LG. 2006. Haploinsufficiency of C2GnT-I glycosyltransferase renders T lymphoma cells resistant to cell death. *Blood*. 108:2399–2406.

Cabrera PV, Pang M, Marshall JL, Kung R, Nelson SF, Stalnaker SH, Wells L, Crosbie-Watson RH, Baum LG. 2012. High throughput screening for compounds that alter muscle cell glycosylation identifies new role for N-glycans in regulating sarcolemmal protein abundance and laminin binding. *J Biol Chem*. 287:22759–22770.

Chandrasekharan K, Yoon JH, Xu Y, deVries S, Camboni M, Janssen PM, Varki A, Martin PT. 2010. A human-specific deletion in mouse Cmah increases disease severity in the mdx model of Duchenne muscular dystrophy. *Sci Transl Med*. 2:42ra54.

Chou HH, Takematsu H, Diaz S, Iber J, Nickerson E, Wright KL, Muchmore EA, Nelson DL, Warren ST, Varki A. 1998. A mutation in human CMP-sialic acid hydroxylase occurred after the Homo-Pan divergence. *Proc Natl Acad Sci USA*. 95:11751–11756.

Chu FK. 1986. Requirements of cleavage of high mannose oligosaccharides in glycoproteins by peptide N-glycosidase F. *J Biol Chem*. 261:172–177.

Clerk A, Morris GE, Dubowitz V, Davies KE, Sewry CA. 1993. Dystrophin-related protein, utrophin, in normal and dystrophic human fetal skeletal muscle. *Histochem J*. 25:554–561.

Cummings RD, Kornfeld S. 1982. Characterization of the structural determinants required for the high affinity interaction of asparagine-linked oligosaccharides with immobilized Phaseolus vulgaris leukoagglutinating and erythroagglutinating lectins. *J Biol Chem*. 257:11230–11234.

Endo T. 2015. Glycobiology of α-dystroglycan and muscular dystrophy. *J Biochem*. 157:1–12.

Ervasti JM, Burwell AL, Geissler AL. 1997. Tissue-specific heterogeneity in alpha-dystroglycan sialoglycosylation. Skeletal muscle alpha-dystroglycan is a latent receptor for Vicia villosa agglutinin b4 masked by sialic acid modification. *J Biol Chem*. 272:22315–22321.

Ervasti JM, Campbell KP. 1993. A role for the dystrophin-glycoprotein complex as a transmembrane linker between laminin and actin. *J Cell Biol*. 122:809–823.

Fuhrmann U, Bause E, Legler G, Ploegh H. 1984. Novel mannosidase inhibitor blocking conversion of high mannose to complex oligosaccharides. *Nature*. 307:755–758.

Gasimli L, Hickey AM, Yang B, Li G, dela Rosa M, Nairn AV, Kulik MJ, Dordick JS, Moremen KW, Dalton S, et al. 2014. Changes in glycosaminoglycan structure on differentiation of human embryonic stem cells towards mesoderm and endoderm lineages. *Biochim Biophys Acta*. 1840:1993–2003.

Greenaway PJ, LeVine D. 1973. Binding of N-acetyl-neuraminic acid by wheat-germ agglutinin. *Nat New Biol*. 241:191–192.

Gundry RL, Raginski K, Tarasova Y, Tchernyshyov I, Bausch-Fluck D, Elliott ST, Boheler KR, Van Eyk JE, Wollscheid B. 2009. The mouse C2C12 myoblast cell surface N-linked glycoproteome: identification, glycosite occupancy, and membrane orientation. *Mol Cell Proteomics*. 8:2555–2569.

Hedberg C, Oldfors A, Darin N. 2014. B3GALNT2 is a gene associated with congenital muscular dystrophy with brain malformations. *Eur J Hum Genet*. 22:707–710.

Iwata Y, Suzuki O, Wakabayashi S. 2013. Decreased surface sialic acid content is a sensitive indicator of muscle damage. *Muscle Nerve*. 47:372–378.

James M, Simmons C, Wise CJ, Jones GE, Morris GE. 1995. Evidence for a utrophin-glycoprotein complex in cultured cell lines and a possible role in cell adhesion. *Biochem Soc Trans*. 23:398S.

Kanagawa M, Michele DE, Satz JS, Barresi R, Kusano H, Sasaki T, Timpl R, Henry MD, Campbell KP. 2005. Disruption of perlecan binding and matrix assembly by post-translational or genetic disruption of dystroglycan function. *FEBS Lett*. 579:4792–4796.

Konami Y, Yamamoto K, Osawa T, Irimura T. 1994. Strong affinity of Maackia amurensis hemagglutinin (MAH) for sialic acid-containing Ser/Thr-linked carbohydrate chains of N-terminal octapeptides from human glycophorin A. *FEBS Lett*. 342:334–338.

Lee EU, Roth J, Paulson JC. 1989. Alteration of terminal glycosylation sequences on N-linked oligosaccharides of Chinese hamster ovary cells by expression of beta-galactoside alpha 2,6-sialyltransferase. *J Biol Chem*. 264:13848–13855.

Live D, Wells L, Boons GJ. 2013. Dissecting the molecular basis of the role of the O-mannosylation pathway in disease: α-dystroglycan and forms of muscular dystrophy. *Chembiochem*. 14:2392–2402.

Lotan R, Skutelsky E, Danon D, Sharon N. 1975. The purification, composition, and specificity of the anti-T lectin from peanut (Arachis hypogaea). *J Biol Chem*. 250:8518–8523.

Magalhães A, Marcos-Pinto R, Nairn AV, Dela Rosa M, Ferreira RM, Junqueira-Neto S, Freitas D, Gomes J, Oliveira P, Santos MR, et al. 2015. Helicobacter pylori chronic infection and mucosal inflammation switches the human gastric glycosylation pathways. *Biochim Biophys Acta*. 1852:1928–1939.

Marshall JL, Holmberg J, Chou E, Ocampo AC, Oh J, Lee J, Peter AK, Martin PT, Crosbie-Watson RH. 2012. Sarcospan-dependent Akt activation is required for utrophin expression and muscle regeneration. *J Cell Biol*. 197:1009–1027.

Martin PT, Camboni M, Xu R, Golden B, Chandrasekharan K, Wang CM, Varki A, Janssen PM. 2013. N-Glycolylneuraminic acid deficiency worsens cardiac and skeletal muscle pathophysiology in α-sarcoglycan-deficient mice. *Glycobiology*. 23:833–843.

Martin PT, Kaufman SJ, Kramer RH, Sanes JR. 1996. Synaptic integrins in developing, adult, and mutant muscle: selective association of alpha1, alpha7A, and alpha7B integrins with the neuromuscular junction. *Dev Biol*. 174:125–139.

McDearmon EL, Combs AC, Ervasti JM. 2001. Differential Vicia villosa agglutinin reactivity identifies three distinct dystroglycan complexes in skeletal muscle. *J Biol Chem*. 276:35078–35086.

Mega T, Oku H, Hase S. 1992. Characterization of carbohydrate-binding specificity of concanavalin A by competitive binding of pyridylamino sugar chains. *J Biochem*. 111:396–400.

Meier T, Ruegg MA. 2000. The role of dystroglycan and its ligands in physiology and disease. *News Physiol Sci*. 15:255–259.

Monti E, Preti A, Nesti C, Ballabio A, Borsani G. 1999. Expression of a novel human sialidase encoded by the NEU2 gene. *Glycobiology*. 9:1313–1321.

Nairn AV, York WS, Harris K, Hall EM, Pierce JM, Moremen KW. 2008. Regulation of glycan structures in animal tissues: transcript profiling of glycan-related genes. *J Biol Chem*. 283:17298–17313.

Nguyen HH, Jayasinha V, Xia B, Hoyte K, Martin PT. 2002. Overexpression of the cytotoxic T cell GalNAc transferase in skeletal muscle inhibits muscular dystrophy in mdx mice. *Proc Natl Acad Sci USA*. 99:5616–5621.

Patnaik SK, Stanley P. 2005. Mouse large can modify complex N- and mucin O-glycans on alpha-dystroglycan to induce laminin binding. *J Biol Chem*. 280:20851–20859.

Praissman JL, Live DH, Wang S, Ramiah A, Chinoy ZS, Boons GJ, Moremen KW, Wells L. 2014. B4GAT1 is the priming enzyme for the LARGE-dependent functional glycosylation of α-dystroglycan. *Elife*. 3. DOI:10.7554/eLife.03943.

Praissman JL, Willer T, Sheikh MO, Toi A, Chitayat D, Lin YY, Lee H, Stalnaker SH, Wang S, Prabhakar PK, et al. 2016. The functional O-mannose glycan on α-dystroglycan contains a phospho-ribitol primed for matriglycan addition. *Elife*. 5. DOI:10.7554/eLife.14473.

Sanes JR, Cheney JM. 1982. Lectin binding reveals a synapse-specific carbohydrate in skeletal muscle. *Nature*. 300:646–647.

Scott LJ, Bacou F, Sanes JR. 1988. A synapse-specific carbohydrate at the neuromuscular junction: association with both acetylcholinesterase and a glycolipid. *J Neurosci*. 8:932–944.

Shibuya N, Goldstein IJ, Broekaert WF, Nsimba-Lubaki M, Peeters B, Peumans WJ. 1987. The elderberry (Sambucus nigra L.) bark lectin recognizes the Neu5Ac(alpha 2-6)Gal/GalNAc sequence. *J Biol Chem*. 262:1596–1601.

Song WK, Wang W, Foster RF, Bielser DA, Kaufman SJ. 1992. H36-alpha 7 is a novel integrin alpha chain that is developmentally regulated during skeletal myogenesis. *J Cell Biol*. 117:643–657.

Stevens E, Carss KJ, Cirak S, Foley AR, Torelli S, Willer T, Tambunan DE, Yau S, Brodd L, Sewry CA, et al. 2013. Mutations in B3GALNT2 cause congenital muscular dystrophy and hypoglycosylation of α-dystroglycan. *Am J Hum Genet*. 92:354–365.

Tidball JG. 1991. Force transmission across muscle cell membranes. *J Biomech*. 24(Suppl 1):43–52.

Tintignac LA, Brenner HR, Rüegg MA. 2015. Mechanisms regulating neuromuscular junction development and function and causes of muscle wasting. *Physiol Rev*. 95:809–852.

Van Ry PM, Wuebbles RD, Key M, Burkin DJ. 2015. Galectin-1 protein therapy prevents pathology and improves muscle function in the mdx mouse model of Duchenne muscular dystrophy. *Mol Ther*. 23:1285–1297.

von der Mark H, Williams I, Wendler O, Sorokin L, von der Mark K, Pöschl E. 2002. Alternative splice variants of alpha 7 beta 1 integrin selectively recognize different laminin isoforms. *J Biol Chem*. 277:6012–6016.

Willer T, Inamori K, Venzke D, Harvey C, Morgensen G, Hara Y, Beltrán Valero de Bernabé D, Yu L, Wright KM, et al. 2014. The

glucuronyltransferase B4GAT1 is required for initiation of LARGE-mediated α-dystroglycan functional glycosylation. *Elife*. 3. DOI:10.7554/eLife.03941.

Wu AM, Wu JH, Lin LH, Lin SH, Liu JH. 2003. Binding profile of Artocarpus integrifolia agglutinin (Jacalin). *Life Sci*. 72: 2285–2302.

Xia B, Hoyte K, Kammesheidt A, Deerinck T, Ellisman M, Martin PT. 2002. Overexpression of the CT GalNAc transferase in skeletal muscle alters myofiber growth, neuromuscular structure, and laminin expression. *Dev Biol*. 242:58–73.

Yoshida-Moriguchi T, Yu L, Stalnaker SH, Davis S, Kunz S, Madson M, Oldstone MB, Schachter H, Wells L, Campbell KP. 2010. O-mannosyl phosphorylation of alpha-dystroglycan is required for laminin binding. *Science*. 327:88–92.

Zhang P, Hu H. 2012. Differential glycosylation of α-dystroglycan and proteins other than α-dystroglycan by like-glycosyltransferase. *Glycobiology*. 22:235–247.

CHAPTER FOUR

Lectin binding characterizes the healthy human skeletal muscle glycophenotype and identifies disease specific changes in dystrophic muscle

This chapter has been submitted to *Glycobiology* for publication.

Abstract

Our understanding of muscle glycosylation to date has derived from studies in mouse models and a limited number of human lectin histochemistry studies. As various therapeutic approaches aimed at treating patients with muscular dystrophies are being translated from rodent models to human, it is critical to better understand human muscle glycosylation and relevant disease-specific differences between healthy and dystrophic muscle. Here, we report the first quantitative characterization of human muscle glycosylation, and identify differentiation- and disease-specific differences in human muscle glycosylation. Utilizing a panel of 13 lectins with varying glycan specificities, we surveyed lectin binding to primary and immortalized myoblasts and myotubes from healthy and dystrophic sources. Following differentiation of primary and immortalized healthy human muscle cells, we observed increased binding of NPA, PNA, MAA-II, and WFA to myotubes compared to myoblasts. Following differentiation of immortalized healthy and dystrophic human muscle cells, we observed disease-specific differences in binding of NPA, Jac and TJA-I to differentiated myotubes. We also observed differentiation- and disease-specific differences in binding of NPA, Jac, PNA, TJA-I, and WFA to glycoprotein receptors in muscle cells. Additionally, Jac, PNA and WFA precipitated functionally glycosylated α-DG, that bound laminin, while NPA and TJA-I did not. Lectin histochemistry of healthy and dystrophic human muscle sections identified disease-specific differences in binding of *O*-glycan and sialic acid specific lectins between healthy and dystrophic muscle. These results indicate that specific and discrete changes in glycosylation occur following differentiation, and identify TJA-I, Jac, PNA and NPA as potential lectin biomarkers sensitive to changes in healthy human muscle glycosylation.

Introduction

Myofiber attachment to the extracellular matrix (ECM) is necessary for proper muscle function. The basement membrane plays a critical role in the transfer of contractile forces by facilitating force transmission both longitudinally and laterally. Loss of connection between myofibers and the ECM causes a drop in both the absolute and specific force generated by a muscle [1]. The major adhesion complexes present at the muscle cell surface, or sarcolemma, are the dystrophin-glycoprotein complex (DGC), the homologous utrophin-glycoprotein complex (UGC) expressed at the neuromuscular and myotendinous junctions (NMJ/MTJ), and the α7β1 integrin heterodimer [2]. All three complexes independently bind laminins in the ECM and intracellular actin cytoskeleton to provide myofiber-ECM attachment [2]. Loss of various components of each adhesion complex cause various muscular dystrophies. For example, loss of dystrophin expression in Duchenne Muscular Dystrophy (DMD) prevents the entire DGC from being present at the sarcolemma [3-5]. Similarly, loss of any of the sarcoglycans (SGs) from the DGC causes various limb-girdle muscular dystrophies (LGMDs) [6-9] and loss of α7-integrin is known to cause a congenital myopathy [10,11].

In addition to the presence of adhesion complexes at the sarcolemma, proper glycosylation of component glycoproteins in the complexes is necessary for myofiber-ECM binding. Improper glycosylation of alpha-dystroglycan (α-DG) in the DGC results in loss of laminin binding. Specifically, addition of the glucuronic acid-xylose disaccharide repeat known as matriglycan is requisite for laminin binding as are the underlying glycan structures to which matriglycan is added [12-15]. To date, mutations in 24 genes necessary for α-DG glycosylation have been identified. Mutations in these 24 genes cause loss-of-function, disrupt α-DG glycosylation,

and contribute to a wide spectrum of congenital α-DG disorders known as dystroglycanopathies [16].

Various therapeutic approaches for muscular dystrophies are being explored, including restoring dystrophin expression (e.g. exon skipping or gene editing), modulating immune responses, potential stem cell therapies, and different strategies to upregulate utrophin, to compensate for the loss of dystrophin [17-23] . One method for upregulating utrophin utilization currently being studied focuses on manipulating the glycosylation status of α-DG. In rodent muscle, differential glycosylation of α-DG correlates with cellular localization and protein complex association. For example, α-DG expressed ubiquitously throughout the sarcolemma binds the sialic acid and GlcNAc-specific lectin wheat germ agglutinin (WGA) [3,24,25]. In contrast, α-DG associated with the UGC is restricted to the NMJ and MTJ in rodent muscle and binds the GalNAc-specific lectin *Wisteria floribunda* agglutinin (WFA) [24-26]. Thus, various groups have sought to increase utrophin utilization, to increase UCG-mediated adhesion at the sarcolemma in the absence of dystrophin, by manipulating this differential glycosylation of α-DG.

Current approaches to alter α-DG glycosylation in order to increase utrophin utilization still face challenges. Overexpression of the GalNAc-transferase β4Galnt2 increases WFA binding to α-DG and reduces the dystrophic pathology in several dystrophic mouse models by increasing abundance of laminin and various UGC components [24,27-29]. However, the exact mechanism by which β4Galnt2 overexpression reduces muscular dystrophy pathology in mice remains poorly defined. Additionally, potential off-target sites of GalNAc addition resulting from β4Galnt2 overexpression have yet to be determined. Our group previously identified lobeline, a small molecule antagonist of the acetylcholine receptor (AChR), in a high throughput screen for molecules which upregulate WFA binding to murine muscle cells [30]. While lobeline

increased WFA binding to both healthy and dystrophic primary murine muscle cells, we observed no increase in WFA binding following treatment of either healthy or dystrophic human inducible, Directly Reprogrammable Myotubes (iDRMs) generated from control and dystrophic fibroblasts [30].

In 1982, Sanes et al. first demonstrated that the lectin *Dolichos biflorus* agglutinin (DBA) selectively and specifically binds the NMJ and not the extra-synaptic sarcolemma of rodent muscle [31]. In a follow-up study, additional GalNAc-specific lectins (VVA, SBA, HPA) were shown to bind the rodent NMJ specifically while lectins with other glycan specificities (e.g. ConA, WGA, RCA, PHA-L) bound the sarcolemma indiscriminately, demonstrating that the rodent NMJ is uniquely modified with terminal GalNAc structures [32]. However, while VVA binding to rodent muscle is highly specific for the NMJ, VVA binding to human muscle is not NMJ-specific [32], indicating that terminal GalNAc residues may not be restricted to the NMJ in human muscle as observed in rodent muscle. Furthermore, GalNAc-specific lectins such as WFA may be poor biomarkers for disease-specific differences or for the UGC in human skeletal muscle. Beyond our current understanding of the process by which matriglycan is added to α-DG, human muscle glycosylation remains poorly characterized. Additionally, disease-specific differences in human muscle glycosylation have not been evaluated beyond a small collection of immunohistochemistry studies in the 1980s, and to date no glycan structure, present on α-DG or any other glycoprotein, which correlates with the UGC has been identified in human muscle. In the present study, we have characterized the glycophenotype of human skeletal muscle cells during differentiation, and identified differences between healthy and dystrophic muscle. These findings reinforce and extend prior observations regarding differences between rodent and

human muscle cell glycosylation and may identify glycan structures that will be useful biomarkers to evaluate novel therapies for muscular dystrophies.

Results

To quantify changes in glycosylation following differentiation of human myoblasts into fused, multinucleated myotubes, we performed lectin binding assays on fixed primary and immortalized, male, healthy, human skeletal muscle cells (Table 4-1) utilizing a panel of 13 lectins with a wide variety of specificities (Table 4-2) [33]. To quantify changes in *N*-glycosylation, Concanavalin A (ConA) and *Narcissus pseudonarcissus* agglutinin (NPA) were included for oligomannose specificity, while *Phaseolus vulgaris* leucoagglutinin (PHA-L) was included for complex *N*-glycan specificity [34-36]. Four lectins specific for various *O*-glycan structures were included: Peanut agglutinin (PNA), Jacalin (Jac), *Amaranthus caudatus* agglutinin (ACA) and *Ricinus communis* agglutinin I (RCA 120) [37-40]. Four sialic acid binding lectins were also included: *Sambucus nigra* agglutinin (SNA), *Tricosanthes japonica* agglutinin-I (TJA-I), *Maackia amurensis* agglutinin-II (MAA-II) and wheat germ agglutinin (WGA) [41-44]. *Wisteria floribunda* agglutinin (WFA) and *Dolichos biflorus* agglutinin (DBA) both bind glycans terminated with GalNAc residues [45,46] and were included due to use of the lectins historically in identifying the rodent neuromuscular junction [24,25,31,32].

While reactivity of healthy human myoblasts with the various lectins at day 0 (d0) varied considerably, lectin binding to the immortalized human myoblasts recapitulated binding patterns seen in the four primary muscle cells. Following five days of differentiation (d5), distinct increases in binding of four lectins (NPA, PNA, MAA-II, WFA) were observed across all cell sources while no change was observed in the binding of PHA-L and DBA (Figure 1). This

indicates that the increases observed in binding of some lectins was not the result of a global increase in glycosylation following differentiation, but rather, changes in discrete and specific types of glycosylation. For example, ConA and NPA binding increased following differentiation, while no change in binding of PHA-L was observed. Following differentiation, binding of lectins which recognize various *O*-glycans (PNA, Jac, ACA and RCA 120) all increased. Similarly, differentiated healthy myotubes bound substantially more sialic acid specific lectins (MAA-II, SNA and TJA-I) following differentiation. Interestingly, no reactivity at either d0 or d5 with DBA was observed. In total, these results demonstrate that discrete and specific changes in muscle cell glycosylation occur following differentiation and that immortalized human myoblasts recapitulate changes observed in primary human muscle cells.

To identify disease-specific differences in human myoblast glycosylation, we performed lectin binding assays on the immortalized healthy myoblasts and compared this with two immortalized dystrophic lines (Table 4-1). We compared binding of the 13 lectin panel at d0 and d5 across the three cell lines and found disease-specific changes in binding of four lectins following differentiation: NPA, Jac, TJA-I and WFA (Figure 2). Binding of NPA, specific for high mannose *N*-glycans, to healthy cells increased substantially following differentiation while almost no change was observed in NPA binding to dystrophic cells. These changes did not result from increases in total *N*-glycosylation, as no difference was observed in binding of the complex *N*-glycan specific lectin PHA-L to dystrophic myotubes compared to healthy controls. Similarly, binding of Jac to healthy muscle cells increased substantially following differentiation while binding to dystrophic myotubes either decreased or showed no change. Again this was a specific difference, as other lectins which recognize *O*-glycan structures (PNA, ACA, and RCA 120) showed increases following differentiation regardless of disease-state. TJA-I binding changed in

a disease-specific manner as well; TJA binding to healthy muscle cells increased while dystrophic cells showed a substantial reduction in binding following differentiation. Binding of WFA to healthy muscle cells increased following differentiation, while a more modest increase or no change was observed in binding to dystrophic myotubes. No cell lines surveyed bound DBA regardless of differentiation or disease status. The results demonstrated that distinct, disease-specific changes in glycosylation occur following *in vitro* human myoblast differentiation and that NPA, Jac and TJA-I may represent potential lectin biomarkers sensitive to changes in healthy human muscle glycosylation.

To determine if the lectins recognized distinct glycoprotein receptors, we next performed lectin precipitations from lysates of d0 confluent myoblasts and d5 differentiated myotubes. As shown in Figure 3A, NPA, Jac, TJA-I and WFA all precipitated a variety of glycoproteins. Differentiation-specific differences in the glycoproteins precipitated from healthy cells were observed across all four lectins (Figure 3A, arrowheads); most notably, WFA precipitated significantly more glycoproteins from healthy muscle cells at d5 compared to the few bands observed at d0. As reactivity of α-DG with various lectins has been utilized to distinguish between DGC- and UGC-associated α-DG in rodent muscle [3,24,25], we asked if any lectins were able to precipitate α-DG, detected by the monoclonal antibody IIH6, and if the α-DG was capable of binding laminin. Jac, PNA and WFA all precipitated α-DG at d0 and d5 while TJA-I and NPA did not (Figure 3B, data not shown). Of note, these three lectins all precipitated more α-DG at d5 compared to d0, detected by IIH6. We next asked if α-DG precipitated by each of the lectins was functionally *O*-mannosylated and could bind laminin. Interestingly, laminin was not bound by α-DG precipitated by any of the lectins at d0 regardless of disease status. Furthermore, α-DG precipitated from healthy myotubes by Jac, PNA and WFA bound substantially more

laminin compared to α-DG precipitated from dystrophic myotubes, indicating a greater extent of functional *O*-mannosylation in healthy mature myotubes. (Figure 3B, right panels).

As we noted disease specific differences in binding of NPA, TJA-I and Jac to differentiated myotubes *in vitro*, we asked which of the lectins bound to innervated human skeletal muscle in a disease-specific manner. We obtained de-identified, anonymized skeletal muscle biopsies from control and DMD patients through the UCLA Translational Pathology Core Laboratory. Biotinylated lectins were added to sections of paraffin-embedded, formalin-fixed healthy and dystrophic human skeletal muscle, and bound lectins were detected with Texas Red conjugated streptavidin and imaged. In healthy muscle, we observed differential binding of the three lectins with *O*-glycan specificities; Jac bound healthy muscle ubiquitously throughout the sarcolemma, while ACA bound in a very punctate fashion and PNA did not bind regardless of lectin concentration (Figure 4, data not shown). Interestingly, we observed increased binding of all three lectins to dystrophic muscle from DMD patients compared to healthy controls. Most surprisingly, we observed abundant and ubiquitous binding of PNA to the sarcolemma of muscle from a DMD patient, compared to healthy control muscle where we detected no PNA binding. Of the three sialic acid specific lectins assayed, WGA bound the healthy sarcolemma ubiquitously while MAA-II staining was punctate and TJA-I staining was negative. Binding of all three lectins to dystrophic muscle sections was increased compared to healthy controls, with the most striking increase in binding of TJA-I. Binding of NPA, WFA and DBA to section of fixed muscle were negative regardless of disease-status, although we did detect NPA and WFA, but not DBA, binding to dystrophic muscle that was frozen prior to sectioning, rather than formalin-fixed (Figure 4-5). In total, these results indicate disease-specific differences of distinct

glycan types, primarily *O*-glycans detected by PNA and sialic acids detected by TJA-I, in healthy vs. dystrophic human skeletal muscle.

Discussion

While significant progress in the past decade has elucidated the specific glycan structures on α-DG bound by laminin, our understanding of muscle glycosylation outside of α-DG matriglycan remains limited, and has focused on rodent muscle [16,24,47,48]. As previous studies of human skeletal muscle have been limited to qualitative lectin histochemistry [49-54], we sought to perform the first quantitative characterization of human skeletal muscle glycosylation utilizing primary and immortalized cells from healthy and dystrophic patients. Utilizing a panel of 13 lectins, we identified differentiation- and disease-specific changes in muscle cell glycosylation. Following differentiation of both primary and immortalized myotubes, binding of NPA, PNA, MAA-II and WFA increased (Figure 1). Given the specificities of these lectins, glycoproteins at the healthy myotube surface bear more high mannose *N*-glycans, asialo *O*-glycans, and structures terminated with either α2,3-linked sialic acid or GalNAc residues, compared to undifferentiated myoblasts. These lectins may represent appropriate lectin markers of differentiation and may correlate with temporally regulated expression of unique glycoprotein receptors, glycosyltransferases or availability of sugar donor substrates.

In addition to differentiation-specific differences in lectin binding, we were also able to identify disease-specific differences in lectin reactivity. Binding of NPA, Jac and TJA-I to healthy myotubes increased after differentiation, while no change or a reduction in binding to dystrophic myotubes was observed. Healthy myotubes therefore express glycoproteins bearing abundant mannose *N*-glycans as detected by NPA, sialylated *O*-glycans as detected by Jac and glycans terminated with α2,6-linked sialic acid as detected by TJA-I. In contrast, there was little difference in abundance of these glycans between dystrophic myoblasts and myotubes, with no change in NPA reactive high mannose *N*-glycans or sialylated *O*-glycans and fewer α2,6-linked

sialic acid terminated glycans on differentiated dystrophic cells. What drives these disease-specific differences in lectin reactivity? The differentiated, multinucleated healthy myotubes we observed at d5 expressed dystrophin and the DGC, as detected by immunoblotting, while dystrophic myotubes did not, as expected. If NPA, Jac and TJA-I recognize glycans present on glycoproteins composing the DGC, then dystrophic myotubes lacking dystrophin and the DGC would not present these glycans at the sarcolemma, resulting in the disease-specific differences in lectin reactivity we observe. Alternatively, NPA, Jac and TJA-I could bind other sarcolemmal glycoproteins impacted indirectly by the loss of the DGC. For example, loss of the DGC component protein sarcospan has been shown to impair glycosylation of α-DG with WFA reactive structures in mice [25]. Therefore, loss of the DGC may alter intracellular signaling and drive a shift in glycosyltransferase expression affecting the glycan structures present on sarcolemmal glycoproteins, which would alter lectin reactivity.

Manipulating skeletal muscle glycosylation by altering glycosyltransferase expression is one potential therapeutic approach for DMD. In rodent muscle, the NMJ is highly enriched for glycans terminated with WFA-reactive GalNAc residues which correlate with localization of the UGC [25,33]. While both utrophin and WFA reactivity are restricted to the NMJ in healthy murine muscle, utrophin and WFA reactivity both spread ubiquitously throughout the sarcolemma of dystrophic mouse muscle [25,33]. Expression of the GalNac-transferase B4Galnt2 was restricted to the NMJ of healthy mice and therefore proposed to modify UGC-associated α-DG, rationalizing the finding that B4Galnt2 overexpression rescues the dystrophic phenotype in a variety of muscular dystrophy mouse models [24,26-29]. While expression of B4Galnt2 has been observed in murine muscle [26], we did not observe expression in murine C2C12 myoblasts or myotubes previously [33], or in immortalized human muscle cells, regardless of differentiation- or disease-

status (Appendix C). Additionally, our current data demonstrate that an increase in WFA binding to dystrophic human muscle is not the sole disease-specific difference in glycosylation: NPA, PNA and TJA-I ubiquitously bound the sarcolemma of dystrophic human skeletal muscle with no detectable binding to healthy human skeletal muscle (Figure 4-4, Figure 4-5). The exact mechanism by which B4Galnt2 overexpression rescues the dystrophic phenotype in mice is not currently understood [27,55,56]. Furthermore, disease-specific differences in human muscle glycosylation remain poorly understood. Therefore, significant translational hurdles remain for development of B4Galnt2 overexpression as a potential DMD therapy.

The four lectins we assayed precipitated distinct sets of glycoproteins from healthy and dystrophic human myotubes (Figure 3). However, not all lectins bound α-DG and not all α-DG that was precipitated by these lectins was sufficiently modified with matriglycan to bind laminin. Our prior work demonstrated that inhibition of complex *N*-glycan formation via treatment with a mannosidase inhibitor reduced laminin binding to endogenous α-DG, without a concomitant reduction in IIH6 reactivity[30], although both IIH6 and laminin binding are dependent on the activity of LARGE [13]. Our results extend the observation that IIH6 and laminin binding are not exactly equivalent, as Jac, PNA and WFA all precipitated α-DG from d0 myoblasts that bound IIH6 but did not bind laminin (Figure 3B). It is also clear that there is altered glycosylation of cell surface glycoproteins other than α-DG on myotubes compared to myoblasts; while NPA and TJA-I binding increased following muscle cell differentiation in a disease-specific manner (Figure 2), neither lectin precipitated α-DG detected by IIH6 or laminin binding (Figure 3).

Iwata et al. found an approximately 5-fold increase in binding of PNA to dystrophic muscle across multiple muscular dystrophy rodent models including J2N-k hamsters (δ-sarcoglycan$^{-/-}$ model of LGMD2F), *mdx* mice (DMD) and Dy/dy mice (Lama2-/- model of

merosin-deficient muscular dystrophy). In this study, the authors observed increased binding of PNA to muscle sections from one patient with Becker muscular dystrophy and one patient with limb-girdle muscular dystrophy, compared to healthy human skeletal muscle controls [57]. We also saw a robust increase in PNA binding to skeletal muscle from DMD patients, compared to healthy controls which did not bind PNA (Figure 4). Iwata et al. reported very little change in ACA binding to dystrophic tissue, while we observed an increase in ACA binding to multiple dystrophic tissue samples compared to healthy controls. As Iwata et al. observed an increase in PNA binding with relatively no change in binding of ACA, they concluded that cell surface content of sialic acid is reduced in dystrophic muscle. However, we observed no such reduction in sialic content on dystrophic muscle as detected by lectin binding; in contrast, binding of three sialic acid specific lectins (WGA, TJA-I and MAA-II) was increased substantially for dystrophic muscle compared to healthy controls (Figure 4). Collectively, lectin reactivity of healthy and dystrophic tissue samples also underscore species-specific differences in glycosylation of innervated muscle. Increased binding of WFA and PNA represent the only two disease specific differences in lectin binding to dystrophic mouse tissue [25,57]. We observed increased WFA staining of frozen but not FFPE dystrophic human tissue. Increased binding of Jac and lectins specific for sialic acid (WGA, TJA-I, MAA-II) represent novel disease-specific differences in innervated muscle glycosylation not previously reported in human or mouse muscle.

Here we report differentiation-specific differences in binding of lectins specific for high mannose *N*-glycans (NPA), *O*-glycans (PNA), sialic acid residues (MAA-II) and GalNAc terminated structures (WFA) (Figure 1). Increases in binding of NPA and MAA-II following differentiation represent species-specific differences in glycosylation, as we previously found no increase in ConA (also specific for high mannose *N*-glycans) or MAA-II (or any other sialic acid

specific lectins) binding following differentiation of murine C2C12 cells [33]. These species-specific differences highlight the need to use human muscle cell sources *in vitro* when studying glycosylation. C2C12 cells have long been the preferred *in vitro* model due to ease of use and lack of appropriate alternative cell sources, and their use has provided insight into murine integrin and glycolipid glycosylation [47,48]. Our results demonstrate that immortalized human myotubes recapitulate changes observed in primary human myotubes and therefore provide an appropriate alternative for *in vitro* study of human muscle glycobiology. Moreover, identification of lectin biomarkers to identify and follow disease-specific differences in muscle glycosylation and to directly interrogate the glycan products on the cell surface may allow facile and cost-effective analysis of the effects of novel therapeutics on human muscle cells. As lectins bind glycan structures independent of glycoprotein backbone, unlike glycan-specific antibodies, lectins may be sensitive biomarkers for changes in glycosylation agnostic to expression of specific proteins.

Our current findings represent the first quantitative characterization of human muscle glycosylation, and highlight differentiation- and disease-specific differences in lectin reactivity to human skeletal muscle cells and tissue. Disease-specific differences in TJA-I binding were observed on *in vitro* myotube cultures as well as *ex vivo* tissue sections. Future research should focus on understanding the mechanisms driving this difference, as well as those observed in binding of *O*-glycan and sialic acid specific lectins. Furthering our understanding of human muscle glycosylation specifically will allow for the selection of an appropriate lectin biomarker for the healthy human muscle 'glycophenotype' which could aid in the discovery of novel therapeutics [30], and provide a sensitive endpoint measure for other therapeutics currently under development for muscular dystrophy.

Materials and Methods

Cells

Immortalized healthy human myoblasts LHCN-M2 [58] were a generous gift from Woodring Wright Lab (UT Southwestern, Dallas, TX) and immortalized dystrophic human myoblasts DMD 6311 and DMD 6594 [59] were a kind gift from Vincent Mouly Lab (UPMC Université Paris, Paris, FR). Four distinct lots of primary human skeletal muscle cells (HSMCs) were purchased and randomly numbered 1-4 (HSMC1-4) (PromoCell GmbH, Heidelberg, Germany). Immortalized and primary human muscle cells were grown in skeletal muscle cell growth medium (Promocell GmbH, Heidelburg, Germany) plus ciprofloxacin (10 µg/mL) on 0.1% porcine gelatin and passaged when approximately 60% confluent.

Reagents

The following biotinylated lectins and proteins were purchased (Vector Laboratories, Burlingame, CA): Concanavalin A (ConA), *Narcissus psuedonarcissus* agglutinin (NPA), *Phaseolus vulgaris* leucoagglutinin (PHA-L), peanut agglutinin (PNA), jacalin agglutinin (Jac), *Ricinus communis* agglutinin I (RCA 120), *Amaranthus caudatus* agglutinin (ACA), wheat germ agglutinin (WGA), *Sambucus nigra* agglutinin (SNA), *Maackia amurensis* lectin II (MAA II), *Wisteria floribunda* agglutinin (WFA), *Dolichos biflorus* agglutinin (DBA) and bovine serum albumin (BSA). *Tricosanthes japonica* agglutinin I (TJA-I) was purchased (Medicago, Uppsala, Sweden) and biotinylated using EZ-Link™ Sulfo-NHS-Biotin kit (21335) (ThermoFisher Scientific, Waltham, MA) according to manufacturer's instruction and stored in 10 mM HEPES, 0.15 M NaCl, pH 7.5, 0.1 mM Ca^{2+} at -20 ^{o}C.

Antibodies against matriglycan (IIH6C4) (EMD Millipore, Billerica, MA) and laminin (L939) (Sigma-Aldrich, St. Louis, MO) and secondary goat anti-mouse IgG+M (H+L)-HRP and donkey anti-rabbit IgG (H+L)-HRP (Jackson ImmunoResearch, West Grove, PA) antibodies were purchased. The following reagents were purchased: streptavidin conjugated horseradish peroxidase (SA-HRP; Jackson ImmunoResearch), EHS Laminin (L2020), protease inhibitor cocktail (PIC; P8340) (Sigma-Aldrich), SYPRO® Ruby protein gel stain (S12000), 1-Step Ultra TMB-ELISA Substrate solution (34029), SuperSignal™ West Femto Maximum Sensitivity Substrate (34094, Thermo Fisher Scientific), VECTASHIELD™ Antifade Mounting Medium with DAPI (H-1500), Texas-Red conjugated Avidin D (A-2006), streptavidin-agarose (SA-5010), and Avidin/Biotin blocking kit (SP-2001) (Vector Laboratories).

Lectin binding assays

Lectin binding assays were performed in 96-well plates as described previously with the following modification [33]. $5x10^3$ healthy or dystrophic, immortalized or primary human myoblasts were plated per well coated with 0.1% porcine gelatin. Cells were grown until approximately 80-85% confluent and differentiated for 5 days. Cells were collected at the time of differentiation (D0) or 5 days following differentiation and fixed overnight at 4^{o}C in 2% paraformaldehyde in PBS. Non-specific binding to fixed cells was blocked by incubating in 1%BSA in PBS for 1 h at room temperature. Triplicate wells were then incubated in the following lectins overnight at 4^{o}C: ConA (5 ng/mL), NPA (2.5 µg/mL), PHA-L (10 ng/mL), PNA (100 ng/mL), Jac (5 µg/mL), RCA 120 (10 ng/mL), ACA (50 ng/mL), WGA (5 ng/mL), SNA (2.5 µg/mL), TJA-I (2.5 µg/mL), MAA II (100 ng/mL), WFA (250 ng/ml), and DBA (5 µg/mL). Control cells were incubated with equivalent concentrations of biotinylated BSA.

Following overnight incubation, cells were rinsed with 1% BSA/0.1% Tween-20/1x PBS solution and incubated with SA-HRP (50 ng/mL). Bound lectins were detected using 1-Step Ultra TMB-ELISA Substrate solution per manufacturer's instructions with a colorimetric spectrophotometer (Bio-Rad Benchmark Plus) at 450 nm.

Lectin precipitations

For enrichment of lectin receptors, $1x10^6$ healthy or dystrophic myoblasts were plated per 10 cm dish coated with 0.1% porcine gelatin, and collected once confluent (day 0) and following 5 days of differentiation (day 5). At appropriate time points, cells were washed with ice-cold PBS and scraped in ice-cold radioimmunoprecipitation assay buffer (RIPA; 25 mM Tris•HCl pH 7.6, 150 mM NaCl, 1% NP-40, 1% sodium deoxycholate, 0.1% SDS) containing protease inhibitor cocktail. Lysates were rotated at 4 ºC for 1 h and clarified by centrifugation at 13,300 rpm for 20 min at 4 ºC. Protein concentration was determined by Pierce™ BCA Protein Assay (Thermo Fisher Scientific). Lysates (150 µg) were added to 25 µg biotinylated lectin and 20 µL streptavidin-agarose overnight at 4 ºC. Following lectin precipitation, beads were washed three times with cold lysis buffer plus protease inhibitor cocktail and denatured in NuPAGE sample buffer and reducing agent (Thermo Fisher Scientific). Proteins were then separated on 3-8% BisTris polyacrylamide gels for staining with SYPRO® Ruby protein gel stain as described previously in [33].

Laminin overlay

Laminin overlays were performed on separated lectin receptors as described previously [30]. Briefly, lectin receptors precipitated per above were separated on 3-8% BisTris gels, transferred to nitrocellulose and blocked in 5% non-fat dry milk in laminin binding buffer. Blots were then sequentially incubated in EHS laminin, rabbit anti-laminin (1:1000), and donkey anti-rabbit HRP (1:3000). Bound antibody was detected by enhance chemiluminesence on a LI-COR Odyssey Fc.

Tissue staining

Deidenitified, anonymized, five micrometer, paraffin-embedded or frozen human muscle tissue sections were provided by the Translational Pathology Core Laboratory at UCLA (David Geffen School of Medicine, UCLA). Paraffin-embedded tissue sections were deparaffinized with xylene, ethanol and rehydrated with 1x phosphate-buffered saline (1x PBS). Sections were stained as described previously [33]. Briefly, non-specific binding to tissue sections was blocked with 1% BSA/1x PBS and Avidin/Biotin blocking kit according to manufacturer's instructions. Serial sections were incubated overnight at 4 ^{o}C in biotinylated lectins: ConA (5µg/mL), NPA (10 µg/mL), PHA-L (10 µg/mL), PNA (10 µg/mL), Jac (10 µg/mL), RCA-120 (10 µg/mL), ACA (5µg/mL), SNA (10 µg/mL), TJA-I (10 µg/mL), MAA-II (5µg/mL), WGA (10 µg/mL), WFA (25 µg/mL), and DBA (25 µg/mL). Bound antibodies and lectins were detected via fluorescein-avidin, mounted with VECTASHIELD™ to prevent photobleaching and visualized on an Olympus BX51 fluorescence microscope and Olympus DP2-BSW software (Olympus America Inc., Center Valley, PA).

Funding

This work was supported by Muscular Dystrophy Association RG 254647 (to LGB), NIH P30 AR057230 (to the UCLA Center for Duchenne Muscular Dystrophy) and the UCLA Center for Duchenne Muscular Dystrophy Fellowship (to BJM).

Acknowledgements

We thank Mabel Pang and Katrin Schaefer (Baum Lab) for helpful discussion, Negar Khanlou for assistance with muscle tissue sample acquisition, Rachelle Crosbie-Watson for assistance with fluorescence microscopy, and Alison Nairn and Kelley Moremen for analysis of glycotranscript expression. We thank the UCLA Translational Pathology Core Laboratory for their preparation of de-identified human skeletal muscle tissue and the UCLA Center for Duchenne Muscular Tissue Repository for immortalized healthy and dystrophic human cell lines.

Conflict of interest statement

The authors declare no conflict of interest

Abbreviations

ACA- *Amaranthus caudatus* agglutinin, AChR- acetylcholine receptor, α-DG- alpha dystroglycan, B4Galnt2- beta-1,4-*N*-acetylgalactosaminyltransferase 2, BSA-bovine serum albumin, ConA- Concanavalin A, DBA- *Dolichos biflorus,* DGC- dystrophin-glycoprotein complex, DMD- Duchenne muscular dystrophy, ECM- extracellular matrix, iDRM- inducible, directly reprogrammable myotube, LGMD- limb-girdle muscular dystrophy, Jac- jacalin, MAA-II- *Maackia amurensis* agglutinin-II, MTJ- myotendous junction, NMJ- neuromuscular junction, NPA- *Narcissus pseudonarcissus* agglutinin, PHA-L- *Phaseolus vulgaris* leucoagglutinin, PNA-

peanut agglutinin, RCA 120- *Ricinus communis* agglutinin I, SG- sarcoglycan, SNA- *Sambucus nigra* agglutinin, TJA-I- *Tricosanthes japonica* agglutinin-I, WGA- wheat germ agglutinin, WFA- *Wisteria floribunda* agglutinin

Table 4-1: Primary and immortalized, healthy and dystrophic human myoblast cell sources

Cell	Muscle Source	Genotype	Vendor/Source
HSMC-1	26 yo gastrocnemius	Healthy	Promocell
HSMC-2	53 yo psoas major	Healthy	Promocell
HSMC-3	19 yo thigh	Healthy	Promocell
HSMC-4	27 yo gastrocnemius	Healthy	Promocell
LHCN-M2	41 yo pectoralis major	Healthy	UCLA CDMD Cell Repository Core
DMD 6311	23 mo	*DMD* exon 45-52 del	UCLA CDMD Cell Repository Core
DMD 6594	20 mo	*DMD* exon 48-50 del	UCLA CDMD Cell Repository Core

Table 4-2: Panel of lectins with varying glycan structure specificities

Lectin	Nominal Specificity	Reference
ConA	High Mannose	Mega et al. 1992
NPA	High Mannose	Kaku et al. 1990
PHA-L	Complex N-glycans	Cummings and Kornfeld 1982
PNA	Asialo O-glycans	Lotan et al. 1975
Jac	Sialylated O-glycans	Wu et al. 2003
ACA	LacNAc, tolerates sialylation	Rinderle et al. 1989
RCA 120	LacNAc	Drysdale et al. 1968
SNA	2,6-linked sialic acid	Shibuya et al. 1987
TJA-I	2,6-linked sialic acid	Yamashita et al. 1992
MAA II	2,3-linked sialic acid	Konami et al. 1994
WGA	Sialic acid, GlcNAc	Greenaway and LeVine 1973
WFA	Terminal GalNAc	Uchida et al. 1978
DBA	Terminal GalNAc	Etzler et al. 1981

Figure 4-1: Changes in cell surface glycosylation following differentiation of primary and immortalized healthy human myotubes.

Healthy primary (HSMC-1, -2, -3, -4) and immortalized (LHCN-M2) human myoblasts (d0, solid bars) and myotubes (d5, hatched bars) were characterized with a panel of 13 lectins. Increased binding of four *O*-glycan specific lectins as well as NPA and MAA-II (high-mannose *N*-glycan and sialic acid-specific, respectively) was observed for both immortalized healthy human muscle cells and four primary healthy human muscle cell preparations.

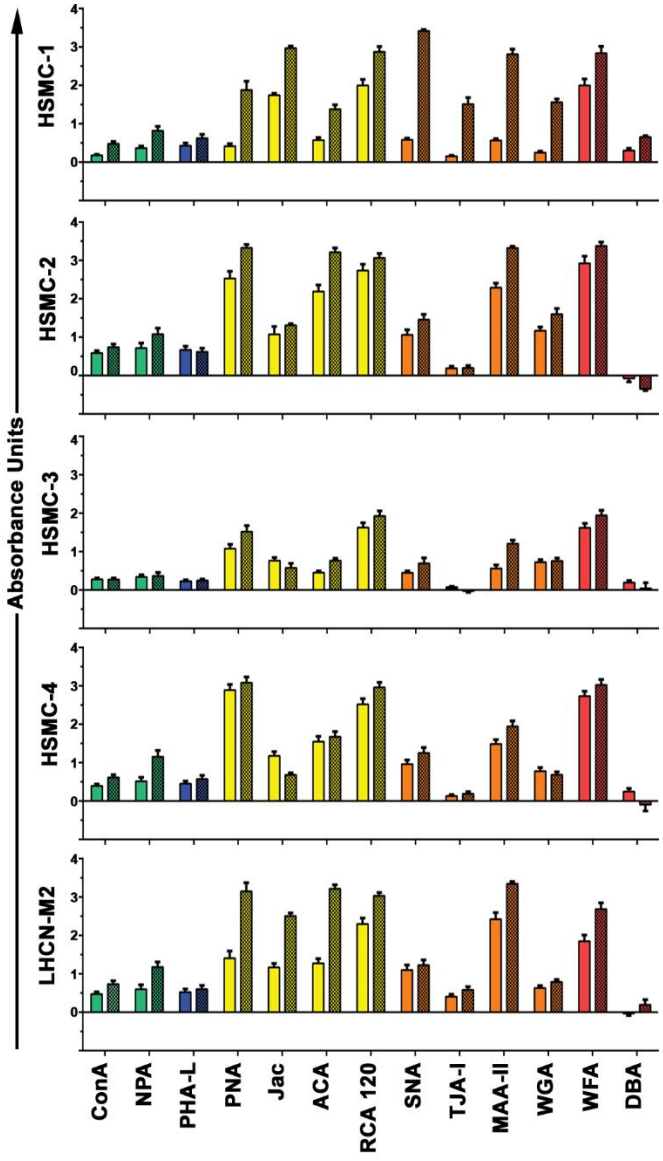

Absorbance Units
HSMC-1
HSMC-2
HSMC-3
HSMC-4
LHCN-M2
0
1
2
3
4
ConA
NPA
PHA-L
PNA
Jac
ACA
RCA 120
SNA
TJA-I
MAA-II
WGA
WFA
DBA

Figure 4-2: Disease-specific changes in lectin binding to human skeletal muscle cells. Healthy (LHCN) immortalized human myoblasts (d0, open bars) and myotubes (d5, black bars) were compared to immortalized muscle cells from two patients with Duchenne muscular dystrophy (6311 and 6594). NPA, Jac and TJA-I binding to healthy myotubes increased on d5 compared to day 0, while binding of these lectins to dystrophic myotubes did not change or decreased. Increased binding of PHA-L, PNA, ACA, RCA 120, MAA-II, and WGA to d5 myotubes were observed regardless of disease status. Human muscle cells did not bind DBA regardless of differentiation- or disease-status.

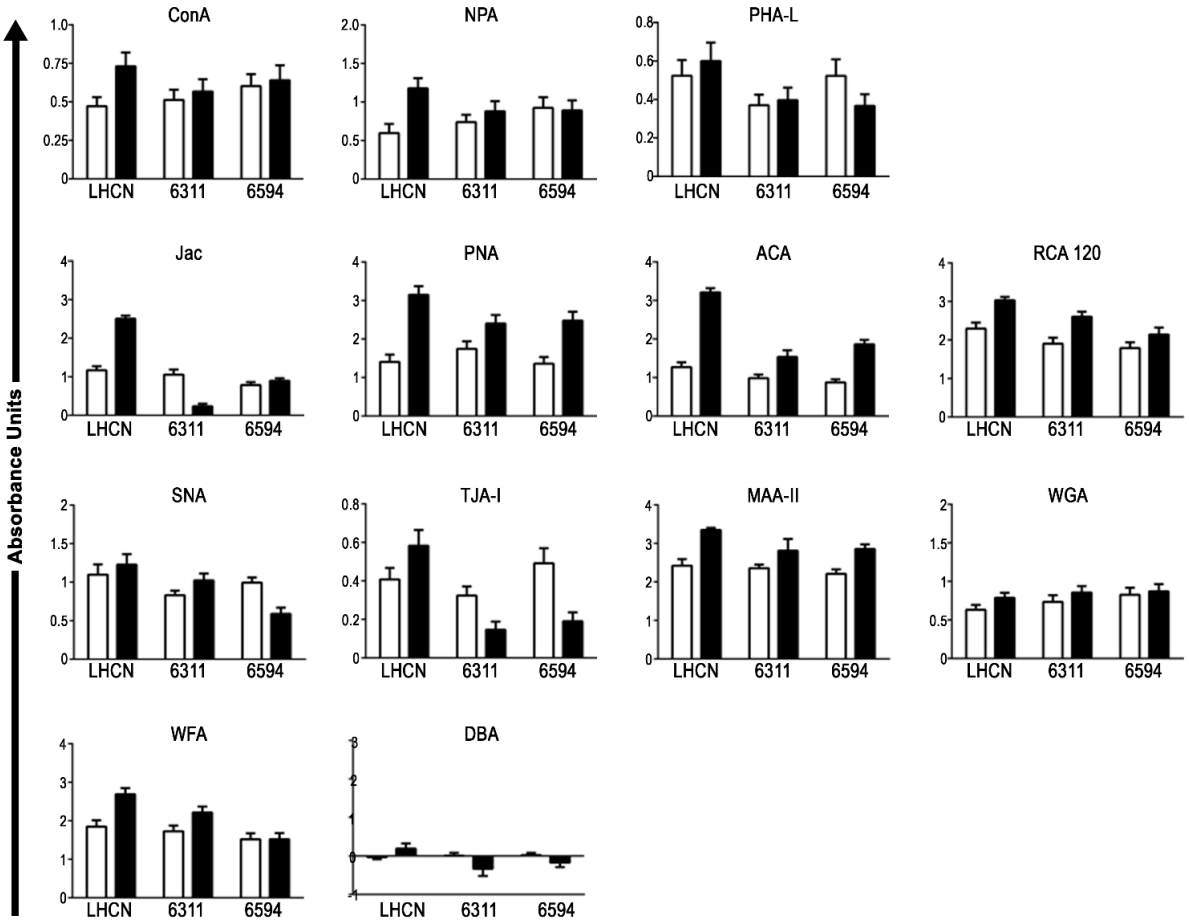

Absorbance Units
ConA
NPA
PHA-L
Jac
PNA
ACA
RCA 120
SNA
TJA-I
MAA-II
WGA
WFA
DBA
LHCN
6311
6594

Figure 4-3: Different lectins precipitate different glycoproteins from healthy and dystrophic human myotubes.

NPA, Jac, THA-1, WFA and PNA were added to lysates of healthy (LHCN) or dystrophic (DMD 6311 (6311)/DMD 6594 (6594)) d0 myoblasts and d5 myotubes. Precipitates were separated by SDS-PAGE and detected by SYPRO® Ruby Protein gel stain (A). Parallel blots were probed for matriglycan with mAb IIH6 (B, left panels) and functional *O*-mannosylation by laminin binding (B, right panels).

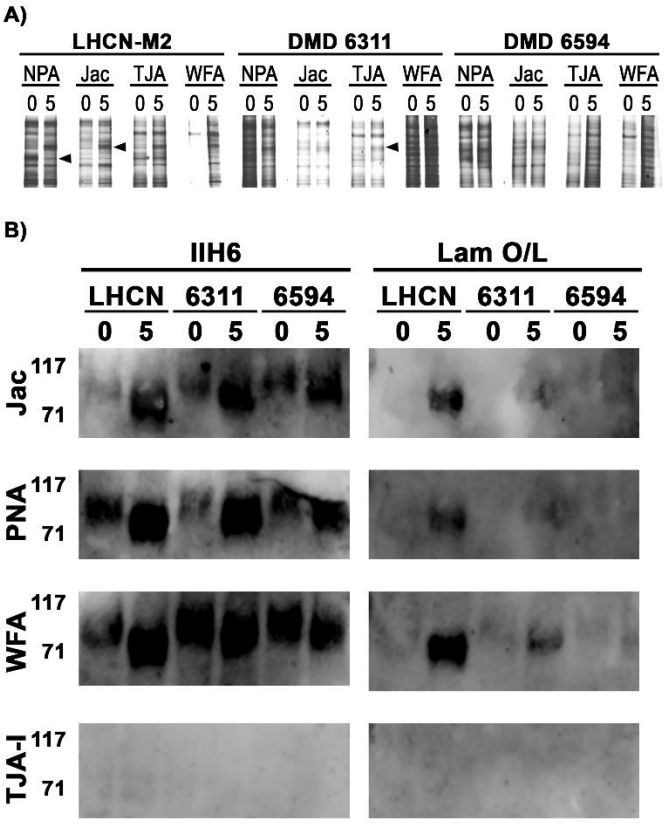

A)
LHCN-M2
DMD 6311
DMD 6594
NPA Jac TJA WFA NPA Jac TJA WFA NPA Jac TJA WFA
0 5 0 5 0 5 0 5 0 5 0 5 0 5 0 5 0 5 0 5 0 5 0 5
B)
IIH6
Lam O/L
LHCN 6311 6594 LHCN 6311 6594
0 5 0 5 0 5 0 5 0 5 0 5
Jac
PNA
WFA
TJA-I
117
71

Figure 4-4: Disease-specific differences in *O*-glycan and sialic acid-specific lectin binding to human skeletal muscle.

Serial transverse 5 µm sections of anonymized, formalin-fixed, paraffin-embedded, healthy and dystrophic human skeletal muscle were rehydrated and stained with biotinylated lectins: Jac, ACA, PNA, WGA, TJA-I, MAA-II, NPA, WFA and DBA. Bound lectins were detected with Texas Red-Avidin D (red) and sections were counterstained with DAPI. 'Other' lectin nominal specificities: NPA- high mannose *N*-glycans, WFA- GalNAc, DBA- GalNAc. Scale bar is 100 µm.

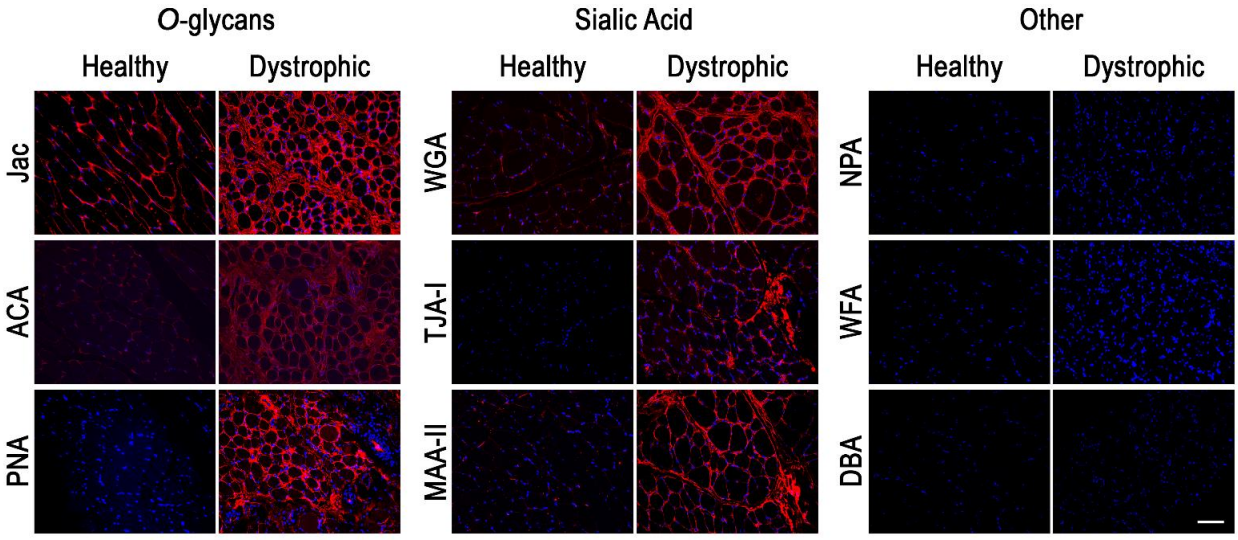
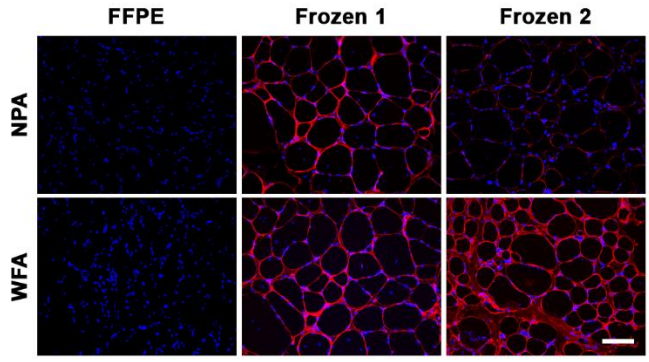

O-glycans
Sialic Acid
Other
Healthy
Dystrophic
Healthy
Dystrophic
Healthy
Dystrophic
Jac
ACA
PNA
WGA
TJA-I
MAA-II
NPA
WFA
DBA

Figure 4-5: Lectin binding to frozen versus fixed skeletal muscle.

Serial transverse 5 µm sections of anonymized, formalin-fixed, paraffin-embedded or frozen dystrophic human muscle sections were stained with biotinylated NPA and WFA. Bound lectins were detected with Texas Red-Avidin D (red) and counterstained with DAPI. Fixed tissue sections were negative for binding NPA and WFA while both lectins bound tissue frozen sections. Scale bar is 100 µM.


FFPE
Frozen 1
Frozen 2
NPA
WFA

References

1 Holmberg, J. & Durbeej, M. Laminin-211 in skeletal muscle function. *Cell Adh Migr* **7**, 111-121, doi:10.4161/cam.22618 (2013).

2 Marshall, J. L., Kwok, Y., McMorran, B. J., Baum, L. G. & Crosbie-Watson, R. H. The potential of sarcospan in adhesion complex replacement therapeutics for the treatment of muscular dystrophy. *FEBS J* **280**, 4210-4229, doi:10.1111/febs.12295 (2013).

3 Campbell, K. P. & Kahl, S. D. Association of dystrophin and an integral membrane glycoprotein. *Nature* **338**, 259-262, doi:10.1038/338259a0 (1989).

4 Ervasti, J. M. & Campbell, K. P. A role for the dystrophin-glycoprotein complex as a transmembrane linker between laminin and actin. *J Cell Biol* **122**, 809-823 (1993).

5 Ibraghimov-Beskrovnaya, O. *et al.* Primary structure of dystrophin-associated glycoproteins linking dystrophin to the extracellular matrix. *Nature* **355**, 696-702, doi:10.1038/355696a0 (1992).

6 Roberds, S. L. *et al.* Missense mutations in the adhalin gene linked to autosomal recessive muscular dystrophy. *Cell* **78**, 625-633 (1994).

7 Mizuno, Y. *et al.* Selective defect of sarcoglycan complex in severe childhood autosomal recessive muscular dystrophy muscle. *Biochem Biophys Res Commun* **203**, 979-983 (1994).

8 Bönnemann, C. G. *et al.* Beta-sarcoglycan (A3b) mutations cause autosomal recessive muscular dystrophy with loss of the sarcoglycan complex. *Nat Genet* **11**, 266-273, doi:10.1038/ng1195-266 (1995).

9 Noguchi, S. *et al.* Mutations in the dystrophin-associated protein gamma-sarcoglycan in chromosome 13 muscular dystrophy. *Science* **270**, 819-822 (1995).

10 Mayer, U. *et al.* Absence of integrin alpha 7 causes a novel form of muscular dystrophy. *Nat Genet* **17**, 318-323, doi:10.1038/ng1197-318 (1997).

11 Hayashi, Y. K. *et al.* Mutations in the integrin alpha7 gene cause congenital myopathy. *Nat Genet* **19**, 94-97, doi:10.1038/ng0598-94 (1998).

12 Hara, Y. *et al.* Like-acetylglucosaminyltransferase (LARGE)-dependent modification of dystroglycan at Thr-317/319 is required for laminin binding and arenavirus infection. *Proc Natl Acad Sci U S A* **108**, 17426-17431, doi:10.1073/pnas.1114836108 (2011).

13 Inamori, K. *et al.* Dystroglycan function requires xylosyl- and glucuronyltransferase activities of LARGE. *Science* **335**, 93-96, doi:10.1126/science.1214115 (2012).

14 Yoshida-Moriguchi, T. *et al.* O-mannosyl phosphorylation of alpha-dystroglycan is required for laminin binding. *Science* **327**, 88-92, doi:10.1126/science.1180512 (2010).

15 Briggs, D. C. *et al.* Structural basis of laminin binding to the LARGE glycans on dystroglycan. *Nat Chem Biol* **12**, 810-814, doi:10.1038/nchembio.2146 (2016).

16 Yoshida-Moriguchi, T. & Campbell, K. P. Matriglycan: a novel polysaccharide that links dystroglycan to the basement membrane. *Glycobiology* **25**, 702-713, doi:10.1093/glycob/cwv021 (2015).

17 Campbell, C. *et al.* Myostatin inhibitor ACE-031 treatment of ambulatory boys with Duchenne muscular dystrophy: Results of a randomized, placebo-controlled clinical trial. *Muscle Nerve* **55**, 458-464, doi:10.1002/mus.25268 (2017).

18 Lim, K. R., Maruyama, R. & Yokota, T. Eteplirsen in the treatment of Duchenne muscular dystrophy. *Drug Des Devel Ther* **11**, 533-545, doi:10.2147/DDDT.S97635 (2017).

19 Reinig, A. M., Mirzaei, S. & Berlau, D. J. Advances in the Treatment of Duchenne Muscular Dystrophy: New and Emerging Pharmacotherapies. *Pharmacotherapy* **37**, 492-499, doi:10.1002/phar.1909 (2017).

20 Mendell, J. R. *et al.* Longitudinal effect of eteplirsen versus historical control on ambulation in Duchenne muscular dystrophy. *Ann Neurol* **79**, 257-271, doi:10.1002/ana.24555 (2016).

21 Ricotti, V. *et al.* Safety, Tolerability, and Pharmacokinetics of SMT C1100, a 2-Arylbenzoxazole Utrophin Modulator, following Single- and Multiple-Dose Administration to Pediatric Patients with Duchenne Muscular Dystrophy. *PLoS One* **11**, e0152840, doi:10.1371/journal.pone.0152840 (2016).

22 Young, C. S. *et al.* A Single CRISPR-Cas9 Deletion Strategy that Targets the Majority of DMD Patients Restores Dystrophin Function in hiPSC-Derived Muscle Cells. *Cell Stem Cell* **18**, 533-540, doi:10.1016/j.stem.2016.01.021 (2016).

23 Guiraud, S. *et al.* Second-generation compound for the modulation of utrophin in the therapy of DMD. *Hum Mol Genet* **24**, 4212-4224, doi:10.1093/hmg/ddv154 (2015).

24 Nguyen, H. H., Jayasinha, V., Xia, B., Hoyte, K. & Martin, P. T. Overexpression of the cytotoxic T cell GalNAc transferase in skeletal muscle inhibits muscular dystrophy in mdx mice. *Proc Natl Acad Sci U S A* **99**, 5616-5621, doi:10.1073/pnas.082613599 (2002).

25 Marshall, J. L. *et al.* Sarcospan-dependent Akt activation is required for utrophin expression and muscle regeneration. *J Cell Biol* **197**, 1009-1027, doi:10.1083/jcb.201110032 (2012).

26 Xia, B. *et al.* Overexpression of the CT GalNAc transferase in skeletal muscle alters myofiber growth, neuromuscular structure, and laminin expression. *Dev Biol* **242**, 58-73, doi:10.1006/dbio.2001.0530 (2002).

27 Thomas, P. J., Xu, R. & Martin, P. T. B4GALNT2 (GALGT2) Gene Therapy Reduces Skeletal Muscle Pathology in the FKRP P448L Mouse Model of Limb Girdle Muscular Dystrophy 2I. *Am J Pathol* **186**, 2429-2448, doi:10.1016/j.ajpath.2016.05.021 (2016).

28 Xu, R., Chandrasekharan, K., Yoon, J. H., Camboni, M. & Martin, P. T. Overexpression of the cytotoxic T cell (CT) carbohydrate inhibits muscular dystrophy in the dyW mouse model of congenital muscular dystrophy 1A. *Am J Pathol* **171**, 181-199, doi:10.2353/ajpath.2007.060927 (2007).

29 Xu, R., DeVries, S., Camboni, M. & Martin, P. T. Overexpression of Galgt2 reduces dystrophic pathology in the skeletal muscles of alpha sarcoglycan-deficient mice. *Am J Pathol* **175**, 235-247, doi:10.2353/ajpath.2009.080967 (2009).

30 Cabrera, P. V. *et al.* High throughput screening for compounds that alter muscle cell glycosylation identifies new role for N-glycans in regulating sarcolemmal protein abundance and laminin binding. *J Biol Chem* **287**, 22759-22770, doi:10.1074/jbc.M111.334581 (2012).

31 Sanes, J. R. & Cheney, J. M. Lectin binding reveals a synapse-specific carbohydrate in skeletal muscle. *Nature* **300**, 646-647 (1982).

32 Scott, L. J., Bacou, F. & Sanes, J. R. A synapse-specific carbohydrate at the neuromuscular junction: association with both acetylcholinesterase and a glycolipid. *J Neurosci* **8**, 932-944 (1988).

33 McMorran, B. J. *et al.* Differentiation-related glycan epitopes identify discrete domains of the muscle glycocalyx. *Glycobiology* **26**, 1120-1132, doi:10.1093/glycob/cww061 (2016).

34 Cummings, R. D. & Kornfeld, S. Characterization of the structural determinants required for the high affinity interaction of asparagine-linked oligosaccharides with immobilized Phaseolus vulgaris leukoagglutinating and erythroagglutinating lectins. *J Biol Chem* **257**, 11230-11234 (1982).

35 Mega, T., Oku, H. & Hase, S. Characterization of carbohydrate-binding specificity of concanavalin A by competitive binding of pyridylamino sugar chains. *J Biochem* **111**, 396-400 (1992).

36 Kaku, H., Van Damme, E. J., Peumans, W. J. & Goldstein, I. J. Carbohydrate-binding specificity of the daffodil (Narcissus pseudonarcissus) and amaryllis (Hippeastrum hybr.) bulb lectins. *Arch Biochem Biophys* **279**, 298-304 (1990).

37 Lotan, R., Skutelsky, E., Danon, D. & Sharon, N. The purification, composition, and specificity of the anti-T lectin from peanut (Arachis hypogaea). *J Biol Chem* **250**, 8518-8523 (1975).

38 Wu, A. M., Wu, J. H., Lin, L. H., Lin, S. H. & Liu, J. H. Binding profile of Artocarpus integrifolia agglutinin (Jacalin). *Life Sci* **72**, 2285-2302 (2003).

39 Rinderle, S. J., Goldstein, I. J., Matta, K. L. & Ratcliffe, R. M. Isolation and characterization of amaranthin, a lectin present in the seeds of Amaranthus caudatus, that recognizes the T- (or cryptic T)-antigen. *J Biol Chem* **264**, 16123-16131 (1989).

40 Drysdale, R. G., Herrick, P. R. & Franks, D. The specificity of the haemagglutinin of the Castor bean, Ricinus communis. *Vox Sang* **15**, 194-202 (1968).

41 Greenaway, P. J. & LeVine, D. Binding of N-acetyl-neuraminic acid by wheat-germ agglutinin. *Nat New Biol* **241**, 191-192 (1973).

42 Shibuya, N. *et al.* The elderberry (Sambucus nigra L.) bark lectin recognizes the Neu5Ac(alpha 2-6)Gal/GalNAc sequence. *J Biol Chem* **262**, 1596-1601 (1987).

43 Konami, Y., Yamamoto, K., Osawa, T. & Irimura, T. Strong affinity of Maackia amurensis hemagglutinin (MAH) for sialic acid-containing Ser/Thr-linked carbohydrate chains of N-terminal octapeptides from human glycophorin A. *FEBS Lett* **342**, 334-338 (1994).

44 Yamashita, K., Umetsu, K., Suzuki, T. & Ohkura, T. Purification and characterization of a Neu5Ac alpha 2-->6Gal beta 1-->4GlcNAc and HSO3(-)-->6Gal beta 1-->GlcNAc specific lectin in tuberous roots of Trichosanthes japonica. *Biochemistry* **31**, 11647-11650 (1992).

45 Etzler, M. E., Gupta, S. & Borrebaeck, C. Carbohydrate binding properties of th Dolichos biflorus lectin and its subunits. *J Biol Chem* **256**, 2367-2370 (1981).

46 Uchida, T. *et al.* Reconstitution of hybrid toxin from Fragment A of diphtheria toxin and a subunit of Wistaria floribunda lectin. *J Biol Chem* **253**, 6307-6310 (1978).

47 Go, S. *et al.* Altered expression of ganglioside GM3 molecular species and a potential regulatory role during myoblast differentiation. *J Biol Chem* **292**, 7040-7051, doi:10.1074/jbc.M116.771253 (2017).

48 Gundry, R. L. *et al.* The mouse C2C12 myoblast cell surface N-linked glycoproteome: identification, glycosite occupancy, and membrane orientation. *Mol Cell Proteomics* **8**, 2555-2569, doi:10.1074/mcp.M900195-MCP200 (2009).

49 Capaldi, M. J., Dunn, M. J., Sewry, C. A. & Dubowitz, V. Altered binding of Ricinus communis I lectin by muscle membranes in Duchenne muscular dystrophy. *J Neurol Sci* **63**, 129-141 (1984).

50 Capaldi, M. J., Dunn, M. J., Sewry, C. A. & Dubowitz, V. Binding of Ricinus communis I lectin to the muscle cell plasma membrane in diseased muscle. *J Neurol Sci* **64**, 315-324 (1984).

51 Capaldi, M. J., Dunn, M. J., Sewry, C. A. & Dubowitz, V. Lectin binding in human skeletal muscle: a comparison of 15 different lectins. *Histochem J* **17**, 81-92 (1985).

52 Capaldi, M. J., Dunn, M. J., Sewry, C. A. & Dubowitz, V. Lectin blotting of human muscle. Identification of a high molecular weight glycoprotein which is absent or altered in Duchenne muscular dystrophy. *J Neurol Sci* **68**, 225-231 (1985).

53 Dunn, M. J., Sewry, C. A. & Dubowitz, V. Cytochemical studies of lectin binding by diseased human muscle. *J Neurol Sci* **55**, 147-159 (1982).

54 Voit, T., Sewry, C. A., Dunn, M. J. & Dubowitz, V. Binding of Ricinus communis I lectin to developing dystrophic muscle in human fetus. *J Neurol Sci* **84**, 301-314 (1988).

55 Xu, R., Camboni, M. & Martin, P. T. Postnatal overexpression of the CT GalNAc transferase inhibits muscular dystrophy in mdx mice without altering muscle growth or neuromuscular development: evidence for a utrophin-independent mechanism. *Neuromuscul Disord* **17**, 209-220, doi:10.1016/j.nmd.2006.12.004 (2007).

56 Yoon, J. H. *et al.* The synaptic CT carbohydrate modulates binding and expression of extracellular matrix proteins in skeletal muscle: Partial dependence on utrophin. *Mol Cell Neurosci* **41**, 448-463, doi:10.1016/j.mcn.2009.04.013 (2009).

57 Iwata, Y., Suzuki, O. & Wakabayashi, S. Decreased surface sialic acid content is a sensitive indicator of muscle damage. *Muscle Nerve* **47**, 372-378, doi:10.1002/mus.23632 (2013).

58 Zhu, C. H. *et al.* Cellular senescence in human myoblasts is overcome by human telomerase reverse transcriptase and cyclin-dependent kinase 4: consequences in aging muscle and therapeutic strategies for muscular dystrophies. *Aging Cell* **6**, 515-523, doi:10.1111/j.1474-9726.2007.00306.x (2007).

59 Mamchaoui, K. *et al.* Immortalized pathological human myoblasts: towards a universal tool for the study of neuromuscular disorders. *Skelet Muscle* **1**, 34, doi:10.1186/2044-5040-1-34 (2011).

CHAPTER FIVE

Conclusions and future directions

Over the past decade, substantial work has focused on elucidating the *O*-mannosyl glycan structures present on α-DG that are bound by laminin, as well as on identifying and characterizing the enzymes responsible for the synthesis of this unique glycan (Chapter 1, Figure 1-3). Outside of α-DG *O*-mannosylation, research has focused on the differential glycosylation of α-DG with WGA- or WFA-reactive structures, primarily in rodent skeletal muscle. This differential glycosylation of α-DG correlates with association of α-DG in either the DGC or UGC and the localization of the DGC and UGC in mouse muscle (Chapter 1, Figure 1-2)[1-4]. WGA-reactive α-DG associates with the DGC that is expressed ubiquitously throughout the healthy rodent sarcolemma, while WFA-reactive α-DG associates with the UGC that is restricted to the NMJ/MTJ. This differential glycosylation of α-DG, and the ability to correlate complex association with differential glycosylation via lectin binding, has spurred interest in therapeutic approaches to ameliorate DMD, and other muscular dystrophies, by manipulating α-DG glycosylation to increase utrophin and UGC utilization.

Several potential new therapies have been explored that are based on this differential glycosylation of α-DG. However, the applicability of these new approaches may be limited by species-specific differences in muscle glycosylation. To date, very little is known about human skeletal muscle glycosylation, as a limited number of qualitative lectin histochemistry studies performed decades ago represents the bulk of our knowledge regarding human muscle glycosylation[5-8]. However, even as early as 1988, species-specific differences in VVA binding to human versus rodent muscle were apparent. VVA binding to skeletal muscle sections from various rodents species was highly specific for the NMJ while VVA binding to human muscle sections was not NMJ-specific[2]. Therefore, specific differences in muscle glycosylation exist between rodent and human muscle. Altering muscle glycosylation may still provide promising

approaches to ameliorating muscular dystrophies, however, substantial research is needed to appropriately characterize human v. rodent muscle glycosylation and to understand the complicated mechanisms regulating the process of glycosylation.

To further our understanding of muscle glycosylation, this work sought to identify and quantify differentiation-, species-, and disease-specific differences in muscle glycosylation in mouse and human skeletal muscle. Differentiation-specific differences in muscle glycosylation were identified following differentiation of both mouse and human myotubes. Differentiated mouse myotubes bound GalNAc- and *O*-glycan-specific lectins to a greater degree than undifferentiated myotubes (Chapter 3) while differentiation of human myotubes increased binding of lectins specific for high mannose *N*-glycan, *O*-glycan and sialic acid specific (Chapter 4). Interestingly, these differentiation-specific differences also highlighted species-specific differences. No change in binding of the high mannose *N*-glycan specific lectin ConA or any sialic specific lectins to mouse myotubes was observed following differentiation while increases were observed in binding of 2 lectins specific for high mannose glycans and four sialic acid specific lectins following differentiation of human myotubes.

This work also identified disease-specific differences in human muscle glycosylation both quantitatively and qualitatively. A panel of 13 lectins with varying glycan structure specificities were used to quantify changes in glycosylation following differentiation of healthy and dystrophic myotubes. Four lectins that characterized disease-specific differences in glycosylation of healthy and dystrophic myotubes were identified: NPA (high mannose *N*-glycans), Jac (sialylated core 1 *O*-glycans), TJA-I (α2,6-linked sialic acid) and WFA (GalNAc). Binding of NPA, Jac, TJA-I and WFA increased following differentiation of healthy human myotubes, while binding to dystrophic human myotubes decreased or did not change following

differentiation (Chapter 4). Staining human muscle tissue sections from DMD patients and healthy controls also identified disease-specific differences in glycosylation of innervated skeletal muscle. Dystrophic tissue bound increased amounts of all lectins recognizing sialic acid and *O*-glycans, with the most stark increases observed in binding of PNA and TJA-I. Healthy control human skeletal muscle sections did not bind PNA or TJA-I, regardless of concentration, while both lectins strongly bound ubiquitously throughout the sarcolemma of dystrophic skeletal muscle sections. These disease-specific differences in human muscle glycosylation demonstrate that altered distribution of WFA binding throughout the dystrophic sarcolemma that has been observed in *mdx* mouse muscle is not the sole change in glycosylation of dystrophic human muscle.

The disease-specific differences in muscle glycosylation identified in this work are simultaneously a significant contribution to characterizing and understanding muscle glycobiology, as well as only a small fraction of that which remains to be understood. These findings provide many avenues of possible future work including, but not limited to, determining the specificity of these differences in lectin binding to healthy vs. dystrophic human skeletal muscle in various types of muscular dystrophies, identifying specific glycan structures bound by each lectin, and understandind the relevance of these glycan structures in muscular dystrophy disease progression. These findings should be further validated on additional cell and tissue sources from DMD patients, as well as patients with other muscular dystrophies, to determine if these findings are specific to loss of dystrophin, as in DMD, or result from general instability of the sarcolemma and thus applicable to other muscular dystrophies. Mass spectrometric analysis of glycans and glycoproteins from healthy and dystrophic cell sources would identify specific

glycan structures bound by each lectin and determine what specific changes in glycan presentation occur during disease progression [3,9,10].

Understanding the mechanisms which drive changes in glycosylation during muscular dystrophy pathology will help identify potential therapeutic approaches for manipulating glycosylation to ameliorate the dystrophic phenotype. What drives disease-specific differences in muscle glycosylation? As glycosylation is the result of a non-templated biologic process, many factors can influence the glycan structures present at the sarcolemma. For example, presentation of glycan structures at the sarcolemma requires the expression of protein backbone substrates, without which glycans would be absent. Many muscular dystrophies result from the loss of specific adhesion complex component glycoproteins. Glycans endogenously present on those proteins would be missing in dystrophic tissue and could manifest as disease-specific differences in lectin binding. Additionally, disease progression could influence sarcolemmal glycan presentation by altering expression of glycosylation-related transcripts. For example, changes in SSPN expression levels alter α-DG glycosylation by modulating expression of B4GALNT2 via integrin-related Akt signaling[4]. Identifying the underlying causes of disease-specific differences in lectin reactivity and muscle glycosylation will further our understanding of muscle biology and muscular dystrophy pathology.

Lectins have proved to be powerful tools for studying glycobiology since their first use decades ago. Cheap to produce, lectins bind glycan structures independent of the underlying glycoprotein backbone, unlike many glycosylation specific antibodies, and therefore represent powerful tools for studying glycobiology. However, to ensure the knowledge gained from lectin binding assays is placed in the appropriate context, glycan structures preferentially bound by each lectin must be identified. For example, most lectins have nominal glycan specificities which

were determined via inhibitory assays performed with sugar monomers in solution. More specifically, WFA, VVA, DBA, and SBA have been utilized interchangeably to identify the NMJ as binding of all four could be inhibited by binding in the presence of GalNAc in solution. Chapter 3 of this work highlights significant differences in the glycan types and glycoproteins bound by each lectin. Understanding the glycan structures and glycoproteins bound by a specific lectin in a tissue specific manner will underscore any specific differences in binding that might result from disease pathology. Utilizing lectin biomarkers for healthy muscle glycosylation will further require a thorough understanding of the glycans necessary for tissue-specific lectin binding. For example, DBA does not precipitate α-DG from skeletal muscle (Chapter 3, [11]) but precipitates α-DG from rabbit brain[11]. Furthermore, how tissue samples are handled post-excision can alter lectin binding. Specifically, processing of formalin-fixed, paraffin-embedded (FFPE) tissues requires rehydration via organic solvents capable of extracting glycolipids from the cell membrane. Distinct binding patterns for both WFA and NPA were observed on frozen tissue compared to FFPE samples. While FFPE samples did not stain either WFA or NPA, frozen tissue sections bound both ubiquitously throughout the sarcolemma. Tissue processing, therefore, may alter lectin binding and diminish the utility of a specific lectin as a biomarker.

By providing the first quantitative and qualitative characterization of human muscle glycosylation, this work provides a significant contribution to the field of muscle glycosylation. However, substantial work remains to fully understand the processes and mechanisms that underlay healthy muscle glycosylation as well as those that drive disease-specific changes in muscle glycosylation. For example, this work has focused on characterizing human muscle glycosylation by utilizing plant lectins with well-defined glycan specificities. Endogenous muscle lectins, such as the galectin family, remain significantly understudied within the context

of muscle biology and disease progression. While some studies have focused on the role of galectin-1 in myoblast fusion, muscle regeneration and potential immunosuppressive functions within the context of muscle[12-15], other galectin family members (galectin-3, -8) were detected at the transcript level in both human and mouse muscle cells (Chapter 3 and 4, Appendix C), yet remain relatively unstudied in muscle.

The discovery of dystrophin and the associated DGC over three decades ago revolutionized our understanding of muscle biology[16,17]. As the field of muscle biology continues to evolve and mature[18], integrating an understanding of muscle-specific glycobiology will supplement our understanding of the various sarcolemmal adhesion complexes and provide an additional layer of information regarding glycoprotein function. Understanding the changes in glycosylation which occur physiologically during development, as well as those which occur during disease progression will further our understanding of muscle biology. Further progress in the field of muscle glycobiology may identify novel disease-specific differences in muscle and provide novel avenues of therapeutic approaches for a variety of muscle diseases.

References

1 Sanes, J. R. & Cheney, J. M. Lectin binding reveals a synapse-specific carbohydrate in skeletal muscle. *Nature* **300**, 646-647 (1982).

2 Scott, L. J., Bacou, F. & Sanes, J. R. A synapse-specific carbohydrate at the neuromuscular junction: association with both acetylcholinesterase and a glycolipid. *J Neurosci* **8**, 932-944 (1988).

3 Cabrera, P. V. *et al.* High throughput screening for compounds that alter muscle cell glycosylation identifies new role for N-glycans in regulating sarcolemmal protein abundance and laminin binding. *J Biol Chem* **287**, 22759-22770, doi:10.1074/jbc.M111.334581 (2012).

4 Marshall, J. L. *et al.* Sarcospan-dependent Akt activation is required for utrophin expression and muscle regeneration. *J Cell Biol* **197**, 1009-1027, doi:10.1083/jcb.201110032 (2012).

5 Dunn, M. J., Sewry, C. A. & Dubowitz, V. Cytochemical studies of lectin binding by diseased human muscle. *J Neurol Sci* **55**, 147-159 (1982).

6 Capaldi, M. J., Dunn, M. J., Sewry, C. A. & Dubowitz, V. Altered binding of Ricinus communis I lectin by muscle membranes in Duchenne muscular dystrophy. *J Neurol Sci* **63**, 129-141 (1984).

7 Capaldi, M. J., Dunn, M. J., Sewry, C. A. & Dubowitz, V. Binding of Ricinus communis I lectin to the muscle cell plasma membrane in diseased muscle. *J Neurol Sci* **64**, 315-324 (1984).

8 Capaldi, M. J., Dunn, M. J., Sewry, C. A. & Dubowitz, V. Lectin binding in human skeletal muscle: a comparison of 15 different lectins. *Histochem J* **17**, 81-92 (1985).

9 Orlando, R. *et al.* IDAWG: Metabolic incorporation of stable isotope labels for quantitative glycomics of cultured cells. *J Proteome Res* **8**, 3816-3823, doi:10.1021/pr8010028 (2009).

10 Fang, M., Lim, J. M. & Wells, L. Quantitative Glycomics of Cultured Cells Using Isotopic Detection of Aminosugars with Glutamine (IDAWG). *Curr Protoc Chem Biol* **2**, 55-69, doi:10.1002/9780470559277.ch090207 (2010).

11 Ervasti, J. M., Burwell, A. L. & Geissler, A. L. Tissue-specific heterogeneity in alpha-dystroglycan sialoglycosylation. Skeletal muscle alpha-dystroglycan is a latent receptor for Vicia villosa agglutinin b4 masked by sialic acid modification. *J Biol Chem* **272**, 22315-22321 (1997).

12 Cerri, D. G. *et al.* Degeneration of dystrophic or injured skeletal muscles induces high expression of Galectin-1. *Glycobiology* **18**, 842-850, doi:10.1093/glycob/cwn079 (2008).

13 Svensson, A. & Tågerud, S. Galectin-1 expression in innervated and denervated skeletal muscle. *Cell Mol Biol Lett* **14**, 128-138, doi:10.2478/s11658-008-0039-0 (2009).

14 Georgiadis, V. *et al.* Lack of galectin-1 results in defects in myoblast fusion and muscle regeneration. *Dev Dyn* **236**, 1014-1024, doi:10.1002/dvdy.21123 (2007).

15 Lecourt, S. *et al.* Human Muscle Progenitor Cells Displayed Immunosuppressive Effect through Galectin-1 and Semaphorin-3A. *Stem Cells Int* **2012**, 412610, doi:10.1155/2012/412610 (2012).

16 Hoffman, E. P., Knudson, C. M., Campbell, K. P. & Kunkel, L. M. Subcellular fractionation of dystrophin to the triads of skeletal muscle. *Nature* **330**, 754-758, doi:10.1038/330754a0 (1987).

17 Campbell, K. P. & Kahl, S. D. Association of dystrophin and an integral membrane glycoprotein. *Nature* **338**, 259-262, doi:10.1038/338259a0 (1989).

18 Bi, P. *et al.* Control of muscle formation by the fusogenic micropeptide myomixer. *Science* **356**, 323-327, doi:10.1126/science.aam9361 (2017).

APPENDIX A

C2C12 myoblast and myotube glycotranscript expression

This is a version of Supplemental Table 1 from *Glycobiology*, 2016, vol. 26, no. 10, 1120-1132, reprinted with copyright permission from Oxford University Press

		Relative Transcript Abundance (normalized to Rpl4)				
Transferases		**Myoblast (Average)**	**Stdev**	**Myotube (Average)**	**Stdev**	**MT/MB Fold Δ**
GT01_M22	Alg13	3.009E-03	2.003E-04	1.108E-03	8.017E-05	-2.71
GT02_M04	Has 1	5.957E-03	1.530E-03	1.589E-03	2.970E-04	-3.75
GT02_M06	Has 3	3.282E-05	6.516E-06	1.106E-05	3.133E-06	-2.97
GT03_M01	Gys 1	2.684E-03	2.511E-04	5.810E-03	7.348E-04	2.16
GT04_M03	PigA	2.081E-03	2.762E-04	7.419E-04	1.212E-04	-2.81
GT07_M07	B4galt6	7.083E-03	4.914E-05	3.490E-03	9.242E-04	-2.03
GT07_M09	B4galnt4	9.491E-05	2.370E-05	9.885E-06	7.056E-07	-9.60
GT07_M10	B4galnt3	5.729E-05	4.925E-06	2.301E-04	3.891E-05	4.02
GT07_M13	Chgn2	8.919E-03	5.817E-04	1.839E-03	3.875E-04	-4.85
GT08_M05	Glt8d2	2.930E-03	3.138E-04	9.428E-04	1.089E-04	-3.11
GT08_M08	Glt8d3/Gxylt1	1.344E-04	2.544E-05	6.635E-05	2.117E-05	-2.03
GT10_M03	Fut7	8.412E-06	4.448E-07	4.884E-05	8.161E-06	5.81
GT10_M04	Fut9	3.143E-05	1.212E-05	9.033E-05	1.286E-05	2.87
GT11_M01	Fut1	5.373E-05	1.212E-06	1.339E-03	4.890E-05	24.92
GT11_M02	Fut2	2.829E-06	1.362E-06	1.143E-05	2.276E-06	4.04
GT11_M03	Sec1	5.071E-05	5.861E-07	1.515E-04	3.183E-05	2.99
GT14_M01	Gcnt2	3.612E-06	1.275E-06	1.000E-06	1.421E-14	-3.61
GT14_M03	Gcnt3	6.042E-05	1.289E-05	1.482E-05	2.745E-06	-4.08
GT29_M14	St8sia2, STX	8.105E-05	1.150E-05	3.596E-04	9.241E-05	4.44
GT29_M15	St8sia4, PST	2.934E-06	1.597E-06	1.426E-05	6.289E-07	4.86
GT31_M03	B3gnt4	1.039E-04	2.072E-05	3.876E-05	4.978E-06	-2.68
GT31_M05	B3galt5	1.280E-04	2.457E-05	9.609E-04	1.394E-04	7.51
GT31_M06	B3galt1	3.352E-05	6.248E-06	1.292E-05	4.458E-06	-2.59
GT31_M07	B3galt2	1.278E-04	3.663E-05	7.856E-04	2.089E-04	6.15
GT31_M10	Lfng	6.466E-03	1.471E-03	1.760E-03	1.535E-04	-3.67
GT35_M01	Pygl	1.749E-05	9.961E-07	4.622E-06	1.043E-06	-3.78
GT35_M02	Pygm	2.813E-03	4.056E-04	5.422E-02	3.190E-03	19.27
GT39_M01	Pomt1	3.519E-03	7.317E-04	1.679E-03	3.876E-04	-2.10
GT43_M03	B3gat2	2.620E-04	7.093E-06	1.218E-04	3.818E-05	-2.15
GT47_M03	Extl1	4.109E-05	6.905E-06	9.088E-04	1.957E-04	22.12
GT54_M03	Mgat4a	1.416E-04	9.355E-06	3.642E-05	1.026E-05	-3.89
GT57_M01	Alg6	3.958E-04	8.048E-05	1.706E-04	1.160E-05	-2.32

Hydrolases		Myoblasts (Average)	Stdev	Myotubes (Average)	Stdev	MT/MB Fold Δ
GH01_M04	Lctl	5.171E-05	1.607E-05	4.719E-04	2.654E-05	9.13
GH13_M01	Amy1	2.480E-05	7.549E-06	6.985E-05	2.298E-05	2.82
GH13_M02	Amy2	3.207E-06	2.619E-06	9.718E-06	3.988E-06	3.03
GH13_M03	Slc3a2	1.957E-02	1.075E-03	9.525E-02	9.397E-03	4.87
GH18_M02	Bclp2	2.673E-04	4.058E-05	8.551E-06	3.601E-06	-31.26
GH18_M04	Chi3l1	5.349E-06	2.185E-06	2.415E-05	6.291E-06	4.51
GH23_M01	Lyg1	1.974E-05	7.608E-06	1.000E-06	1.421E-14	-19.74
GH31_M01	Gaa	1.392E-02	2.132E-03	3.147E-02	5.797E-04	2.26
GH31_M04	AI464131	5.798E-03	5.441E-04	2.076E-02	3.550E-03	3.58
GH33_M01	Neu2	1.028E-04	3.184E-05	1.912E-03	6.674E-04	18.60
GH33_M04	Neu1	3.857E-03	8.030E-05	1.025E-02	7.449E-04	2.66
GH37_M01	Treh	3.890E-06	2.729E-06	1.000E-06	1.421E-14	-3.89
GH38_M02	Man2b1	8.365E-05	1.899E-05	3.919E-05	6.086E-06	-2.13
GH47_M01	Man1a	1.777E-03	1.551E-04	5.362E-04	1.141E-05	-3.31
GH47_M06	Edem3	4.671E-03	1.349E-03	1.003E-02	5.711E-04	2.15
GH56_M06	Hyal1	5.579E-04	2.181E-05	1.142E-03	1.529E-04	2.05
GH79_M01	Hpse	8.846E-04	8.912E-05	1.475E-04	1.158E-05	-6.00
Carbohydrate Binding Modules		**Myoblasts (Average)**	**Stdev**	**Myotubes (Average)**	**Stdev**	**MT/MB Fold Δ**
CBM13_M02	Aim1	5.137E-03	8.986E-05	1.934E-03	7.060E-05	-2.66
CBM13_M04	Aim1l	2.187E-05	7.650E-06	4.485E-05	5.825E-06	2.05
CBM13_M06	Crybg3	1.376E-03	1.274E-04	4.293E-04	1.331E-04	-3.21
CBM20_M03	Epm2a	1.032E-04	2.262E-06	3.730E-04	5.989E-05	3.62
CBM21_M02	Ppp1r3c	2.372E-05	8.807E-06	2.503E-04	5.796E-05	10.55
CBM21_M03	Ppp1r3a	2.541E-06	5.647E-07	1.381E-04	2.465E-05	54.35
CBM21_M04	Ppp1r3b	1.431E-05	6.441E-06	2.327E-06	2.944E-08	-6.15
Carbohydrate Esterases		**Myoblasts (Average)**	**Stdev**	**Myotubes (Average)**	**Stdev**	**MT/MB Fold Δ**
CE01_M01	Esd	1.927E-02	2.201E-03	5.769E-03	1.187E-03	-3.34
CE10_M01	Ache	2.664E-05	6.823E-06	2.532E-04	2.423E-05	9.50
CE10_M03	Bche	1.269E-05	2.189E-06	1.000E-06	1.421E-14	-12.69
CE10_M09	Ces2	9.417E-06	3.366E-06	6.243E-05	3.050E-06	6.63
CE10_M10	Ces2g	3.718E-05	6.743E-06	5.622E-04	1.584E-05	15.12
CE10_M21	Nlgn3	1.000E-06	1.421E-14	2.918E-06	1.511E-06	2.92
CE10_M22	Ces7	8.046E-06	2.032E-06	2.373E-05	1.712E-06	2.95
CE13_M01	Notum	1.415E-05	1.607E-06	1.000E-06	1.421E-14	-14.15

Lectins		Myoblasts (Average)	Stdev	Myotubes (Average)	Stdev	MT/MB Fold Δ
LCR_M01	Mgl1	8.527E-05	2.196E-06	8.879E-06	4.245E-06	-9.60
LCR_M04	Asgr1	8.770E-04	1.272E-04	2.279E-05	6.298E-06	-38.48
LCR_M17	Fcer2a	2.948E-06	2.590E-06	1.150E-05	1.072E-06	3.90
LCR_M21	Colec12	3.063E-03	3.207E-04	1.104E-02	1.517E-03	3.60
LCC_M08	Collec11	2.113E-06	1.332E-07	8.707E-06	2.372E-06	4.12
LCS_M02	Selectin L	1.053E-05	1.325E-06	1.000E-06	1.421E-14	-10.53
LCS_M03	Selectin P	1.220E-04	1.065E-05	4.639E-06	2.464E-06	-26.31
LCE_M04	Clec14a	1.000E-06	1.421E-14	2.930E-06	3.285E-07	2.93
LCNKR_M01	Cd69	2.329E-05	6.091E-06	4.012E-06	7.618E-07	-5.81
LCNKR_M02	Cd72	1.000E-06	1.421E-14	2.137E-05	1.823E-06	21.37
LCNKR_M03	Klrd1	2.242E-05	6.094E-06	1.000E-06	1.421E-14	-22.42
LCNKR_M09	Klra2	7.241E-05	1.063E-05	1.673E-05	5.931E-06	-4.33
LCNKR_M29	Clecsf5	1.434E-05	4.397E-06	4.625E-05	1.063E-05	3.23
LCNKR_M35	Clec2d	6.708E-04	3.415E-05	3.266E-03	4.985E-04	4.87
LCNKR_M36	Olr1	1.169E-04	2.644E-05	4.237E-05	1.242E-05	-2.76
LINS_M04	L1cam	9.361E-03	5.733E-04	2.634E-03	4.679E-04	-3.55
LINS_M07	Icam5	1.000E-06	1.421E-14	1.531E-05	6.042E-06	15.31
LINS_M08	Ncam1	2.569E-02	1.262E-03	1.231E-01	7.252E-03	4.79
LSG_M01	Lgals1	5.024E+00	3.339E-01	2.413E+00	8.325E-02	-2.08
LSG_M03	Lgals3	4.865E-01	9.775E-02	2.079E-01	9.370E-03	-2.34
LSG_M04	Lgals9	2.244E-02	3.104E-03	1.013E-02	7.299E-04	-2.21
LSG_M05	Lgals12	3.963E-06	2.444E-06	1.086E-04	1.817E-05	27.39
LSG_M06	Lgals4	5.692E-05	9.838E-06	6.508E-04	6.587E-05	11.43
LSG_M07	Lgals6	7.838E-05	1.265E-05	1.357E-03	2.012E-04	17.32
LSG_M09	Lgals8	1.431E-02	9.920E-05	6.405E-03	6.215E-04	-2.23
LCST_M01	Layn	1.622E-04	4.138E-05	2.464E-05	6.787E-06	-6.58
LCT_M02	Clec11a	5.188E-05	1.696E-05	1.408E-04	4.223E-05	2.71
LCT_M03	Clec3b	5.394E-05	2.084E-07	1.254E-04	2.327E-05	2.33
LMHC_M01	CD1d1	1.681E-03	2.813E-04	5.836E-04	4.894E-05	-2.88
LAN_M01	Anxa4	9.532E-02	1.950E-02	4.115E-02	6.175E-03	-2.32
LAN_M04	Anxa9	6.618E-04	1.145E-04	2.778E-04	2.259E-05	-2.38
LGB_M01	RHAMM	4.705E-02	8.498E-03	8.160E-03	7.054E-04	-5.77
LGB_M03	Sdcbp	9.492E-02	1.086E-02	4.447E-02	3.318E-03	-2.13
LGB_M06	Habp2	1.000E-06	1.421E-14	1.545E-05	2.360E-06	15.45
LGB_M07	Sdcdp2	1.094E-04	2.153E-05	2.087E-05	5.242E-06	-5.24
LAP_M02	Masp2	1.000E-06	1.421E-14	1.671E-05	6.063E-06	16.71
LL_M01	Lman1l	4.714E-05	9.235E-06	1.620E-04	2.788E-05	3.44
LCB_M03	Cd302	1.643E-03	1.711E-04	4.087E-03	1.134E-04	2.49

Nucleotide Sugar Synthesis		**Myoblasts (Average)**	**Stdev**	**Myotubes (Average)**	**Stdev**	**MT/MB Fold Δ**
NSN_M09	Renbp	5.883E-03	1.389E-03	1.893E-02	3.254E-03	3.22
NSN_M14	Gfpt2	1.958E-05	6.065E-06	9.877E-05	1.047E-05	5.04
NSN_M18	Nans	3.360E-02	1.963E-03	1.318E-02	7.773E-04	-2.55
NSN_M24	Uap1	1.428E-02	2.706E-03	5.271E-03	1.371E-03	-2.71
NSN_M25	Gale	1.151E-02	9.246E-04	2.762E-03	2.183E-04	-4.17
NSN_M26	Udgh	5.031E-02	1.590E-03	1.603E-02	1.504E-03	-3.14
NSN_M36	Hk2	2.752E-03	1.365E-04	8.575E-03	2.638E-03	3.12
NSN_M44	Mpi	3.473E-03	3.964E-04	7.717E-03	0.000E+00	2.22
NSN_M47	Cyb5r1	6.326E-03	1.419E-04	4.805E-02	1.677E-02	7.60
Transporters		**Myoblasts (Average)**	**Stdev**	**Myotubes (Average)**	**Stdev**	**MT/MB Fold Δ**
TR_M07	Slc2a1	4.919E-02	2.742E-03	1.115E-02	4.251E-04	-4.41
TR_M08	Slc2a5	1.465E-05	2.917E-07	7.158E-06	3.181E-06	-2.05
TR_M12	Slc2a4	7.690E-05	1.416E-05	6.247E-04	9.782E-05	8.12
TR_M13	Slc5a1	2.597E-06	6.223E-07	1.000E-06	1.421E-14	-2.60
TR_M16	Slc2a10	7.803E-05	8.182E-06	2.357E-04	7.521E-06	3.02
TR_M19	Slc2a12	1.251E-04	1.184E-05	5.155E-05	7.146E-06	-2.43
TR_M25	Slc35b3	3.649E-03	9.934E-04	1.623E-03	4.417E-04	-2.25
TR_M37	Slc26a9	5.642E-06	2.472E-06	1.000E-06	1.421E-14	-5.64
TR_M42	Slc2a6	8.780E-04	1.863E-04	8.335E-03	3.767E-04	9.49
TR_M46	Slc35a5	6.851E-05	7.571E-06	2.771E-05	6.388E-06	-2.47
TR_M47	Slc5a2	5.777E-06	2.542E-06	1.000E-06	1.421E-14	-5.78
TR_M51	Ctns	2.636E-03	4.283E-04	6.025E-03	4.896E-04	2.29
Carbohydrate Metabolism		**Myoblasts (Average)**	**Stdev**	**Myotubes (Average)**	**Stdev**	**MT/MB Fold Δ**
CM_M2	G6pdx	2.612E-02	1.539E-03	1.091E-02	2.774E-03	-2.39
CM_M3	Pfkl	4.428E-02	3.533E-03	1.172E-02	1.371E-03	-3.78
CM_M5	Hk2	5.797E-03	1.663E-03	1.478E-02	2.826E-03	2.55
CM_M8	Pfkm	9.034E-03	3.471E-04	4.956E-02	6.881E-03	5.49
CM_M14	Pgm5	2.925E-05	2.920E-06	2.338E-04	3.837E-05	7.99
CM_M15	Aldo3	1.387E-04	1.264E-05	6.659E-05	3.253E-06	-2.08
CM_M17	Mpi1	6.808E-03	1.313E-03	1.798E-02	3.005E-03	2.64
CM_M18	Npl	1.000E-06	1.421E-14	3.811E-06	1.370E-06	3.81
Arylsulfatase		**Myoblasts (Average)**	**Stdev**	**Myotubes (Average)**	**Stdev**	**MT/MB Fold Δ**
SAS_M03	Sts	5.588E-05	1.120E-05	1.303E-04	1.947E-05	2.33
SAS_M09	Arsi	3.320E-06	8.695E-07	2.780E-05	4.137E-06	8.37
SAS_M10	Arsj	5.275E-03	1.394E-03	2.584E-03	4.558E-04	-2.04
Sulfatase		**Myoblasts (Average)**	**Stdev**	**Myotubes (Average)**	**Stdev**	**MT/MB Fold Δ**
ST_M01	Galns	1.350E-03	1.941E-04	2.909E-03	1.010E-04	2.15

Sulfotransferse		Myoblasts (Average)	Stdev	Myotubes (Average)	Stdev	MT/MB Fold Δ
STR_M07	Gal3st1	1.253E-05	3.036E-06	1.000E-06	1.421E-14	-12.53
STR_M08	Gal3st2	1.421E-06	9.643E-08	9.340E-06	2.559E-06	6.57
STR_M12	Chst5	2.187E-05	6.002E-06	2.539E-04	6.752E-05	11.61
STR_M15	Hs3st1	1.698E-05	1.340E-06	1.186E-04	1.801E-05	6.99
STR_M16	Hs3st3b1	7.809E-05	1.118E-05	1.697E-04	6.673E-06	2.17
STR_M18	Hs6st2	3.049E-05	1.155E-05	2.168E-04	1.511E-05	7.11
STR_M20	Chst1	4.760E-03	4.446E-04	2.260E-03	2.115E-04	-2.11
STR_M23	Ndst3	1.436E-04	2.362E-05	5.133E-05	3.519E-06	-2.80
STR_M26	Hs3st3a1	1.143E-04	4.660E-06	2.719E-04	5.659E-05	2.38
STR_M34	Hs3st5	8.491E-05	2.588E-05	1.574E-05	6.035E-06	-5.39
Glycolipid-related		**Myoblasts (Average)**	**Stdev**	**Myotubes (Average)**	**Stdev**	**MT/MB Fold Δ**
GL_M03	Lass1	1.835E-04	6.944E-06	3.114E-03	7.522E-04	16.97
GL_M04	Lass4	2.264E-05	4.445E-06	4.569E-05	1.102E-05	2.02
GL_M07	Lass6	6.194E-03	1.335E-03	1.918E-02	1.589E-03	3.10
GL_M11	SPHK1	5.908E-04	1.327E-04	1.184E-03	6.176E-05	2.00
GL_M15	CERT	3.525E-03	2.993E-04	7.927E-03	1.924E-04	2.25
GL_M18	ASAH3	1.000E-06	1.421E-14	6.031E-06	2.520E-06	6.03
GL_M28	Tram2	3.868E-03	3.477E-04	1.185E-02	2.119E-03	3.06
GL_M30	Ppap2a	2.275E-02	3.051E-03	5.968E-02	1.201E-03	2.62
GL_M31	Ppap2b	6.067E-05	1.840E-05	1.756E-04	2.511E-05	2.89
GL_M32	Ppap2c	3.080E-02	3.366E-03	1.367E-02	7.536E-04	-2.25
GL_M38	Scd4	1.452E-05	3.988E-06	3.602E-05	6.820E-06	2.48
GAG-related		**Myoblasts (Average)**	**Stdev**	**Myotubes (Average)**	**Stdev**	**MT/MB Fold Δ**
GR_M01	Decorin	1.724E-02	1.943E-03	3.554E-02	2.602E-03	2.06
GR_M02	Biglycan	4.503E-02	4.039E-03	2.285E-01	2.452E-02	5.08
GR_M03	Fibromodulin	9.246E-06	1.543E-06	6.544E-04	4.949E-05	70.77
GR_M04	Lumican	1.688E-06	5.561E-07	2.421E-05	2.524E-06	14.34
GR_M06	Glypican 2	1.000E-06	1.421E-14	5.873E-06	2.691E-06	5.87
GR_M08	Glypican 4	1.000E-06	1.421E-14	5.799E-06	2.393E-06	5.80
GR_M12	Syndecan 2	1.067E-01	2.335E-02	2.328E-01	4.037E-02	2.18
GR_M17	Neuroglycan	1.000E-06	1.421E-14	4.252E-05	2.600E-06	42.52
GR_M20	CD44 (Epican)	4.640E-01	3.157E-02	1.300E-01	1.882E-03	-3.57
GR_M27	Collagen Type XIV	4.538E-04	6.393E-05	1.624E-04	4.415E-05	-2.79
GR_M29	Dystroglycan	1.808E-02	3.199E-03	9.682E-02	5.367E-03	5.36
GR_M34	Plaur	2.432E-02	1.599E-03	3.407E-03	4.459E-04	-7.14
GR_M36	Dse2	2.164E-03	2.404E-04	1.017E-03	2.479E-05	-2.13
GR_M37	Ptn	7.056E-03	6.828E-04	1.909E-02	1.454E-03	2.71
GR_M40	Ogn	4.088E-02	2.023E-03	8.550E-02	5.751E-03	2.09
GR_M44	Tnr	1.000E-06	1.421E-14	1.470E-05	6.154E-06	14.70
GR_M45	Aspn	1.148E-03	6.281E-05	6.507E-03	2.301E-04	5.67
GR_M51	Hapln4	1.344E-04	2.042E-05	3.156E-04	4.329E-05	2.35
GR_M53	Spock2	8.652E-05	2.535E-05	3.503E-04	8.809E-05	4.05
GR_M59	Lepre1	1.216E-03	2.842E-04	2.637E-03	6.235E-04	2.17

Fibroblast growth factors		**Myoblasts (Average)**	**Stdev**	**Myotubes (Average)**	**Stdev**	**MT/MB Fold Δ**
FGF_M01	Fgf1	1.977E-05	4.481E-06	6.552E-06	1.799E-06	-3.02
FGF_M02	Fgf2	8.855E-04	1.495E-04	2.118E-03	4.557E-04	2.39
FGF_M08	Fgf9	7.453E-06	4.604E-06	2.565E-04	4.843E-05	34.42
FGF_M09	Fgf10	1.585E-05	3.663E-06	5.052E-05	1.050E-05	3.19
FGF_M10	Fgf11	1.181E-03	1.283E-04	3.230E-03	3.254E-04	2.74
FGF_M11	Fgf12	1.000E-06	1.421E-14	1.488E-05	2.034E-06	14.88
FGF_M12	Fgf13	3.591E-05	4.221E-07	2.953E-04	5.502E-05	8.22
FGF_M14	Fgf15	2.281E-06	5.465E-07	1.000E-06	1.421E-14	-2.28
FGF_M18	Fgf20	6.856E-06	3.865E-06	1.000E-06	1.421E-14	-6.86
FGF_M19	Fgf21	8.799E-03	1.775E-03	1.401E-01	2.990E-02	15.92
Fibroblast growth factor receptors		**Myoblasts (Average)**	**Stdev**	**Myotubes (Average)**	**Stdev**	**MT/MB Fold Δ**
FGFR_M03	Fgfr3	1.000E-06	1.421E-14	7.745E-06	1.711E-06	7.75
FGFR_M04	Fgfr4	1.496E-03	2.127E-04	3.272E-03	3.948E-04	2.19
Lipid Linked Oligosaccharide -related		**Myoblasts (Average)**	**Stdev**	**Myotubes (Average)**	**Stdev**	**MT/MB Fold Δ**
LLO_M01	Mpdu1	1.972E-02	4.757E-03	7.790E-03	1.645E-04	-2.53
LLO_M09	Rft1	6.045E-05	9.788E-06	1.640E-05	4.692E-06	-3.69
GPI-related		**Myoblasts (Average)**	**Stdev**	**Myotubes (Average)**	**Stdev**	**MT/MB Fold Δ**
GPI_M03	PigF	1.119E-02	2.137E-03	5.345E-03	4.804E-04	-2.09
Miscellaneous		**Myoblasts (Average)**	**Stdev**	**Myotubes (Average)**	**Stdev**	**MT/MB Fold Δ**
MISC_M1	Gnptab	5.439E-03	3.791E-04	2.383E-03	4.696E-04	-2.28

APPENDIX B:

Glycan structures preferentially bound by nominally GalNAc-specific lectins: WFA, VVA-B4, SBA and DBA

This is a version of Supplemental Table 2 from *Glycobiology*, 2016, vol. 26, no. 10, 1120-1132, reprinted with copyright permission from Oxford University Press

Lectin	Structures within 90% of Top Hit Average Signal		
WFA	**Structure**	**Average Signal**	**Terminal GalNAc?**
1	GalNAcb1-3Gala1-4Galb1-4GlcNAc	54878.555	
2	GalNAca1-3GalNAc	54039.582	
3	Galb1-4GalNAcb1-3(Fuca1-2)Galb1-4GlcNAc	50483.082	No
4	GalNAcb1-4GlcNAc	49395.98	
5	GalNAca	48323.477	
6	GalNAcb	47747.645	
7	GalNAca1-3Gal	47230.836	
8	Biantennary N-glycan with 1 Galb1-4GlcNAcb1-2Man/branch	46701.85	No
9	NeuAca2-8NeuAca2-8NeuAca2-8(GalNAcb1-4)Galb1-4Glc	45489.28	
10	Galb1-4GlcNAcb1-6GlcNAc	45317.586	No
11	Galb1-3GlcNAcb1-3Galb1-4(Fuca1-3)GlcNAc	45208.395	No
12	Galb1-3GalNAcb1-4(NeuAca2-3)Galb1-4Glc	42301.72	No
13	Galb1-4GlcNAcb1-6(Galb1-3)GalNAc	40374.82	No
14	Galb1-4GlcNAcb1-6(Galb1-3)GalNAc	39134.77	No
15	Galb1-4Glc[6S]	37583.86	No
16	Galb1-3GlcNAc	33539.883	No
17	Galb1-4GlcNAcb1-3Galb1-4Glc	313990.752	No
18	Galb1-4GlcNAcb1-3GalB1-4(Fuca1-3)GlcNAcb1-3Galb1-4(Fuca1-3)GlcNAc	27388.68	No
19	Galb1-3GalNAcb1-3Gala1-4Galb1-4Glc	21600.78	No
20	Galb1-2Gal	12907.149	No
21	NeuAca2-6(Galb1-3)GlcNAcb1-4Galb1-4Glc	11742.102	No
22	Gala1-3(Gala1-4)Galb1-4GlcNAc	10595.416	No
23	Fuca1-2Galb1-3GalNAcb1-4(NeuAca2-3)Galb1-4Glc	7941.242	No
VVA-B4			
1	GalNAcb1-4GlcNAcb1-3GalNAcb1-4GlcNAc	15114.617	
2	GalNAcb1-4GlcNAc[6S]	11470.912	
3	GalNAcb1-4GlcNAcb1-2Man	7086.3306	
4	GalNAca	5367.427	
5	GalNAcb1-4GlcNAc	1712.2303	

SBA			
1	Biantennary N-glycan terminating with Gala1-4Galb1-3GlcNAc on each branch	36534.97	No
2	GalNAcb1-4GlcNAcb1-2Man	34775.08	
3	GalNAcb1-4GlcNAc	31030.377	
4	GalNAc	29120.102	
5	GalNAca1-3GalNAcb1-3Gala1-4Galb1-4Glc	28051.396	
6	GalNAcb1-4GlcNAc	36440.941	
7	Biantennary N-glycan terminating with GalNAcb1-4GlcNAc on each branch	24020.35	
8	GalNAcb	17463.256	
9	GalNAcb1-3Gala1-4Galb1-4GlcNAcb1-3Galb1-4Glc	15338.711	
10	GalNAcb1-3Gala1-4Galb1-4GlcNAc	13592.017	
11	GalNAca	8140.083	
12	NeuAca2-8NeuAca2-3(GalNAcb1-4)Galb1-4Glcb	3696.9182	
DBA			
1	GalNAca1-3GalNAcb1-3Gala1-4Galb1-4Glc	22755.984	
2	GalNAca1-3GalNAcb1-3Gala1-4Galb1-4GlcNAc	15271.574	
3	NeuAca2-3(GalNAcb1-4)Galb1-4GlcNAcb	7656.855	

APPENDIX C:

Healthy and dystrophic, human myoblast and myotube glycotranscript expression

REFSEQ gene name	Control_d0 TPM	Control_d2 TPM	DMD6594_d 0 TPM	DMD6594_d 2 TPM	DMD6311_d 0 TPM	DMD6311_d 2 TPM
A3GALT2	0.037	0.162	0.000	0.000	0.159	0.045
A4GALT	38.108	52.076	52.836	31.800	58.597	53.461
A4GNT	0.000	0.023	0.000	0.000	0.115	0.235
AADAC	0.095	0.000	0.261	0.000	1.143	0.000
ABO	0.000	0.000	0.000	0.000	0.000	0.029
ACAN	0.515	5.621	35.120	4.193	23.361	1.781
ACER1	0.035	0.000	0.000	0.135	0.150	0.042
ACER3	7.472	4.765	5.932	4.725	6.257	5.940
ACHE	0.644	21.747	0.557	3.714	0.410	0.673
ADAMTS1	273.431	23.664	136.260	32.027	157.878	78.544
ADAMTS10	0.018	0.237	1.795	2.677	3.280	9.491
ADAMTS15	0.088	0.270	0.081	1.883	1.631	142.151
ADAMTS2	60.874	42.371	80.276	11.358	98.510	277.326
ADAMTS4	1.421	9.905	6.036	5.537	3.587	2.494
ADAMTS5	8.072	34.572	4.323	43.501	3.853	29.408
ADAMTS8	0.010	0.011	0.034	0.050	0.022	0.050
ADAMTS9	0.669	3.469	0.716	0.608	1.444	5.595
AGA	5.566	3.838	9.010	5.610	9.448	6.393
AGL	1.964	6.692	2.218	5.123	2.109	4.872
AGRN	19.624	88.784	86.872	116.811	24.075	24.160
AIM1	15.270	1.180	0.817	0.399	4.958	2.045
AIM1L	0.000	0.016	0.008	0.035	0.000	0.009
AKR1B1	234.640	240.324	140.418	162.965	157.724	211.232
ALDOA	2066.869	1635.616	1962.468	1753.319	1838.904	1121.780
ALDOB	0.016	0.068	0.000	0.030	0.017	0.076
ALDOC	43.076	78.491	131.310	259.030	26.973	14.068
ALG1	17.435	13.244	16.937	16.857	20.131	19.672
ALG10	4.206	1.469	3.028	1.774	3.143	1.580
ALG11	6.860	7.154	8.071	10.075	8.110	7.986
ALG12	33.918	48.472	36.833	48.112	39.423	43.258
ALG13	7.740	10.472	7.010	7.541	7.289	9.051
ALG14	17.979	14.014	13.954	13.206	16.320	12.888
ALG2	27.606	30.690	40.092	41.895	38.912	42.051
ALG3	69.442	35.823	47.729	27.776	56.776	43.860
ALG5	47.787	40.046	54.751	53.965	57.086	46.558
ALG6	7.305	3.191	4.872	3.705	8.166	5.383
ALG8	42.294	23.501	22.477	21.644	32.756	17.432
ALG9	12.128	8.691	10.392	8.736	10.120	7.981
AMDHD2	23.293	23.655	28.855	22.748	51.265	37.609

AMY2A	0.046	0.518	0.050	0.109	0.291	1.678
ANXA1	470.282	334.401	534.477	227.197	500.700	283.796
ANXA4	71.652	126.542	82.236	115.193	99.970	109.212
ANXA5	1680.111	1110.708	1717.870	1043.923	2291.036	985.485
ANXA7	118.883	155.019	123.069	141.758	136.382	127.073
ANXA9	0.147	1.248	0.230	1.591	0.671	2.253
AOAH	0.000	0.000	0.000	0.014	0.000	0.000
APEH	117.079	98.369	99.935	94.925	98.284	82.442
APOO	25.536	12.534	15.550	14.284	26.332	13.497
APOOL	4.363	6.321	5.488	5.970	5.789	6.712
ARSA	20.709	34.981	37.104	28.621	28.636	33.796
ARSB	11.107	12.447	20.539	7.666	21.279	11.470
ARSD	6.580	12.709	11.261	11.708	10.771	14.157
ARSE	3.569	4.994	1.194	3.538	1.330	3.479
ARSF	0.081	0.317	0.018	0.125	0.139	0.236
ARSG	4.141	2.982	8.457	4.857	6.596	3.393
ARSH	0.000	0.024	0.000	0.130	0.000	0.000
ARSI	1.557	1.267	2.090	1.067	4.468	1.079
ARSJ	29.139	6.412	45.797	9.517	34.277	9.654
ARSK	8.687	8.819	7.729	5.765	7.961	7.524
ASAH1	38.790	284.952	67.390	169.699	75.873	142.735
ASAH2	1.202	0.770	0.832	0.547	0.708	0.382
ASGR1	0.661	0.853	0.558	0.244	0.597	0.399
ASGR2	0.025	0.000	0.027	0.024	0.000	0.030
ASPN	0.045	0.033	0.050	0.015	0.097	0.128
ATHL1	4.739	15.548	3.590	2.023	17.071	12.420
ATRN	24.936	24.054	48.385	49.563	30.823	39.258
ATRNL1	7.536	2.006	8.786	2.760	5.009	3.282
B3GALNT1	1.386	1.511	9.045	6.800	6.631	4.147
B3GALNT2	10.098	15.073	8.729	15.662	11.012	12.910
B3GALT1	0.035	0.038	0.193	0.407	0.414	0.405
B3GALT2	5.464	92.629	81.120	180.140	49.470	105.786
B3GALT4	0.027	0.054	0.403	0.715	0.310	0.931
B3GALT5	0.369	0.385	0.237	0.709	0.353	0.491
B3GALT6	43.371	34.826	39.259	39.681	46.111	28.232
B3GALTL	7.551	3.653	10.761	3.741	12.855	4.187
B3GAT1	0.000	0.023	0.011	0.020	0.011	0.025
B3GAT2	0.000	0.000	0.000	0.000	0.000	0.028
B3GAT3	85.798	69.115	79.034	49.569	78.870	43.153
B3GNT2	17.164	26.219	18.656	22.797	17.920	8.029
B3GNT3	0.042	0.046	0.031	0.041	0.000	0.102

B3GNT4	0.280	0.110	1.894	0.440	0.841	0.092
B3GNT5	51.247	7.336	21.779	7.288	17.576	9.195
B3GNT6	0.405	0.553	0.247	0.332	0.721	0.707
B3GNT7	0.116	0.628	0.127	0.740	0.236	0.726
B3GNT8	0.020	0.088	0.022	0.314	0.131	0.197
B3GNT9	62.777	70.620	73.123	52.871	60.056	52.268
B3GNTL1	6.995	3.889	5.060	5.737	6.399	5.943
B4GALNT1	2.935	1.222	0.494	0.219	0.837	0.414
B4GALNT2	0.000	0.020	0.040	0.035	0.000	0.000
B4GALNT3	0.389	1.902	1.877	1.571	0.154	0.134
B4GALNT4	0.565	0.335	0.109	0.138	0.118	0.147
B4GALT1	73.224	71.472	120.059	108.789	77.102	78.579
B4GALT2	117.561	71.046	100.997	70.957	111.162	44.655
B4GALT3	34.880	44.529	38.761	43.259	33.283	33.921
B4GALT4	25.143	32.222	26.609	26.743	26.909	22.023
B4GALT5	32.582	31.984	44.391	36.509	29.729	23.855
B4GALT6	0.191	0.069	2.829	2.480	2.516	1.094
B4GALT7	58.693	52.445	75.819	53.176	57.192	35.241
B4GAT1	24.050	58.446	34.533	73.521	36.111	76.025
BCAN	0.094	0.664	0.497	0.934	0.081	0.114
BCHE	0.047	0.186	5.942	11.619	0.967	3.208
BGN	2.112	0.948	6.755	1.819	56.799	22.522
C1GALT1	80.794	27.969	56.707	23.435	59.179	13.467
C1GALT1C1	18.978	22.144	33.604	30.483	36.175	25.514
CADM1	0.200	0.282	0.095	0.059	0.028	0.105
CALR	2155.101	980.572	2772.430	1286.980	2330.681	826.789
CALR3	0.000	0.032	0.065	0.028	0.000	0.000
CANX	319.853	277.519	403.715	359.411	348.457	306.304
CD1D	0.303	0.241	0.244	0.107	0.129	0.342
CD207	0.000	0.022	0.022	0.000	0.022	0.000
CD209	0.596	0.692	0.502	0.531	0.663	1.356
CD22	0.464	0.352	0.610	0.279	2.042	0.322
CD248	0.045	0.065	0.524	1.120	0.223	1.661
CD302	4.670	5.012	5.927	7.643	4.479	17.243
CD33	0.309	0.308	0.104	0.000	0.000	0.057
CD34	0.313	4.048	1.178	2.627	0.508	1.643
CD44	199.521	70.018	142.727	84.805	138.969	67.738
CD69	0.000	0.000	0.000	0.000	0.000	0.000
CD72	0.890	7.008	0.867	2.803	0.660	15.404
CD74	0.023	0.074	0.075	0.131	0.121	0.027
CD83	0.652	0.213	1.296	1.661	2.443	1.960

CD93	0.017	0.025	0.025	0.011	0.018	0.048
CEL	0.705	0.936	0.299	0.908	1.179	2.458
CERCAM	142.124	139.255	275.139	138.467	159.111	124.600
CERK	76.085	50.191	60.716	37.205	82.047	53.459
CERS1	4.394	5.929	5.556	8.704	3.630	4.178
CERS2	207.119	149.221	202.338	173.669	292.619	287.621
CERS3	0.000	0.000	0.020	0.009	0.000	0.011
CERS4	0.042	0.114	0.092	0.263	0.045	0.254
CERS5	24.378	24.896	30.701	32.117	28.799	21.772
CERS6	26.728	17.998	17.963	13.813	19.639	26.200
CES1	0.000	0.000	0.000	0.018	0.000	0.046
CES2	38.072	47.816	41.931	52.128	27.789	37.585
CES3	0.310	0.833	0.320	0.442	0.491	0.759
CES5A	0.000	0.017	0.000	0.000	0.000	0.000
CES5AP1	0.000	0.000	0.000	0.000	0.000	0.000
CHGA	0.075	0.142	0.102	0.036	0.040	0.090
CHI3L1	0.125	1.329	0.684	2.400	0.466	0.302
CHI3L2	0.831	0.745	0.026	0.342	0.051	1.462
CHIA	0.021	0.045	0.000	0.020	0.000	0.000
CHID1	38.236	43.381	56.567	61.389	41.997	36.583
CHIT1	0.784	7.067	0.066	6.332	0.080	3.170
CHODL	0.014	0.162	0.000	0.000	0.044	0.016
CHPF	141.994	387.285	286.170	273.880	282.519	308.953
CHPF2	118.829	161.826	113.433	107.221	82.280	70.958
CHST1	1.087	0.347	0.170	0.233	0.621	0.434
CHST10	18.100	12.787	18.910	18.650	17.732	19.739
CHST11	7.789	3.063	7.381	1.458	2.885	1.729
CHST12	23.465	20.348	18.210	20.546	19.616	27.927
CHST13	0.000	0.116	0.047	0.041	0.000	0.052
CHST14	43.716	58.149	44.302	52.862	60.224	61.303
CHST15	20.654	27.353	12.832	12.157	7.132	14.595
CHST2	84.115	5.271	210.424	11.508	135.875	29.635
CHST3	62.111	69.763	60.721	43.040	55.565	51.514
CHST4	0.083	0.000	0.000	0.000	0.035	0.000
CHST5	0.376	0.586	0.258	0.452	0.502	0.696
CHST6	0.827	0.607	0.548	0.448	1.137	1.160
CHST7	8.207	11.707	10.433	7.127	7.764	3.304
CHST8	0.000	0.000	0.029	0.013	0.000	0.000
CHST9	0.017	0.000	0.000	0.000	0.000	0.000
CHSY1	31.370	21.370	51.514	32.504	34.157	22.135
CHSY3	10.315	23.769	12.071	9.425	10.277	5.488

CLC	0.000	0.000	0.000	0.116	0.000	0.000
CLEC10A	0.000	0.000	0.000	0.000	0.000	0.026
CLEC11A	46.253	38.376	79.542	40.467	66.431	37.086
CLEC12A	0.000	0.036	0.018	0.016	0.018	0.040
CLEC12B	0.000	0.000	0.024	0.000	0.023	0.013
CLEC14A	0.000	0.017	0.000	0.000	0.155	0.000
CLEC17A	0.069	0.205	0.038	0.132	0.073	0.228
CLEC18A	0.079	0.257	0.417	0.259	0.423	0.651
CLEC1A	0.000	0.028	0.014	0.025	0.028	0.079
CLEC1B	0.000	0.000	0.000	0.000	0.000	0.000
CLEC2A	0.000	0.000	0.000	0.060	0.000	0.000
CLEC2B	5.628	13.379	3.084	3.713	0.680	1.994
CLEC2D	34.722	29.217	18.528	28.383	24.149	42.884
CLEC2L	0.000	0.000	0.130	0.000	0.000	0.036
CLEC3A	0.000	0.000	0.000	0.000	0.000	0.000
CLEC3B	3.007	2.088	24.196	5.864	8.233	16.530
CLEC4A	0.358	0.388	0.196	0.172	0.287	1.226
CLEC4C	0.116	0.378	0.064	0.084	0.155	0.141
CLEC4D	0.000	0.000	0.000	0.038	0.021	0.024
CLEC4E	0.071	0.096	0.058	0.085	0.113	0.150
CLEC4F	0.015	0.084	0.000	0.000	0.000	0.019
CLEC4G	0.000	0.000	0.000	0.000	0.000	0.034
CLEC4M	0.000	0.000	0.000	0.000	0.000	0.000
CLEC5A	0.087	0.000	0.012	0.000	0.000	0.000
CLEC6A	0.000	0.000	0.000	0.000	0.000	0.000
CLEC7A	0.922	1.644	0.996	1.016	1.736	2.359
CLEC9A	0.000	0.000	0.000	0.000	0.000	0.000
CLECL1	0.000	0.000	0.000	0.000	0.000	0.000
CLGN	0.014	0.000	0.282	0.208	0.130	0.180
CMAS	35.572	28.645	32.395	29.404	34.233	29.884
COG1	31.548	38.626	31.948	28.456	41.331	41.432
COG2	13.822	39.306	15.246	37.665	15.844	23.167
COG3	13.511	15.034	16.346	16.840	13.904	19.693
COG4	60.294	73.076	53.303	60.621	67.820	87.302
COG5	10.518	12.372	9.543	9.890	9.943	11.070
COG6	5.759	7.041	8.871	8.831	6.363	7.956
COG7	15.232	18.610	19.417	19.662	19.286	16.886
COG8	27.204	29.263	28.522	35.209	32.799	34.649
COL10A1	0.674	12.501	4.750	2.490	1.401	0.098
COL14A1	0.189	62.461	0.732	33.466	2.681	94.361
COL15A1	2.320	13.362	39.126	66.253	36.862	28.181

COL19A1	0.013	0.081	0.014	0.623	0.023	0.069
COL1A1	3218.117	4680.815	6661.887	2773.308	4504.216	3951.667
COL4A3BP	14.735	23.309	14.656	16.955	14.532	35.781
COL9A2	0.041	0.073	0.281	0.078	0.115	1.191
COLEC10	0.135	0.243	0.098	0.086	0.072	0.108
COLEC11	0.000	0.104	0.052	0.092	0.000	0.096
COLEC12	0.244	0.436	0.053	0.000	0.104	0.781
COLGALT1	130.671	87.105	193.958	117.706	199.440	97.405
COLGALT2	3.150	1.994	4.712	2.109	3.569	1.073
CRYBG3	6.282	2.766	5.950	4.570	6.194	6.081
CSGALNACT 1	0.110	0.076	0.163	0.165	0.200	0.189
CSGALNACT 2	39.819	33.900	38.766	24.921	38.681	22.727
CSPG4	26.484	49.232	253.860	52.691	235.645	33.243
CSPG5	0.723	0.367	0.404	0.468	0.315	0.214
CST3	228.825	175.838	424.183	354.380	263.300	286.131
CST5	0.000	0.000	0.056	0.049	0.054	0.062
CST7	0.041	0.000	2.163	0.671	0.044	0.000
CSTA	1.063	0.350	0.152	0.400	0.049	0.112
CSTB	196.020	309.967	269.679	292.855	430.101	390.345
CTBS	9.852	10.354	12.026	8.280	10.876	11.243
CTNS	12.819	30.525	20.341	22.977	22.297	29.961
CTSA	241.233	597.549	557.422	692.589	525.795	746.211
CTSB	523.355	259.794	1235.118	339.853	1419.179	542.676
CTSD	710.023	1651.843	2104.676	2933.426	1440.696	2193.268
CTSH	25.722	168.262	46.218	151.636	56.708	86.135
CTSK	2.514	9.715	4.584	9.721	3.087	18.573
CTSS	1.033	1.159	0.806	1.002	0.844	1.226
CYB5R1	192.390	892.769	344.539	790.107	243.440	280.182
CYB5R3	312.519	336.013	570.018	352.875	677.104	513.863
DAD1	334.580	335.521	377.585	286.652	504.573	302.370
DAG1	55.102	175.451	90.872	356.495	98.823	281.884
DCN	497.662	474.308	19.706	146.661	87.641	456.336
DDOST	331.954	271.280	433.724	369.139	351.877	348.905
DEGS1	225.672	135.921	227.417	159.418	254.525	149.477
DEGS2	0.027	0.236	0.000	0.131	0.000	0.362
DGCR2	34.151	62.601	44.839	82.115	43.929	70.561
DOLK	30.763	34.862	38.498	35.251	44.592	39.431
DPAGT1	50.232	33.012	33.978	23.443	51.042	32.423
DPM1	69.351	58.408	97.648	98.624	82.339	66.421
DPM2	89.951	42.366	66.076	35.760	88.339	31.691
DPM3	67.875	92.660	63.349	105.166	79.547	128.146

DPP10	0.006	0.007	0.000	0.000	0.007	0.000
DPP4	12.363	45.991	44.221	63.249	65.311	200.835
DSE	19.091	73.015	15.076	39.826	13.805	39.737
DSEL	49.433	22.771	51.543	108.367	52.719	70.291
EDEM1	19.836	13.597	24.243	14.340	30.361	16.443
EDEM2	36.746	36.907	56.013	62.165	32.927	39.280
EDEM3	14.396	13.401	15.169	12.751	15.194	16.356
ELOVL1	226.930	137.264	217.882	116.966	203.273	98.171
ELOVL2	0.000	0.000	0.021	0.063	0.080	0.011
ELOVL3	3.557	3.266	0.856	0.958	0.862	4.914
ELOVL4	5.985	3.178	4.478	3.685	4.465	5.267
ELOVL5	65.801	72.600	50.395	66.575	68.870	107.407
ELOVL6	35.024	41.388	20.296	33.095	31.416	12.198
ENGase	8.304	22.207	7.282	10.495	13.766	28.781
EOGT	17.520	13.709	13.658	11.533	19.613	18.487
EPM2A	4.149	9.457	2.926	7.887	4.531	6.903
EPYC	0.000	0.134	0.082	0.286	0.026	0.060
ERLEC1	44.737	44.998	58.338	45.611	49.179	43.656
ESD	167.090	174.008	171.188	168.601	194.493	250.332
ESM1	25.295	0.079	10.972	0.088	21.396	0.066
EXT1	37.076	37.673	124.468	90.235	94.014	96.061
EXT2	51.894	63.085	80.392	70.257	69.132	74.302
EXTL1	0.238	6.308	4.363	5.344	0.396	1.576
EXTL2	23.495	20.504	16.912	19.369	20.318	20.459
EXTL3	24.058	36.150	37.433	39.502	35.596	28.266
FAM20B	28.372	35.405	30.668	46.959	30.314	29.030
FBN1	84.819	153.807	313.347	361.320	172.724	381.657
FBP1	0.000	0.000	0.023	0.020	0.045	0.000
FBP2	0.000	0.062	0.000	0.779	0.000	0.000
FBXO17	17.020	16.842	10.895	13.162	21.208	25.774
FBXO2	0.089	0.193	0.366	1.946	0.226	0.781
FBXO27	2.284	3.261	2.929	3.689	4.113	5.146
FBXO44	1.485	4.669	11.262	20.332	9.360	21.825
FBXO6	1.851	4.274	13.417	9.794	6.292	11.328
FCER2	0.000	0.000	0.000	0.000	0.000	0.000
FCN1	0.000	0.000	0.000	0.000	0.032	0.000
FCN2	0.000	0.000	0.000	0.000	0.039	0.000
FCN3	0.148	0.000	0.244	0.107	0.158	0.000
FGF1	9.636	1.784	13.751	8.197	9.165	2.722
FGF10	0.427	3.168	0.067	0.176	0.000	0.074
FGF11	48.796	51.602	18.180	22.583	1.387	0.420

FGF12	0.006	0.032	0.020	0.011	0.025	0.036
FGF13	0.997	1.366	0.012	0.032	0.083	0.107
FGF14	2.023	1.067	1.566	1.215	3.762	7.009
FGF16	0.000	0.000	0.000	0.000	0.000	0.000
FGF17	0.028	0.090	0.060	0.159	0.029	0.300
FGF18	0.424	0.251	1.416	0.445	0.905	2.446
FGF19	0.000	0.000	0.000	0.000	0.000	0.000
FGF2	12.643	4.143	27.791	12.384	27.288	15.668
FGF20	0.000	0.041	0.041	0.000	0.000	0.000
FGF21	0.000	0.000	0.000	0.083	0.000	0.000
FGF22	0.119	0.129	0.391	0.229	0.000	0.503
FGF23	0.076	0.055	0.069	0.024	0.054	0.077
FGF3	0.000	0.000	0.000	0.000	0.000	0.000
FGF4	0.000	0.000	0.000	0.000	0.000	0.000
FGF5	15.098	2.813	71.956	14.376	57.135	11.120
FGF6	0.000	0.000	0.000	0.000	0.000	0.000
FGF7	0.243	16.872	0.149	2.352	0.093	0.223
FGF8	0.207	0.522	0.226	0.132	0.184	0.915
FGF9	0.017	0.365	0.009	0.276	0.018	0.061
FGFR1	48.251	30.919	62.926	42.727	46.660	42.691
FGFR2	0.185	0.282	0.128	0.191	0.263	0.389
FGFR3	0.560	0.093	0.585	0.099	0.901	0.395
FGFR4	6.222	57.060	0.914	54.001	1.843	102.401
FKRP	18.601	24.404	17.971	15.575	19.756	21.214
FKTN	9.210	10.499	9.986	13.312	9.386	12.870
FMOD	1.479	4.294	2.213	0.835	3.681	2.977
FPGT	5.870	6.357	6.978	7.240	7.289	9.344
FUCA1	7.893	12.157	17.853	16.207	12.579	15.138
FUCA2	89.993	66.822	68.919	58.705	77.175	64.137
FUK	4.179	10.558	5.952	6.911	7.609	8.959
FUT1	0.342	0.497	0.217	0.355	0.499	0.511
FUT10	3.557	4.234	3.993	7.042	6.680	13.071
FUT11	39.765	22.978	45.673	41.983	42.710	24.733
FUT2	0.642	1.616	0.919	1.126	1.237	2.518
FUT3	0.074	0.144	0.065	0.057	0.142	0.285
FUT4	4.071	2.155	2.972	1.525	3.142	2.527
FUT5	0.000	0.000	0.021	0.018	0.000	0.000
FUT6	0.390	0.541	0.321	0.539	0.689	0.677
FUT7	0.000	0.000	0.000	0.000	0.017	0.020
FUT8	12.130	6.993	8.672	9.394	10.973	17.965
FUT9	0.051	0.084	0.069	0.046	0.073	0.152

G6PC	0.322	0.428	0.161	0.274	0.421	0.510
G6PC2	0.087	0.094	0.082	0.036	0.040	0.165
G6PD	155.757	165.474	142.829	200.570	151.030	188.861
GAA	63.184	112.163	58.438	74.196	123.394	181.105
GAL3ST1	0.064	0.185	0.070	0.246	0.046	0.155
GAL3ST2	0.000	0.086	0.058	0.025	0.169	0.127
GAL3ST3	0.276	0.199	0.050	0.011	0.540	0.070
GAL3ST4	3.523	18.961	4.586	12.090	7.963	16.816
GALC	10.720	12.931	18.305	15.554	13.049	19.509
GALE	75.360	17.726	60.708	16.034	74.316	7.878
GALK1	75.545	57.154	60.742	54.710	51.477	68.129
GALK2	6.620	10.635	6.770	6.616	7.671	8.039
GALNS	22.734	32.166	72.009	64.592	40.004	42.171
GALNT1	74.439	57.385	120.811	78.397	77.066	52.506
GALNT10	82.276	39.688	118.778	80.630	84.033	40.291
GALNT11	49.653	71.543	38.254	51.273	39.266	58.050
GALNT12	1.342	0.620	1.532	0.725	1.819	1.300
GALNT13	0.052	0.630	0.007	0.000	0.007	0.024
GALNT14	0.022	0.000	0.000	0.000	0.000	0.041
GALNT15	0.445	1.747	8.189	9.332	2.504	28.019
GALNT16	7.640	10.399	4.463	5.626	3.133	26.877
GALNT18	6.340	2.566	0.200	0.000	0.016	0.073
GALNT2	117.633	95.667	122.238	117.263	97.222	101.928
GALNT3	1.170	0.823	0.077	0.112	0.262	0.664
GALNT4	4.358	2.156	5.698	3.790	4.920	4.173
GALNT5	48.018	18.752	23.486	10.700	18.821	10.250
GALNT6	0.440	0.412	5.330	0.666	12.495	1.686
GALNT7	48.578	53.058	19.506	57.118	22.734	51.505
GALNT8	0.000	0.039	0.000	0.000	0.000	0.043
GALNT9	0.039	0.014	0.043	0.063	0.000	0.000
GALNTL5	0.000	0.000	0.000	0.000	0.000	0.000
GALNTL6	0.013	0.058	0.000	0.064	0.000	0.081
GALT	20.329	29.714	28.778	30.512	29.954	48.905
GANAB	397.863	276.900	421.631	318.735	359.235	319.084
GANC	4.481	6.374	5.382	5.544	5.793	10.243
GBA	90.311	103.862	127.909	98.834	132.129	111.630
GBA3	0.000	0.000	0.019	0.017	0.000	0.000
GBE1	138.471	79.948	187.193	167.230	156.620	189.387
GBGT1	0.241	0.301	1.587	2.034	1.505	4.553
GCK	0.012	0.040	0.164	0.920	0.027	0.601
GCNT1	16.133	1.170	16.738	1.208	13.231	6.749

GCNT2	0.089	0.153	0.034	0.055	0.112	0.114
GCNT3	0.172	1.024	0.000	0.760	0.202	0.894
GCNT4	0.367	0.205	0.329	0.214	0.178	0.108
GCNT7	0.037	0.100	0.081	0.053	0.099	0.157
GFPT1	21.255	14.904	27.301	16.398	22.664	10.781
GFPT2	106.251	24.336	48.775	33.586	53.688	74.227
GLA	25.778	26.465	22.457	24.144	22.374	21.200
GLB1	72.894	125.976	136.826	149.150	94.941	157.769
GLB1L	4.913	6.409	5.897	5.905	5.364	7.099
GLB1L2	0.000	0.000	0.000	0.000	0.000	0.015
GLB1L3	0.156	0.281	0.171	0.112	0.402	0.455
GLCE	13.435	6.670	8.350	12.339	9.744	17.901
GLT1D1	0.000	0.000	0.015	0.027	0.000	0.000
GLT6D1	0.000	0.000	0.000	0.000	0.053	0.030
GLT8D1	50.459	70.750	61.842	63.209	59.061	79.460
GLT8D2	14.402	18.803	5.759	14.052	11.276	31.637
GLTP	72.983	43.097	107.010	50.174	81.630	40.787
GLYCAM1	0.000	0.000	0.054	0.000	0.000	0.000
GM2A	27.215	35.665	36.696	40.969	28.528	51.199
GMDS	16.728	12.225	17.689	12.878	17.030	14.509
GMPPA	91.061	77.223	98.383	54.208	71.380	52.867
GMPPB	60.718	19.275	42.745	16.721	54.278	12.721
GNB1	427.325	364.959	468.762	332.507	387.714	209.102
GNB2L1	2597.911	3267.140	1899.882	3534.113	2351.941	3352.725
GNE	13.260	14.167	13.796	15.094	13.904	14.597
GNPDA1	77.604	107.556	96.260	145.625	108.990	179.622
GNPDA2	19.753	11.436	14.789	12.518	17.757	16.590
GNPNAT1	72.101	14.210	50.168	17.525	52.709	16.000
GNPTAB	14.004	10.745	15.160	14.341	13.799	13.451
GNPTG	92.140	163.037	155.476	200.747	142.021	189.531
GNS	92.742	131.648	162.070	165.153	129.204	187.680
GPAA1	184.520	130.373	167.845	110.202	216.350	126.758
GPC1	283.980	958.381	469.066	1007.149	294.500	454.716
GPC2	5.047	20.265	1.941	7.684	2.849	4.848
GPC3	0.064	0.017	0.000	0.000	0.034	0.000
GPC4	2.347	45.854	0.316	0.673	1.976	3.083
GPC5	0.026	0.028	0.014	0.012	0.042	0.031
GPC6	12.356	8.191	15.871	7.965	14.654	13.817
GPCPD1	11.977	9.292	24.423	14.528	16.457	18.965
GPI	271.635	169.873	291.262	215.996	304.402	159.207
GPLD1	0.269	0.442	0.316	0.454	0.414	0.595

GPNMB	191.876	837.711	218.912	615.611	947.387	2483.593
GRIFIN	0.000	0.000	0.000	0.000	0.000	0.000
GTDC1	8.217	13.822	11.391	16.142	8.701	11.865
GUSB	86.486	75.968	79.482	55.525	74.482	68.793
GXYLT1	13.021	3.581	8.119	4.297	9.084	5.778
GXYLT2	6.736	38.026	4.912	34.450	3.302	21.055
GYG1	39.655	69.472	49.028	51.196	51.732	60.702
GYG2	1.239	11.151	2.456	11.372	0.805	4.230
GYLTL1B	0.015	0.000	0.016	0.014	0.016	0.000
GYS1	212.347	308.044	294.165	259.255	173.673	97.391
GYS2	0.012	0.053	0.027	0.106	0.078	0.236
H6PD	40.841	22.603	32.862	28.490	29.266	47.057
HABP2	0.000	0.000	0.000	0.012	0.013	0.000
HABP4	30.704	48.114	43.960	42.000	41.499	29.508
HAPLN1	0.016	0.035	0.036	0.102	0.061	0.020
HAPLN2	0.022	0.070	0.071	0.021	0.023	0.104
HAPLN3	4.080	15.453	7.681	4.366	7.109	16.441
HAPLN4	0.089	0.313	1.426	0.962	0.901	1.531
HAS1	4.293	0.510	0.159	0.174	0.019	0.022
HAS2	128.608	11.022	82.798	16.158	30.724	1.385
HAS3	0.258	0.659	0.300	0.493	0.516	0.962
HEXA	135.340	255.403	257.369	309.805	184.540	298.095
HEXB	101.419	83.744	111.557	72.006	165.637	137.406
HEXDC	5.501	21.180	3.821	16.346	5.544	26.945
HGSNAT	44.491	55.065	46.047	35.860	60.107	52.438
HK1	247.164	120.212	326.438	132.604	239.390	70.998
HK2	40.355	17.383	49.633	23.787	32.777	55.083
HK3	0.000	0.013	0.027	0.012	0.013	0.015
HMGB1	305.822	99.684	167.198	78.744	215.269	133.140
HMMR	33.715	0.592	6.895	0.643	23.768	5.237
HPSE	1.685	0.824	0.746	0.607	1.512	1.732
HPSE2	0.000	0.000	0.000	0.008	0.000	0.010
HS2ST1	19.889	15.947	24.823	25.115	16.851	17.619
HS3ST1	0.953	0.253	0.000	0.000	1.390	0.235
HS3ST2	0.000	0.000	0.043	0.000	0.042	0.000
HS3ST3A1	20.288	5.518	24.039	3.858	17.365	4.564
HS3ST3B1	10.734	3.946	20.655	2.986	21.107	9.005
HS3ST4	0.012	0.013	0.000	0.000	0.000	0.000
HS3ST5	0.111	1.312	1.298	7.001	0.803	1.195
HS3ST6	0.000	0.000	0.000	0.000	0.000	0.000
HS6ST1	18.934	24.771	21.332	31.166	20.617	25.168

HS6ST2	0.000	0.091	0.000	0.097	0.000	0.010
HS6ST3	0.069	0.032	0.043	0.028	0.063	0.077
HSD3B7	65.538	78.091	53.495	61.249	48.085	23.613
HSPG2	129.837	245.950	257.071	303.251	271.079	638.800
HYAL1	0.207	0.687	0.099	0.212	0.539	0.548
HYAL2	65.408	54.323	55.983	61.793	48.133	38.158
HYAL3	3.907	6.630	2.850	3.513	4.104	3.964
HYAL4	0.048	0.103	0.052	0.214	0.102	0.250
ICAM1	1.496	3.646	8.403	7.786	7.375	12.248
ICAM2	0.395	0.457	0.153	0.138	0.000	0.000
ICAM3	28.849	10.600	22.857	11.949	24.720	10.818
IDS	43.900	77.073	51.910	56.976	52.707	54.246
IDUA	9.926	30.667	14.529	17.806	20.987	31.725
IGF2R	64.637	148.277	102.891	130.499	144.249	153.708
IL1B	0.000	0.000	0.112	0.000	0.027	0.000
IL6	1.163	4.578	0.849	3.599	0.792	0.273
ITGA3	487.888	622.383	753.561	708.528	925.582	377.303
ITGB1	965.697	491.091	1211.695	501.500	1286.074	572.146
ITGB2	21.261	118.004	39.344	50.140	41.334	37.132
ITLN1	0.000	0.000	0.000	0.000	0.000	0.000
ITLN2	0.000	0.000	0.000	0.000	0.000	0.000
KDELC1	14.155	13.157	18.932	22.316	26.496	33.115
KDELC2	72.055	36.712	37.789	27.165	31.311	17.310
KDSR	32.337	24.119	37.411	24.989	41.125	45.147
KERA	0.000	0.000	0.000	0.000	0.000	0.000
KHK	0.847	0.211	1.726	1.093	1.876	0.901
KIAA1161	6.057	6.291	2.522	2.747	3.024	2.343
KL	0.000	0.000	0.000	0.015	0.008	0.000
KLB	0.164	0.327	0.179	0.193	0.215	0.471
KLRB1	0.000	0.000	0.000	0.000	0.055	0.000
KLRC1	0.042	0.091	0.023	0.000	0.045	0.178
KLRC2	0.221	0.102	0.242	0.091	0.134	1.294
KLRC3	0.067	0.289	0.146	0.128	0.036	0.363
KLRD1	1.026	1.344	0.774	0.723	1.422	1.720
KLRF1	0.000	0.000	0.000	0.000	0.000	0.000
KLRG1	0.813	2.013	0.352	1.151	0.502	1.395
KLRK1	0.178	0.104	0.026	0.069	0.000	1.157
L1CAM	0.678	0.892	4.908	17.463	0.288	0.661
LAMP1	405.482	403.545	544.657	460.940	590.878	559.069
LAMP2	32.260	44.127	48.706	53.111	55.377	73.666
LARGE	10.367	11.504	20.407	25.219	9.144	13.619

LAYN	4.579	6.986	7.800	8.402	4.811	5.780
LBP	0.020	0.044	0.044	0.019	0.022	0.219
LCT	0.006	0.007	0.000	0.006	0.013	0.022
LCTL	0.797	0.718	0.361	0.360	0.701	0.569
LEPREL2	73.766	47.960	98.218	53.980	90.767	52.349
LFNG	8.229	1.547	10.837	13.820	8.531	4.318
LGALS1	6128.726	3500.637	6310.021	3850.442	3755.938	2628.116
LGALS12	0.017	0.216	0.018	0.271	0.018	0.160
LGALS14	0.106	0.038	0.039	0.000	0.000	0.298
LGALS2	0.072	1.019	0.238	0.765	0.000	0.175
LGALS3	102.639	114.519	105.265	149.359	149.116	194.917
LGALS3BP	281.999	527.780	993.339	818.909	422.743	394.753
LGALS4	0.060	0.162	0.098	0.029	0.032	0.614
LGALS7	0.000	0.000	0.085	0.074	0.000	0.000
LGALS8	16.097	17.705	27.323	19.560	22.586	28.177
LGALS9	0.022	0.493	0.831	0.625	0.208	0.681
LGALSL	0.380	0.735	0.755	0.566	0.480	0.471
LIAS	8.221	13.567	5.864	13.527	9.081	20.683
LIPA	44.915	66.441	62.379	61.422	26.398	41.366
LMAN1	81.764	45.972	74.344	49.584	71.876	63.505
LMAN1L	0.066	0.000	0.000	0.042	0.000	0.080
LMAN2	290.591	248.617	363.886	304.199	257.347	228.742
LMAN2L	14.358	17.130	21.071	26.264	16.349	20.649
LUM	9.740	105.689	2.158	2.500	4.009	14.599
LY75	0.088	0.107	0.329	0.344	0.394	0.838
LYG1	0.618	2.633	0.508	1.410	0.700	2.752
LYG2	0.000	0.143	0.048	0.000	0.000	0.000
LYZ	0.908	1.064	0.719	0.775	1.829	1.797
LYZL1	0.000	0.000	0.000	0.000	0.000	0.000
LYZL4	0.000	0.046	0.000	0.000	0.000	0.000
LYZL6	0.000	0.039	0.000	0.000	0.000	0.000
M6PR	119.215	150.003	118.235	160.552	202.001	194.281
MADCAM1	0.000	0.135	0.027	0.143	0.000	0.270
MAG	0.000	0.000	0.017	0.000	0.000	0.000
MAN1A1	48.877	9.367	11.427	4.567	15.397	10.848
MAN1A2	17.933	22.677	16.284	28.900	16.311	35.027
MAN1B1	83.589	85.818	126.296	106.813	102.002	91.974
MAN1C1	0.700	5.260	0.424	3.657	1.204	40.517
MAN2A1	39.547	57.865	34.733	71.279	28.375	39.952
MAN2A2	10.704	21.536	13.535	19.729	18.091	22.554
MAN2B1	38.876	71.290	66.475	81.157	49.759	77.331

MAN2B2	54.722	71.500	79.923	61.030	60.653	58.499
MAN2C1	48.817	66.944	33.123	37.031	62.760	96.526
MANBA	11.999	37.664	40.293	67.732	29.363	59.301
MANEA	17.544	11.402	13.661	13.425	15.778	11.204
MANEAL	11.211	14.622	16.911	26.211	23.599	24.865
MASP1	0.004	0.025	0.025	0.114	0.008	0.134
MASP2	0.249	1.315	0.064	0.464	0.875	3.431
MBL2	0.000	0.012	0.000	0.000	0.000	0.000
MDK	41.053	95.930	82.033	121.421	44.100	50.485
MFNG	0.090	0.077	0.039	0.017	0.038	0.000
MGAM	0.625	0.019	0.071	0.006	0.006	0.007
MGAT1	142.449	100.670	193.332	146.094	145.312	112.305
MGAT2	74.652	61.110	87.047	78.997	70.715	48.851
MGAT3	0.007	0.040	0.097	0.247	0.086	0.151
MGAT4A	0.117	0.185	0.148	0.125	0.206	0.249
MGAT4B	220.956	341.278	301.623	308.447	288.981	240.332
MGAT4C	0.020	0.000	0.022	0.000	0.000	0.000
MGAT4D	0.000	0.000	0.000	0.000	0.000	0.000
MGAT5	25.758	31.755	23.463	26.550	19.381	13.833
MGAT5B	0.146	0.140	3.014	1.420	0.321	0.228
MGEA5	36.715	58.413	50.738	56.866	56.207	69.368
MMP1	0.037	0.000	4.057	0.000	325.111	0.627
MOGS	45.817	51.509	45.432	39.766	52.472	57.168
MPDU1	145.099	57.947	92.007	65.158	98.651	48.232
MPI	46.029	61.160	58.197	58.051	37.144	33.585
MRC1	0.007	0.000	0.000	0.000	0.000	0.044
MRC2	311.453	310.415	424.459	220.478	416.691	422.404
MUC2	0.000	0.000	0.010	0.009	0.000	0.000
MUC5AC	0.000	0.000	0.000	0.006	0.000	0.000
NAGA	30.263	21.832	34.197	22.764	38.887	28.542
NAGK	117.149	110.527	147.198	82.993	154.154	69.868
NAGLU	64.034	129.080	83.952	82.394	70.288	105.533
NAGPA	18.884	25.357	24.617	33.352	27.449	49.303
NANS	92.476	56.825	100.189	56.849	89.355	39.884
NCAM1	23.089	304.332	13.438	180.758	7.805	14.880
NCAM2	0.344	0.273	0.008	0.000	0.073	0.175
NCAN	0.042	0.013	0.026	0.017	0.006	0.029
NCEH1	58.350	8.774	31.384	7.781	58.134	10.027
NDST1	87.114	125.828	107.182	114.540	63.524	69.081
NDST2	12.851	19.860	25.165	19.847	18.043	26.925
NDST3	0.219	0.230	0.155	0.142	0.295	0.295

NDST4	0.000	0.012	0.013	0.000	0.000	0.000
NEU1	7.034	18.723	13.075	22.427	10.601	21.648
NEU2	0.000	0.000	0.000	0.032	0.000	0.000
NEU3	3.854	1.822	3.614	2.807	4.022	4.453
NEU4	0.000	0.030	0.000	0.120	0.030	0.084
NGLY1	16.324	9.404	16.247	13.679	18.993	16.146
NLGN2	16.328	28.525	21.888	30.251	25.463	48.930
NLGN3	0.144	0.685	0.084	0.369	0.297	0.997
NLGN4X	0.046	0.019	0.232	0.203	0.421	0.449
NLGN4Y	0.494	0.411	3.520	2.849	5.143	5.255
NOTUM	0.897	1.978	1.021	1.690	0.166	0.604
NPL	2.053	2.026	1.535	1.775	2.112	2.815
NT5M	6.140	13.783	6.227	6.223	9.399	10.905
NYX	0.000	0.000	0.000	0.000	0.000	0.000
OGN	0.000	0.013	0.000	0.000	0.000	0.105
OGT	27.607	66.681	23.954	35.475	51.332	107.819
OLR1	0.046	0.066	0.033	0.044	0.049	0.092
OS9	190.467	317.979	331.945	342.615	252.625	376.676
OST4	449.046	460.048	503.917	455.241	550.098	417.777
OVGP1	0.119	0.960	0.206	0.754	0.291	2.719
P3H1	86.985	93.387	116.544	95.788	98.781	95.193
P3H2	4.899	0.673	3.302	0.784	3.151	1.690
PAPSS1	61.415	115.875	67.301	114.595	55.106	82.036
PAPSS2	65.170	17.299	59.822	17.110	70.694	20.707
PDIA3	396.982	239.436	552.774	290.203	431.289	210.261
PECAM1	0.189	0.520	0.235	0.445	0.403	0.550
PFKFB1	0.061	0.198	0.067	0.058	0.022	0.049
PFKFB2	0.899	3.249	2.855	7.164	2.141	7.818
PFKFB3	49.610	19.684	61.595	53.569	40.100	11.924
PFKL	219.842	163.565	267.358	264.035	237.550	104.310
PFKM	44.941	66.381	30.913	71.683	45.629	90.584
PFKP	451.030	82.949	342.712	136.863	351.293	65.663
PGAP1	1.858	2.640	1.146	3.289	1.842	3.727
PGM1	102.334	79.548	98.239	94.770	80.314	46.741
PGM2	32.662	7.923	30.837	10.244	42.694	12.407
PGM3	18.245	12.151	26.086	16.433	24.562	11.356
PGM5	0.046	0.657	2.774	31.991	0.342	0.249
PHACTR1	6.264	2.298	1.353	0.995	1.713	1.891
PHPT1	146.893	116.507	112.936	132.657	121.834	79.881
PIGA	7.055	2.442	5.974	3.525	4.701	2.522
PIGB	7.980	8.985	6.833	6.440	7.114	8.024

PIGC	26.510	23.309	20.839	29.339	24.550	33.186
PIGF	33.158	34.203	29.665	34.395	28.861	34.636
PIGG	17.543	20.528	20.107	20.222	21.447	25.786
PIGH	19.931	10.604	20.529	13.657	15.815	17.100
PIGK	15.832	13.795	14.840	16.949	16.965	21.366
PIGL	9.360	13.433	8.184	8.769	9.629	20.363
PIGM	10.837	9.210	12.089	11.610	10.492	11.678
PIGN	8.620	9.599	12.042	15.417	11.803	15.023
PIGO	21.430	17.105	24.589	19.201	20.899	17.466
PIGP	8.322	14.093	13.594	23.390	12.736	23.275
PIGQ	42.079	48.750	34.967	35.725	48.129	44.676
PIGS	59.104	95.512	85.872	106.047	76.550	89.670
PIGT	221.394	243.594	341.807	322.080	183.236	216.629
PIGU	27.550	17.752	39.316	35.711	33.791	16.611
PIGV	6.133	11.286	9.897	14.333	8.156	16.736
PIGW	17.838	6.752	10.238	6.223	13.021	6.348
PIGX	14.686	9.899	11.406	11.390	19.540	14.347
PIGY	38.180	40.918	35.381	56.185	40.028	59.645
PIGZ	3.853	6.330	5.278	6.250	5.926	12.054
PKD1	37.162	70.089	53.420	62.036	76.644	97.159
PKD1L2	0.009	0.563	0.025	0.571	0.055	28.553
PKD2	22.780	70.825	59.332	62.171	51.973	65.106
PLA2R1	1.548	6.639	7.172	9.917	5.526	9.509
PLAC8	1.418	2.342	1.002	1.721	1.473	1.510
PLAUR	190.782	16.892	227.053	11.727	250.841	25.373
PLOD1	446.810	156.235	566.120	297.909	567.331	559.321
PLOD2	284.425	75.191	286.785	144.564	132.724	69.081
PLOD3	282.422	135.427	203.859	80.662	217.353	92.323
PMM1	144.033	107.681	161.658	126.436	144.081	111.106
PMM2	54.070	30.974	55.753	30.741	50.523	23.834
POFUT1	62.050	35.630	76.951	62.751	52.731	35.753
POFUT2	24.609	32.719	37.756	39.948	33.078	36.966
POGLUT1	9.010	9.773	10.307	14.174	10.808	14.111
POMGNT1	101.903	85.760	98.392	77.920	84.242	60.700
POMGNT2	18.654	26.338	29.212	48.993	26.756	36.530
POMK	2.309	1.377	2.737	3.780	1.206	1.423
POMT1	16.295	30.732	23.301	33.848	24.617	36.072
POMT2	16.098	18.005	12.697	16.212	20.273	21.828
PPAP2A	12.673	61.310	12.898	42.016	20.137	45.654
PPAP2B	106.663	67.630	113.707	48.549	87.133	164.398
PPAP2C	0.025	0.000	0.985	0.647	0.240	0.181

PPBP	0.322	0.000	0.032	0.000	0.000	0.000
PPP1R3A	0.000	0.019	0.000	0.000	0.000	0.000
PPP1R3B	7.211	22.633	23.092	40.717	15.501	39.897
PPP1R3C	71.984	47.680	81.994	146.379	67.993	108.201
PPP1R3F	4.080	11.134	3.591	8.718	3.139	5.385
PRG2	0.124	0.080	0.136	0.143	0.185	0.299
PRG3	0.000	0.000	0.000	0.000	0.000	0.000
PRG4	0.194	0.145	0.154	0.067	1.334	1.152
PRKCSH	423.376	351.166	386.408	302.157	386.268	327.861
PTN	6.237	1.205	1.898	0.856	0.449	0.269
PTPRZ1	0.037	0.051	0.087	0.140	0.190	0.736
PXYLP1	3.325	3.890	5.637	5.469	3.340	5.407
PYGB	173.196	64.964	251.109	153.010	154.641	95.339
PYGL	53.741	96.037	18.124	52.974	38.616	43.029
PYGM	0.032	0.092	0.023	0.183	0.034	3.576
RDH13	5.790	3.903	7.950	7.355	10.405	6.859
REG1A	0.000	0.000	0.000	0.000	0.000	0.000
REG1B	0.000	0.000	0.000	0.000	0.000	0.000
REG3A	0.000	0.000	0.000	0.000	0.000	0.000
REG3G	0.000	0.000	0.000	0.000	0.000	0.000
REG4	0.034	0.000	0.074	0.000	0.018	0.000
RENBP	0.754	9.873	7.833	12.161	5.877	6.938
RFNG	45.034	71.842	47.081	56.508	52.269	72.954
RFT1	16.860	9.894	15.074	11.197	21.742	13.994
RNF123	19.135	37.538	25.394	34.063	27.044	39.092
RPN1	380.924	209.548	394.556	271.857	343.366	223.725
RPN2	290.468	196.610	451.386	330.357	311.808	183.484
RTFDC1	112.538	147.859	227.245	264.273	128.885	162.910
S100A12	0.000	0.000	0.000	0.000	0.000	0.000
S100A8	0.000	0.000	0.000	0.000	0.000	0.000
S100A9	0.000	0.000	0.000	0.000	0.000	0.000
SCD	168.202	1338.893	366.469	1937.549	299.916	1884.786
SCD5	9.261	17.325	5.952	18.572	9.260	16.916
SDC1	51.124	5.324	22.658	4.531	60.234	4.217
SDC2	9.052	28.150	38.787	27.311	16.792	11.620
SDC3	82.871	46.127	124.908	151.384	65.769	56.556
SDC4	124.999	23.745	293.480	75.282	137.173	74.357
SDCBP	136.579	183.232	163.963	193.385	204.307	368.904
SDCBP2	0.728	2.072	1.519	2.019	1.883	2.719
SELE	0.000	0.000	0.000	0.000	0.000	0.000
SELL	0.031	0.000	0.000	0.000	0.000	0.000

SELP	0.000	0.000	0.000	0.000	0.000	0.000
SELPLG	4.931	36.814	15.216	17.786	9.638	14.596
SERPINC1	0.072	0.078	0.052	0.207	0.077	0.173
SERPINE1	16485.995	160.471	12239.773	423.330	12464.288	932.948
SFTPA1	0.000	0.000	0.000	0.016	0.000	0.000
SFTPA2	0.017	0.019	0.038	0.000	0.019	0.000
SFTPB	0.323	0.519	0.251	0.441	0.400	0.705
SFTPC	0.000	0.035	0.000	0.000	0.000	0.000
SFTPD	0.060	0.097	0.261	0.401	0.127	0.144
SGMS1	12.623	15.986	12.661	14.212	14.441	12.919
SGMS2	11.273	8.170	11.655	5.564	10.197	2.985
SGPL1	22.674	24.837	32.611	29.246	26.324	25.654
SGPP2	0.255	0.000	0.210	0.000	0.170	0.038
SGSH	36.095	47.833	59.884	43.157	49.870	62.825
SHH	0.000	0.289	0.000	0.000	0.000	0.000
SI	0.000	0.000	0.007	0.000	0.000	0.000
SIAE	15.173	27.704	17.967	21.753	30.460	45.694
SIGLEC1	0.000	0.012	0.012	0.350	0.018	0.076
SIGLEC10	1.430	1.280	0.951	0.747	1.314	1.660
SIGLEC11	0.230	0.314	0.079	0.197	0.335	0.496
SIGLEC12	0.000	0.000	0.000	0.000	0.000	0.000
SIGLEC15	2.210	0.220	27.061	2.075	43.436	0.399
SIGLEC5	0.030	0.016	0.000	0.000	0.000	0.000
SIGLEC6	0.000	0.000	0.000	0.000	0.000	0.000
SIGLEC7	0.000	0.000	0.000	0.021	0.023	0.053
SIGLEC8	0.156	0.309	0.242	0.162	0.401	0.485
SIGLEC9	0.038	0.020	0.083	0.000	0.000	0.000
SLC17A5	15.784	37.331	28.511	20.085	30.099	20.065
SLC26A1	1.290	1.193	1.902	1.003	1.897	2.922
SLC26A10	0.266	1.544	0.062	0.262	0.196	0.627
SLC26A11	6.788	16.222	18.157	16.412	15.575	22.309
SLC26A2	19.457	13.174	12.796	8.944	11.464	7.228
SLC26A3	0.013	0.000	0.000	0.013	0.000	0.000
SLC26A4	4.167	0.621	1.148	3.332	1.771	2.849
SLC26A5	0.000	0.100	0.000	0.000	0.071	0.080
SLC26A6	19.977	15.491	28.594	11.190	40.614	39.811
SLC26A7	0.006	0.042	0.000	0.006	0.007	0.023
SLC26A8	0.000	0.011	0.000	0.020	0.000	0.051
SLC26A9	0.000	0.000	0.000	0.000	0.000	0.010
SLC2A1	248.221	179.269	421.610	313.759	247.626	105.024
SLC2A10	14.175	24.493	49.806	43.344	22.186	23.901

SLC2A11	1.963	8.561	3.232	6.033	4.021	9.424
SLC2A12	0.280	3.037	0.374	16.573	0.299	4.553
SLC2A13	4.887	2.310	6.761	3.289	5.357	4.359
SLC2A14	4.116	8.552	9.315	6.978	5.763	2.917
SLC2A2	0.011	0.000	0.012	0.021	0.047	0.000
SLC2A3	31.527	54.205	62.808	47.816	39.952	21.939
SLC2A4	0.352	0.723	0.399	0.362	0.466	1.026
SLC2A5	0.013	0.043	0.396	0.270	0.243	0.485
SLC2A6	17.090	32.438	35.861	45.752	25.628	14.818
SLC2A7	0.000	0.000	0.000	0.000	0.000	0.000
SLC2A8	9.643	8.088	5.081	4.285	7.539	5.322
SLC2A9	0.257	0.378	0.464	0.989	0.667	1.155
SLC35A1	11.314	11.267	10.992	14.840	13.565	31.326
SLC35A2	23.929	21.672	30.734	25.100	27.905	19.917
SLC35A3	7.130	6.028	8.647	7.726	8.235	7.776
SLC35A4	121.212	99.305	87.223	62.864	90.478	65.677
SLC35A5	20.766	18.295	26.819	25.744	19.946	22.954
SLC35B1	66.290	63.772	56.933	54.770	62.119	44.371
SLC35B2	104.459	83.927	126.538	121.933	141.655	115.500
SLC35B3	18.070	17.865	16.549	16.125	16.661	18.275
SLC35B4	20.798	13.709	16.238	13.939	16.043	10.421
SLC35C1	29.761	24.054	27.192	18.171	21.344	18.030
SLC35C2	47.892	77.895	102.140	82.394	61.981	57.263
SLC35D1	22.373	11.663	11.552	7.893	16.205	21.702
SLC35D2	7.291	9.617	8.125	9.109	7.089	11.615
SLC35D3	0.016	0.017	0.017	0.031	0.051	0.019
SLC37A4	14.518	10.836	12.709	15.641	18.892	17.499
SLC3A1	0.078	0.000	0.000	0.154	0.085	0.285
SLC3A2	220.782	362.812	367.750	337.315	307.627	252.577
SLC5A1	0.000	0.016	0.000	0.021	0.008	0.000
SLC5A2	0.020	0.091	0.068	0.000	0.065	0.075
SLC5A4	0.000	0.000	0.332	0.000	0.000	0.000
SMC3	47.442	26.172	31.303	24.987	54.288	35.677
SMPD1	105.866	135.263	114.508	72.679	135.079	144.220
SMPD3	0.254	0.377	0.461	0.286	0.774	1.420
SORD	41.746	13.021	23.596	15.261	27.427	16.890
SPACA3	1.120	0.859	0.000	0.090	0.050	0.113
SPACA5	0.000	0.000	0.000	0.000	0.000	0.000
SPAM1	0.000	0.000	0.000	0.000	0.000	0.000
SPHK1	49.154	9.569	23.267	3.407	55.034	6.621
SPHK2	9.077	17.522	9.895	13.422	10.060	15.273

SPOCK1	67.347	17.564	75.459	26.186	55.210	14.235
SPOCK2	0.073	0.562	0.087	0.687	0.111	3.521
SPOCK3	0.000	0.000	0.000	0.000	0.000	0.000
SPTLC1	41.557	35.618	45.625	40.973	42.465	41.027
SPTLC2	10.674	13.101	54.449	23.757	37.109	10.781
SPTLC3	14.429	4.799	0.687	2.541	1.771	22.686
SRD5A3	21.324	9.652	22.701	7.984	23.603	10.285
SRGN	501.047	148.115	934.371	150.251	776.937	102.811
ST3GAL1	7.728	5.971	15.592	8.363	10.401	8.121
ST3GAL2	24.402	15.788	31.807	21.248	26.255	16.261
ST3GAL3	29.166	22.408	23.216	25.362	23.887	20.511
ST3GAL4	31.972	21.074	30.663	42.094	33.851	28.129
ST3GAL5	17.009	35.663	15.524	97.412	8.029	32.633
ST3GAL6	0.740	0.651	2.890	0.951	2.569	1.471
ST6GAL1	0.929	1.014	1.682	1.917	1.922	6.646
ST6GAL2	0.184	0.351	0.231	0.530	0.375	0.353
ST6GALNAC1	0.000	0.030	0.031	0.000	0.000	0.017
ST6GALNAC2	0.527	1.022	0.697	0.785	0.601	0.724
ST6GALNAC3	0.000	0.011	0.012	0.000	0.023	0.026
ST6GALNAC4	35.612	35.992	40.216	45.750	24.502	33.643
ST6GALNAC5	1.543	4.581	0.516	1.537	0.040	0.182
ST6GALNAC6	96.402	178.730	114.530	129.829	69.302	107.703
ST8SIA1	0.295	0.571	0.306	0.473	0.466	0.799
ST8SIA2	6.389	12.341	1.236	2.272	5.226	1.436
ST8SIA3	0.015	0.016	0.037	0.033	0.016	0.018
ST8SIA4	1.315	0.523	0.387	0.884	0.588	0.647
ST8SIA5	1.181	4.022	0.655	2.059	0.606	1.232
ST8SIA6	0.274	0.148	0.150	0.368	0.379	0.099
STBD1	28.526	15.340	20.287	12.012	22.193	16.389
STS	11.260	4.977	14.173	9.050	15.399	27.393
STT3A	87.967	79.600	101.017	81.195	109.158	72.190
STT3B	67.404	73.714	58.016	85.621	62.325	68.344
SULF1	15.742	38.432	143.406	42.290	34.457	7.374
SULF2	0.524	1.459	0.348	0.776	0.009	0.197
SV2A	24.409	17.045	17.114	13.251	28.722	20.048
SVOP	0.580	0.825	0.321	0.551	0.625	0.870
SVOPL	0.000	0.000	0.000	0.000	0.000	0.000
TGDS	9.267	5.264	9.649	7.069	8.941	8.109
TGFBR3	2.839	1.150	0.979	0.853	3.106	15.913
THBD	10.431	14.572	1.808	1.285	5.634	3.516
THBS1	1099.347	2565.567	3198.395	2329.043	2562.665	1048.169

THBS2	15.058	86.122	48.420	161.040	158.322	185.768
THNSL2	4.225	13.590	9.042	15.172	12.426	31.827
TIMP1	3186.097	935.793	3753.104	859.762	5365.579	413.981
TIMP2	253.184	837.786	1100.638	973.960	1093.490	1202.004
TIMP3	10.949	2.723	60.598	64.817	29.392	14.225
TMEM5	21.171	16.791	13.993	16.145	18.531	21.408
TNC	56.078	0.380	9.384	1.918	3.002	0.338
TNF	0.003	0.006	0.003	0.000	0.009	0.011
TNR	0.015	0.000	0.008	0.000	0.016	0.018
TNXB	0.005	0.040	0.090	0.115	0.225	0.433
TPI1	1866.543	910.538	2199.975	1334.463	1836.549	480.954
TPST1	39.671	45.189	25.557	29.445	23.263	46.290
TPST2	30.424	46.700	97.657	81.527	49.173	23.367
TRAM2	179.905	115.943	321.827	201.113	331.871	300.842
TREH	0.000	0.022	0.023	0.020	0.110	0.174
TSTA3	110.597	60.662	88.954	61.187	104.053	41.553
TUSC3	56.556	28.794	52.190	28.146	51.752	27.975
UAP1	170.821	32.077	143.690	44.438	120.693	28.694
UGCG	107.265	38.736	122.140	47.767	68.509	27.128
UGDH	37.386	24.300	40.826	30.482	52.558	30.169
UGGT1	25.656	14.459	21.482	16.571	24.810	15.601
UGGT2	14.770	9.821	15.718	10.709	16.919	12.020
UGP2	300.909	156.088	145.442	105.972	118.156	88.111
UGT1A1	0.000	0.000	0.000	0.000	0.000	0.000
UGT1A10	0.000	0.000	0.000	0.000	0.000	0.000
UGT1A3	0.000	0.000	0.000	0.000	0.000	0.000
UGT1A4	0.000	0.000	0.000	0.000	0.000	0.000
UGT1A5	0.000	0.000	0.000	0.000	0.000	0.000
UGT1A6	0.000	0.000	0.000	0.000	0.000	0.000
UGT1A7	0.000	0.000	0.000	0.000	0.000	0.000
UGT1A8	0.000	0.000	0.000	0.000	0.000	0.000
UGT1A9	0.000	0.000	0.000	0.000	0.000	0.000
UGT2A1	0.078	0.061	0.025	0.032	0.072	0.041
UGT2A2	0.000	0.000	0.000	0.000	0.000	0.000
UGT2A3	0.000	0.000	0.000	0.000	0.000	0.000
UGT2B10	0.005	0.035	0.010	0.009	0.045	0.129
UGT2B11	0.000	0.000	0.049	0.000	0.024	0.217
UGT2B15	0.076	0.128	0.028	0.065	0.072	0.051
UGT2B17	0.000	0.010	0.000	0.000	0.000	0.000
UGT2B28	0.000	0.023	0.000	0.020	0.000	0.000
UGT2B4	0.079	0.221	0.086	0.393	0.134	0.304

UGT2B7	0.871	3.377	0.799	2.414	2.658	15.857
UGT3A1	0.000	0.008	0.008	0.007	0.000	0.000
UGT3A2	0.000	0.000	0.000	0.031	0.000	0.000
UGT8	0.928	0.847	0.772	0.742	1.300	1.392
UST	6.313	3.383	4.609	2.660	6.455	16.458
UTP14C	10.496	17.088	16.270	19.995	12.442	16.114
UXS1	36.628	25.598	38.825	29.638	35.679	13.972
VCAM1	0.048	0.220	0.157	0.459	1.732	2.523
VCAN	41.721	72.507	35.895	30.509	40.850	14.356
VTN	0.570	1.061	0.899	0.482	0.584	2.588
WBSCR17	0.000	0.000	0.000	0.010	0.000	0.000
XXYLT1	33.739	25.683	50.678	43.943	46.101	39.474
XYLT1	3.502	1.228	1.948	0.610	8.347	15.936
XYLT2	34.424	27.175	51.431	32.827	38.288	32.686